

# Analysis of the dorsal-ventral gene regulatory network of *Nasonia vitripennis*

Inaugural-Dissertation  
zur  
Erlangung des Doktorgrades  
der Mathematisch-Naturwissenschaftlichen Fakultät  
der Universität zu Köln

vorgelegt von  
**Thomas Martin Buchta**  
aus Bretten

Köln 2014

Berichterstatter/in:

Prof. Dr. Siegfried Roth

Prof. Dr. Günter Plickert

Tag der letzten mündlichen Prüfung: 07. April 2014



## Contents

<b>1</b>	<b>Introduction</b> .....	<b>1</b>
1.1	Introduction Summary .....	1
1.2	In <i>Drosophila</i> the main body axes are determined during oogenesis.....	2
1.3	Establishment of the anterior-posterior (AP) axis in <i>Drosophila</i> .....	3
1.4	Establishment of the dorsal-ventral (DV) axis in the <i>Drosophila</i> .....	4
1.4.1	The spatial cues for the DV axis originates in the follicular epithelium.....	4
1.4.2	A protease cascade transmits the ventralizing signal to the embryo .....	5
1.4.3	The translation of an extracellular into an intracellular gradient.....	8
1.4.4	A gradient of nuclear Dorsal patterns the dorsal-ventral (DV) axis .....	9
1.4.5	The BMP pathway .....	11
1.5	The DV axis in the beetle <i>Tribolium castaneum</i> .....	14
1.6	The wasp <i>Nasonia vitripennis</i> .....	16
1.7	Objective .....	17
<b>2</b>	<b>Publications &amp; Manuscripts</b> .....	<b>18</b>
2.1	Patterning the dorsal-ventral axis of the wasp <i>Nasonia vitripennis</i> .....	18
2.2	Novel deployment of Toll and BMP signaling pathways leads to a convergent patterning output in a wasp .....	41
2.3	Ancient and diverged TGF- $\beta$ signaling components in <i>Nasonia vitripennis</i> ..	59
<b>3</b>	<b>Additional Material &amp; Methods</b> .....	<b>83</b>
3.1	<i>Nasonia vitripennis</i> Stock Keeping.....	83
3.2	Ovary preparation & Fixation.....	83
3.3	Embryo Collection & Fixation .....	83
3.4	<i>In Situ</i> Hybridization Probe & dsRNA Synthesis.....	84
3.4.1	Obtaining the Sequence.....	84
3.4.2	Designing the primers.....	85
3.4.3	PCR.....	86
3.4.4	Making dig labelled probes.....	87
3.4.5	Making dsRNA .....	88
3.5	<i>In Situ</i> Hybridization (ISH) .....	89
3.6	Analysis of Toll pathway components .....	93

3.6.1	NCBI Accession numbers.....	93
3.6.2	Phylogenetic analysis.....	100
3.6.3	ISH Primers of Toll Pathway genes.....	100
<b>3.7</b>	<b>Transcriptome .....</b>	<b>102</b>
3.7.1	RNA isolation .....	102
3.7.2	cDNA generation .....	102
3.7.3	Quantitative polymerase chain reaction (qPCR).....	103
3.7.4	Transcriptome data generation and evaluation.....	107
3.7.5	High through-put ISH Primers .....	108
3.7.6	High through-put in ISH.....	109
<b>4</b>	<b>Additional Results.....</b>	<b>110</b>
<b>4.1</b>	<b>The Toll signaling cascade in <i>Nasonia vitripennis</i> .....</b>	<b>110</b>
<b>4.2</b>	<b>Analyses of Toll pathway components .....</b>	<b>112</b>
4.2.1	Analysis of components of the follicular epithelium.....	113
4.2.2	Analysis of perivitelline fluid components .....	116
4.2.3	Analysis of Toll.....	126
4.2.4	Analysis intracellular Components.....	130
<b>4.3</b>	<b>Transcriptome .....</b>	<b>137</b>
4.3.1	Quantitative polymerase chain reaction (qPCR).....	138
4.3.2	High through put ISH.....	139
<b>5</b>	<b>Discussion and outlook.....</b>	<b>144</b>
<b>5.1</b>	<b>The fate mapping analysis.....</b>	<b>144</b>
5.1.1	Dynamic gene expression on the ventral side.....	144
5.1.2	Lateral gene expression .....	146
5.1.3	Gene expression on the dorsal side.....	147
<b>5.2</b>	<b>Functional analysis .....</b>	<b>148</b>
5.2.1	Toll knockdown embryos are still polarized .....	148
5.2.2	Toll signaling in the absence of BMP.....	150
5.2.3	Future functional analyses.....	151
<b>5.3</b>	<b>Analysis of Toll pathway components .....</b>	<b>152</b>
<b>5.4</b>	<b>DV axis formation without <i>short gastrulation (sog)</i> .....</b>	<b>157</b>

5.4.1	Sog is not conserved in the <i>Nasonia vitripennis</i> genome .....	157
5.4.2	A BMP gradient without Sog .....	158
5.5	<b>Transcriptome</b> .....	<b>159</b>
<b>6</b>	<b>References</b> .....	<b>162</b>
<b>7</b>	<b>Summary</b> .....	<b>171</b>
<b>8</b>	<b>Zusammenfassung</b> .....	<b>172</b>
<b>9</b>	<b>Anhang über die Eigenbeteiligung an den aufgeführten</b>	
	<b>Veröffentlichungen</b> .....	<b>174</b>
<b>9.1</b>	<b>Patterning the dorsal-ventral axis of the wasp <i>Nasonia vitripennis</i></b> .....	<b>174</b>
9.1.1	Gene identification .....	174
9.1.2	Primer design .....	175
9.1.3	cDNA generation .....	175
9.1.4	<i>In situ</i> hybridization (ISH) probe synthesis.....	175
9.1.5	Single/two color fluorescent ISH with DAPI.....	175
9.1.6	DAPI staining .....	175
9.1.7	Microscopy, picture processing and figure design .....	176
9.1.8	Embryo collection and fixation .....	176
9.1.9	Waspinator .....	177
9.1.10	Text.....	177
<b>9.2</b>	<b>Novel deployment of Toll and BMP signaling pathways leads to a convergent</b>	
	<b>patterning output in a wasp</b> .....	<b>177</b>
9.2.1	Gene identification .....	177
9.2.2	Primer design .....	177
9.2.3	cDNA generation .....	178
9.2.4	<i>In situ</i> hybridization (ISH) probe synthesis.....	178
9.2.5	Two-color and three-color fluorescent ISH with DAPI.....	178
9.2.6	Double stranded RNA synthesis.....	178
9.2.7	dsRNA single and double injections .....	178
9.2.8	Microscopy, picture processing and figure design .....	179
9.2.9	Embryo collection and fixation .....	179

9.2.10	Text.....	179
<b>9.3</b>	<b>Ancient and diverged TGF-<math>\beta</math> signaling components</b>	
	<b>in <i>Nasonia vitripennis</i>.....</b>	<b>180</b>
9.3.1	Gene identification .....	180
9.3.2	Primer design .....	181
9.3.3	cDNA generation .....	181
9.3.4	<i>In situ</i> hybridization (ISH) probe synthesis.....	181
9.3.5	Single/ two color fluorescent ISH with DAPI.....	181
9.3.6	Double stranded RNA synthesis.....	181
9.3.7	dsRNA injection .....	182
9.3.8	Microscopy, picture processing, tree generation and figure design.....	182
9.3.9	Embryo collection and fixation.....	182
9.3.10	Text.....	182
	<b>Danksagung.....</b>	<b>183</b>
	<b>Erklärung.....</b>	<b>184</b>
	<b>Lebenslauf .....</b>	<b>185</b>

# 1 Introduction

## 1.1 Introduction Summary

All bilaterally symmetric animals share the feature of possessing two major body axes. The long axis also called anterior posterior (AP) axis extends from head to abdomen. Orthogonal to the AP axis extends the short or dorsal ventral (DV) axis. Signaling pathways that are highly conserved throughout the whole animal kingdom regulate the establishment of both body axes. They interact with each other in gene regulatory networks (GRN). One of the most studied and best-understood GRNs establishes the DV axis in the long germ embryo of the fruit fly *Drosophila melanogaster* (*Dm*). The basic mechanism underlying this GRN is a hierarchical signaling cascade that is triggered on the ventral side of the *Drosophila* egg chamber. Center of this signaling cascade is the transmembrane receptor Toll (Hashimoto et al., 1988) which transmits the ventralising signal into the embryo. In the early syncytial blastoderm embryo, Toll signaling generates a stable morphogen gradient of nuclear Dorsal (Roth et al., 1989; Rushlow et al., 1989; Steward, 1989), a NF- $\kappa$ B transcription factor (Huguet et al., 1997), which provides the majority of pattern information along the DV axis in the early embryo by activating a huge number of downstream target genes in a concentration dependent manner (Hong et al., 2008; Roth et al., 1989; Stathopoulos and Levine, 2004). The BMP pathway, like the Toll pathway, is a highly conserved signal transduction cascade. During *Drosophila* embryogenesis the BMP homolog Dpp creates a morphogen gradient, which is essential to pattern the dorsal side of the embryo. This gradient in turn is regulated by Toll associated inhibition (O'Connor et al., 2006). Studies in other organisms indicate that the hierarchical arrangement of the Toll pathway and its dominance in *Drosophila* embryogenesis is a derived feature and not even conserved within insects (Nunes da Fonseca et al., 2008).

## 1.2 In *Drosophila* the main body axes are determined during oogenesis

In *Drosophila melanogaster* body axes induction is under maternal control and both axes are established in the ovary during oogenesis (Roth and Lynch, 2009). Each of the two *Drosophila* ovaries consists of sixteen ovarioles (Lin and Spradling, 1993), whereas each ovariole itself is a string of connected egg chambers (Fig. 1.1 top panel). This tube-like structure already exhibits an anatomical polarity with two axes. The long axis is constituted by the string of connected egg chambers and the short axis extends orthogonal to this and is defined by the plane of cross section through an egg chamber (Roth and Lynch, 2009).

*Drosophila* uses a polytrophic meroistic mode of oogenesis. The anterior most region of each ovariole consists of the germarium, a compartment that holds both somatic stem cells as well as the germline stem cell (GSC) niche (Fig. 1.1 bottom panel left). The development of each egg chamber begins in the germarium with an asymmetric division of a GSC into a self-renewing GSC and one differentiating cell called cystoblast (Fuller and Spradling, 2007; Lin and Spradling, 1993). The cystoblast undergoes four incomplete mitotic divisions resulting in 16 cells (the cystocytes), which are connected by ring canals (Margolis and Spradling, 1995; Robinson and Cooley, 1996). Only one of the cystocytes will develop into an oocyte while the remaining fifteen will develop into nurse cells. These specialized polyploid cells contribute to the development of the oocyte by synthesizing massive amounts of RNAs and proteins that are to be deposited in the oocyte by microtubule (MT) dependent transport (Bastock and St Johnston, 2008). Oocyte and nurse cells go through fourteen stages of development during oogenesis.

A monolayer of somatic cells called follicle epithelium encompasses the oocyte-nurse cell compartment (Fig. 1.1). Besides its function in synthesizing the vitelline membrane and chorion of the eggshell (Pascucci et al., 1996), the follicle epithelium plays a crucial role in axis determination. It degenerates prior to the end of oogenesis.

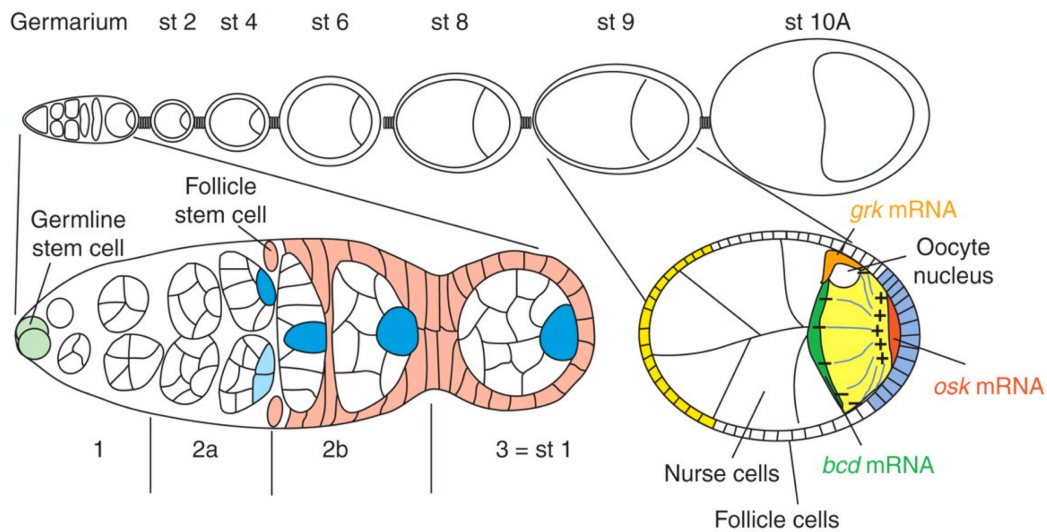


**Figure 1.1 Oogenesis in *Drosophila melanogaster***

Schematic drawing of a *Drosophila* ovariole (top), germarium (bottom left) and egg chamber (bottom right). Oogenesis starts at the germarium and completes 14 stages during egg maturation. (Roth and Lynch, 2009)

### 1.3 Establishment of the anterior-posterior (AP) axis in *Drosophila*

During oogenesis one of the first symmetry-breaking events inside the oocyte is the migration of the oocyte nucleus to the posterior cortex of the oocyte. The *grk* mRNA, which surrounds the nucleus, is translated and secreted. Gurken protein, a TGF- $\alpha$  homolog (Neuman-Silberberg and Schüpbach, 1993) binds as ligand to the epidermal growth factor receptor (EGFR) Torpedo (González-Reyes et al., 1995). Binding of Gurken to its receptor specifies the respective follicle cells as posterior follicle cells. A yet unknown response signal of the affected follicle cells to the oocyte leads to the repolarization of the oocyte MT network (Januschke et al., 2006; Roth, 2003). Subsequent MT-Dynein dependent transport localizes *bicoid* mRNA to the anterior pole of the oocyte and MT-Kinesin dependent transport localizes *oskar* mRNA at the opposite, posterior pole (Fig. 1.1 bottom panel right) (Cha et al., 2001; Kugler and Lasko, n.d.; Roth and Lynch, 2009). Localization of these mRNAs is maintained during oogenesis and early embryogenesis and is essential for the specification of the anterior-posterior axis (St Johnston and Nüsslein-Volhard, 1992).

## 1.4 Establishment of the dorsal-ventral (DV) axis in the *Drosophila*

### 1.4.1 The spatial cues for the DV axis originates in the follicular epithelium

Similar to the AP axis, polarization of the DV axis is initiated by asymmetric reposition of the oocyte nucleus followed by a localized activation of the EGF receptor (Roth and Schüpbach, 1994) (Fig. 1.1). This process again differentiates the adjacent follicle cells and defines the dorsal domain of the follicular epithelium. Specification of the ventral domain starts in the ventral follicle cells. From there, a protease cascade is triggered, which is located in the perivitelline space. The cascade culminates in the generation of the Spätzle morphogen gradient in the perivitelline fluid. Here, Spätzle protein binds as ligand to the transmembrane receptor Toll, which itself is evenly distributed across the oocyte plasmamembrane. Finally, asymmetric activation of the Toll receptor transfers the polarity of the follicular epithelium to the oocyte.

To re-localize the oocyte nucleus, polarized microtubules push it to an anterior cortical position that is asymmetric in relation to the short axis (Zhao et al., 2012). Subsequently, Gurken protein surrounding the oocyte nucleus is secreted and binds to the EGF-receptor in the follicle cells overlying the oocyte nucleus (Roth and Schüpbach, 1994). Activation of the EGF receptor leads to the transcriptional repression of *pipe* by *mirror (mirr)* in those cells (Andreu et al., 2012).

Follicle cells unaffected by EGF signaling adopt a ventral identity and continue to express *pipe* (Sen et al., 1998). Sub-cellular transportation of Pipe protein from the endoplasmic reticulum (ER) to the Golgi apparatus is a crucial step in defining the ventral domain and requires the protein-disulfide isomerase *windbeutel*, which is uniformly expressed in the follicular epithelium (Konsolaki and Schüpbach, 1998; Ma et al., 2003; Sen et al., 2000). The role of *pipe* in transferring the defined DV polarity of the follicular epithelium to the embryo is not completely understood. However, it is assumed that Pipe mediates the sulfation of some ventrally localized glycoprotein or



glycosaminoglycan, which in turn triggers the activation of a spatially restricted protease cascade in the perivitelline fluid (Fig. 1.2A).

It has been shown that *slalom* (*sll*), which encodes a Golgi transporter for the universal sulfate donor in sulfotransferase reactions 3'-phosphoadenosine 5'-phosphosulfate (PAPS), is essential for the specification of the ventral domain. Most likely Sll Protein provides PAPS for the reaction carried out by Pipe (Kamiyama et al., 2003; Lüders et al., 2003). One assumed Pipe substrate is the vitelline membrane-like (VML) protein, a sulfated eggshell component whose sulfation on the ventral side is provably increased in *Drosophila* ovaries with enhanced levels of *pipe* expression (Zhang et al., 2009a).

Nevertheless, no outright connection between *pipe* activity in the follicle cells and the subsequent protease cascade in the perivitelline fluid has been established, yet.

#### **1.4.2 A protease cascade transmits the ventralizing signal to the embryo**

Nudel together with Pipe and Windbeutel triggers a protease cascade consisting of Gastrulation defective (Gd) (Konrad et al., 1998), Snake (Snk) (DeLotto and Spierer, 1986) and Easter (Ea) (Chasan and Anderson, 1989) (Fig. 1.2B). It is expressed in all follicle cells surrounding the oocyte and therefore seems to be independent of the ventrally restricted *pipe* activity (Hong and Hashimoto, 1995).

*nudel* encodes a large modular protein, that structurally resembles extracellular matrix proteins along with two central serine protease domains (Hong and Hashimoto, 1995). The Nudel protease is activated by autocatalytic cleavage. So far, no other Nudel substrates have been identified. Three dimensional computer models have shown that Nudel is able to bind Gd, which is the first of three sequentially acting serine proteases that process the Toll receptor ligand Spätzle. This suggests that Nudel may indeed also cleave Gd and thus could potentially be involved in the activation of the cascade (Rose et al., 2003). However, Nudel alone is not necessarily needed to activate Gd since exogenously injected Gd was shown to be able to trigger Toll signaling in

a *nudel* mutant background (Han et al., 2000). Hence, it needs to be shown what actually activates Gd. At the moment it cannot be ruled out, that Gd is not activated by Nudel but rather by an unidentified protease or alternatively, it activates itself by autocatalytic cleavage. Nevertheless, the fact that Nudel activity is not restricted to the ventral side and the finding that it is also required for eggshell biogenesis (LeMosy and Hashimoto, 2000) raises the possibility that Nudel acts indirectly in DV patterning by modifying the extracellular matrix.

Gd itself is initially expressed in the oocyte. After secretion of its inactive precursor it becomes accumulated in the ventral region of the perivitelline fluid. After activation it is required to facilitate the interaction of Snake and Easter to create active Easter, which ultimately leads to the generation of the active Toll receptor ligand C-Spätzle (Fig. 1.2B) (Chasan and Anderson, 1989; Chasan et al., 1992; DeLotto and Spierer, 1986; Konrad et al., 1998).

Spätzle actually competes with Serpin 27A (Spn27A) for the interaction with Easter (Fig. 1.2B). Spn27A is a serine protease inhibitor. It targets and irreversibly binds the catalytic center of the Easter protease. Spn27A's role as suicide substrate for Easter is assumed to control the Dorsal gradient by preventing excessive or ectopic cascade activation to lateral and dorsal regions of the embryo (Hashimoto et al., 2003; Ligoxygakis et al., 2003; Misra et al., 1998).

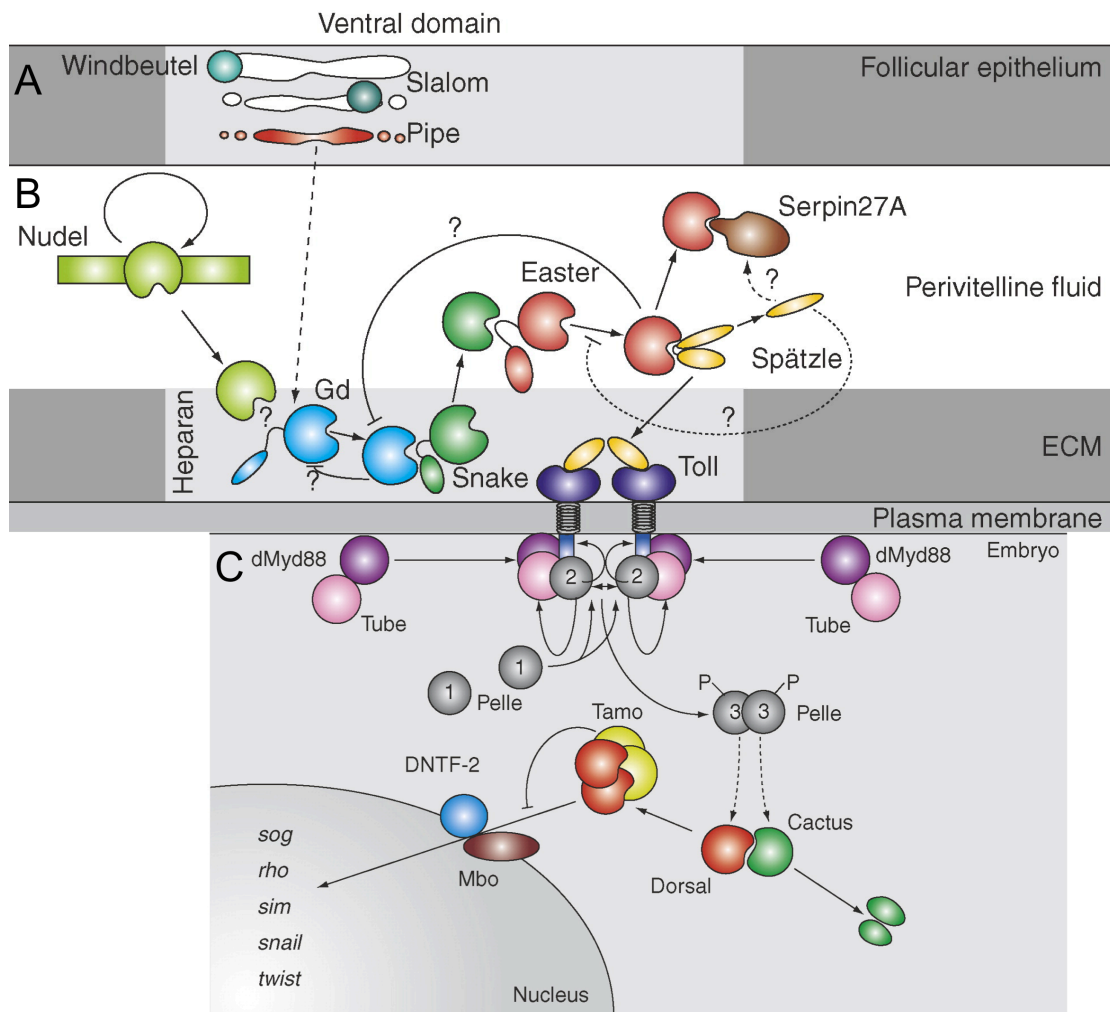


**Figure 1.2 The Toll/NF- $\kappa$ B signaling cascade in *Drosophila melanogaster***

(A) Activation of the Toll receptor is initiated in the follicle cells. The expression of Pipe specifies the ventral domain of the follicular epithelium. Windbeutel transports Pipe to the Golgi, where Slalom provides the substrate (PAPS) for the sulfo- transferase reaction carried out by Pipe. (B) In the perivitelline fluid, within the *pipe* expression domain, a protease cascade consisting of Nudel, Gd and Snake activates another protease, Easter. Active Easter processes the Toll receptor ligand Spätzle, a process negatively regulated by Serpin27A. (C) Activation by Spätzle leads Toll to the formation of an intracellular trimeric complex with dMyd88 and Tube. This complex recruits Pelle and thereby enhances its activity through autophosphorylation. Pelle phosphorylates Cactus, which leads to its degradation and enables Dorsal to dimerise and translocate through a nuclear pore consisting of DNTF-2 and Mbo to the nucleus, a process negatively regulated by Tamo. In the nucleus Dorsal regulates gene expression of many genes. ECM = Extracellular Matrix; P = phosphate; Gd = Gastrulation defective; dMyd88 = *Drosophila* Myeloid differentiation primary response gene (88); DNTF-2 = *Drosophila* Nuclear Transport Factor-2; Mbo = Members-only; *sog* = *short gastrulation*; *rho* = *rhomboid*; *sim* = *single-minded*; PAPS = 3'-phosphoadenosine 5'-phosphosulfate.

(Moussian and Roth, 2005)modified

### 1.4.3 The translation of an extracellular into an intracellular gradient

After binding Spätzle, the activated Toll receptor recruits and binds a membrane-localized heterodimer consisting of Myd88 and the IRAK4 homolog Tube (Towb et al., 2009) with its intracellular TIR (Toll and Interleukin Receptor) domain (Hu et al., 2004; Medzhitov et al., 1998; Towb et al., 1998). The resulting trimeric complex interacts via the death domain of Tube with the death domain of the serine/threonine-kinase Pelle (Pll) (Fig. 1. 2C) (Grosshans et al., 1994; Hu et al., 2004). In non-signaling conditions, Pelle is equally distributed in the cytoplasm (Grosshans et al., 1994). The recruitment of Pelle, by the Toll-Myd88-Tube complex increases the Pelle concentration on the ventral side. The result is an asymmetric distribution of Pelle inside the embryo, which makes Pelle a crucial factor for the transmission of the extracellular to an intracellular gradient.

Putative direct targets of Pelle mediated phosphorylation are the I- $\kappa$ B homolog Cactus and the NF- $\kappa$ B transcription factor Dorsal (Drier et al., 2000, 1999; Edwards et al., 1997). Both are evenly distributed in the cytoplasm. In the absence of Toll signaling, Cactus is bound to Dorsal (Dl) or Dif (Dorsal related immune factor), respectively and inhibits their translocation to the nucleus and thus the activation of target gene expression. To enable Dorsal's nuclear activity, Cactus needs to be degraded. It is assumed that Pelle phosphorylates Cactus in two distinct N-terminal motifs, causing its ubiquitination and proteasomal degradation (Fig. 1.2C) (Bergmann et al., 1996; Fernandez et al., 2001; Reach et al., 1996; Towb et al., 2001). After Dorsal is phosphorylated, too, it dimerises and enters the nucleus. Nuclear translocation of Dorsal is modulated by a transport machinery comprising Tamo and the nuclear pore proteins *Drosophila* Nuclear Transport Factor-2 (DNTF-2) and Members-only (Mbo) (Fig. 1.2C) (Minakhina et al., 2003; Uv et al., 2000). Having arrived in the nucleus, Dorsal acts as a transcription factor and regulates transcription of approximately fifty genes (Hong et al., 2008; Isoda and Nüsslein-Volhard, 1994; Stathopoulos and Levine, 2004).

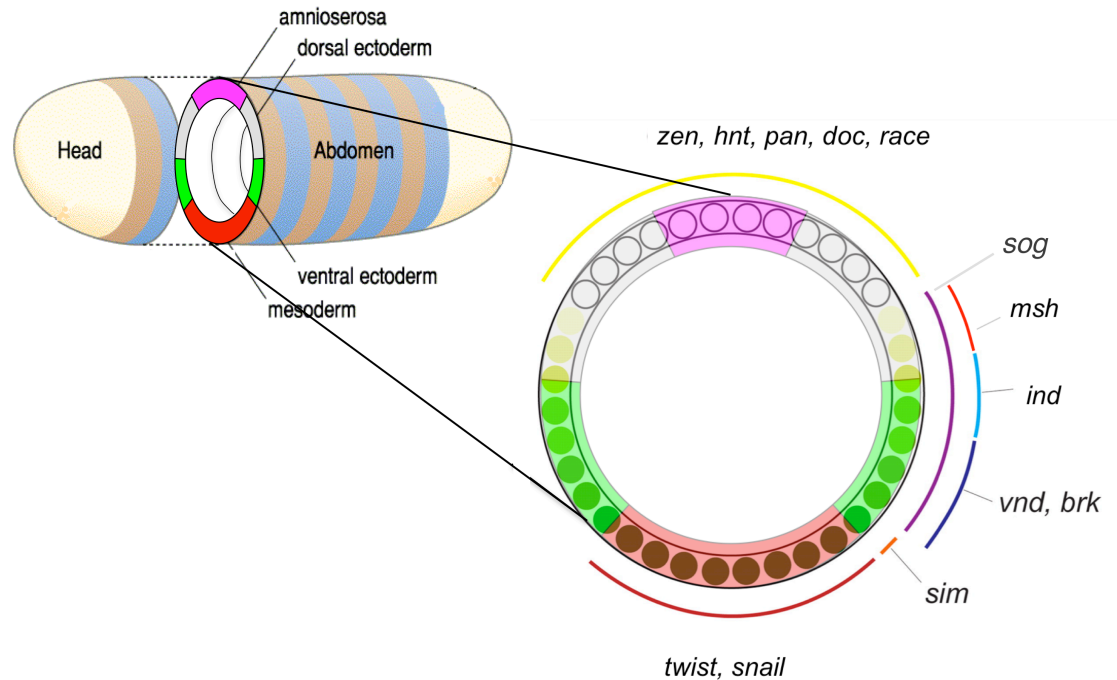


### Figure 1.3 The Nuclear Dorsal gradient

Cut section of a schematic *Drosophila melanogaster* embryo (**left side**). Along the dorsal-ventral axis the different embryonic fates are indicated: mesoderm (red), ventral/neurogenic ectoderm (green), dorsal/non-neurogenic ectoderm (grey), and amnioserosa (pink). The dorsal gradient regulates target gene expression in a concentration-dependent manner across the DV axis (**right side**). Filled circles represent high levels of nuclear Dorsal protein, shaded and yellow circles represent intermediate and low levels, respectively.

*zen* = *zerknüllt*; *hnt* = *hindsight*; *pan* = *pannier*, *doc* = *dorsocross*; *race* = *angiotensin converting enzyme*; *sog* = *short gastrulation*; *msh* = *muscle segment homeo-box*; *ind* = *intermediate neuroblast defective*; *vnd* = *ventral nervous system defective*; *brk* = *brinker*; *sim* = *single-minded*. (Hong et al., 2008; Wolper et al., 2007) (modified)

#### 1.4.4 A gradient of nuclear Dorsal patterns the dorsal-ventral (DV) axis

Dorsal is a member of the NF- $\kappa$ B/ Rel-family of transcription factors (Steward, 1987). After the degradation of its inhibitor Cactus, Dorsal translocates to the nucleus, where it specifically binds to kappa B consensus sequences in enhancer regions of zygotic genes. As a result of the previously described Pelle mediated activation, the nuclear Dorsal distribution is graded along the DV axis. Highest

nuclear Dorsal concentration is measured on the most ventral side of the blastoderm embryo. It decreases towards the dorsal side, creating a symmetric morphogen gradient with intermediate to low concentration of nuclear Dorsal on both lateral sides (Fig. 1.3) (Roth et al., 1989; Steward, 1989). Along this gradient, target genes that respond to different nuclear Dorsal concentrations are activated or inhibited respectively, thereby establishing the different embryonic fates mesoderm (ventral), neurogenic ectoderm (ventrolateral), dorsal- or non-neurogenic ectoderm (dorsolateral) and amnioserosa (dorsal) (Fig. 1.3).

Depending on their domains of expression and their threshold-dependent responsiveness to nuclear Dorsal, these target genes have been subdivided into three categories (Type-I, II and III). Type-I target genes like the transcription factors *twist (twi)* and *snail (sna)* require high nuclear dorsal concentrations to be activated since they have low affinity binding sites in their enhancers. Those genes are expressed on the ventral side, where their activity specifies the mesodermal fate. Type-II genes like *ventral nervous system defective (vnd)* and *intermediate neuroblasts defective (ind)* possess enhancer-binding sites, which respond to intermediate to low levels of nuclear Dorsal and therefore they are expressed in ventrolateral to lateral regions. They specify the neuroectoderm or ventral ectoderm. Type-III genes like *short gastrulation (sog)* and *zerknüllt (zen)* have enhancers with high affinity Dorsal binding sites. They are further subdivided into genes that are activated (Type-III<sup>+</sup>, e.g. *sog*) and repressed (Type-III<sup>-</sup>, e.g. *zen*) by Dorsal (Reeves et al., 2012).

On the dorsal side, in the absence of Dorsal activity, BMP signaling is active. In the early blastoderm embryo, the BMP ligand Dpp establishes an activity gradient with several zones of dose-dependent gene activation that subdivides the dorsal embryo hemisphere into dorsal ectoderm and presumptive amnioserosa (Ashe et al., 2000; Ferguson and Anderson, 1992a, 1992b; Ray et al., 1991; Wharton et al., 1993). The Dorsal and BMP dependent regulation of target genes is described in more detail in chapter 2.1.

#### 1.4.5 The BMP pathway

Like the Toll signaling cascade, BMP signaling is highly conserved and found throughout the whole animal kingdom (Kingsley, 1994). BMPs (Bone Morphogenic Proteins) are members of the TGF- $\beta$  superfamily. They are involved in the development of almost all tissues and organs (Hogan, 1996). In vertebrates BMP-2 and BMP-4 have been described to have anti-neuralizing effects (Mizutani and Bier, 2008). As extracellular ligand BMP-2/4 binds to a tetrameric receptor complex, composed of dimers of type-I and type-II transmembrane serin/threonine kinases (Massagué, 1998; Yamashita et al., 1996). The intracellular kinase of the receptor phosphorylates members of the SMAD protein family. There are three subclasses of SMADs (Attisano and Wrana, 1998; Kretzschmar and Massagué, 1998; Whitman, 1998): receptor-regulated SMADs (R- SMADs) are directly phosphorylated by type-I receptors and form complexes with common SMADs (Co-SMADs) or inhibitory SMADs (Anti-SMADs/I-SMADs), which compete with Co-SMADs to bind R-SMADs (Hayashi et al., 1997; Imamura et al., 1997; Massagué et al., 2005; Nakao et al., 1997; Nakayama et al., 2000; Tsuneizumi et al., 1997). SMADs are characterized by an amino-terminal Mad homology 1 (MH1) and a carboxyl-terminal MH2 domain (Kretzschmar and Massagué, 1998). Both domains are important for protein-protein interaction and DNA binding (Schmierer and Hill, 2007). In response to receptor mediated phosphorylation, SMADs form a heterotrimer of two R-SMADs and one Co-SMAD (Lagna et al., 1996; Zhang et al., 1997). This complex translocates into the nucleus where it facilitates transcriptional activation of target genes (Fig. 1.4) (Dennler et al., 1998; Derynck and Feng, 1997; Jonk et al., 1998).

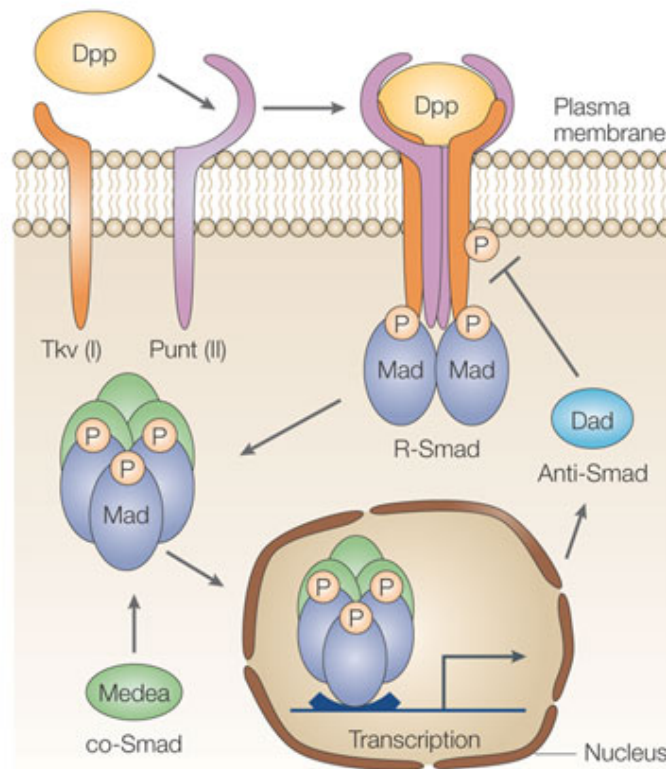


**Figure 1.4 The transforming growth factor- $\beta$  (TGF- $\beta$ )–Decapentaplegic (Dpp) pathway**

Extracellular interaction of the TGF- $\beta$  ligand Decapentaplegic (Dpp) to transmembrane serine/threonine kinases called type-I receptor (Thickveins, Tkv) and type-II receptor (Punt) results in the formation of a tetrameric complex. The type-I receptor transduces the signal by phosphorylating the R-SMAD Mothers against Dpp (Mad), a cytoplasmic transcription factor. Phosphorylated Mad associates with Co-SMAD Medea. R-SMADs and Co-SMADs translocate to the nucleus where they can bind to DNA and regulate the transcription of target genes. Receptor mediated phosphorylation of Mad is antagonized by the I-SMAD Daughters against Dpp (Dad). (Häcker et al., 2005)

In the early *Drosophila* embryo, the BMP-2/4 homolog Decapentaplegic (Dpp) establishes a morphogen gradient on the dorsal side. Dpp binds as ligand to a dimer consisting of the type-I receptor Thickveins (Tkv) or Saxophon (Sax) and the type-II receptor Punt (Put). Receptor activation propagates the generation of an intracellular heteromer of the R-SMAD Mad (Mothers Against Dpp) and the Co-SMAD Medea (Das et al., 1998; Hudson et al., 1998; Wisotzkey et al.,



1998). The complex translocates to the nucleus, where it activates genes like *zerknüllt* (*zen*) that are important for the specification of dorsal ectoderm and amnioserosa (Fig. 1.4).

The peak level of Dpp signaling is stabilized via an inverse gradient of the laterally expressed Chordin homolog Short gastrulation (*Sog*) (Fig. 1.5) (François and Bier, 1995; Srinivasan et al., 2002). Activation of *sog* expression is under direct control of Dorsal. *Sog* protein is secreted and diffuses dorsally, thereby generating a gradient. On its way to the dorsal side it concurrently binds the ventrally diffusing BMP receptor ligand Dpp, transporting it towards the dorsal midline. There, *Sog* releases Dpp after it is cleaved by the dorsally expressed metalloprotease Tolloid (Fig. 1. 5) (Ashe and Levine, 1999; Biehs et al., 1996; Marqués et al., 1997; Shimell et al., 1991).

In addition, the laterally expressed Dorsal target gene *brinker* (*brk*) acts parallel as a specific transcriptional repressor of low and intermediate level Dpp target genes (Jaźwińska et al., 1999). Thus, via the *brk* and *sog* mediated inhibition, Toll signaling regulates the BMP gradient.

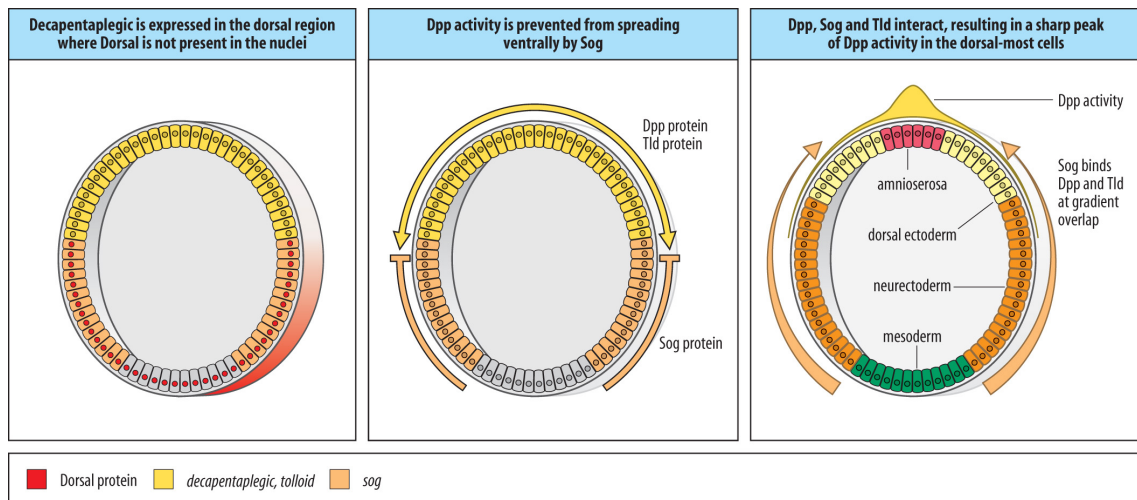


**Figure 1.5 Establishment of Dpp peak levels requires Toll dependent Sog transport**

**Left panel:** Nuclear Dorsal Protein activates the type-III gene *short gastrulation (sog)*, which encodes the secreted Protein Sog. Throughout the dorsal side *decapentaplegic (dpp)* is expressed, which also encodes a secreted protein, Dpp. *tolloid (tld)*, which encodes a metalloprotease is co-expressed with *dpp*. **Middle Panel:** Dpp protein generates a dorsal to ventral gradient while Sog protein generates an inverse ventral to dorsal gradient. Where Sog meets Dpp, it binds it and thus prevents Dpp interacting with its receptors. **Right panel:** Dpp bound by Sog is transported towards the dorsal side by the developing Sog gradient, thereby concentrating its activity in a sharp peak in the dorsal most region. Tld protein binds to the Sog-Dpp complex and cleaves Sog, which releases Dpp and enables it to bind to its receptors. The interaction of Sog, Dpp and Tld subdivides the dorsal region into a region of high Dpp signaling (amnioserosa) and a zone of lower Dpp signaling (dorsal ectoderm) (Wolper et al., 2007)

## 1.5 The DV axis in the beetle *Tribolium castaneum*

The above described dorsal-ventral gene network of *Drosophila melanogaster* (*Dm*) has been studied in detail and belongs to the best-understood GRNs.

However, in recent years it became apparent that highly derived mechanisms of *Drosophila* embryogenesis are only partially conserved.

*Drosophila* development uses a long germ mode of embryogenesis, where all segments along the AP and DV axis are established simultaneously (Davis and Patel, 2002). This long germ mode of embryogenesis is only found in holometabolous insects and for that reason considered a derived mode of embryogenesis. All hemi- and only some holometabolous insects go through a short germ mode of embryogenesis where initially only anterior segments are

established and subsequently developing segments derive from a posterior growth zone (Davis and Patel, 2002).

It was shown that the hierarchical adjustment of the *Drosophila* GRN where the Toll dependent signaling cascade serves as sole inductor for DV axis polarization in the early blastoderm (Anderson et al., 1985a, 1985b) is not representative for more basally branching insects like the beetle *Tribolium castaneum* (*Tc*) (Nunes da Fonseca et al., 2008). Studies on the short germ embryo of *Tribolium* revealed interesting similarities to *Drosophila*, however, also differences.

The *Tribolium* dorsal-ventral GRN comprises many components homologous to *Drosophila* (Lynch and Roth, 2011). Nevertheless, the GRN of *Tribolium* differs in its basic mechanism. Unlike *Drosophila*, where the unidirectional Toll signaling cascade dictates the expression boundaries of downstream targets through a stable nuclear Dorsal gradient, the *Tribolium* network is organized in self-regulatory circuits, where the nuclear Dorsal gradient is regulated by feedback loops. Studies on *Tribolium* revealed that *Tc*-Dorsal similar to *Dm*-Dorsal activates downstream target genes like *twist*, *snail* and *vnd* (Nunes da Fonseca et al., 2008). However, in contrast to *Drosophila*, *Tc* Dorsal also controls transcription of its own upstream activator *Tc*-Toll as well as its own inhibitor *Tc*-Cactus (Nunes da Fonseca et al., 2008). So, instead of a stable morphogen gradient, as observed in *Drosophila*, this feedback regulation results in a dynamic nuclear Dorsal gradient (Chen et al., 2000; Kanodia et al., 2009; Liberman et al., 2009). Initially, a broad domain of nuclear Dorsal is formed in the early blastoderm embryo. This domain rapidly shrinks during successive nuclear cycles to a narrow stripe on the ventral side before it disappears prior to the onset of gastrulation (Chen et al., 2000).

Additionally, *Tribolium* embryos lacking Toll signaling display a zygotic DV patterning system that involves the BMP homolog *decapentaplegic* (*Tc-dpp*), indicating a Toll-independent second level of self-organized patterning (Nunes da Fonseca et al., 2008). In *Drosophila* *Bmp/dpp* signaling and especially the maintenance of its peak levels on the dorsal side is a result of Toll mediated

inhibition (see chapter 1.4.4 and 1.4.5). Thus, the hierarchical nature of Toll signaling and its dominance in early axis determination, is not conserved within the insect clade.

### 1.6 The wasp *Nasonia vitripennis*

Initially, the Toll pathway and its role in dorsal-ventral pattern formation has been identified in a saturation mutagenesis screen performed by C. Nüsslein-Volhard and E.F. Wieschaus (Anderson et al., 1985a; Schüpbach and Wieschaus, 1989). Later studies revealed the role of Toll signaling in innate immunity (Lemaitre et al., 1996). In the following it was shown, that Toll's participation in immune response constitutes the conserved function of the pathway, whereas its role in DV axis formation and in particular its dominance in DV axis formation of *Drosophila* seems to be a derived function. So far, Toll signaling has not been observed to play a role in body axis formation outside the insect phyla, (Lynch and Roth, 2011). Instead, BMP signaling is most commonly used (Robertis, 2008). Due to this observation it is reasonable, that DV axis polarization of the prototype bilateria (the last common ancestor of insects and other bilateria) was induced by BMP and during insect evolution a switch in the regulation of the GRN from a BMP-only to a Toll-dominated mechanism has occurred.

In spiders, which represent an arthropod outside the insect phylum, Toll signaling does not seem to play a role in body axis formation (M. Pechmann unpublished data). However, it has been shown that *sog* and *dpp* are required for axis specification (Akiyama-Oda and Oda, 2006).

One of the more recent model organisms, *Nasonia vitripennis*, represents an interesting starting point for analyzing the evolution of DV axis formation within the insect phylum. *Nasonia's* phylogenetic position on the base of the holometabola (Savard et al., 2006) makes it an appealing candidate for reconstructing features of the ancestral DV patterning mechanism within the insects. Another interesting aspect is *Nasonia's* similarity to *Drosophila* concerning its mode of embryogenesis. *Nasonia* has a drosophila-like, however,

independently derived long germ mode of embryogenesis (Lynch et al., 2012). Hence, *Nasonia* might answer questions about which characteristics of the *Drosophila* DV patterning system is due to its mode of embryogenesis. Furthermore, the *Nasonia* genome is sequenced and annotated (Werren et al., 2010), which makes it an ideal candidate for direct comparison to *Drosophila*. Especially, with regard to functional analyses since the *Nasonia* genome is amenable to parental RNA interference (pRNAi) (Lynch and Desplan, 2006).

### **1.7 Objectives**

The aim of this project was the analysis of the GRN that establishes the DV axis in the early embryo of *Nasonia vitripennis*. The focus was the investigation of the Toll/NF- $\kappa$ B signaling pathway.

## 2 Publications & Manuscripts

### 2.1 Patterning the dorsal-ventral axis of the wasp *Nasonia vitripennis*

Developmental Biology 381 (2013) 189–202



Contents lists available at ScienceDirect

Developmental Biology

journal homepage: [www.elsevier.com/locate/developmentalbiology](http://www.elsevier.com/locate/developmentalbiology)



### Patterning the dorsal–ventral axis of the wasp *Nasonia vitripennis*



Thomas Buchta<sup>a,1</sup>, Orhan Özüak<sup>a,1</sup>, Dominik Stappert<sup>a</sup>, Siegfried Roth<sup>a,\*</sup>,  
Jeremy A. Lynch<sup>a,b,\*\*</sup>

<sup>a</sup> Institute for Developmental Biology, University of Cologne, Zùlpichstrasse 47b, 50674 Cologne, Germany

<sup>b</sup> Department of Biological Sciences, University of Illinois at Chicago, 900S Ashland Ave., Chicago, IL 60607, USA

#### ARTICLE INFO

Article history:  
Received 29 November 2012  
Received in revised form  
14 May 2013  
Accepted 24 May 2013  
Available online 2 June 2013

Keywords:  
Nasonia  
Tribolium  
Fate map  
Dorsal–ventral patterning  
Mesoderm  
Extraembryonic  
Patterning  
Embryo

#### ABSTRACT

Regulatory networks composed of interacting genes are responsible for pattern formation and cell type specification in a wide variety of developmental contexts. Evolution must act on these regulatory networks in order to change the proportions, distribution, and characteristics of specified cells. Thus, understanding how these networks operate in homologous systems across multiple levels of phylogenetic divergence is critical for understanding the evolution of developmental systems. Among the most thoroughly characterized regulatory networks is the dorsal–ventral patterning system of the fly *Drosophila melanogaster*. Due to the thorough understanding of this system, it is an ideal starting point for comparative analyses. Here we report an analysis of the DV patterning system of the wasp, *Nasonia vitripennis*. This wasp undergoes a mode of long germ embryogenesis that is superficially nearly identical to that of *Drosophila*, but one that was likely independently derived. We have found that while the expression of genes just prior to the onset of gastrulation is almost identical in *Nasonia* and *Drosophila*, both the upstream network responsible for generating this pattern, and the downstream morphogenetic movements that it sets in motion, are significantly diverged. From this we conclude that many network structures are available to evolution to achieve particular developmental ends.

© 2013 Elsevier Inc. All rights reserved.

#### Introduction

All bilaterally symmetric animals face the problem of setting up two orthogonal body axes during embryogenesis. The mechanisms employed in these processes are variable across evolutionary time, with embryological and environmental factors influencing the strategies employed in various lineages. In order to understand how axis determination and patterning processes can change in the course of evolution, a comparative approach that incorporates highly detailed descriptions of homologous developmental processes is required. The establishment and patterning of the dorsal–ventral axis of the fruit fly *Drosophila melanogaster* is one of the most thoroughly described embryonic patterning systems among the bilateria, and thus serves as a valuable point of comparison for studies focused on the evolution of patterning processes.

The chain of events that leads to cell fate determination along the DV axis of the *Drosophila* (and other insects (Lynch et al., 2010)) embryo begins in the ovary (reviewed in (Roth and Schùpbach, 1994)). Here, *gurken* mRNA localized anteriorly and

asymmetrically with regard to the short axis of the oocyte, leads to the localized activation of EGF signaling in the overlying follicle cells, and this signal specifies the future dorsal side of the egg (Neuman-Silberberg and Schùpbach, 1993; Roth, 2003). EGF signaling also precisely restricts the expression of the sulfotransferase *pipe* to the ventral follicle cells, which in turn leads to a localized activation of a protease cascade in the perivitelline space (Sen et al., 1998; Cho et al., 2010). The outcome of the activated protease cascade is the graded cleavage, and thus activation, of the Toll ligand Spätzle (Spz) in the ventral half of the perivitelline space (Moussian and Roth, 2005).

In the early embryo, cleaved Spz protein binds the maternally provided Toll receptor present in the plasma membrane. Upon Toll activation by Spz the IκB homolog Cactus (Cact) becomes phosphorylated and degraded, which in turn leads to the release and translocation of the NF-κB transcription factor Dorsal to the nucleus, creating a stable DV gradient of nuclear Dorsal with peak levels at the ventral midline (Moussian and Roth, 2005). Dorsal acts as a morphogen, directly regulating around 50 genes in a concentration dependent manner (Stathopoulos et al., 2002; Hong et al., 2008).

Dorsal target genes contain enhancers that vary in the number, affinity, and arrangement of Dorsal binding sites and determine their sensitivity to nuclear Dorsal concentrations (Stathopoulos and Levine, 2004; Hong et al., 2008). The expression of genes with

\* Corresponding author.

\*\* Corresponding author.

E-mail addresses: [siegfried.roth@uni-koeln.de](mailto:siegfried.roth@uni-koeln.de) (S. Roth),

[jlynch42@uic.edu](mailto:jlynch42@uic.edu) (J.A. Lynch).

<sup>1</sup> These authors contributed equally.

enhancers containing low affinity Dorsal binding sites can only be activated by high levels of nuclear Dorsal, and are thereby restricted to the ventral region of the embryo. Examples are genes like *twist* and *snail*, which are involved in the specification and morphogenesis of mesoderm. Genes such as *ventral neuroblasts defective (vnd)* and *brinker (brk)* that react to moderate and low nuclear Dorsal concentrations are characterized by enhancers containing high affinity Dorsal binding sites in combination with binding sites for bHLH, Suppressor of Hairless and/or ETS domain transcription factors. They have lateral, stripe like expression domains, due to repression by Snail ventrally. Finally, genes like *short gastrulation (sog)* and *zerknuellt (zen)*, that react to low levels of Dorsal, are characterized by enhancers containing high affinity Dorsal binding sites with either activating (e.g. *sog* enhancer) or repressing influence (e.g. *zen* enhancer) depending on the presence of closely linked co-activator or co-repressor binding sites, respectively (Rusch and Levine, 1996; Reeves and Stathopoulos, 2009).

Several Dorsal target genes are transcription factors that interact with each other and which further refine and elaborate the expression of downstream target genes. Dorsal not only patterns the ventral and lateral parts of the *Drosophila* embryo, but also plays a major role in regulating the BMP signaling pathway, which patterns the dorsal half of the embryo. By activating the BMP inhibitor *sog* in a broad lateral domain and repressing the BMP2/4-like ligand *decapentaplegic (dpp)* and the metalloprotease *tolloid (tld)* in the ventral half of the embryo, Dorsal facilitates the establishment of a gradient of BMP activation with a sharp peak at the dorsal midline (O'Connor et al., 2006).

Although the *Drosophila* DV patterning system is one of the best understood gene regulatory networks (GRNs), and thus is the gold standard to which other insects will be compared, the fly is not typical of insects in many respects. It shows highly derived features and undergoes a long germ mode of embryogenesis, which is only found among holometabolous insects. In this type of embryogenesis all segments are specified simultaneously within the blastoderm stage embryo (Davis and Patel, 2002). In contrast, all hemimetabolous and some holometabolous insects, such as the beetle *Tribolium castaneum*, undergo a short germ mode of embryogenesis. In this mode of embryogenesis only the head and thoracic segments are specified prior to gastrulation, while the remaining segments are generated and patterned progressively after gastrulation (Davis and Patel, 2002). Thus, short germ patterning requires at least two steps in DV patterning: one acting at the blastoderm stage which partitions the head and thoracic segments, and a second one being active in the post-gastrulation growth zone.

The Dorsal protein of *Tribolium* (Tc-Dorsal), like its *Drosophila* counterpart, forms a gradient during early embryogenesis, and is involved in patterning cell fates along the DV axis of the early embryo (Chen et al., 2000; Nunes da Fonseca et al., 2008). However, the function of Tc-Dorsal differs from that of fly Dorsal in two fundamental ways. First, the Tc-Dorsal gradient is dynamic over developmental time, while the shape of the *Drosophila* gradient is relatively stable (Chen et al., 2000; Kanodia et al., 2009; Liberman et al., 2009). The domain of nuclear Tc-Dorsal is initially weak and shallowly graded, then progressively shrinks to form a steeply graded stripe straddling the ventral midline, before finally disappearing completely just prior to gastrulation. The dynamics of the Tc-Dorsal gradient are a result of a feedback loop of zygotic target genes of Tc-Dorsal, which include both its upstream activating receptor Tc-Toll, and its inhibitor, Tc-Cactus (Nunes da Fonseca et al., 2008). *Tc-Toll*, *Tc-cactus*, and at least one additional zygotic target of Tc-Dorsal (*Tc-twist*) are expressed in dynamic patterns that seem to follow the changes in the Tc-Dorsal gradient (Nunes da Fonseca et al., 2008).

A second difference between the fly and beetle systems is that Tc-Dorsal is only directly involved in specifying cell fates along the DV axis in a fraction of the embryo, since the Tc-Dorsal nuclear gradient is only present prior to gastrulation, and does not operate in the growth zone (Chen et al., 2000). In contrast, fly Dorsal assigns DV cell fates to all segmental primordia prior to gastrulation.

These differences between *Tribolium* and *Drosophila* Dorsal function lead to questions about which characteristics of the *Drosophila* DV patterning system are due to its mode of embryogenesis, and which characteristics of the *Tribolium* system are truly representative of the ancestral mode for insects.

To begin to address these questions, we have initiated an examination of the DV patterning process of the wasp *Nasonia vitripennis*. This wasp has a mode of long germ embryogenesis similar to, but independently derived from, that of the fly, which makes it an ideal model for understanding the patterning requirements for long germ embryogenesis (Lynch et al., 2012). On the other hand, it is a member of the Hymenoptera, the most basally branching order of the Holometabola (fully metamorphosing insects), and *Nasonia* thus represents a key phylogenetic sampling point for reconstructing features of the ancestral DV patterning mechanism within this clade (Lynch et al., 2012).

To fully understand how establishment and patterning of the DV axis come about at a functional level, the process must first be well described observationally. Only after such a thorough description can perturbations of the system be robustly interpreted. Thus, to provide a basis for future functional experiments, and to gain insights into how DV axial patterning comes about in *Nasonia*, we have cloned and analyzed the expression of *Nasonia* orthologs of *Drosophila* DV marker genes covering the entire embryonic axis. We have found that the expression patterns of these genes just prior to gastrulation are highly similar between *Nasonia* and *Drosophila*. However, our results also show that some aspects of the gene regulatory networks both upstream and downstream of this conserved arrangement have diverged significantly between the wasp and the fly. Finally, incorporation of gene expression data from the beetle *Tribolium* into this comparative work has shed light onto features and components of DV patterning that were likely present in the last common ancestor of the Holometabola.

## Results

### Characterization of early *Nasonia* embryogenesis

In order to best be able to interpret the dynamics of gene expression, the process of *Nasonia* embryogenesis needed further characterization. We took two approaches to this end. One was timed egg collections and DAPI staining to characterize the stages present at different time points at 29 °C (the temperature at which embryos were laid and incubated) (Fig. S1). The other was to take advantage of the optically clear embryo of *Nasonia* to make time lapse DIC movies of embryogenesis (supplemental movie 1). These two approaches were complementary, and led us to the same conclusions about early *Nasonia* embryogenesis, that were generally consistent with previous work (Bull, 1982). Like *Drosophila*, there are rapid, synchronous syncytial divisions of nuclei before the onset of gastrulation. In *Nasonia*, there are 12 of these divisions, rather than 13 observed in *Drosophila*. The initial pole cell bud occurs after 6 divisions (02:00, supplemental movie 1), one cycle prior to the appearance of the rest of the nuclei on the egg surface (02:20, supplemental movie 1). This is in contrast to *Drosophila*, where the pole cells form simultaneously with the arrival of nuclei to the embryo surface.

Supplementary material related to this article can be found online at doi:10.1016/j.ydbio.2013.05.026.

Once nuclei have arrived at the egg surface, they undergo 5 division cycles of increasing duration. Once the 12th division has been completed, there is a long period before gastrulation (~1 h), during which membrane furrows form between the nuclei, and a clear boundary forms between the nuclei and the yolk sac, completing the process of cellularization (07:00, supplemental movie 1). Once this boundary is completed the embryo begins the process of gastrulation with the mesoderm internalizing ventrally starting at the anterior, and progressing posteriorly, and the posterior gut invaginating posterior-dorsally. As these processes complete, cells on the dorsal side differentiate and migrate ventrally over the ectoderm, forming the serosa (onset at 09:00, supplemental movie 1). All of these morphogenetic movements are distinct from equivalent events occurring in the *Drosophila* embryo (see Discussion).

These observations were made with embryos deriving from both mated and virgin females, which should give rise to mostly female embryos, and all male embryos, respectively. We could not detect any differences between male or female embryos in our time lapse, or in our DAPI analyses. This was somewhat surprising, since in *Drosophila*, haploid embryos undergo an additional, and triploid embryos undergo one less, division cycle prior to gastrulation (Erickson and Quintero, 2007). It may be that since *Nasonia* is obligately haplodiploid, it has developed means to ensure a consistent number of blastoderm nuclei prior to gastrulation between the sexes.

Aside from the morphological movements, the structure of the blastoderm and the arrangement of cell fates prior to gastrulation appear to be almost identical between *Nasonia* and *Drosophila* as described above. Since this similarity is likely due to convergent evolution, it is of interest to compare the molecular patterning processes occurring during this time. We have identified and examined *Nasonia* orthologs of genes known to play a crucial role in DV patterning in other insects, and examined their expression to understand how the mesoderm (ventral region), ectoderm (lateral regions) and extraembryonic membranes (dorsal region) are specified and patterned.

#### Dynamic gene expression on the ventral side

Two transcription factors, Twist and Snail, are critical factors both in patterning the *Drosophila* DV axis and in specifying the ventral most tissue, the mesoderm (Leptin, 1991). Both of these transcription factors are direct targets of Dorsal, and are expressed in broad overlapping stripes that are initiated weakly and slightly narrower than their broad, largely overlapping final domains (Fig. 1A"–C").

Orthologs of these genes were cloned, and their expression was observed in the blastoderm embryo of *Nasonia*. Like their fly counterparts, both of these genes are expressed ventrally. However the dynamics of their patterns over time are distinct. Both *Nv-twi* and *sna* are initially detected at cycle 11 in very narrow stripes covering 3–4 ventral nuclei (Fig. 1D"). Over the course of cycle 11, *Nv-twi* and *sna* expression domains expand more or less in concert (Fig. 1E"), until they reach their final width (16–17 nuclei) and take on their characteristic "slug" shape in cycle 12 (Fig. 1F"). We do not observe any major differences between patterns of *Nv-sna* and *twi* expression during the dynamic or final domain stages, in contrast to the graded *twi* and extremely sharp "on/off" character of *sna* (Fig. 1C and C') in *Drosophila*. Aside from its expression on the blastoderm, *Nv-sna* is expressed in the yolk nuclei (Fig. 1D"–F").

Given the apparent dynamic nature of the ventral patterning system in *Nasonia*, it was of interest to compare our wasp results

with another system with known dynamic patterning properties: the beetle *T. castaneum*. It is known that the Dorsal gradient and the expression of its early target genes are dynamic in the early *Tribolium* embryo, and it was of interest to determine whether the pattern of simultaneous gene expression in the beetle resembled that of *Nasonia*.

In *Tribolium*, both the temporal and spatial relationship between *Tc-twi* and *Tc-sna* appear to be quite different from that found in either *Nasonia* or *Drosophila*. *Tc-twist* is a very early target of the dynamic Tc-Dorsal gradient, and is first easily detectable as a fairly broad ventral stripe (approximately 9 nuclei wide) expressed over most (Fig. 1G), or the entire length (see Fig. 2G) of the AP axis. This stripe then retracts from the anterior pole, narrows and increases in intensity (Fig. 1H and I). *Tc-sna* expression is not detectable in the early stages of development (Fig. 1G'), and was only seen after *Tc-twi* expression retracts from the anterior pole (Fig. 1H'). *Tc-sna* is not only expressed later, but it is initially expressed in a domain that is significantly narrower than the concurrent *Tc-twi* domain (Fig. 1H"). Prior to gastrulation the *Tc-sna* domain becomes nearly coincident with the slightly broader *Tc-twi* domain (Fig. 1I").

In the course of our analysis of DV marker genes in *Nasonia*, we unexpectedly observed that the temporal and spatial pattern of *Nv-sim* early expression resembled strongly those of *Nv-sna* and *twi*. The *Nv-sim* stripe starts narrowly, just as the *Nv-sna* and *twi* stripes do (Fig. 2D", S2E"), and undergoes expansion and refinement as well. The *Nv-sim* domain is consistently wider than both the *Nv-twi* and *Nv-sna* domains, but is largely coexpressed with the other two markers during cycle 11 and a portion of cycle 12 (Fig. 2D" and E"). In the latter portion of cycle 12 *Nv-sim* begins to clear ventrally (Fig. 2F", S2F"). The end result of this clearing is that *Nv-sim* is no longer co-expressed at any position with *Nv-twi* or *Nv-sna*, and is found in stripes of 1–2 cells wide flanking the domains of the mesodermal genes (Fig. 2F", S2H"). After gastrulation, these stripes will constitute the leading edge of the migrating ectoderm, and eventually fuse, forming the ventral midline (Fig. S3A and B).

The early and dynamic expression of *Nv-sim* is in stark contrast to the pattern of *sim* expression in *Drosophila*. Here, *sim* is not detected prior to cycle 14 (Fig. 2A'), and is initially expressed only in a posterior domain (Fig. 2B'). Only after *sna* and *twi* achieve their final domains, is striped *sim* expression observed (Fig. 2C', S2C'). These stripes emerge somewhat gradually in the cells directly adjacent to the lateral edges of the *sna* domain (Fig. 2B', S2C').

The *Tribolium* mode of generating *sim* stripes contains elements of both the *Nasonia* and *Drosophila* systems, but also differs from both. Like *Drosophila*, *Tc-sim* expression is initiated well after the first appearance of a ventral *Tc-twi* domain (Fig. 2G"). Like *Nasonia*, *Tc-sim* appears at a slightly later stage and is expressed in a stripe that is slightly broader than, and completely covering the *Tc-twi* domain (Fig. 2H"). Later, *Tc-sim* is repressed in the most ventral regions, leading to the production of two stripes of 1–4 cells wide flanking the mesoderm (Fig. 2I"). The clearing of *Tc-sim* from the ventral region seems to be correlated with the onset of *Tc-sna* expression (Fig. S2K"–M"), in contrast to *Nasonia*, where *Nv-sim* and *Nv-sna* are initially completely overlapping ventrally (Fig. S2E).

In *Tribolium*, the *cactus* gene was an important marker that gave great insight into how the dynamic, self-regulatory DV patterning system functions in the beetle embryo. It is initially expressed very broadly, then narrows progressively over time, mimicking the pattern of nuclear Tc-Dorsal (Nunes da Fonseca et al., 2008). Given the apparent dynamic nature of ventral patterning in *Nasonia*, as indicated by the behavior of *Nv-twi*, *Nv-sna*, and *Nv-sim*, it was of interest to determine how the



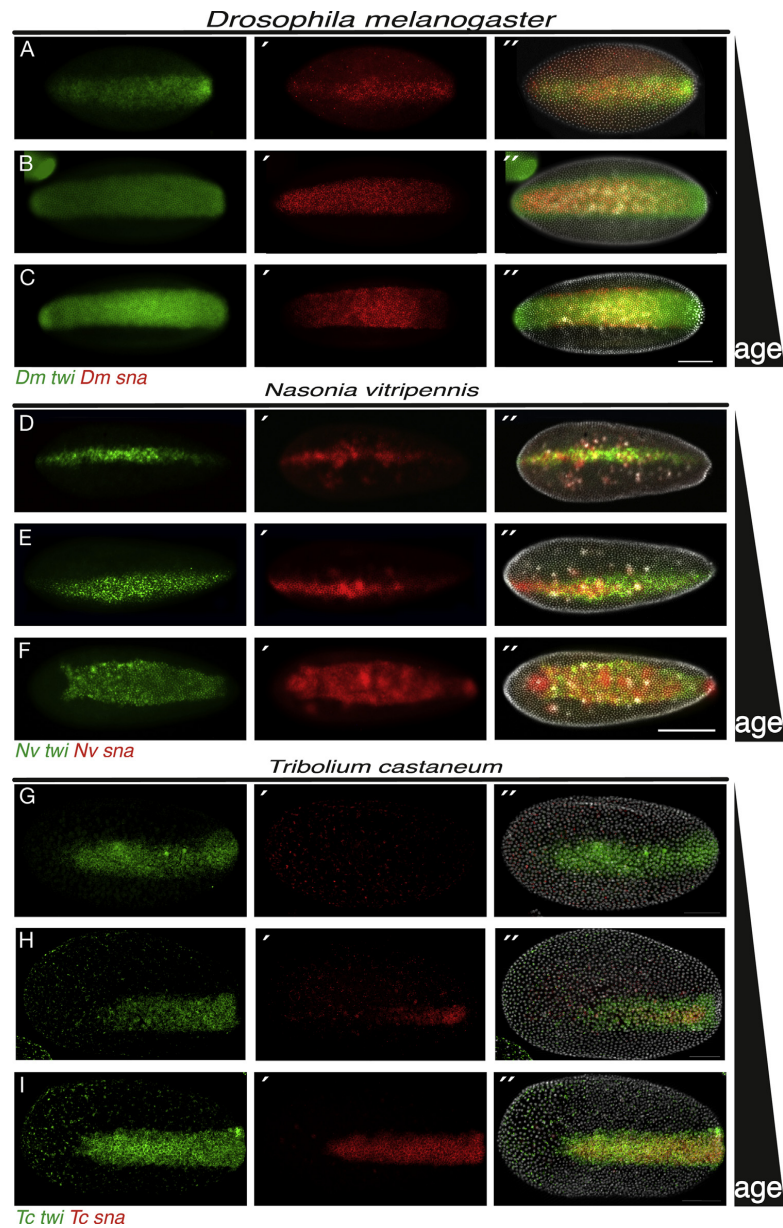


**Fig. 1.** Simultaneous detection of *twist* and *snail* in *Nasonia*, *Drosophila* and *Tribolium* embryos. (A)–(C<sup>''</sup>) Ventral views of *Drosophila* embryos in cycle 13 (A)–(A<sup>''</sup>) and cycle 14 (B)–(B<sup>''</sup>) comparing *Dm-tw1* (A)–(C) and *Dm-sna* (A<sup>''</sup>)–(C<sup>''</sup>). Overlays with DAPI (white) (A<sup>''</sup>)–(C<sup>''</sup>). (D)–(F<sup>''</sup>) Ventral views of *Nasonia* embryos in cycle 11 (D)–(E<sup>''</sup>) and cycle 12 (F)–(F<sup>''</sup>) comparing *Nv-tw1* (D)–(F) with *Nv-sna* (D<sup>''</sup>)–(F<sup>''</sup>). Overlays with DAPI (white) (D<sup>''</sup>)–(F<sup>''</sup>). (G)–(I<sup>''</sup>) Ventral views of *Tribolium* embryos in undifferentiated blastoderm (G)–(G<sup>''</sup>), early differentiated blastoderm (H)–(H<sup>''</sup>) and late differentiated blastoderm (I)–(I<sup>''</sup>) comparing *Tc-tw1* (G)–(I) and *Tc-sna* (G<sup>''</sup>)–(I<sup>''</sup>) expression. Overlays with DAPI (white) (G<sup>''</sup>)–(I<sup>''</sup>). Embryos in panels (A<sup>''</sup>), (D<sup>''</sup>), (E<sup>''</sup>), and (G<sup>''</sup>) are at an equivalent developmental stage (penultimate nuclear division before gastrulation). Embryos in (B<sup>''</sup>), (C<sup>''</sup>), (F<sup>''</sup>), (H<sup>''</sup>), and (I<sup>''</sup>) are also at an equivalent stage in the last division directly preceding gastrulation. Scale bar 100  $\mu$ m. Anterior is left.

*Nasonia cactus* gene behaves in the early embryo, as it could provide insight into the potential for feedback regulation in the *Nasonia* embryo.

In *Nasonia* there are three *cact* paralogs tandemly arrayed in the genome. Only one of these (XM\_001602977) is differentially

expressed along the DV axis. In the early stages, (cycle 11) this gene is expressed in a narrow ventral stripe (Fig. 3A'), similar to the early narrow stripes of *Nv-tw1*, *sna*, and *sim* (Fig. 1D–D', Fig. 2D–D'). In contrast to the other *Nasonia* ventral genes, the *Nv-cact1* expression domain does not expand over the course of development

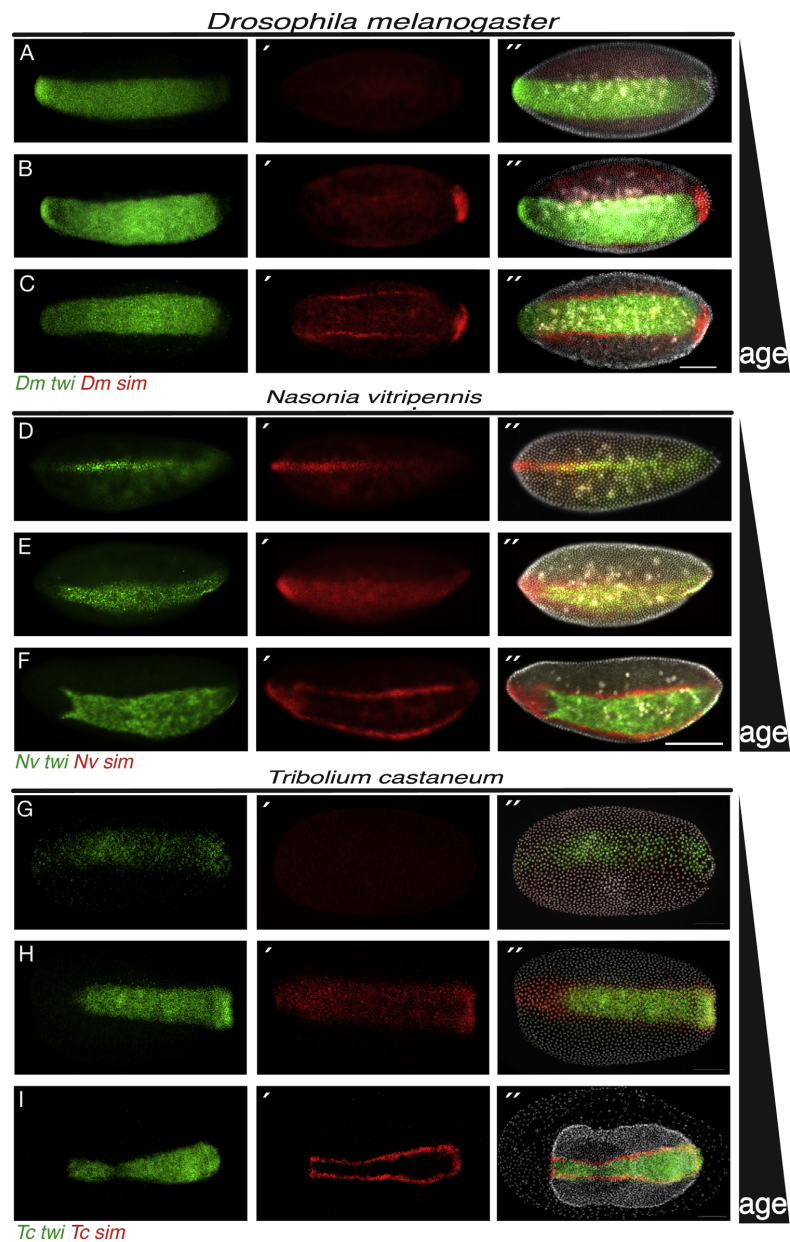


**Fig. 2.** Simultaneous detection of *twist* and *single-minded* in *Nasonia*, *Drosophila* and *Tribolium* embryos. (A)–(C<sup>\*</sup>) Ventral views of *Drosophila* embryos in cycle 14 (A)–(A<sup>\*</sup>) and (B)–(B<sup>\*</sup>) and at initiation of gastrulation (C)–(C<sup>\*</sup>) comparing *Dm-tw1* (A)–(C) and *Dm-sim* (A<sup>\*</sup>)–(C<sup>\*</sup>). Overlays with DAPI (white) (A<sup>\*</sup>)–(C<sup>\*</sup>). (D)–(F<sup>\*</sup>) Ventral views of *Nasonia* embryos in cycle 10 (D)–(D<sup>\*</sup>), cycle 11 (E)–(E<sup>\*</sup>) and cycle 12 (F)–(F<sup>\*</sup>) comparing *Nv-tw1* (D)–(F) and *Nv-sim* (D<sup>\*</sup>)–(F<sup>\*</sup>). Overlays with DAPI (white) (D<sup>\*</sup>)–(F<sup>\*</sup>). (G)–(I<sup>\*</sup>) Ventral views of *Tribolium* embryos in undifferentiated blastoderm (G)–(G<sup>\*</sup>), start of primitive pit formation (H)–(H<sup>\*</sup>) and before serosal window closes (I)–(I<sup>\*</sup>) comparing *Tc-tw1* (G)–(I) and *Tc-sim* (G<sup>\*</sup>)–(I<sup>\*</sup>). Overlays with DAPI (white) (G<sup>\*</sup>)–(I<sup>\*</sup>). Embryos in (A<sup>\*</sup>), (B<sup>\*</sup>), (F<sup>\*</sup>), (H<sup>\*</sup>) are at equivalent stages, while (D<sup>\*</sup>), (E<sup>\*</sup>), and (G<sup>\*</sup>) are at earlier stages, and (C<sup>\*</sup>) and (I<sup>\*</sup>) are at later (post-gastrulation) stages. Scale bar 100  $\mu$ m. Anterior is left.

(Fig. 3B'). Rather, the narrow stripe disappears, leaving two terminal spots at each of the AP poles, during cycle 12, prior to gastrulation (Fig. 3C'). Thus unlike *Tc-cact*, *Nv-cact* is not dynamic in early development, which may have implications for the nature of the Dorsal gradient behavior in *Nasonia*.

#### Lateral markers

The specification and pattern of the neurogenic ectoderm is another function of DV patterning in insect embryos. In *Drosophila*, genes involved in this process are typically expressed in symmetric

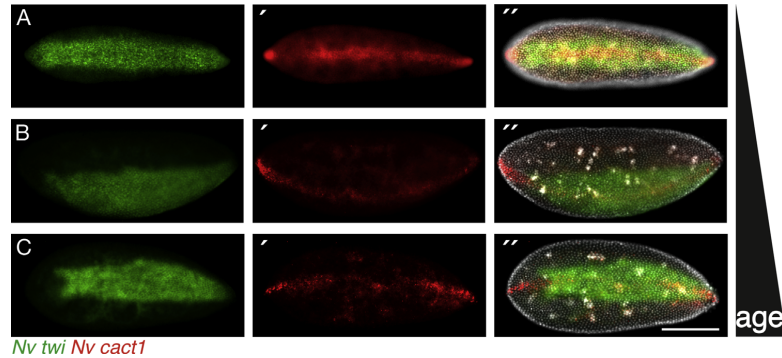


**Fig. 3.** Characterization of the expression and dynamics of *cact* in *Nasonia*. (A)–(A') Ventral view of a *Nasonia* embryo in cycle 11 comparing *Nv-twi* (green) and *Nv-cact1* (red) and DAPI (white). (B)–(B') Ventro-lateral view of a *Nasonia* embryo in cycle 12 comparing *Nv-twi* (green) and *Nv-cact1* (red) and DAPI (white). (C)–(C') Ventral view of a *Nasonia* embryo in late cycle 12 comparing *Nv-twi* (green) and *Nv-cact1* (red) and DAPI (white). Scale bar 100  $\mu$ m. Anterior is left. (For interpretation of the references to color in this figure legend, the reader is referred to the web version of this article.)

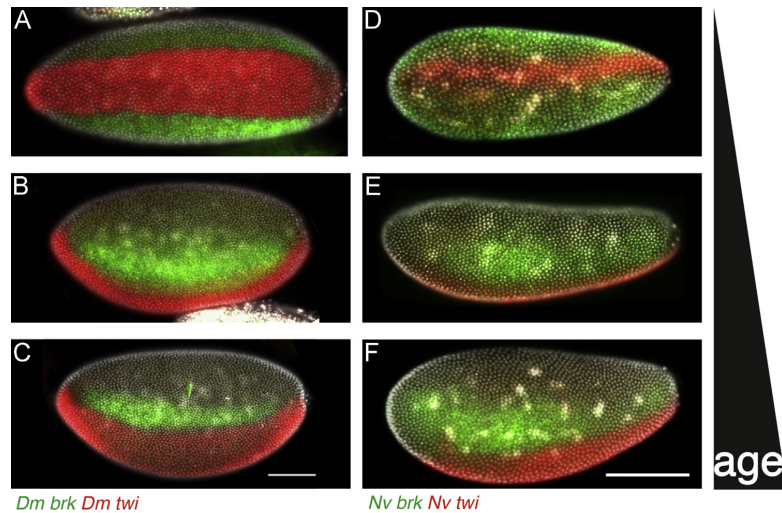


**Fig. 4.** Comparison of *brinker* expression dynamics in *Drosophila* and *Nasonia*. (A) Ventral, and (B) and (C) lateral views of *Drosophila* embryos comparing *Dm-brk* (green) mRNA and *Dm-twi* (red) expression with DAPI (white) in *Drosophila* during cycle 14. (D) Ventral, and (E) and (F) lateral views of *Nv-brk* mRNA expression with DAPI (white) in cycle 10 (D), cycle 11 (E) and cycle 12 (F) in *Nasonia*. Scale bar 100  $\mu$ m. Embryos arranged from youngest to oldest from top to bottom in each species panel. Anterior is left. (For interpretation of the references to color in this figure legend, the reader is referred to the web version of this article.)

lateral stripes, reflecting their activation by low to moderate levels of nuclear Dorsal, as well as repression on the ventral side by Snail. Here three markers of differential fates within the neuroectoderm were examined in *Nasonia*: *ventral neuroblasts defective (vnd)*, *intermediate neuroblasts defective (ind)* and *muscle segment homeobox (msh)* (Von Ohlen and Doe, 2000). In addition, an important specifier of general neuroectoderm fate, *brinker (brk)* was also examined in the wasp.

In *Drosophila*, *brk* (Jaźwińska et al., 1999) is expressed in two lateral stripes with sharp ventral borders adjacent to the mesoderm and with relatively fuzzy dorsal borders extending into the region of the dorsal neurogenic ectoderm (Fig. 4A and B). This pattern is somewhat dynamic, being initially broad (Fig. 4A and B), narrowing early in cycle 14 (Fig. 4C), then expanding again just prior to gastrulation (not shown, (Jaźwińska et al., 1999)).

In *Nasonia*, *Nv-brk* is the only neurogenic gene examined that shows expression at the time when the ventral markers (e.g., *Nv-twi*)

are expressed in early, very narrow stripes (Fig. 4D). At this stage *Nv-brk* is expressed in broad ventro-lateral domains with relatively fuzzy borders on both the ventral and dorsal edges, and is excluded from the domain of the ventral markers (Fig. 4D). As the embryo ages and the expression domain of *Nv-twi* expands, *Nv-brk* expression is correspondingly cleared from the ventral side (Fig. 4E). During this time, the dorsal border of the *Nv-brk* domain becomes more defined, until the domains of *Nv-twi* and *Nv-brk* are very similar to their counterparts in *Drosophila* (Fig. 4C and F).

The neurogenic ectoderm in *Drosophila* is subdivided by a set of factors known as the columnar genes (*vnd*, *ind*, and *msh*, listed in order of expression from ventral to dorsal). *vnd* is a direct target of the Dorsal gradient, is expressed in stripes of 7–8 nuclei (Jiménez et al., 1995) that lie just dorsally to the stripes of *sim* expression, and its expression is stable at the blastoderm stage. Expression can be detected early in cycle 14 in stripes that correspond well with the AP and DV extent of the final domain prior to gastrulation



(Fig. 5A). These stripes intensify and become more refined in the time approaching gastrulation (Fig. 5B and C).

*ind* is expressed just dorsal to *vnd*, in a stripe of approximately the same width, and with limited dynamics (Fig. 5B and C). Like *vnd*, *ind* expression is initiated in a stripe that is complete along the AP axis (Fig. 5B). *ind* initiation occurs later than *vnd*, as we have observed multiple embryos with *vnd* stripes lacking the *ind* domain (Fig. 5A).

In *Nasonia*, the final domain of *Nv-vnd* is also in the form of two broad stripes directly dorsal to the *Nv-sim* domain (not shown). Unlike *Drosophila vnd* and *Nv-brk*, the *Nv-vnd* domain appears relatively late in embryogenesis, just prior to gastrulation. In

addition, *Nv-vnd* expression is dynamic with respect to the AP axis. It is first observed at the anterior in stripes extending to approximately 40% egg length (Fig. 5D). These stripes progressively lengthen over time, finally extending to the posterior pole of the embryo just prior to the initiation of gastrulation (Fig. 5E and F, S3C). During gastrulation, *Nv-vnd* marks most of the ectoderm that migrates over the mesoderm (Fig. S3D). Once gastrulation is completed, *Nv-vnd* is expressed in two stripes flanking the ventral midline (S3E).

*Nv-ind* is initiated later than *Nv-vnd*, and is first detected after the *Nv-vnd* stripe has extended most of the way toward the posterior pole (Fig. 5E). Like *Nv-vnd*, *Nv-ind* expression is also

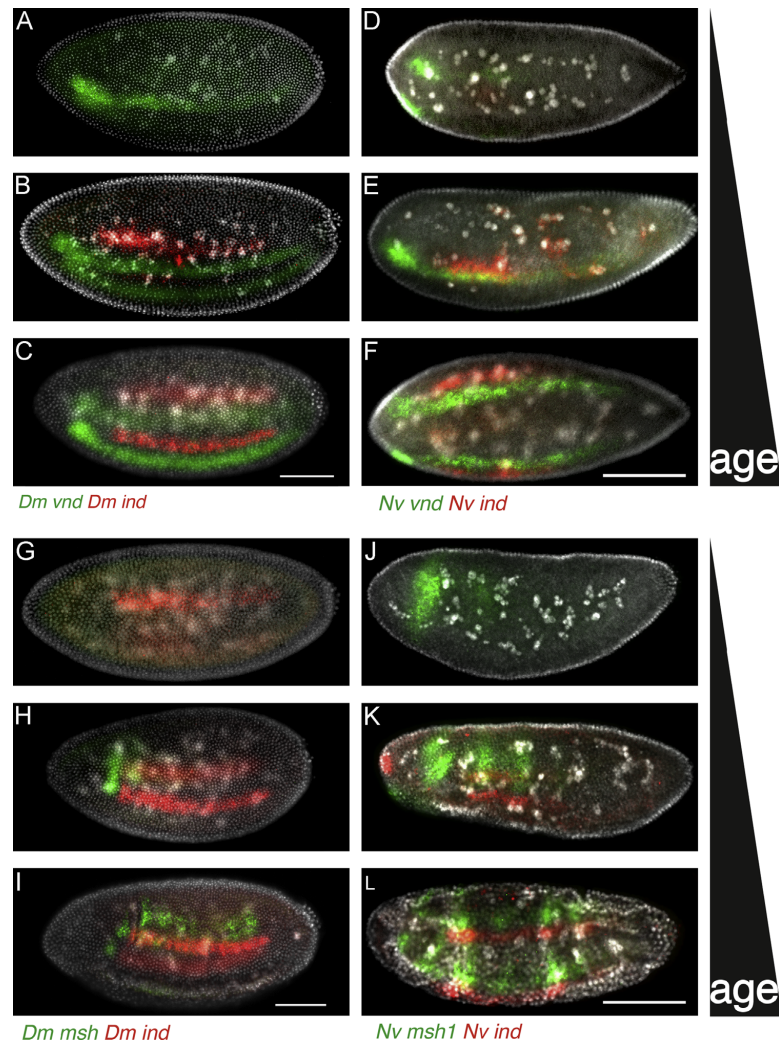


**Fig. 5.** Comparison of columnar gene dynamics in *Drosophila* and *Nasonia*. (A)–(C) Lateral views of *Drosophila* embryos in cycle 14 comparing *Dm-vnd* (green) and *Dm-ind* (red) mRNA expression with DAPI (white) in *Drosophila*. (D) and (E) Lateral and (F) ventral views of *Nasonia* embryos in cycle 11–12 comparing *Nv-vnd* (green) and *Nv-ind* (red) mRNA expression with DAPI (white) in *Nasonia*. (G)–(I) Lateral views of *Drosophila* embryos in cycle 14 (G) and (H) and early gastrulating embryo (I) comparing *Dm-msh* (green) and *Dm-ind* (red) mRNA expression with DAPI (white). (J)–(L) Lateral views of *Nasonia* embryos in cycle 11–12 (J), early gastrulation (K) and ongoing gastrulation (L) comparing *Nv-msh1* (green) and *Nv-ind* (red) mRNA expression with DAPI (white). Scale bar 100  $\mu$ m. Embryos arranged from youngest to oldest from top to bottom in each species panel. Anterior is left. (For interpretation of the references to color in this figure legend, the reader is referred to the web version of this article.)

initially restricted to the anterior portion of the embryo, and then extends over time toward the posterior pole (Fig. 5E, F, K and L). This process of extension is not completed until after gastrulation has been initiated at the anterior of the embryo.

The most dorsally expressed of the *Drosophila* columnar genes is *msh*, which is initiated still later than *ind* (Fig. 5G). The first evidence of *msh* expression is in the form of a stripe in the head region of the embryo, that extends ventrally in nuclei just anterior to the *ind* domain (Fig. 5H). Subsequently to this, a segmentally modulated stripe of *msh* appears dorsally to the *ind* domain (Fig. 5I). Again this stripe appears all at once, with no detectable AP progression.

As is the case in *Tribolium*, there are two *msh*-like genes in the *Nasonia* genome (Wheeler et al., 2005; Nunes da Fonseca et al., 2008). Only one of these genes is expressed in a columnar pattern in *Nasonia*, and we refer to this gene as *Nv-msh1*. *Nv-msh1* expression shares characteristics with both fly *msh* expression, and with the other *Nasonia* columnar genes, but also exhibits some differences. The first evidence of *Nv-msh1* is a stripe covering the dorsal part of the embryonic head anlage, quite similar to that seen in the fly (Fig. 5J). At the time of the appearance of this stripe, a second stripe can be seen arising toward the posterior. This indicates that the initiation of the neurogenic ectoderm domain of *Nv-msh1* occurs prior to the onset of *Nv-ind*, which is in contrast to the pattern observed for both *Drosophila* and *Tribolium ind* and *msh* (Fig. 5K) (Von Ohlen and Doe, 2000; Wheeler et al., 2005). Over time, the full *Nv-msh1* expression domain appears progressively, again, from anterior to posterior, in segmental blocks (Fig. 5K). The full extent of the *Nv-msh1* domain is not completed until well after the initiation of gastrulation (Fig. 5L).

#### Complexity of dorsal ectodermal and extraembryonic patterning

In *Drosophila* a set of genes is expressed in the dorsal part of the embryo that is used to pattern and differentiate the dorsal ectoderm and amnioserosa (the single extraembryonic tissue in the fly embryo) (Ashe et al., 2000). The novelty of the higher dipteran amnioserosa (Schmidt-Ott, 2000) makes a comparison to *Nasonia* dorsal genes significant, as this wasp which exhibits an independently derived mode of long germ embryogenesis, but has been proposed to possess the ancestral complement of extraembryonic tissues (amnion+serosa) (Bull, 1982; Fleig and Sander, 1988). These two tissues have been described to arise from a narrow dorsal domain that is more similar to the fly amnioserosal anlage than to the typical pattern for amnion and serosa specification found in short and intermediate germ insects, such as *Tribolium* (Van der Zee et al., 2005).

The homeodomain transcription factor *zerknüllt* (*zen*) is a highly conserved marker of extraembryonic fate throughout the insects so far examined (Falciani et al., 1996; Dearden et al., 2000; Panfilio et al., 2006). In *Drosophila* it is initially expressed in a very broad domain covering most of the dorsal side of the embryo (Fig. S4A'). This broad domain later resolves into a narrow stripe that corresponds to the future amnioserosal cells (Fig. S4B' and C') (Rushlow et al., 1987).

*Drosophila zen* is part of a BMP signaling dependent gene regulatory network that produces different threshold outputs of gene expression on the dorsal half of the embryo, which leads to the patterning and subdivision of the amnioserosa and dorsal ectoderm. Genes such as *pannier* (*pnr*) are expressed in broad domains covering most of the dorsal surface of the embryo, and respond to the lowest threshold levels of BMP signaling+*zen*

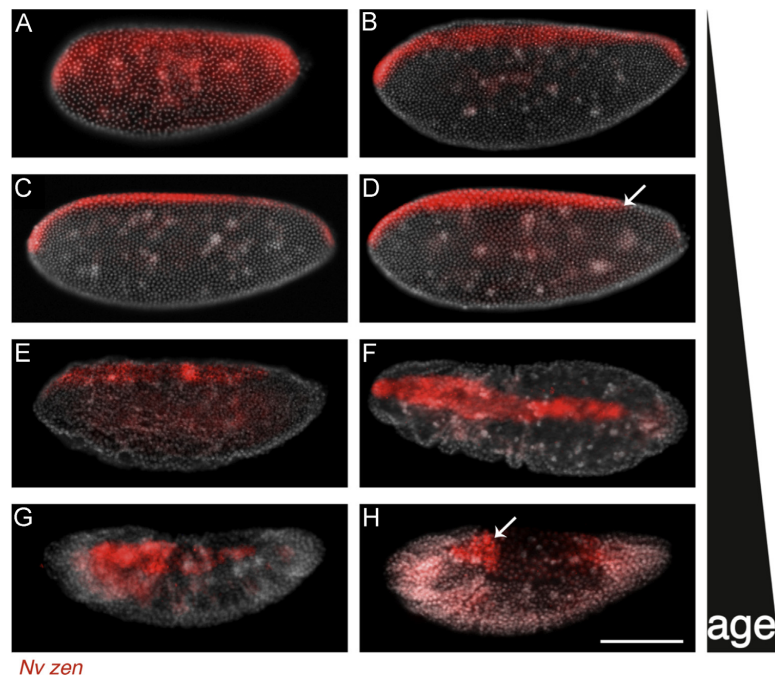


**Fig. 6.** Dynamics of *Nv-zen* expression in *Nasonia* embryos. (A)–(E) Lateral and (F)–(H) dorso-lateral views of *Nasonia* embryos expressing *Nv-zen* with DAPI (white) in cycle 9 (A), cycle 12 (B)–(D), initiation of gastrulation (E), continuation of gastrulation (F), onset of germ band extension (G) and completion of germ band extension (H). Arrow in D indicates retraction of *Nv-zen* on the posterior pole. Arrow in H indicates *Nv-zen* expression in anterior portion of the serosa. Scale bar 100  $\mu$ m. Anterior is left.

(Fig. S5A–C). Genes such as *tail-up* (*tup*) and *dorsocross* (*doc*) respond to moderate to high levels of BMP+Zen (Fig. S6B and C). Peak levels of BMP signaling are required to activate a third class of genes that includes genes such as *RACE* and *hindsight* (*hnt*) (Fig. S4A–C). In other insects, many of these have conserved roles in the amnion and/or serosa (Van der Zee et al., 2006; Goltsev et al., 2007; Rafiqi et al., 2010). We have cloned and analyzed orthologs of the above mentioned genes from *Nasonia* in order to understand the patterning and tissue specification of the extraembryonic membranes and dorsal ectoderm of the wasp.

*Nasonia zen*, like its *Drosophila* ortholog is expressed in a narrow stripe over the dorsal midline in the last nuclear cycle before gastrulation. *Nv-zen* is one of the earliest detectable dorsal genes in the embryo. We have detected it in cycle 9 where it is weakly expressed in a rather broad domain (Fig. 6A). In the next cycle, the *Nv-zen* domain is found in a narrow stripe with fuzzy borders that extends from the extreme anterior to posterior pole (Fig. 6B). After the 12th nuclear division, the *Nv-zen* stripe further refines, gains sharp borders and retracts from the posterior pole (Fig. 6C and D). After gastrulation, *Nv-zen* expression is initially strong, then progressively reduced in the presumptive serosa, with strong staining remaining only in the anterior portion of the tissue (Fig. 6E–H).

*RACE* has a strong requirement both for peak levels of BMP signaling, and for the late phase of narrow zen expression to be fully expressed in the *Drosophila* embryo (Ashe et al., 2000). To determine whether a similar gene regulatory network may be operating in the *Nasonia* embryo, we cloned the *Nasonia* ortholog of this gene, and examined its expression. *Nv-RACE* appears late relative to *Nv-zen*, just before gastrulation, in a stripe that mostly overlaps the *Nv-zen* domain (Fig. 7A"). After gastrulation, *Nv-RACE* expressing cells of the serosa break their epithelial continuity with ectodermal cells, and spread over the surface of the embryo (Fig. S7). The function of *RACE* in the fly amnioserosa is not clear, but our results indicate that this factor was included in the extraembryonic GRN in the common ancestor of the holometabolous insects.

Another high level target of the BMP+Zen GRN in *Drosophila* is *hnt*. This gene is expressed in a narrow stripe similar in width to the zen domain, but restricted to the posterior half of the embryo (Fig. S4C"). *Nv-hnt* is unique among the DV genes examined so far. It is initially detected ubiquitously in embryos at cycle 11 (Fig. 7B) and earlier stages (not shown). In cycle 12, most of the transcript disappears leaving a continuous stripe covering both the ventral and dorsal midlines (Fig. 7C). Eventually, the ventral half of this ring disappears, and what remains is a dorsal narrow stripe that corresponds exactly with the *Nv-zen* domain (Fig. 7D"). Again, this gene remains expressed in the presumptive serosa after gastrulation (not shown).

We examined two *Nasonia* orthologs of genes that respond to moderate levels of BMP+Zen, *Nv-tup* and *Nv-doc*. *tup* is expressed in a moderately broad stripe in *Drosophila*, similar to that of *doc*. In the wasp, however, the *Nv-tup* expression is quite dynamic, and rather different from *Nv-doc*. *Nv-tup* is first detected in spot-like domains just anterior and posterior to the *Nv-zen* expression stripe, just prior to gastrulation (Fig. 8A). As gastrulation proceeds, and the presumptive serosa begins to expand, *Nv-tup* expression becomes localized to the lateral margins of the serosal region, which may represent the *Nasonia* amnion (Fig. 8B and C).

*Nv-doc* also has a rather complex expression pattern in *Nasonia* (Fig. 8D and F). Dorsally, the *Nv-doc* stripe is variable in width. It is broader than the *Nv-zen* domain anteriorly (Fig. 8E"). Starting at about 50% egg length, the *Nv-doc* domain gets narrower than the *Nv-zen* domain. Then, close to the posterior pole, it is wider again. In addition, its domain extends over the extreme anterior pole of the embryo and continues on the ventral side in the presumptive head region (Fig. 8E), unlike most of the dorsally expressed genes that we have examined. This stripe terminates in a broad domain on the ventral side (Fig. 8F).

We next describe the expression of *Nv-pnr*, whose *Drosophila* ortholog is expressed broadly, covering most of the dorsal surface of the embryo (Fig. S5A'). Just before gastrulation, *Nv-pnr* is expressed in a very broad domain straddling the dorsal midline, and extending several cell rows wider than *Nv-zen* (Fig. 9A" and B").

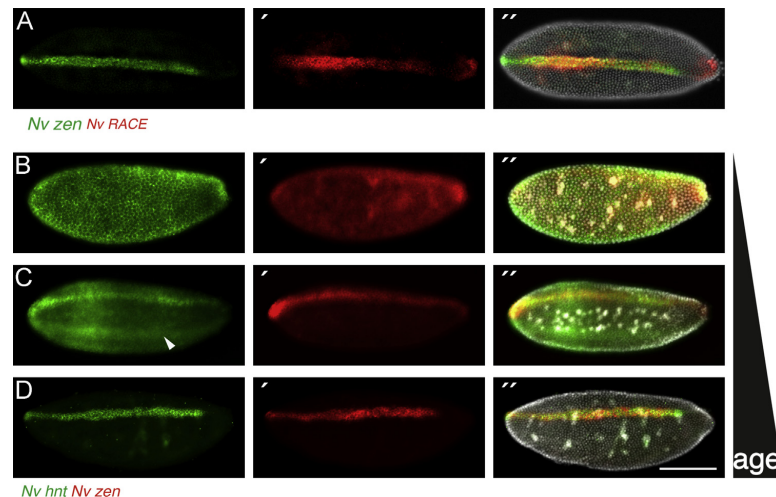


**Fig. 7.** Dynamics of *Nv-RACE* and *Nv-hnt* in relation to those of *Nv-zen*. (A)–(A") Dorsal view of a *Nasonia* embryo between cycle 11 and 12 comparing *Nv-zen* (green) and *Nv-RACE* (red) expression with DAPI (white). (B)–(B") Lateral view of a *Nasonia* embryo in cycle 11–12 comparing *Nv-hnt* (green) and *Nv-zen* (red) expression with DAPI (white). (C)–(C") Dorso-lateral view of a *Nasonia* embryo in cycle 11 comparing *Nv-hnt* (green) and *Nv-zen* (red) expression with DAPI (white). Note the ventral stripe of *Nv-hnt* is still discernable (arrowhead in C), despite being out of focus. Dorsal view of a *Nasonia* embryo in cycle 12 comparing *Nv-hnt* (green) and *Nv-zen* (red) expression with DAPI (white). Scale bar 100  $\mu$ m. Anterior is left. (For interpretation of the references to color in this figure legend, the reader is referred to the web version of this article.)

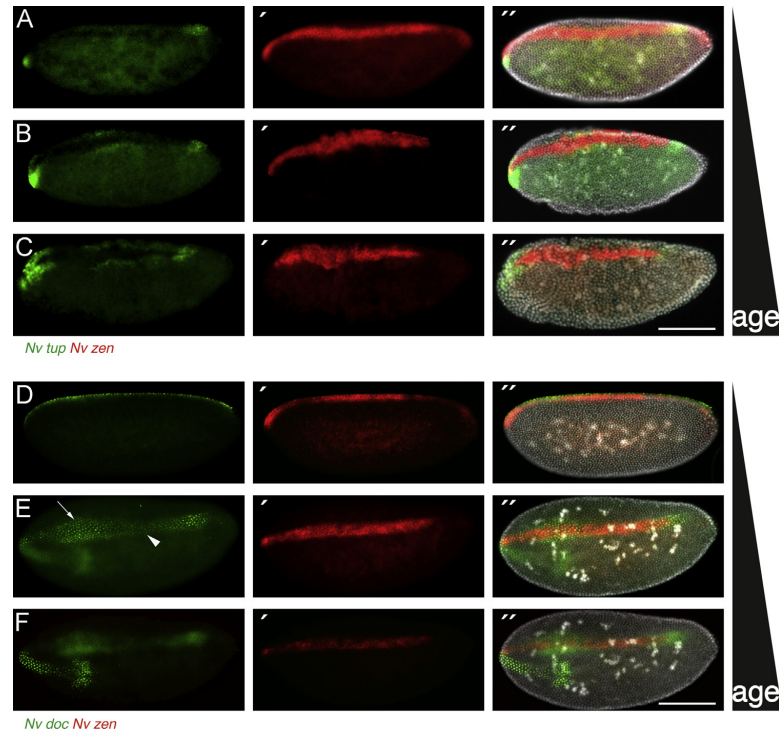


**Fig. 8.** Dynamics of *Nv-tup* and *Nv-doc* in relation to those of *Nv-zen*. (A)–(C) Lateral views of *Nasonia* embryos in cycle 11 (A), at initiation of gastrulation (B) and completion of gastrulation (C) comparing *Nv-tup* (A)–(C) and *Nv-zen* (A)–(C) with DAPI (white). (D)–(D\*) Lateral view of a *Nasonia* embryo in cycle 11 comparing *Nv-doc* (green) and *Nv-zen* (red) with DAPI (white). (E)–(F) Ventro-lateral views of a *Nasonia* embryo in cycle 11–12 comparing *Nv-doc* (green) and *Nv-zen* (red) with DAPI (white) focusing on the dorsal side (E)–(E\*) and ventral side (F)–(F\*). Arrow in E indicates broadened area of *Nv-doc* expression, arrowhead in E indicates narrowed area. Scale bar 100  $\mu$ m. Anterior is left. (For interpretation of the references to color in this figure legend, the reader is referred to the web version of this article.)

As development proceeds, *Nv-pnr* is cleared from the presumptive serosal region, and flanks the expanding *Nv-zen* domain in a very similar way to *Nv-tup* (Fig. 9C”).

Finally, we examined the expression of the single *Nasonia* ortholog of the *Drosophila iro-c* genes *araucan/caupolican* (referred to here as *Nv-ara*). In the fly, these genes are expressed late in the dorsal ectodermal region, but the single *Tribolium* ortholog (referred to as *Tc-iroquois*) has served as a useful marker for the amnion (Nunes da Fonseca et al., 2010). *Nv-ara* expression is first detected in two broad patches toward the posterior end of the embryo that flank the domain of *Nv-zen* (Fig. 9D”). As the embryo nears gastrulation, the stripe-like expression extends anteriorly, until the *Nv-ara* domain completely flanks the presumptive serosa, with the stripes being narrow at the anterior, and becoming quite broad at the posterior (Fig. 9E”). After gastrulation, *Nv-ara* refines to two broad, even stripes flanking the serosa (Fig. 9F”).

## Discussion

With our analyses of time lapse movies and DAPI stainings in *Nasonia* embryos, we have shown that in general the cellular processes leading up to gastrulation are quite similar, with some interesting differences, between *Nasonia* and *Drosophila*. In our gene expression analyses, we have uncovered points of strong convergence between these embryos, and also cases of major

divergence between them in the three main DV domains (ventral (mesoderm), lateral (ectoderm), dorsal (extraembryonic)).

### Ventral side

One of our striking results is the observation that the expression of *Nv-cact1*, *twi*, *sna*, and *sim* all start out as very narrow stripes at the ventral midline. The latter three expand over time until they reach their full domains, while *Nv-cact* remains the same width until it is cleared from most of the ventral side. This result gives some insights into the patterning system operating in the *Nasonia* blastoderm embryo. First, it appears that there is a very restricted peak of initial gene activation in early (cycle 11) embryos, covering only a few nuclei at the ventral midline. The sharp edges of these early stripes indicate that the activation is either very steeply graded with a sharp peak at the ventral side, or that these target genes are exquisitely sensitive to specific threshold levels of activation that are only present in this region (or a combination of both). This differs from *Drosophila*, where the early DV regulated domains of *twi* and *sna* are only slightly narrower, weaker, and more graded than their mature domains, likely reflecting the increasing amplitude of the broad, stably shaped nuclear Dorsal gradient (Lieberman et al., 2009).

The expansion of the *Nv-twi*, *sim*, and *sna* domains from their initial very narrow domains to their broad, final shape indicates that the ventral patterning GRN has strong dynamic, and possibly self-regulatory, properties. In this respect, the *Nasonia* system has



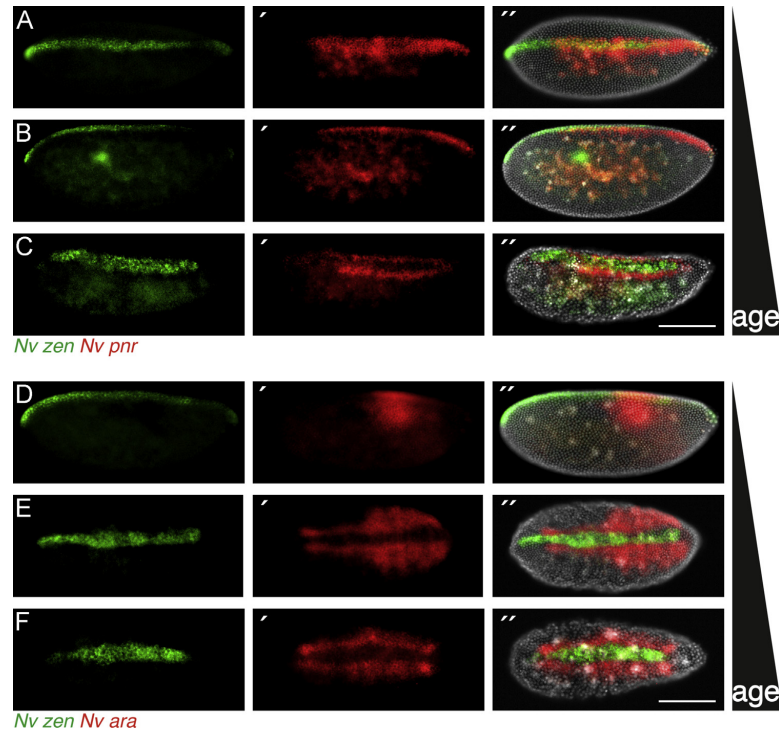


**Fig. 9.** Dynamics of *Nv-pnr* and *Nv-ara* expression in relation to those of *Nv-zen*. (A)–(A<sup>''</sup>) Dorsal view of a *Nasonia* embryo in cycle 11 comparing *Nv-zen* (green) and *Nv-pnr* (red) with DAPI (white). (B)–(B<sup>''</sup>) Lateral view of a *Nasonia* embryo in cycle 12 comparing *Nv-zen* (green) and *Nv-pnr* (red) with DAPI (white). (C)–(C<sup>''</sup>) Dorso-lateral view of a *Nasonia* embryo in continuation of gastrulation comparing *Nv-zen* (green) and *Nv-pnr* (red) with DAPI (white). (D)–(D<sup>''</sup>) Lateral view of a *Nasonia* embryo in cycle 11 comparing *Nv-zen* (green) and *Nv-ara* (red) with DAPI (white). (E)–(E<sup>''</sup>) and (F)–(F<sup>''</sup>) Dorsal view of *Nasonia* embryos in continuation of gastrulation comparing *Nv-zen* (green) and *Nv-ara* (red) with DAPI (white). Scale bar 100 μm. Embryos arranged from youngest to oldest from top to bottom in each species panel. Anterior is left. (For interpretation of the references to color in this figure legend, the reader is referred to the web version of this article.)

more in common with that of *Tribolium* than with *Drosophila*. In *Tribolium*, a self-regulatory loop composed of components and direct targets of the Toll signaling pathway leads to a dynamic source of DV patterning information in the form of a gradient of nuclear Dorsal that progressively narrows over the course of embryonic development (Nunes da Fonseca et al., 2008). In contrast, while there is quite some crosstalk among Dorsal target genes in the process of refinement of their domains, the *Drosophila* system does not appear to have significant dynamic self-regulatory properties downstream of Toll activation.

While the apparent use of a highly dynamic, and self-regulatory system for patterning the ventral side appears to be conserved between *Tribolium* and *Nasonia*, it is clear that the regulatory mechanism responsible for these features are not the same. In *Tribolium*, the changes in dynamic ventral genes such as *Tc-twist* are due to the shrinking and refinement of the Dorsal nuclear gradient toward the ventral side. In *Nasonia*, the changes in gene expression domains proceeds in the opposite direction, from narrow to broad.

At present it is not clear at which level the dynamic behavior of ventral genes in the *Nasonia* embryo is generated. Preliminary evidence indicates that Toll signaling is required for the activation of ventral genes in *Nasonia* (in preparation), so one explanation could be that the Dorsal gradient is itself dynamic in *Nasonia*. Other possibilities include the presence of feed-forward or feed-back interactions among ventrally expressed genes. A more

complete characterization of all of the genes expressed in the ventral region, the distribution of protein products, and the functional connections among genes expressed in this region, are needed to differentiate among these possibilities.

Our analyses also provide insights into the evolution of *sim* regulation among the insects. In *Drosophila*, the *sim* stripes appear very late in embryogenesis, and seem to arise de novo in a single row of cells flanking the presumptive mesoderm (Fig. 2A'–C'). The pattern is very different in *Nasonia*, where *Nv-sim* appears simultaneously with *Nv-twi* and *sna* in a stripe that is narrow, but noticeably broader than the expression of *Nv-twi* and *sna*. The *Nv-sim* stripe remains broader than *Nv-sna* and *twi* and is largely coexpressed with them throughout most of blastodermal development. Only toward the end of cycle 12 is *Nv-sim* finally cleared from the ventral side of the embryo, leading to the production of two stripes that in the end cover a single row of nuclei flanking the mesoderm (Fig. 2D'–F', S2E'–H').

A similar pattern is seen in *Tribolium*, where *Tc-sim* is a relatively early target of the Tc-Dorsal gradient, appearing later than *Tc-twist* but before *Tc-snail* (Fig. 2G', S2I'–J'). The initial domain of *Tc-sim* is similar to that of its *Nasonia* counterpart, in that it initially covers the ventral side of the embryo in an unbroken domain, and persists in being coexpressed with *Tc-sna* for a significant period of time, before being cleared from the ventral side at the onset of gastrulation (Fig. S2I'–M'). Thus, an early broad stripe of *sim* expression is likely ancestral for at least the holometabolous insects.



### Lateral genes

*Nv-brk* is the first of the lateral genes to be expressed, and appears at about the same time as the early, narrow stripes of *Nv-twi*, *sim* and *sna* (Fig. 4D). This indicates that *Nv-brk* might have an important role in the early interpretation and further refinement of positional information in the *Nasonia* embryo.

Our results also raise an interesting question about the origin of the use of *brinker* in insect embryonic patterning, since *brinker* is not expressed in the embryo of *Tribolium*. (R.N. da Fonseca, personal communication). Thus, either embryonic *brinker* was present in the common ancestor of the Holometabola, and was lost in the beetle lineage, or it was independently recruited for DV patterning in the wasp and fly lineages.

In contrast to the early expression of *Nv-brk*, genes involved in the partitioning of the neurogenic ectoderm are expressed relatively late in embryogenesis, at about the time just preceding gastrulation. The first of these to appear is *Nv-vnd*, which is the ventral-most of the columnar genes. Unlike the fly *vnd* domain, the *Nv-vnd* domain is initially incomplete along the AP axis, and is only present in presumptive thoracic regions (Fig. 5D). As development progresses, this stripe extends to the posterior end of the embryo, just as the morphogenetic movements of gastrulation are beginning (Fig. 5E and F). *Nv-ind* and *msh1* columnar expression is initiated later, and again in an anteriorly restricted pattern, at a stage where *Nv-vnd* is extended most of the way to the posterior pole (Fig. 5F and K). Thus, there appear to be two temporal gradients of gene activation that affect columnar gene expression: one along the DV axis and one along the AP axis.

Another potentially useful marker for ectoderm fate would have been *short-gastrulation* (*sog*), which is a BMP inhibitor, and responds to the lowest levels of nuclear Dorsal in the fly embryo (Rusch and Levine, 1996; Reeves and Stathopoulos, 2009). To date we have found no evidence that this gene exists in *Nasonia*. It is absent from all three *Nasonia* genome sequences and was not detected in any of the numerous EST and next generation sequencing projects deposited in Genbank. In addition, we have sequenced the transcriptome of the *Nasonia* embryo between blastoderm formation and gastrulation, and were not able to detect any *sog* expression. Together, these data indicate that *sog* has been lost from the *Nasonia* genome. This may not be so surprising, as *sog* appears to have no role in establishing early polarity in honeybee (Wilson and Dearden, 2011). In addition the other known function of *Drosophila sog* is in patterning the wing veins. These structures are strongly reduced in *Nasonia*, a trait that is diagnostic for the Chalcid family of wasps (Grissell and Schauff, 1990), to which *Nasonia* belongs. Thus, the combination of a loss of a role in embryonic patterning early in hymenopteran evolution (prior to the divergence of *Nasonia* and *Apis* lineages), and the lineage specific reduction in wing veins, may have allowed the loss of *sog* somewhere along the lineage leading to *Nasonia*.

### Dorsal side

One of the characteristic features of the insect embryo is the presence of extra-embryonic membranes, which are critical for the protection of the embryo from the environment, and for morphogenetic movements taking place after gastrulation. Insects vary widely in regard to the proportion of the egg surface which is dedicated to the production of these membranes, as well as where these structures are specified within the coordinates of the egg axes. *Drosophila* is one extreme, where the extraembryonic membranes are reduced to a single tissue type (the amnioserosa), which is restricted to the extreme dorsal pole of the embryo. On the other hand, most other insects generate two distinct extraembryonic tissues, the amnion and the serosa. In short germ

insects, these tissues typically derive from both anterior and dorsal egg regions (Panfilio, 2008).

At first glance the *Nasonia* embryo looks very much like that of *Drosophila* in terms of its arrangement of, and egg surface area commitment to, extraembryonic membranes. The best known *Drosophila* marker for this tissue, *zen*, is expressed initially in a very broad pattern, which then refines to a narrow stripe at the dorsal midline (Fig. S4A'–C'). A similar pattern is observed for *Nv-zen*, which in a very early division cycle (10) is expressed in a fairly broad domain restricted to the dorsal side of the embryo (Fig. 6A), and very quickly refines to a narrow stripe of about 4 nuclei wide covering the dorsal midline in the next nuclear division cycle (Fig. 6B and C). It is not yet clear whether the same molecular mechanisms for generating the two phases of *zen* expression in the fly (ubiquitous activation+repression by Dorsal, followed by refinement and amplification of BMP signaling) are also employed in *Nasonia*.

The expression patterns of two of our dorsal marker genes give an intriguing insight into the possible mechanisms used to generate DV polarity in the wasp. Both *Nv-hnt* and *Nv-doc* show expression in a stripe that covers the dorsal midline and continues over one or both poles onto the ventral side of the embryo (Fig. 7C, Fig. 8E–F). *Nv-hnt* is particularly striking, since it has a transient stripe completely covering the embryo circumference, before disappearing from the ventral side (Fig. 7C and D). The above observations indicate that there is a shared characteristic of both the dorsal and ventral midlines of *Nasonia* that allows the initial circumpolar expression of *Nv-hnt* and *Nv-doc*, and that breaking of DV asymmetry allows differential expression at the two midlines.

BMP signaling in *Drosophila* has three threshold outputs on the dorsal side of the embryo, with genes such as *RACE* and *hnt* expressed in narrow dorsal domains, genes such as *tup* and *doc* expressed in somewhat broader stripes, while genes such as *pnr* are expressed quite broadly, and can be activated in the presence of low levels of BMP activity (Ashe et al., 2000). We have also found that there are genes expressed very narrowly (*Nv-RACE*, *Nv-hnt*), moderately more broadly (*Nv-tup*, *Nv-doc*), and significantly more broadly (*Nv-ara*) along the dorsal surface of the *Nasonia*. This indicates that there might be a gradient of positional information on the dorsal side of the *Nasonia* embryo with threshold outputs similar in nature to the one found in *Drosophila*. It is clear that while the location and width of the *Nv-zen* stripe is quite similar to that of its fly counterpart, the behavior of the tissue in which it is expressed is quite different. The fly amnioserosa maintains a border with the surrounding ectoderm throughout development until the end of dorsal closure. In contrast, *Nasonia* serosal cells eventually migrate and surround the entire embryo. This latter behavior is typical of the serosal coverings present in most insects. However the *Nasonia* serosal behavior differs from that of most insects, in that its movement involves a severing of this tissue from the flanking epithelium, and the migration of a free edge over the surface of the ectoderm. This behavior is similar to that observed in the honeybee (Fleig and Sander, 1988), indicating that this type of migration is an ancestral character of the higher hymenoptera. Interestingly, this mode of serosal migration is also found in some fly species, such as the scutellfly *Megaselia* (Rafiqi et al., 2008). This may be an additional case of convergent evolution between hymenoptera and dipterans.

Many of the dorsal/extraembryonic markers analyzed here have also been examined in other insect species, and have been used as indicators of serosa or amnion fate. *zen* orthologs are generally reliable markers of the serosa, but also have roles in the amnion in *Tribolium* and *Megaselia* (Van der Zee et al., 2005; Rafiqi et al., 2010). *hnt* orthologs seem to vary in their expression, with a narrow, *zen*-like, serosal expression in *Nasonia*, a broader domain encompassing both the amnion and serosa in *Megaselia* (Rafiqi

et al., 2012), and a domain flanking the presumptive serosa in the mosquito *Anopheles* (Goltsev et al., 2007). Expression of *hnt* has so far not been reported in *Tribolium*. In both *Megaselia* and *Anopheles*, *tup* and *doc* are expressed in domains flanking the serosa, which will give rise to the amnion (Goltsev et al., 2007; Rafiqi et al., 2010). While *Nasonia* *tup* matches this pattern, and likely also is an amnion marker in the wasp, *Nv-doc* differs in that it is only slightly broader than the serosal primordium, and is not repressed at the dorsal midline. *Tribolium* *doc* is also exceptional, as it is expressed in the dorsal serosa (Van der Zee et al., 2006). *Tribolium* *pnr* and *ara* are both specific amnion markers, and the expression of *Nv-pnr* and *ara* are also consistent with amniotic roles (Van der Zee et al., 2006; Nunes da Fonseca et al., 2008), with *Nv-ara* likely also having a significant role in the dorsal ectoderm.

Thus it is clear that there is much plasticity in gene regulatory systems in the insect extraembryonic and dorsal ectoderm, but that there also may be a conserved core of factors that are crucial for the specification of amnion, serosa, and dorsal embryonic ectoderm across insects.

## Conclusion

In this work we have shown that the arrangement of cell fates, and the expression of genes that mark these fates, are strongly convergent along the DV axis of the long germ embryo of *Nasonia* just prior to gastrulation when compared to those of *Drosophila* at an equivalent stage (Fig. 10). Given the large evolutionary distances between the wasp and the fly this may represent a developmental constraint impinging on the evolution of rapid long germ embryonic patterning among the holometabolous insects. The stringency and true nature of this constraint can be explored by further sampling additional cases of independent evolution of the long germ mode of embryogenesis in other insect orders. Only in this way can lineage specific traits (which are in themselves interesting) and mere coincidence be distinguished from a true signal of constraint.

In contrast to the similarity seen at the stage just prior to gastrulation, we have found that the dynamics of the generation and interpretation of positional information before this stage is quite diverged (Fig. 10). In addition, the behaviors of cells and tissues during and after gastrulation are also quite different between *Drosophila* and *Nasonia* (Fig. S3, Fig. 10). Together these observations indicate that the GRN governing DV patterning and cell type specification in *Nasonia* is structured rather differently and could have novel components that are not found in the *Drosophila* DV GRN. For these reasons, a comprehensive characterization of the *Nasonia* DV patterning system, at the level of its components, their interactions, and the output of the preceding in regard to cell fate and behavior, will give major insights into how convergent traits can evolve.

## Methods

### Embryo collection and fixation

All *N. vitripennis* embryos were collected using the Waspinator (Fig. S8). This modified petri dish harbors 19 hosts, which can be accessed by up to 120 *Nasonia* females at the same time only from the anterior side. To collect the embryos, parasitized hosts were cracked open at the anterior side and dipped into the fixing solution (5 mL heptane, 2 mL 10% methanol-free formaldehyde, 2 mL 1xPBS, in a 15 mL scintillation vial). Fixation and subsequent hand devitellinization were done as described in Lynch and Desplan (2006).

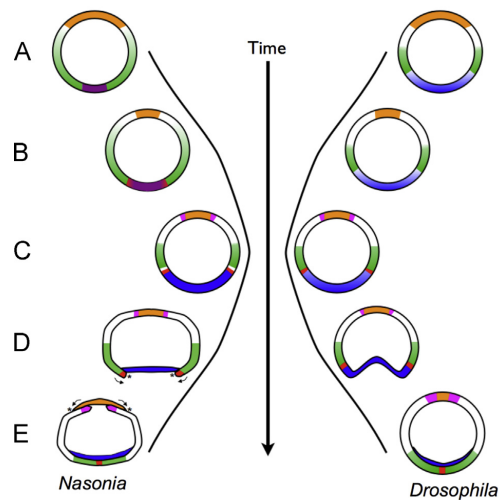


**Fig. 10.** Summary of convergences and divergences between *Nasonia* and *Drosophila* embryos. Schematic representations of embryogenesis of *Nasonia* (left) and *Drosophila* (right) from mid-blastoderm stage (A) until after the completion of gastrulation (E). Colored regions correspond to different exemplar gene expression patterns: blue=*twi*, red=*sim*, green=*brk*, orange=*zen*, magenta=*tup*, purple=blue(*twi*)+red(*sim*). (A) The *Nasonia* embryo diverges from *Drosophila* in that *Nv-twi* and *sim* are expressed in a very narrow, overlapping (red+blue=purple) domain, while in *Drosophila* *twi* expression is broad and *sim* is not yet detected. *Nv-brk* is found quite ventrally, while *Dm-brk* is restricted to the lateral sides. (B) As development proceeds the *Nv-twi-sim* domain dynamically expands, while the *Drosophila* pattern remains for the most part static. In both species, *zen* expression retracts to a very narrow dorsal stripe. (C) *Dm-sim* becomes expressed in two lateral stripes and *Nv-sim* expression is cleared from the *Nv-twi* expression domain resulting in two lateral stripes of *Nv-sim* expression, too. Hence the arrangement of markers of tissue fates are basically identical between *Nasonia* and *Drosophila* just before gastrulation. (D) *Nasonia* and *Drosophila* embryos diverge again at the onset of gastrulation. *Drosophila* mesoderm is internalized through a ventral furrow, whereas the embryonic epithelium remains intact. In contrast, *Nasonia* mesoderm is internalized by a rupturing of the epithelium at the border between *Nv-sim* and *Nv-twi* expressing cells, leading to free edges (‘’) that migrate over the mesoderm, and eventually fuse at the midline (see E). (E) After the completion of gastrulation, morphogenetic movements differ on the dorsal side between *Nasonia* and *Drosophila*. In *Nasonia*, the border between serosal cells and putative amnion is ruptured, leading again to free edges (‘’) that move over the ectodermal surface. In contrast, the fly amnioserosa gradually shrinks as the embryonic flanks expand dorsally. (For interpretation of the references to color in this figure legend, the reader is referred to the web version of this article.)

### In situ hybridization

Single in Situ hybridizations for *Nasonia* and *Drosophila* were performed as previously described (Brent et al., 2003).

Double fluorescent in situ hybridizations in *Nasonia* were performed as described in Lynch et al. (2010). In brief, digoxigenin and biotin labeled probes were hybridized simultaneously. They were detected by anti-dig::POD (Roche, 1:100), and anti-Biotin::AP (Roche, 1:2000) antibodies respectively. Fluorescence was generated with the AlexaFluor 488 TSA kit (Invitrogen), and a modification of the HNPP/Fast Red (Roche) protocol, respectively.

Double fluorescent in situ hybridizations in *Tribolium* were performed using a modified version of the protocol described in Lynch and Desplan (2010). Digoxigenin-labelled and dinitrophenyl (DNP)-labeled probes were added simultaneously and were detected using anti-digoxigenin::AP antibody (1:2500, Roche) coupled with HNPP Fluorescent detection (Roche), and 1st anti-DNP-rabbit antibody (1:400, Molecular Probes) plus 2nd anti-rabbit-HRP antibody (1:100) combined with AlexaFluor 488 TSA

kit (Invitrogen), respectively. A step by step protocol is available at: <http://www.uni-koeln.de/math-nat-fak/ebio/Research/Roth/Protocols/protocols.html>.

Probes were produced as in Lynch et al. (2010), using the gene specific primers listed in the Supplementary Table.

### Acknowledgements

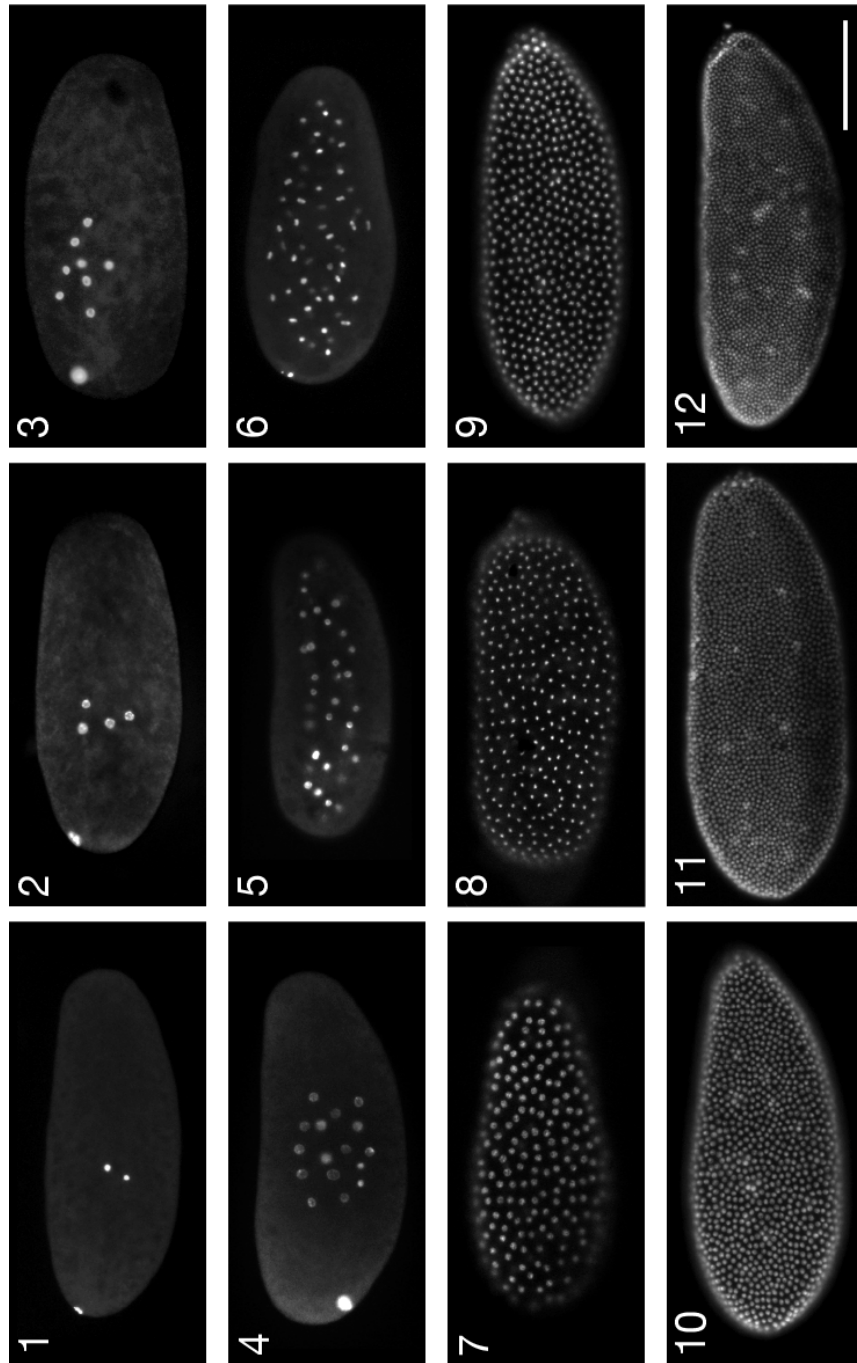
This work was funded and supported by the Collaborative Research Grant “Molecular Basis of Evolutionary Innovations” (SFB 680) from the German Research Foundation (DFG). We also thank Boehringer Ingelheim Fonds for supporting Dominik Stappert with a B.I.F. Ph.D. Fellowship.

### Appendix A. Supporting information

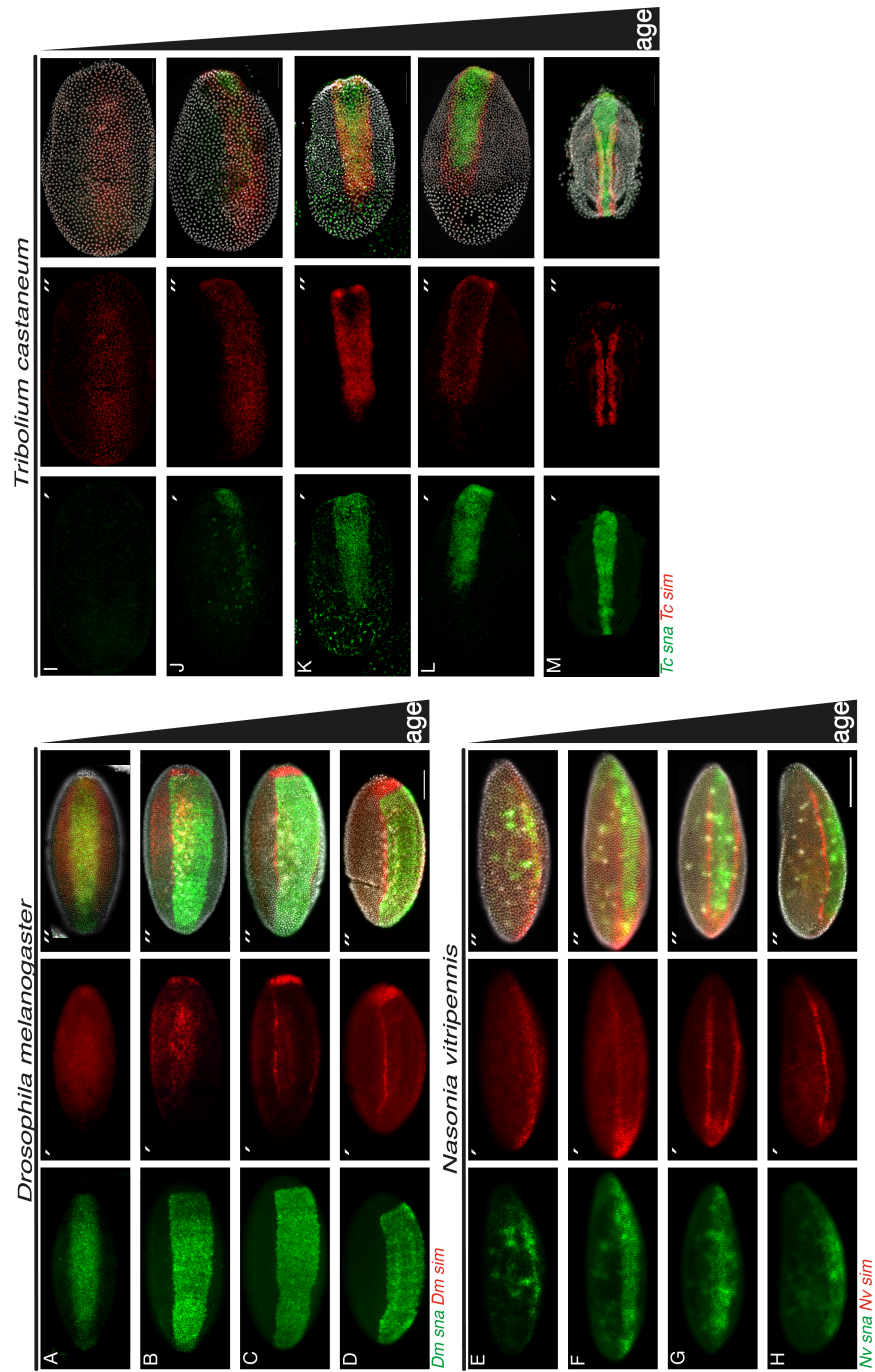
Supplementary data associated with this article can be found in the online version at <http://dx.doi.org/10.1016/j.ydbio.2013.05.026>.

### References

- Ashe, H.L., Mannervik, M., Levine, M., 2000. Dpp signaling thresholds in the dorsal ectoderm of the *Drosophila* embryo. *Development* (Cambridge, England) 127, 3305–3312.
- Brent, A.E., Schweitzer, R., Tabin, C.J., 2003. A somitic compartment of tendon progenitors. *Cell* 113, 235–248.
- Bull, A.L., 1982. Stages of living embryos in the jewel wasp *Mormoniella* (*Nasonia*) *vitripennis* (walker) (hymenoptera: pteromalidae). *Int. J. Insect Morphol. Embryol.* 11, 1–23.
- Chen, G., Handel, K., Roth, S., 2000. The maternal NF- $\kappa$ B/dorsal gradient of *Tribolium castaneum*: dynamics of early dorsoventral patterning in a short-germ beetle. *Development* (Cambridge, England) 127, 5145–5156.
- Cho, Y.S., Stevens, L.M., Stein, D., 2010. Pipe-dependent ventral processing of Easter by Snake is the defining step in *Drosophila* embryo DV axis formation. *Curr. Biol.*: CB 20, 1133–1137.
- Davis, G.K., Patel, N.H., 2002. Short, long, and beyond: molecular and embryological approaches to insect segmentation. *Annu. Rev. Entomol.* 47, 669–699.
- Dearden, P., Grbic, M., Falciani, F., Akam, M., 2000. Maternal expression and early zygotic regulation of the *Hox3/zen* gene in the grasshopper *Schistocerca gregaria*. *Evol. Dev.* 2, 261–270.
- Erickson, J.W., Quintero, J.J., 2007. Indirect effects of ploidy suggest X chromosome dose, not the X:A ratio, signals sex in *Drosophila*. *PLoS Biol.* 5, e332.
- Falciani, F., Hausdorf, B., Schröder, R., Akam, M., Tautz, D., Denell, R., Brown, S., 1996. Class 3 Hox genes in insects and the origin of *zen*. *Proc. Nat. Acad. Sci. U.S.A.* 93, 8479–8484.
- Fleig, R., Sander, K., 1988. Honeybee morphogenesis: embryonic cell movements that shape the larval body 534, 525–534.
- Goltsev, Y., Fuse, N., Frasch, M., Zinzen, R.P., Lanzaro, G., Levine, M., 2007. Evolution of the dorsal–ventral patterning network in the mosquito, *Anopheles gambiae*. *Development* (Cambridge, England) 134, 2415–2424.
- Grissell, E.E., Schauf, M., 1990. A Handbook of the Families of Nearctic Chalcidoidea (Hymenoptera). 1. Entomological Society of Washington, Washington, D.C., pp. 1–85, Handbook.
- Hong, J.-W., Hendrix, D.A., Papatsenko, D., Levine, M.S., 2008. How the Dorsal gradient works: insights from postgenome technologies. *Proc. Nat. Acad. Sci. U.S.A.* 105, 20072–20076.
- Jaźwińska, A., Rushlow, C., Roth, S., 1999. The role of brinker in mediating the graded response to Dpp in early *Drosophila* embryos. *Development* (Cambridge, England) 126, 3323–3334.
- Jiménez, F., Martin-Morris, L.E., Velasco, L., Chu, H., Sierra, J., Rosen, D.R., White, K., 1995. vnd, a gene required for early neurogenesis of *Drosophila*, encodes a homeodomain protein. *EMBO J.* 14, 3487–3495.
- Kanodia, J.S., Rikhy, R., Kim, Y., Lund, V.K., DeLotto, R., Lippincott-Schwartz, J., Shvartsman, S.Y., 2009. Dynamics of the Dorsal morphogen gradient. *Proc. Nat. Acad. Sci. U.S.A.* 106, 21707–21712.
- Leptin, M., 1991. twist and snail as positive and negative regulators during *Drosophila* mesoderm development. *Genes Dev.* 5, 1568–1576.
- Liberman, L.M., Reeves, G.T., Stathopoulos, A., 2009. Quantitative imaging of the Dorsal nuclear gradient reveals limitations to threshold-dependent patterning in *Drosophila*. *Proc. Nat. Acad. Sci. U.S.A.* 106, 22317–22322.
- Lynch, J.A., Desplan, C., 2010. Novel modes of localization and function of nanos in the wasp *Nasonia*. *Development* (Cambridge, England) 137, 3813–3821.
- Lynch, J.A., El-Sherif, E., Brown, S.J., 2012. Comparisons of the embryonic development of *Drosophila*, *Nasonia*, and *Tribolium*. *Wiley Interdisciplinary Reviews. Dev. Biol.* 1, 16–39.
- Lynch, J.A., Desplan, C., 2006. A method for parental RNA interference in the wasp *Nasonia vitripennis* *Nature Protocols* 1, 486–494.
- Lynch, J.A., Peel, A.D., Drechsler, A., Averof, M., Roth, S., 2010. EGF signaling and the origin of axial polarity among the insects. *Curr. Biol.*: CB 20, 1042–1047.
- Moussian, B., Roth, S., 2005. Dorsoventral axis formation in the *Drosophila* embryo —shaping and transducing a morphogen gradient. *Curr. Biol.*: CB 15, R887–R899.
- Nunes da Fonseca, R., Van der Zee, M., Roth, S., 2010. Evolution of extracellular Dpp modulators in insects: the roles of tolloid and twisted-gastrulation in dorsoventral patterning of the *Tribolium* embryo. *Dev. Biol.* 345, 80–93.
- Neuman-Silberberg, F.S., Schüpbach, T., 1993. The *Drosophila* dorsoventral patterning gene *gurken* produces a dorsally localized RNA and encodes a TGF alpha-like protein. *Cell* 75, 165–174.
- Nunes da Fonseca, R., Von Levetzow, C., Kalscheuer, P., Basal, A., Van der Zee, M., Roth, S., 2008. Self-regulatory circuits in dorsoventral axis formation of the short-germ beetle *Tribolium castaneum*. *Dev. Cell* 14, 605–615.
- O’Connor, M.B., Umulis, D., Othmer, H.G., Blair, S.S., 2006. Shaping BMP morphogen gradients in the *Drosophila* embryo and pupal wing. *Development* (Cambridge, England) 133, 183–193.
- Panfilio, K.A., 2008. Extraembryonic development in insects and the acrobatics of blastokinesis. *Dev. Biol.* 313, 471–491.
- Panfilio, K.A., Liu, P.Z., Akam, M., Kaufman, T.C., 2006. *Oncopeltus fasciatus zen* is essential for serosal tissue function in katatrepsis. *Dev. Biol.* 292, 226–243.
- Rafiqi, A.M., Lemke, S., Ferguson, S., Stauber, M., Schmidt-Ott, U., 2008. Evolutionary origin of the amnioserosa in cyclorhaphan flies correlates with spatial and temporal expression changes of *zen*. *Proc. Nat. Acad. Sci. U.S.A.* 105, 234–239.
- Rafiqi, A.M., Lemke, S., Schmidt-Ott, U., 2010. Postgastrular *zen* expression is required to develop distinct amniotic and serosal epithelia in the scutella fly *Megaselia*. *Dev. Biol.* 341, 282–290.
- Rafiqi, A.M., Park, C.-H., Kwan, C.W., Lemke, S., Schmidt-Ott, U., 2012. BMP-dependent serosa and amnion specification in the scutella fly *Megaselia abdita*. *Development* (Cambridge, England).
- Reeves, G.T., Stathopoulos, A., 2009. Graded dorsal and differential gene regulation in the *Drosophila* embryo. *Cold Spring Harbor Perspect. Biol.* 1, a000836.
- Roth, S., 2003. The origin of dorsoventral polarity in *Drosophila*. *Philos. Trans. R. Soc. London, Ser. B* 358, 1317–1329, discussion 1329.
- Roth, S., Schüpbach, T., 1994. The relationship between ovarian and embryonic dorsoventral patterning in *Drosophila*. *Development* (Cambridge, England) 120, 2245–2257.
- Rusch, J., Levine, M., 1996. Threshold responses to the dorsal regulatory gradient and the subdivision of primary tissue territories in the *Drosophila* embryo. *Curr. Opin. Genetics Dev.* 6, 416–423.
- Rushlow, C., Frasch, M., Doyle, H., Levine, M., 1987. Maternal regulation of *zerknüllt*: a homeobox gene controlling differentiation of dorsal tissues in *Drosophila*. *Nature* 330, 583–586.
- Schmidt-Ott, U., 2000. The amnioserosa is an apomorphic character of cyclorhaphan flies. *Dev. Genes Evol.* 210, 373–376.
- Sen, J., Goltz, J.S., Stevens, L., Stein, D., 1998. Spatially restricted expression of pipe in the *Drosophila* egg chamber defines embryonic dorsal–ventral polarity. *Cell* 95, 471–481.
- Stathopoulos, A., Levine, M., 2004. Whole-genome analysis of *Drosophila* gastrulation. *Curr. Opin. Genetics Dev.* 14, 477–484.
- Stathopoulos, A., Van Drenth, M., Erives, A., Markstein, M., Levine, M., 2002. Whole-genome analysis of dorsal–ventral patterning in the *Drosophila* embryo. *Cell* 111, 687–701.
- Van der Zee, M., Berns, N., Roth, S., 2005. Distinct functions of the *Tribolium* *zerknüllt* genes in serosa specification and dorsal closure. *Curr. Biol.*: CB 15, 624–636.
- Van der Zee, M., Stockhammer, O., Von Levetzow, C., Nunes da Fonseca, R., Roth, S., 2006. Sog/Chordin is required for ventral-to-dorsal Dpp/BMP transport and head formation in a short germ insect. *Proc. Nat. Acad. Sci. U.S.A.* 103, 16307–16312.
- Von Ohlen, T., Doe, C.Q., 2000. Convergence of dorsal, dpp, and *egr* signaling pathways subdivides the *drosophila* neuroectoderm into three dorsal–ventral columns. *Dev. Biol.* 224, 362–372.
- Wheeler, S.R., Carrico, M.L., Wilson, B.A., Skeath, J.B., 2005. The *Tribolium* columnar genes reveal conservation and plasticity in neural precursor patterning along the embryonic dorsal–ventral axis. *Dev. Biol.* 279, 491–500.
- Wilson, M.J., Dearden, P.K., 2011. Diversity in insect axis formation: two orthodenticle genes and hunchback act in anterior patterning and influence dorsoventral organization in the honeybee (*Apis mellifera*). *Development* (Cambridge, England) 138, 3497–3507.

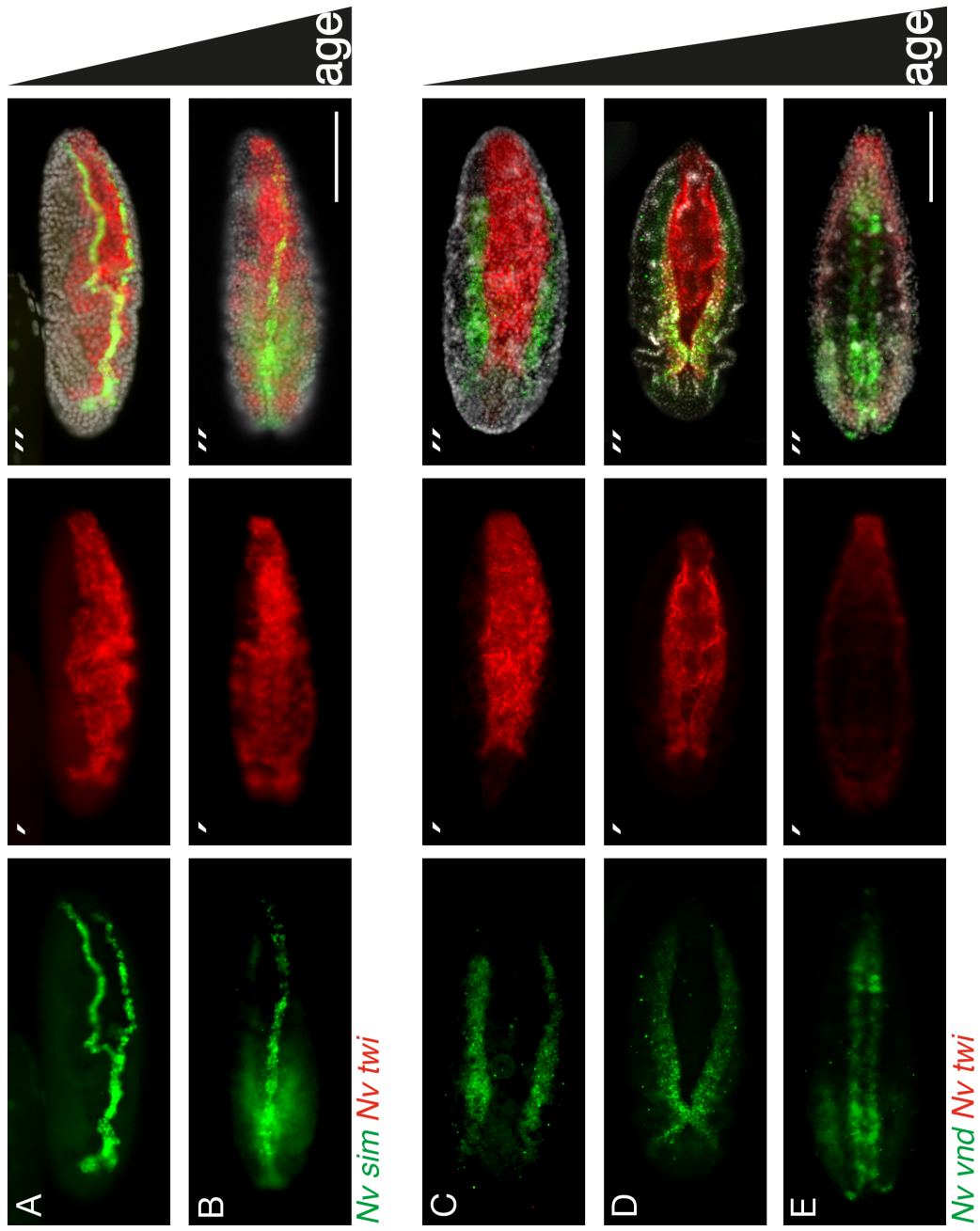


**Supplementary Figure 1. Characterization of syncytial divisions in the early embryo of *Nasonia***

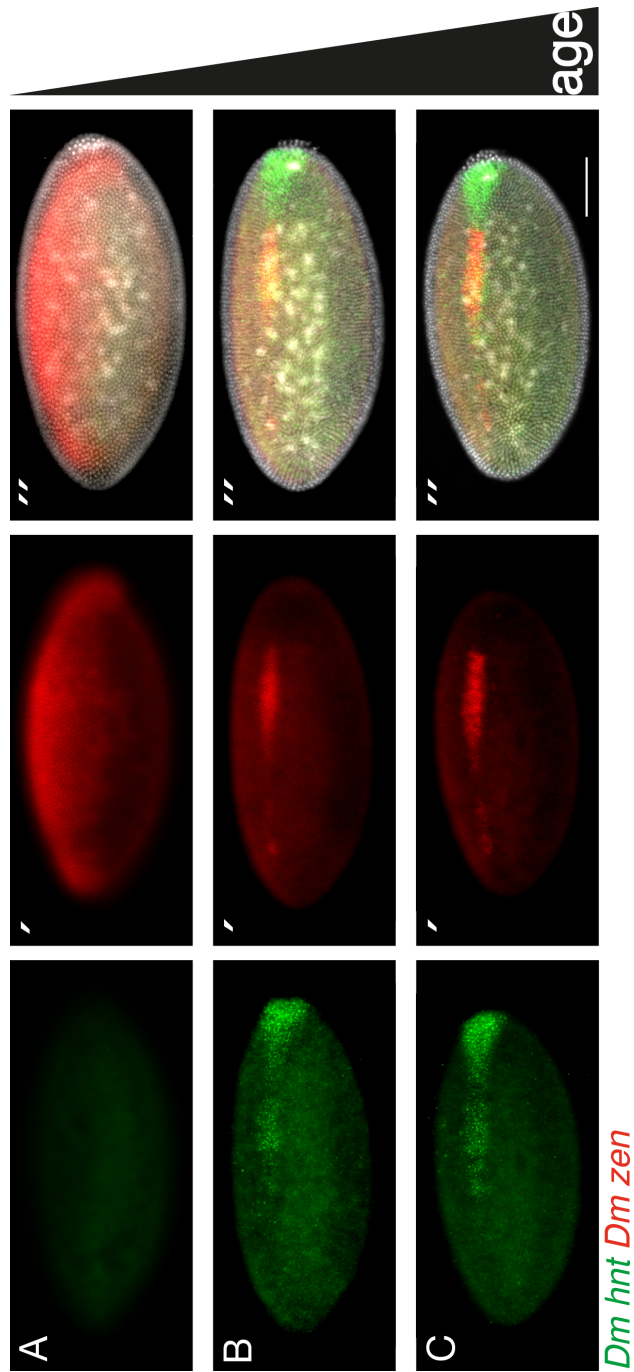


Supplementary Figure 2. Double fluorescent ISH of *snail* (green) and *sim* (red) in *Nasonia*, *Drosophila* and *Tribolium* embryos

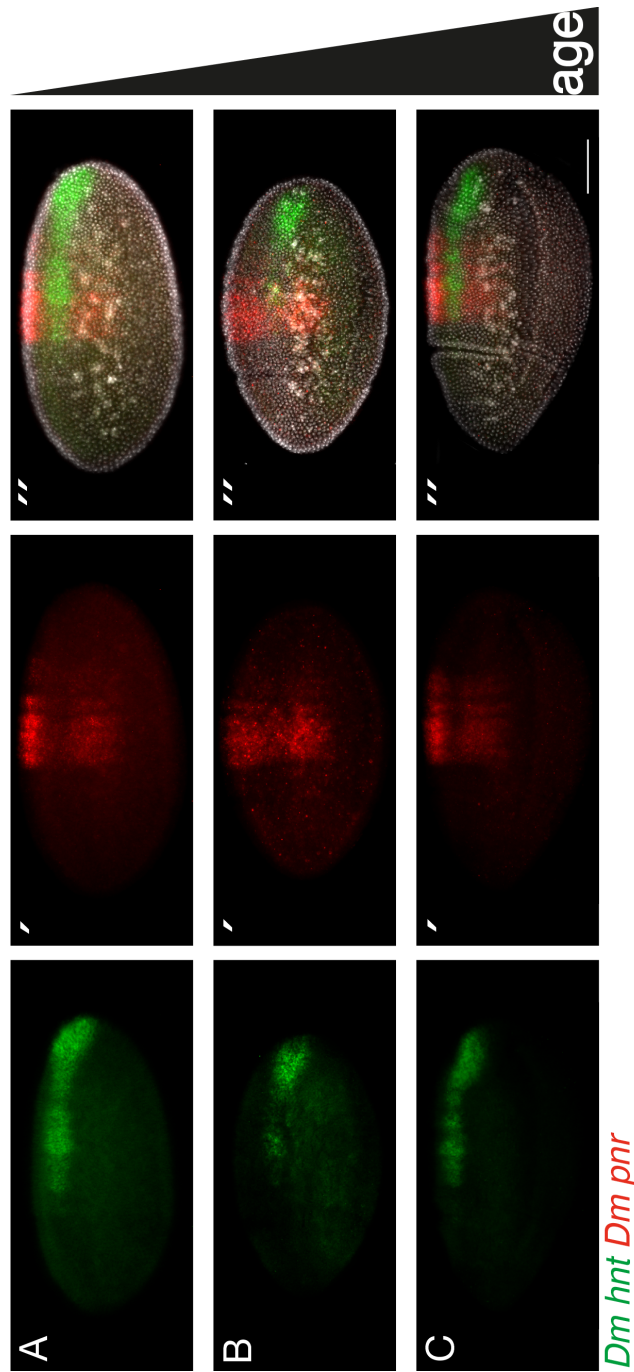




Supplementary Figure 3. Postgastrular dynamics of *Nv-vnd* and *Nv-sim*

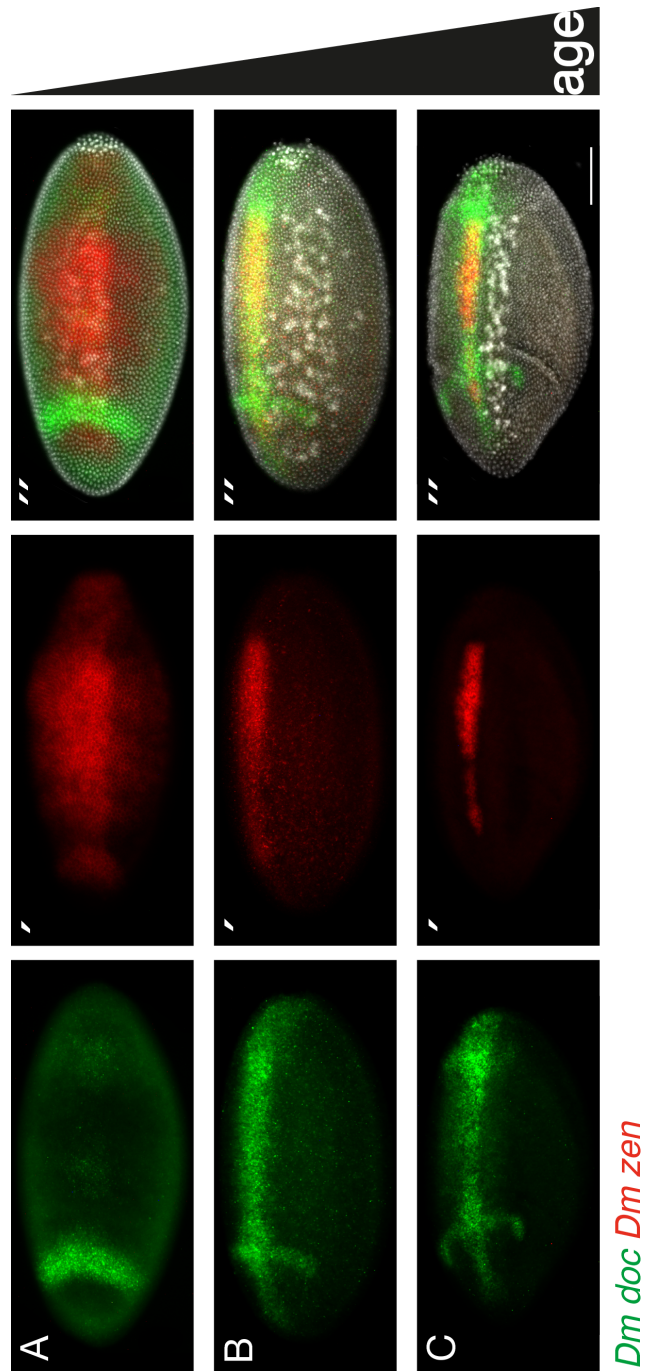


Supplementary Figure 4. Double fluorescent ISH of *hnt* (green) and *zen* (red) in *Drosophila*

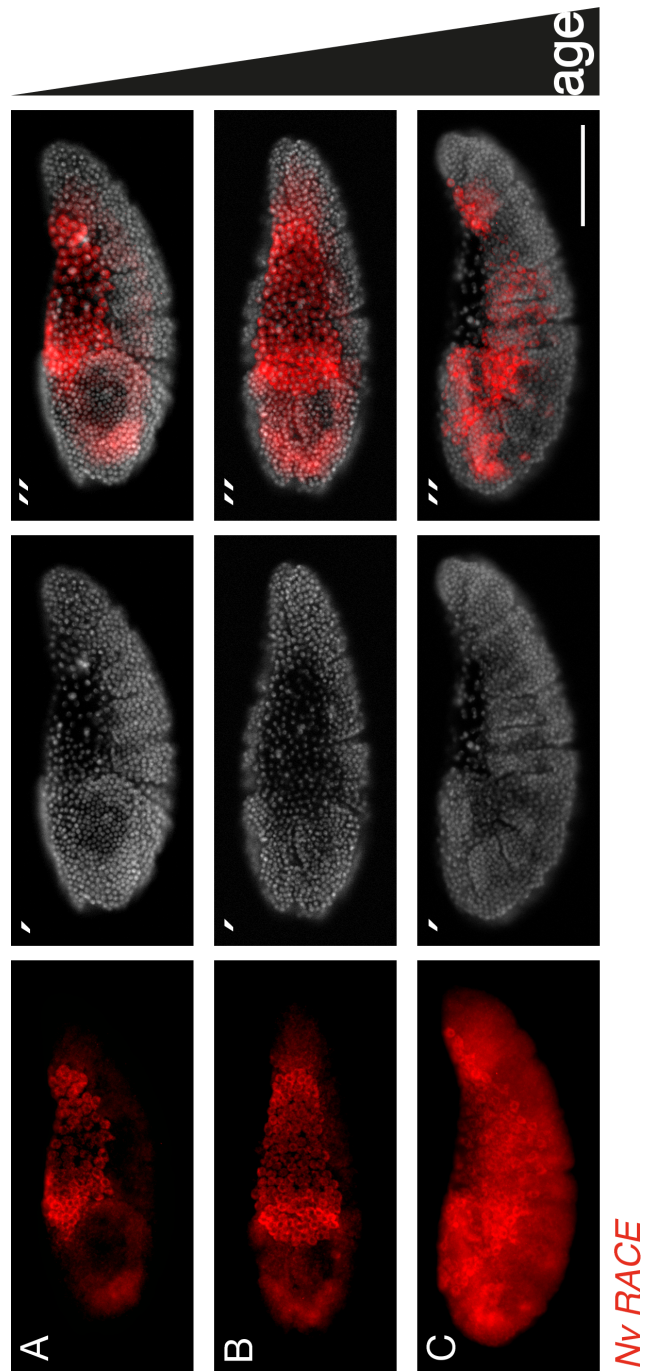


Supplementary Figure 5. Double fluorescent ISH of *hnt* (green) and *pnr* (red) in *Drosophila*

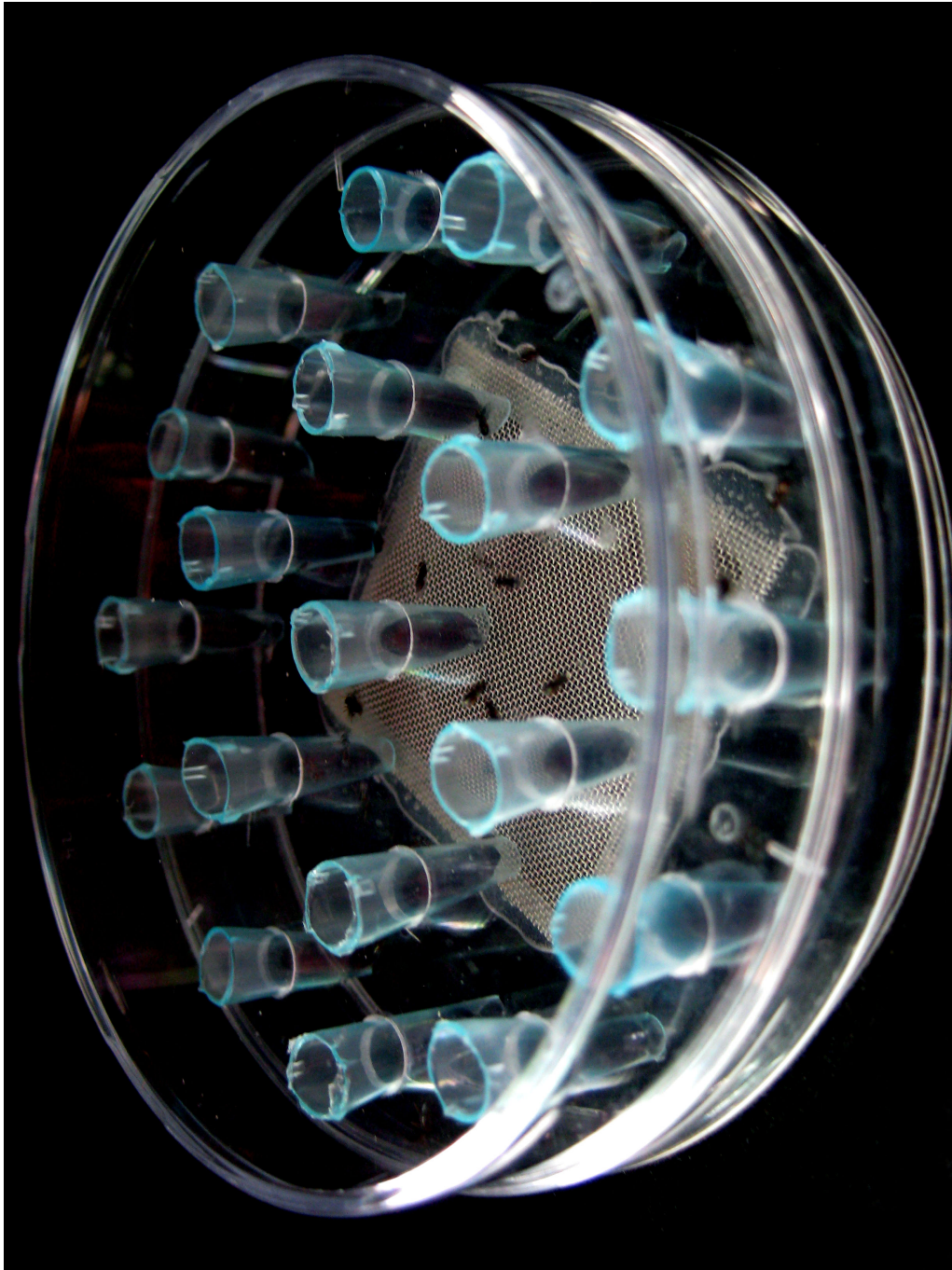




Supplementary Figure 6. Double fluorescent ISH of *doc* (green) and *zen* (red) in *Drosophila*



Supplementary Figure 7. fluorescent ISH of RACE (red) in late (gastrulating and post- gastrulation) *Nasonia* embryos



**Supplementary Figure 8. The “WASPINATOR” egg laying chamber**

### Supplementary Figure 1. Characterization of syncytial divisions in the early embryo of *Nasonia*

Embryos at all stages stained with DAPI to demonstrate the arrangement of the nuclei. Embryos are arranged from youngest to oldest.

### Supplementary Figure 2. Double fluorescent ISH of *snail* (green) and *sim* (red) in *Nasonia*, *Drosophila* and *Tribolium* embryos

(A''-C'') Ventral and (D'') ventro-lateral views of *Drosophila* embryos in cycle 13 (A''), cycle 14 (B''), initiation of gastrulation (C'') and ongoing gastrulation (D'') comparing *Dm-snail* (A-D) and *Dm-sim* (A'-D') mRNA expression with DAPI (white).

(E''/H'') Lateral and (F''-G'') ventro-lateral views of *Nasonia* embryos in cycle 10-12 (E''-H'') comparing *Nv-sna* (E-H) and *Nv-sim* (E'-H') mRNA expression with DAPI (white).

(I''-M'') Ventral views of *Tribolium* embryos in undifferentiated blastoderm (I''-J''), start of pit formation (K''), differentiated blastoderm (H'') and before serosal window closes (M'') comparing *Tc-sna* (I-M) and *Tc-sim* (I'-M') mRNA expression with DAPI (white).

Scale bar 100  $\mu$ m. Embryos arranged from youngest to oldest from top to bottom in each species panel. Anterior is left.

### Supplementary Figure 3. Postgastrular dynamics of *Nv-vnd* and *Nv-sim*

(A-A'') Ventro-lateral view of a gastrulating *Nasonia* embryo comparing *Nv-sim* (green) and *Nv-twi* (red) mRNA expression with DAPI (white).

(B-B'') Ventral view of a *Nasonia* embryo comparing *Nv-sim* (green) and *Nv-twi* (red) mRNA expression with DAPI (white) after gastrulation is completed.

(C''-E'') Ventral views of *Nasonia* embryos comparing *Nv-vnd* (C-E) and *Nv-twi* (C'-E') after initiation of gastrulation (C''), ongoing gastrulation (D'') and after gastrulation is completed.

### Supplementary Figure 4. Double fluorescent ISH of *hnt* (green) and *zen* (red) in *Drosophila*

(A'') Dorsal and (B''-C'') dorso-lateral views of *Drosophila* embryos comparing *Dm-hnt* (A-C) and *Dm-zen* (A'-C') mRNA expression in cycle 14 (A''-C'')

Scale bar 100  $\mu$ m. Embryos arranged from youngest to oldest from top to bottom. Anterior is left.

### Supplementary Figure 5. Double fluorescent ISH of *hnt* (green) and *pnr* (red) in *Drosophila*

(A''-C'') Lateral views of *Drosophila* embryos comparing *Dm-hnt* (A-C) and *Dm-pnr* (A'-C') mRNA expression in cycle 14 (A''), initiation of gastrulation (B'') and ongoing gastrulation (C'').

Scale bar 100  $\mu$ m. Embryos arranged from youngest to oldest from top to bottom. Anterior is left.

### Supplementary Figure 6. Double fluorescent ISH of *doc* (green) and *zen* (red) in *Drosophila*

(A'') Dorsal and (B''-C'') dorso-lateral views of *Drosophila* embryos comparing *Dm-doc* (A-C) and *Dm-zen* (A'-C') mRNA expression in cycle 14 (A''-B'') and initiation of gastrulation (C'').

Scale bar 100  $\mu$ m. Embryos arranged from youngest to oldest from top to bottom. Anterior is left.

**Supplementary Figure 7. fluorescent ISH of RACE (red) in late (gastrulating and post- gastrulation) *Nasonia* embryos**

(A'') Dorso-lateral, (B'') dorsal and (C'') lateral views of *Nasonia* embryos with completed germ band extension comparing *Nv-RACE* (A-C) mRNA expression and DAPI (A'-C'). Scale bar 100  $\mu$ m. Embryos arranged from youngest to oldest from top to bottom. Anterior is left.

**Supplementary Figure 8. The “WASPINATOR” egg laying chamber**

Modified 10 cm plastic Petri dish with cut 1 ml pipette tips to position fly hosts and a grid for airflow. See materials and methods for details.

## 2.2 Novel deployment of Toll and BMP signaling pathways leads to a convergent patterning output in a wasp

Orhan Özüak\*, Thomas Buchta\*, Siegfried Roth, Jeremy A. Lynch

\*These authors contributed equally.

**Abstract**

In *Drosophila*, Toll signaling is the source for all dorsal-ventral (DV) patterning of the embryo. This is in contrast to the majority of the metazoa, where Toll signaling plays no role in embryonic patterning, and BMP signaling plays the major role. We have examined the DV patterning system in the wasp *Nasonia*, whose embryo has many features convergent with *Drosophila*. In contrast to the fly, wasp Toll has a limited role, and BMP is required for almost all DV patterning and polarity of the *Nasonia* embryo. Our results indicate that the ancestral role of Toll in insect embryos was to simply induce mesoderm that BMP played the morphogen role, and that significant alterations in the BMP pathway occurred in the *Nasonia* lineage.

**Results/Discussion**

Toll signaling, which leads to the graded nuclear uptake of the transcription factor Dorsal that acts as a morphogen, patterns the *Drosophila* embryo, and is required for all DV polarity(1-3). It is known that in most other animal species, Toll has no embryonic patterning role (4), and BMP signaling is the most commonly used system to generate DV polarity (5). Even in the beetle

*Tribolium*, the strict hierarchy with Toll at the top is not conserved, indicating that the *Drosophila* system is not representative of the insects (6).

We have shown that while the expression of DV fate markers is almost identical in *Nasonia* and *Drosophila* embryos at the onset of gastrulation, the upstream networks responsible for these patterns are highly diverged (7). This led us to examine the functional basis of DV patterning in *Nasonia*.

Multiplex *in situ* hybridization techniques with *Nv-twist* (*-twi*, mesoderm), *Nv-brinker* (*-brk*, ventral and lateral ectoderm), and *Nv-zerknuellt* (*-zen*, extraembryonic) allow a global view of the *Nasonia* DV axis (Fig. 1A). Parental RNAi (pRNAi) targeting either the *Nasonia* Toll receptor (*Nv-Toll*) or the BMP ligand Decapentaplegic (*Nv-dpp*) allowed a test of the relative roles of the two pathways.

*Nv-Toll* pRNAi embryos show a complete loss *Nv-twist* expression (Fig. 1B). This indicates a conserved role of Toll in mesoderm induction. However, even the most strongly affected embryos are still highly polarized, with normal *Nv-zen* and dorsal border of *Nv-brk* expression (Fig. 1B), indicating that a Toll independent patterning system operates on the dorsal side, which is absent in *Drosophila* (1, 8). In addition, the expansion of the ventral border of *Nv-brk* to cover the ventral side (Fig. 1B) in *Nv-Toll* RNAi indicates a Toll independent mode of ventro-lateral ectoderm specification in *Nasonia* which is also absent in *Drosophila* (compare Fig. 1E to 1F) (1, 9).

*Nv-dpp* knockdown leads to loss of not only the dorsal fates (which is its phenotype in *Drosophila*, Fig. 1F), but also to the expansion of the mesoderm to the dorsal side, (Fig. 1C), whereas the mesoderm is unaffected by loss of BMP in *Drosophila* (Fig. 1F).

Double knockdown of *Nv-dpp* and *Nv-Toll* results in embryos expressing *Nv-brk* only (Fig. 1D). This shows that the ventralization of *Nv-dpp* RNAi embryos requires at least initial induction of mesoderm by *Nv-Toll*. Thus wasps and flies may share a similar ectodermal "ground state" (compare Fig. 1E to 1F) (11-12).

These phenotypes indicate that Nv-Toll signaling has a rather limited role in *Nasonia*, rather than acting as a global morphogen, while BMP signaling appears to have a broad patterning role encompassing most of the embryo. Thus, these end point phenotypes show that *Nasonia* uses novel mechanisms for patterning its DV axis, and we hoped to gain insights into the molecular bases of the differences by looking in more detail how these phenotypes come about.

*Nv-ventral nervous system defective* (*Nv-vnd*) is a marker of ventral ectoderm, and is expressed in stripes flanking the *Nv-twi* domain (Fig. 2A). In weak *Nv-Toll* knockdowns *Nv-twi* narrows (Fig. 2B), while *Nv-vnd* shifts in concert ventrally. In stronger knockdowns, *Nv-twi* and *Nv-vnd* retract from the poles (Fig. 2C). In some cases, *Nv-twi* is completely absent, and only a small patch of *Nv-vnd* remains (Fig. 2D). In the strongest, and by far most common case, both *Nv-twi*, and *Nv-vnd* are absent after *Nv-Toll* RNAi (not shown).

This behavior of *Nv-vnd* provides clues about the role of Toll signaling on the ventral side of the embryo. First, *Nv-vnd*, unlike *Nv-brk*, requires at least a minimal amount of Nv-Toll signaling for its expression. Second, *Nv-vnd* seems able to respond to lower levels of ventralizing influence, since it is always expressed further dorsally than *Nv-twi*. These results alone cannot distinguish whether *Nv-vnd* is directly sensing lower levels of Nv-Toll activity, or whether it is activated by a factor emanating from presumptive mesoderm. The fact that *Nv-vnd* expression is only seen well after the *Nv-twi* domain has been stably established is consistent with the latter possibility.

The almost complete ventralization of late blastoderm embryos after *Nv-dpp* RNAi (Fig. 1C) led us to examine the origin of this phenotype. Our previous analyses showed that ventral genes start from very narrow domains early (division cycles 10 & 11) and expand laterally until cycle 12 (demonstrated in detail in (7)). After *Nv-dpp* RNAi, all early embryos show narrow *Nv-twi* domains that are indistinguishable from wild-type (compare Fig. 2E to 2F, BMP knockdown is confirmed by absence of *Nv-zen*, and dorsal expansion of *Nv-brk*).

This demonstrates that the Nv-Toll dependent activation of *Nv-twi* is initially independent of the state of BMP signaling. It also shows that the *Nv-*



*dpp* pRNAi phenotypes seen at cycle 12 are the result of a dynamic process, as the mesoderm must expand massively from its initially narrow domain to eventually cover the entire embryo.

It is clear from intermediate phenotypes that BMP signaling has a strong influence on both the width of the *Nv-vnd* (compare Fig. 2G to 2C) domain, as well as the position of its dorsal edge (Fig. 2G and H). A similar strong input of BMP into the vertebrate *vnd* ortholog *Nkx2.2* has been described, as has a much weaker influence on fly *vnd* (13, 14). Subtle, but consistent differences in expansion of *Nv-twi* along the AP axis have also been observed (arrows in Fig. 2G, Fig. S1), which may indicate significant cross-talk between the axes, another hallmark of vertebrate systems (5).

These results show that patterning the ventral side of the *Nasonia* embryo involves a two-step process. First, narrow domains of genes such as *Nv-twi* are established in an Nv-Toll dependent manner in the early syncytial stage. The second phase is when the narrow domains expand and sharpen, and the later expressed lateral genes such as *Nv-vnd* are turned on. This phase is negatively regulated by BMP signaling, and indicates that robust ventral patterning is accomplished through a balance between dynamic, self-enhancing interactions among ventral genes and repressive BMP signaling emanating from the dorsal side (Fig. 4)

We next asked: what is the regulatory basis of the expansion of ventral fates in wild-type and *Nv-dpp* RNAi embryos in *Nasonia*?

If the Toll activity gradient itself were dynamic and increasing over time, one would expect all early, direct targets of Toll to expand laterally both in wild-type, and in BMP knockdown embryos. *Nv-cactus* (*Nv-cact*) is likely a direct target of Toll signaling, since: 1) its orthologs are conserved targets and components of Toll signaling (6, 15, 16), 2) its expression is lost in *Nv-Toll* RNAi (Fig. 2J), and 3) a highly significant cluster of Dorsal binding sites is found just upstream of its coding sequence (Fig. S2).

*Nv-cact* does not expand in *Nasonia* embryos, and remains as a narrow stripe at the ventral midline of the embryo (Fig 2I). When BMP is knocked



down, *Nv-cact* expression is unaffected, indicating both that Toll signaling is not increasing in BMP knockdown, and that *Nv-cact* (and thus *Nv-Toll* signaling) is not regulated by BMP signaling (Fig. 2K). This result supports the ideas that only a subset of ventral genes participate in the expansionary feedback loop, and that the loop is both independent of further Toll input, and negatively regulated by BMP signaling (Fig. 4).

Another striking feature of the *Nasonia* DV patterning system from our initial investigation is that *Nv-zen* expression at the dorsal midline is unaffected in Toll knockdown (Figure 1B), which is in contrast to *Drosophila*. We examined a more broadly expressed dorsal marker, *Nv-araucan* (*-ara*, Fig. 2L (7)), which should be more sensitive to subtle fluctuations in BMP activity, to see if there is any weak effect of *Nv-Toll* pRNAi. In all cases, *Nv-ara* appears normal (Fig 2M), even when it is apparent that *Nv-Toll* knockdown is strong (Fig. 2M').

Since *Nasonia* DV patterning depends so strongly on BMP signaling, we used a cross-reactive phosphorylated MAD antiserum to monitor the pattern of BMP activity (17, 18). pMAD is found in a broad, shallowly graded pattern in cycle 10 embryos (Fig. 3A). Over the next division cycle this gradient intensifies and becomes more dorsally restricted, and more obviously graded (Fig. 3B). By cycle 12 it is found in an intense stripe over the dorsal midline with a very sharp lateral borders (Fig. 3C). Eventually, the stripe narrows further and begins to disappear just prior to gastrulation (Fig. 3D).

This pattern is similar to *Drosophila*, in that the gradient of BMP activity starts relatively broad and flat, and then refines and intensifies, generating a high peak at the Dorsal midline (18). However, the transformation of BMP activity all occurs in cycle 14 in *Drosophila*, while the first clear asymmetry in BMP signaling is seen in cycle 10 in *Nasonia*, and the patterns evolves over the next two division cycles.

In *Drosophila* three genes directly regulated by Toll are required for BMP signaling: the ligand *dpp*, the inhibitor *short gastrulation* (*sog*), and the metalloprotease *tolloid* (*tld*) (19). *dpp* and *tld* are expressed in broad dorsal domains and are repressed by Dorsal, while *sog* is activated by Dorsal laterally.

Sog protein binds Dpp, inhibits its signaling, and facilitates its diffusion. Tld cleaves Sog, leading to its destruction, and frees Dpp to signal. The interactions among these and other BMP components are critical for the proper formation of the BMP signaling gradient, particularly the peak levels at the dorsal midline (19).

*Nv-dpp* is expressed maternally, and does not show spatial regulation until after gastrulation (not shown). In addition, no *sog* ortholog has been detected in any genome or transcriptome data set in *Nasonia* (7, 20). The very restricted anterior expression (Fig. 3E) and lack of patterning function of *Nv-tld* (tested by pRNAi, not shown) are also consistent with the absence of a Sog based transport system.

Other components are required for BMP signaling in *Drosophila*. One is *screw*, a highly diverged BMP 5/7 paralog related to *glass bottom boat* (*gbb*) (21). In *Nasonia*, *Nv-gbb* a BMP 5/7-like ligand is expressed maternally, and appears ubiquitously weak throughout early embryogenesis (not shown) and gives an identical pRNAi phenotype to *Nv-dpp* (Fig. 3F). Therefore, BMP signaling requires both *Nv-dpp* and *Nv-gbb* together to induce signaling in *Nasonia*, indicating that Nv-Dpp+Gbb heterodimers may be required for long range BMP signaling in the *Nasonia* embryo, while such heterodimers are only required for peak levels of signaling in *Drosophila* (21).

The BMP binding protein Twisted gastrulation (*Tsg*), has both positive and negative effects on BMP activity in *Drosophila* (22), and is required for peak levels of BMP signaling in the embryo. pRNAi against *Nv-tsg* gives identical phenotypes to *Nv-dpp* and *Nv-gbb*, indicating that *Nv-tsg* is also required for BMP signaling in *Nasonia* (Fig. 3G). An exclusively pro-BMP, *sog*-independent role for *tsg* was also observed in *Tribolium* (23).

Finally, the receptors *thickveins* (*tkv*) and *saxophone* (*sax*) are required for BMP signaling in *Drosophila* (21). We find that both are also required in *Nasonia*, but the lack of either one alone does not completely abrogate the signal (Fig. 3H, only *Nv-tkv* RNAi result shown).

We have shown here the first example of an insect that relies almost completely on BMP signaling for DV axis patterning (Fig. 4, right side). This BMP system is independent of Toll signaling, which is in stark contrast to the *Drosophila* paradigm, where crucial BMP components are regulated by Toll signaling (Fig. 4). We have also shown that Toll signaling induces only a narrow ventral expression domain of genes whose final pattern depends on a combination dynamic expansion, and BMP mediated repression (Fig. 4), rather than on any Toll-based gradient. These results suggest that the original embryonic patterning role for Toll in insects may have been simply to induce a single ventral fate, and that the Toll pathway usurped the ancestral role of BMP some time after the divergence of the Hymenoptera from the clade containing Coleoptera and Diptera.

Furthermore, while the dynamics of BMP signaling (pMAD) are similar between wasp and fly, we have shown that the molecular mechanisms producing the dynamics must be highly diverged, due to the absence of Sog and Tld function in *Nasonia*, the differing roles of Tsg and BMP 5/7 genes, and the lack of any *Nasonia* BMP component with clearly localized mRNA expression during the patterning phase. This shows that not only are the downstream regulatory networks targets of evolutionary change, but that the upstream signaling modules are also prone to significant alterations in the course of evolution.

#### References:

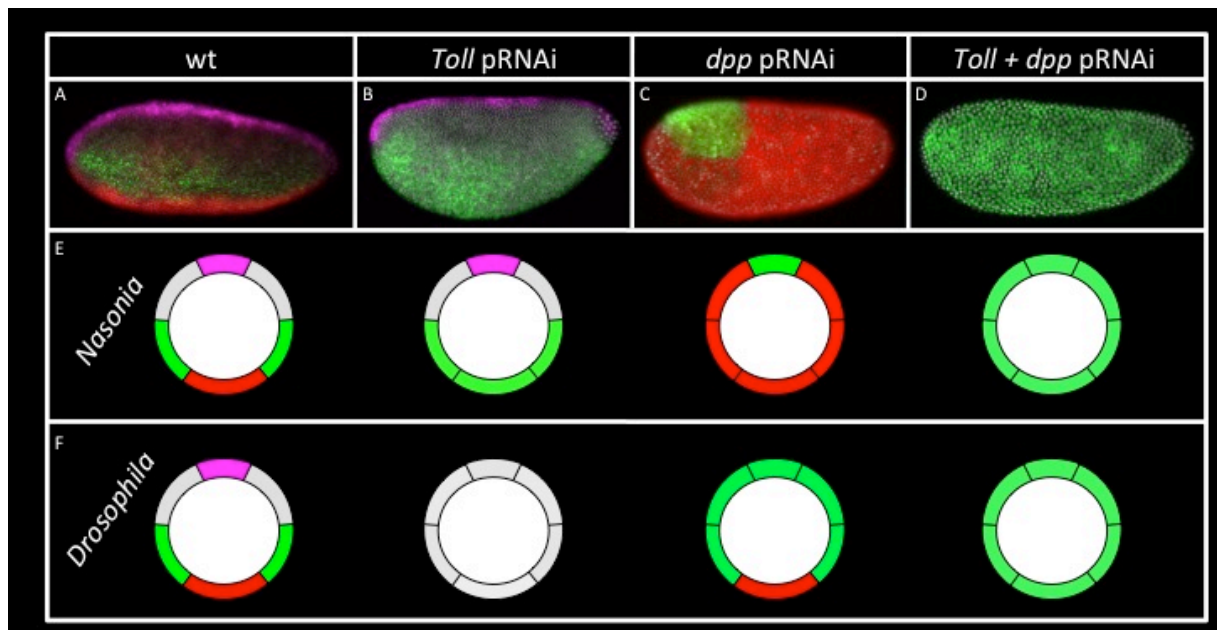
1. K. V. Anderson, L. Bokla, C. Nusslein-Volhard, Establishment of dorsal-ventral polarity in the *Drosophila* embryo: the induction of polarity by the Toll gene product. *Cell* 42, 791-798 (1985); published online EpubOct (0092-8674(85)90275-2 [pii]).
2. K. V. Anderson, G. Jurgens, C. Nusslein-Volhard, Establishment of dorsal-ventral polarity in the *Drosophila* embryo: genetic studies on the

- role of the Toll gene product. *Cell* 42, 779-789 (1985); published online EpubOct (0092-8674(85)90274-0 [pii]).
3. B. Moussian, S. Roth, Dorsoventral axis formation in the *Drosophila* embryo--shaping and transducing a morphogen gradient. *Curr Biol* 15, R887-899 (2005); published online EpubNov 8 (S0960-9822(05)01226-1 [pii] 10.1016/j.cub.2005.10.026).
  4. J. A. Lynch, S. Roth, The evolution of dorsal-ventral patterning mechanisms in insects. *Genes & development* 25, 107-118 (2011); published online EpubJan 15 (10.1101/gad.2010711).
  5. E. M. De Robertis, Evo-devo: variations on ancestral themes. *Cell* 132, 185-195 (2008); published online EpubJan 25 (10.1016/j.cell.2008.01.003).
  6. R. Nunes da Fonseca, C. von Levetzow, P. Kalscheuer, A. Basal, M. van der Zee, S. Roth, Self-regulatory circuits in dorsoventral axis formation of the short-germ beetle *Tribolium castaneum*. *Developmental cell* 14, 605-615 (2008); published online EpubApr (10.1016/j.devcel.2008.02.011).
  7. T. Buchta, O. Ozuak, D. Stappert, S. Roth, J. A. Lynch, Patterning the dorsal-ventral axis of the wasp *Nasonia vitripennis*. *Developmental biology* 381, 189-202 (2013); published online EpubSep 1 (10.1016/j.ydbio.2013.05.026).
  8. S. Roth, D. Stein, C. Nusslein-Volhard, A gradient of nuclear localization of the dorsal protein determines dorsoventral pattern in the *Drosophila* embryo. *Cell* 59, 1189-1202 (1989); published online EpubDec 22 (
  9. A. Jazwinska, C. Rushlow, S. Roth, The role of brinker in mediating the graded response to Dpp in early *Drosophila* embryos. *Development* 126, 3323-3334 (1999); published online EpubAug (
  10. K. A. Wharton, R. P. Ray, W. M. Gelbart, An activity gradient of decapentaplegic is necessary for the specification of dorsal pattern elements in the *Drosophila* embryo. *Development* 117, 807-822 (1993); published online EpubFeb (
  11. T. von Ohlen, C. Q. Doe, Convergence of dorsal, dpp, and egfr signaling pathways subdivides the *drosophila* neuroectoderm into three dorsal-

- ventral columns. *Developmental biology* 224, 362-372 (2000); published online EpubAug 15 (10.1006/dbio.2000.9789).
12. V. F. Irish, W. M. Gelbart, The decapentaplegic gene is required for dorsal-ventral patterning of the *Drosophila* embryo. *Genes & development* 1, 868-879 (1987); published online EpubOct (
  13. C. M. Mizutani, E. Bier, *EvoD/Vo*: the origins of BMP signalling in the neuroectoderm. *Nature reviews. Genetics* 9, 663-677 (2008); published online EpubSep (10.1038/nrg2417).
  14. J. Crocker, A. Erives, A Schnurri/Mad/Medea complex attenuates the dorsal-twist gradient readout at *vnd*. *Developmental biology* 378, 64-72 (2013); published online EpubJun 1 (10.1016/j.ydbio.2013.03.002).
  15. A. Hoffmann, A. Levchenko, M. L. Scott, D. Baltimore, The IkappaB-NF-kappaB signaling module: temporal control and selective gene activation. *Science* 298, 1241-1245 (2002); published online EpubNov 8 (10.1126/science.1071914298/5596/1241 [pii]).
  16. T. Sandmann, C. Girardot, M. Brehme, W. Tongprasit, V. Stolc, E. E. Furlong, A core transcriptional network for early mesoderm development in *Drosophila melanogaster*. *Genes & development* 21, 436-449 (2007); published online EpubFeb 15 (
  17. H. Tanimoto, S. Itoh, P. ten Dijke, T. Tabata, Hedgehog creates a gradient of DPP activity in *Drosophila* wing imaginal discs. *Mol Cell* 5, 59-71 (2000); published online EpubJan (S1097-2765(00)80403-7 [pii]).
  18. R. Dorfman, B. Z. Shilo, Biphasic activation of the BMP pathway patterns the *Drosophila* embryonic dorsal region. *Development* 128, 965-972 (2001); published online EpubMar (
  19. M. B. O'Connor, D. Umulis, H. G. Othmer, S. S. Blair, Shaping BMP morphogen gradients in the *Drosophila* embryo and pupal wing. *Development* 133, 183-193 (2006); published online EpubJan (
  20. J. H. Werren, S. Richards, C. A. Desjardins, O. Niehuis, J. Gadau, J. K. Colbourne, G. Nasonia Genome Working, J. H. Werren, S. Richards, C. A. Desjardins, O. Niehuis, J. Gadau, J. K. Colbourne, L. W. Beukeboom, C.

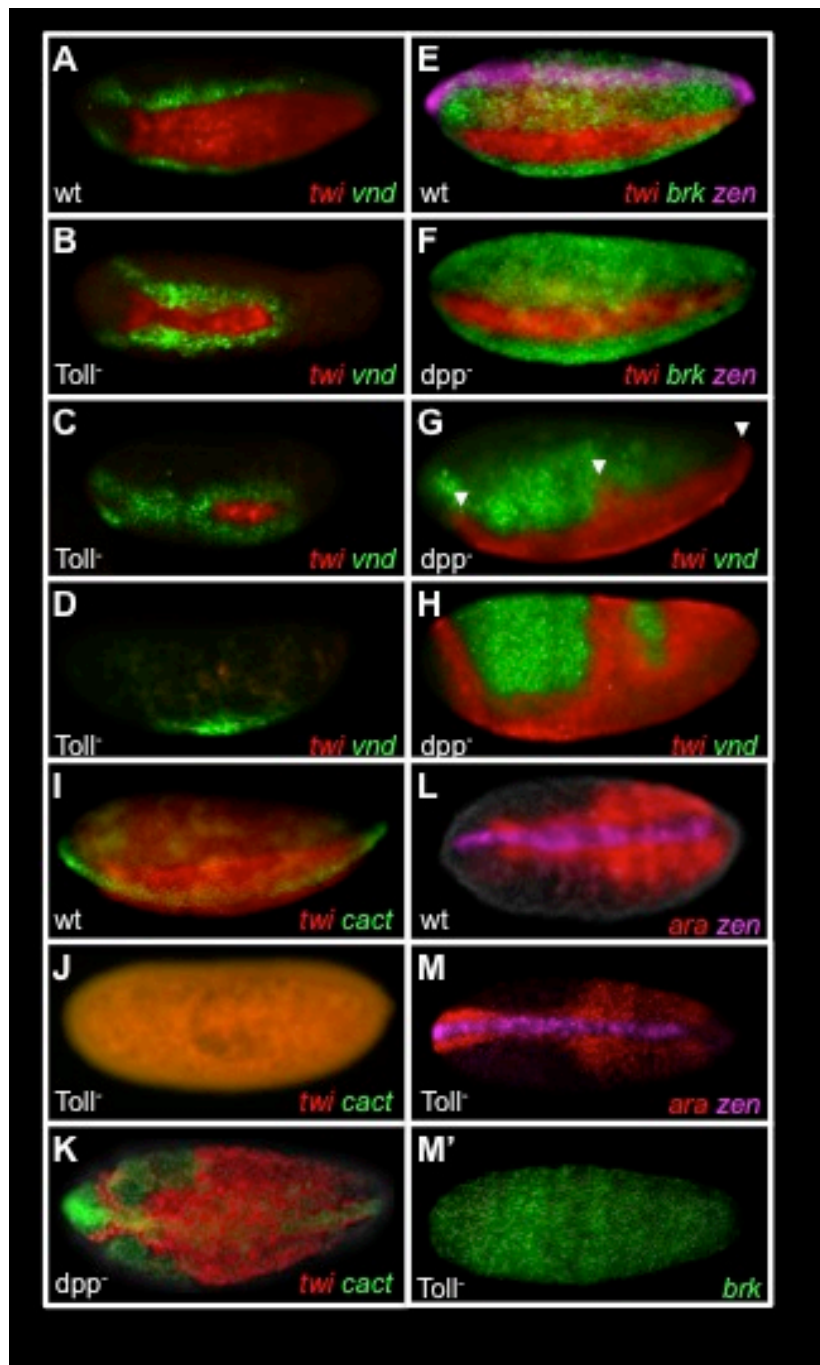
Desplan, C. G. Elsik, C. J. Grimmelikhuijzen, P. Kitts, J. A. Lynch, T. Murphy, D. C. Oliveira, C. D. Smith, L. van de Zande, K. C. Worley, E. M. Zdobnov, M. Aerts, S. Albert, V. H. Anaya, J. M. Anzola, A. R. Barchuk, S. K. Behura, A. N. Bera, M. R. Berenbaum, R. C. Bertossa, M. M. Bitondi, S. R. Bordenstein, P. Bork, E. Bornberg-Bauer, M. Brunain, G. Cazzamali, L. Chaboub, J. Chacko, D. Chavez, C. P. Childers, J. H. Choi, M. E. Clark, C. Claudianos, R. A. Clinton, A. G. Cree, A. S. Cristino, P. M. Dang, A. C. Darby, D. C. de Graaf, B. Devreese, H. H. Dinh, R. Edwards, N. Elango, E. Elhaik, O. Ermolaeva, J. D. Evans, S. Foret, G. R. Fowler, D. Gerlach, J. D. Gibson, D. G. Gilbert, D. Graur, S. Grunder, D. E. Hagen, Y. Han, F. Hauser, D. Hultmark, H. C. t. Hunter, G. D. Hurst, S. N. Jhangian, H. Jiang, R. M. Johnson, A. K. Jones, T. Junier, T. Kadowaki, A. Kamping, Y. Kapustin, B. Kechavarzi, J. Kim, J. Kim, B. Kiryutin, T. Koevoets, C. L. Kovar, E. V. Kriventseva, R. Kucharski, H. Lee, S. L. Lee, K. Lees, L. R. Lewis, D. W. Loehlin, J. M. Logsdon, Jr., J. A. Lopez, R. J. Lozado, D. Maglott, R. Maleszka, A. Mayampurath, D. J. Mazur, M. A. McClure, A. D. Moore, M. B. Morgan, J. Muller, M. C. Munoz-Torres, D. M. Muzny, L. V. Nazareth, S. Neupert, N. B. Nguyen, F. M. Nunes, J. G. Oakeshott, G. O. Okwuonu, B. A. Pannebakker, V. R. Pejaver, Z. Peng, S. C. Pratt, R. Predel, L. L. Pu, H. Ranson, R. Raychoudhury, A. Rechtsteiner, J. T. Reese, J. G. Reid, M. Riddle, H. M. Robertson, J. Romero-Severson, M. Rosenberg, T. B. Sackton, D. B. Sattelle, H. Schluns, T. Schmitt, M. Schneider, A. Schuler, A. M. Schurko, D. M. Shuker, Z. L. Simoes, S. Sinha, Z. Smith, V. Solovyev, A. Souvorov, A. Springauf, E. Stafflinger, D. E. Stage, M. Stanke, Y. Tanaka, A. Telschow, C. Trent, S. Vattathil, E. C. Verhulst, L. Viljakainen, K. W. Wanner, R. M. Waterhouse, J. B. Whitfield, T. E. Wilkes, M. Williamson, J. H. Willis, F. Wolschin, S. Wyder, T. Yamada, S. V. Yi, C. N. Zecher, L. Zhang, R. A. Gibbs, Functional and evolutionary insights from the genomes of three parasitoid *Nasonia* species. *Science* 327, 343-348 (2010); published online EpubJan 15 (10.1126/science.1178028).

21. O. Shimmi, D. Umulis, H. Othmer, M. B. O'Connor, Facilitated transport of a Dpp/Scw heterodimer by Sog/Tsg leads to robust patterning of the *Drosophila* blastoderm embryo. *Cell* 120, 873-886 (2005); published online EpubMar 25 (10.1016/j.cell.2005.02.009).
22. Y. C. Wang, E. L. Ferguson, Spatial bistability of Dpp-receptor interactions during *Drosophila* dorsal-ventral patterning. *Nature* 434, 229-234 (2005); published online EpubMar 10 (10.1038/nature03318).
23. R. Nunes da Fonseca, M. van der Zee, S. Roth, Evolution of extracellular Dpp modulators in insects: The roles of tolloid and twisted-gastrulation in dorsoventral patterning of the *Tribolium* embryo. *Developmental biology* 345, 80-93 (2010); published online EpubSep 1 (10.1016/j.ydbio.2010.05.019).



**Figure 1. Effects of *Toll*, *dpp*, and *Toll/dpp* double pRNAi.**

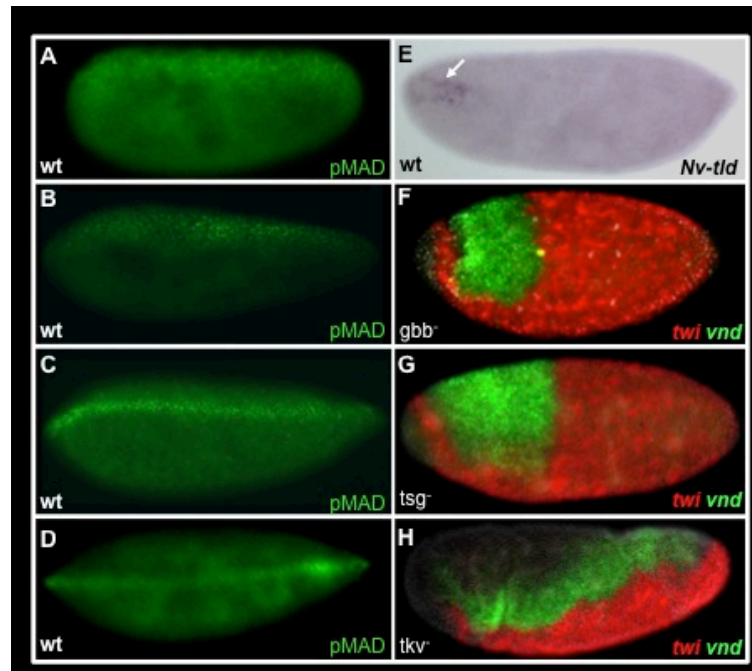
**A-D**, *Nv-zen* (purple), *-brk* (green) and *-twi* (red) expression in wild-type (A) *Nv-Toll* (B), *Nv-dpp* (C) and *Nv-Toll /dpp* (D) RNAi embryos. **E,F**, Schematic cross sections of *Nasonia* (E) and *Drosophila* (F) embryos corresponding to the four different conditions shown in (A-D) (Red=Mesoderm, Green=Neurectoderm, Grey=Dorsal ectoderm, and Magenta=extraembryonic).



**Figure 2. Detailed effects of *Nv-dpp* and *Nv-Toll* pRNAi**

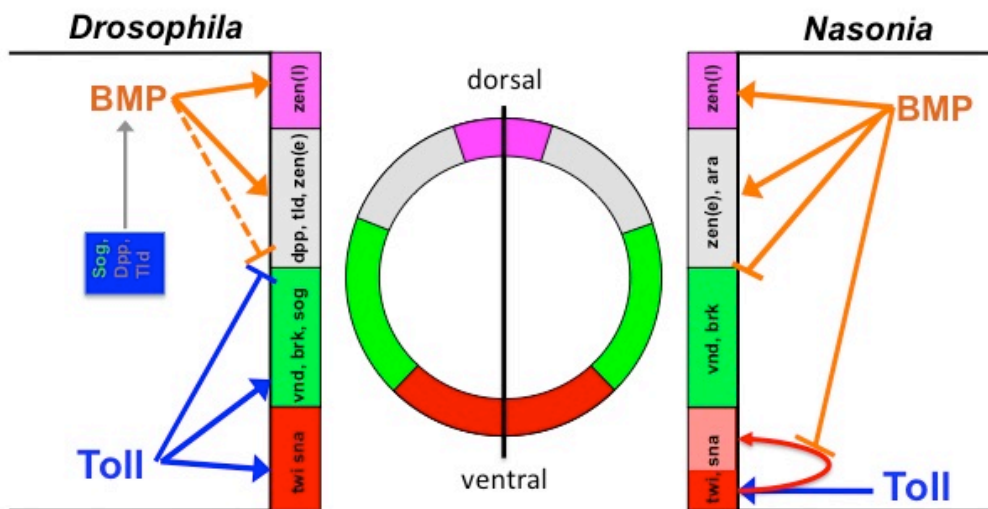
**A-D,G-H,** *Nv-vnd* (green), *Nv-twi* (red) expression in wild-type (A), *Nv-Toll* (B-D) and *Nv-dpp* (G,H) embryos. **E,F** *Nv-twi* (red), *Nv-brk* (green), *Nv-zen* (purple) expression in wild-type (E) and *Nv-dpp* (F) pRNAi embryos. **I-K,** *Nv-cact* (green) and *Nv-twi* (red) expression in wildtype (I), *Nv-Toll* (J) and *Nv-dpp* (K) pRNAi embryos. **L-M,** *Nv-ara* (red), *Nv-zen* (purple) expression in wild-type (L) and *Nv-Toll* RNAi (M) embryos. **M'** is a ventral view of the same embryo in **M** showing *Nv-brk* (green).





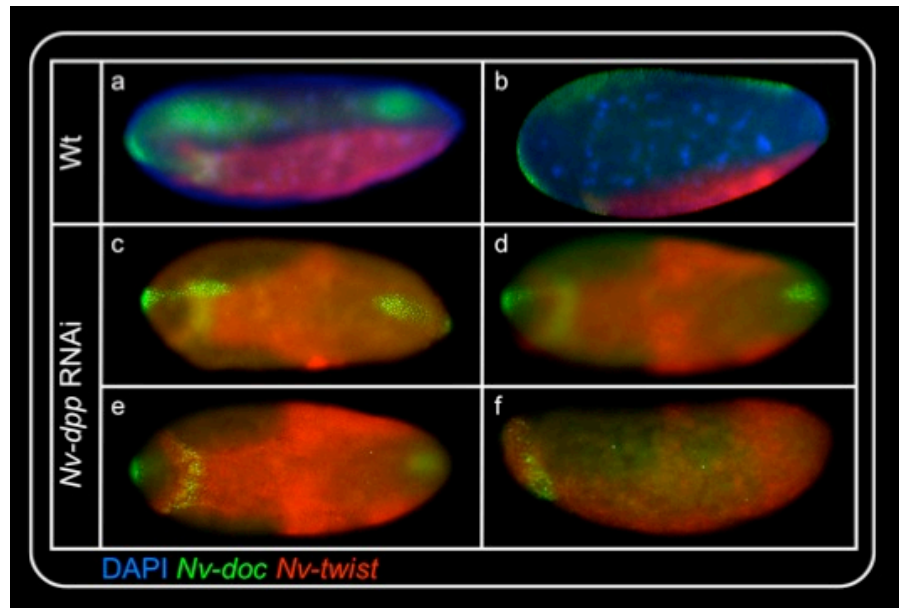
**Figure 3. BMP signaling in the *Nasonia* embryo.**

**A,B,C,D**, Distribution of pMAD (green), arranged from young (cycle 10, **A**) to old (late cycle 12, **D**). **E**, Expression of *Nv-tld* in late cycle 12. **F,H**, *Nv-twi* (red), *Nv-brk* (green) expression in *Nv-gbb* (**F**), *tsg* (**G**) and *tkv* (**H**) pRNAi embryos.



**Fig. 4 Relative roles of BMP and Toll signalling in *Drosophila* and *Nasonia* embryos.**

Summary of *Drosophila* Toll and BMP roles and regulation on left, *Nasonia* at right. Blue and orange arrows and lines indicate regulation by Toll and BMP, respectively. Factors in blue box on left indicate BMP signaling components whose transcription is directly regulated by Toll. Red curved arrow indicates self-activation of ventral genes. zen (e) and zen(l), indicate early and late zen expression, respectively.

Supplement:

**Figure S1. *Nasonia dorsocross* (*Nv-doc*) as a marker in *Nv-dpp* RNAi.**

**A-G,** *twi* (red) and *doc* (green) expression in wild-type (**A,B**) and *dpp* (**C-F**).  
**A**, dorso-lateral view; **C-E**, dorsal view; **B,F**, lateral view.

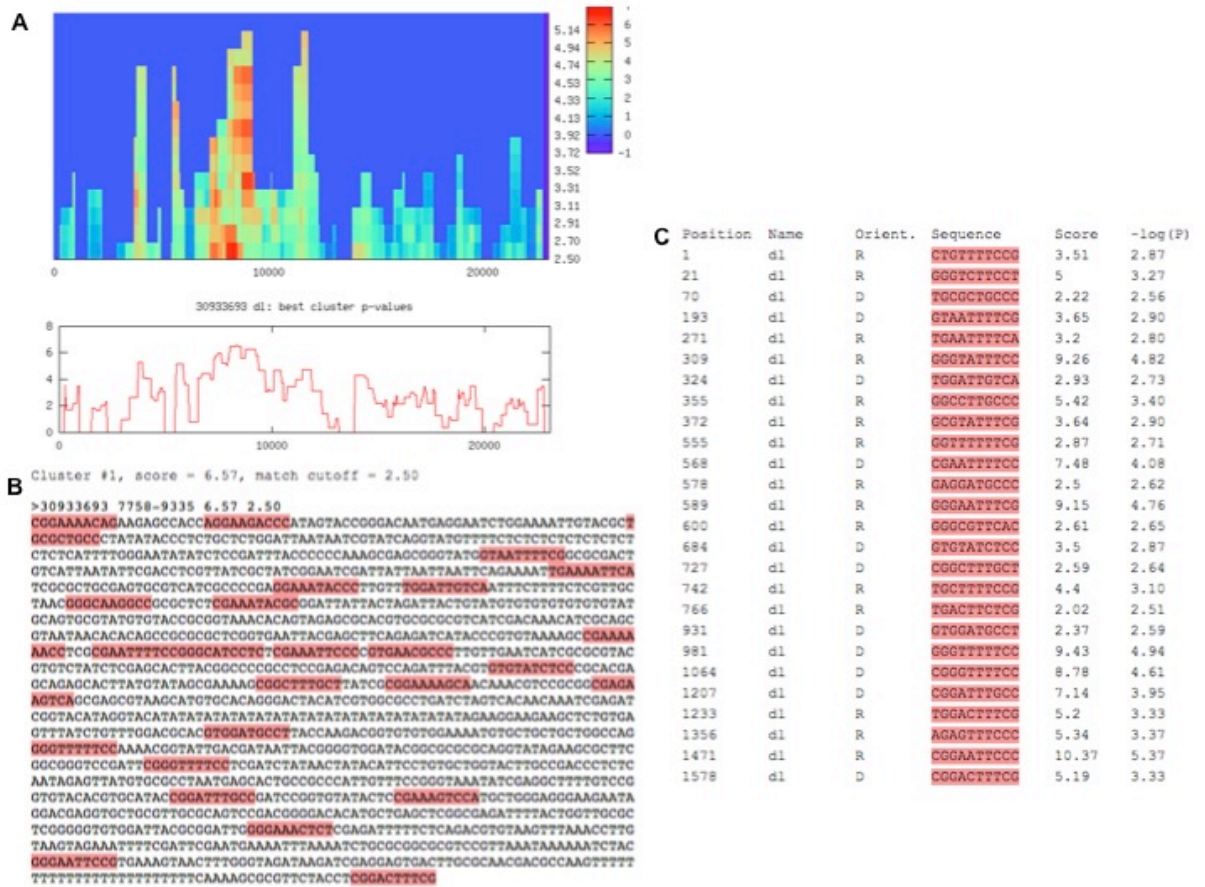


**Figure S2. Illustration of clustered Dorsal binding sites in the *Nv-cact* genomic region.** A genomic fragment including the *Nv-cact1* locus plus 10kb upstream and downstream was submitted to the Clusterdraw web server, using default parameters. Output of the highest scoring cluster is shown. **A).** Heatmap and histogram showing regions with clusters of high scoring Dorsal binding sites. Note that the strongest cluster is located just before the 10kb mark, which is the start of the *Nv-cact* coding locus. **B)** Distribution of Dorsal binding sites in best scoring cluster. **C).** Position and score (higher score~higher affinity) of Dorsal sites in best scoring cluster.

Materials and methods**Embryo collection**

All *N. vitripennis* embryos were collected using the *Waspinator* and fixed as described in [4].

**Double-Stranded RNA (dsRNA) primer**

<i>Toll (Toll)</i>	Fw	ggccgcggGAACTCGCCAAACTGGTCTC
	Rev	cccggggcAACGGATTGTTTCGTCAGCTC
<i>decapentaplegic (dpp)</i>	Fw	ggccgcgggTGGTGGGCGAGGCGGTAAA
	Rev	cccggggcCACGACCTTGTTCTCCTCGT
<i>glass bottom boat 1 (gbb1)</i>	Fw	ggccgcggATCCTGCTGCAGTTCGACTT
	Rev	cccggggcCCCTGATGATCATGTTGTGG

**In Situ hybridization (ISH) primer**

<i>cactus1 (cact1)</i>	Fw	ggccgcggACTTGGATATGGGCAAGTCG
	Rev	cccggggcCTACTGTCGCTGCTGCTGTC
<i>twist (twi)</i>	Fw	ggccgcgggCTTCTCGCCCAGTAACAAC
	Rev	cccggggcACGTTAGCCATGACCCTCTG
<i>ventral nervous system defective (vnd)</i>	Fw	ggccgcgggTCGGACTGCTCAACAACCTG
	Rev	cccggggcAGGTTCCAGGAGCTTCGACT
<i>brinker (brk)</i>	Fw	ggccgcggATCCAAAAGTGGCTCCAGTG
	Rev	cccggggcCTGAAAGTCGTGCTCCTCGT

<i>zerknüllt (zen)</i>	Fw	ggccgcggAAGTCGGCTCCTATTCAGCA
	Rev	cccggggcTAGGAATAGTGGCCCGAAGA
<i>araucaan (ara)</i>	Fw	ggccgcggCACCACCACCTTCTCATCCT
	Rev	cccggggcGCCCTTGTAGAACGGTTTGA
<i>dorsocross1 (doc1)</i>	Fw	ggccgcggATAAAATCGGCACCGAGATG
	Rev	cccggggcAAATAGGCAGCTGCAATGCT

### **RNAi**

Young *N. vitripennis* pupae were injected as in [3].

### **In Situ Hybridisation (ISH) and Immunohistochemistry (IHC)**

Two-color ISH was performed as described in [2]

Three-color ISH is a modified version of the two-color ISH and was performed in 4 days.

First day: Probe incubation using biotin-, fluorescein-, and dig labelled probes as described in [2].

Second day: Antibodies were incubated using  $\alpha$ -fluorescein::AP antibodies (1:2500),  $\alpha$ -digoxigenin::POD antibodies (1:100) and Mouse- $\alpha$ -biotin antibodies (1:100) as described in [2].

Third day: Staining reaction with Fast Red and HNPP (Roche) as substrates for  $\alpha$ -fluorescein::AP antibodies to give a red fluorescent signal with AlexaFluor 488 tyramide (Invitrogen) as a substrate  $\alpha$ -digoxigenin::POD antibodies as described in [2].

After staining reaction POD was destroyed by incubating embryos for 30 min in a 1% H<sub>2</sub>O<sub>2</sub> solution diluted in PBT. Antibody incubation using  $\alpha$ -mouse::POD (1:100) antibodies overnight.

Fourth day: Staining reaction with AlexaFluor 647 (Invitrogen) as substrate for  $\alpha$ -mouse::POD.

Immunohistochemistry was performed as described in [1]. Rabbit monoclonal antibody 41D10, raised against phospho-Smad 1/5, was obtained from Cell Signaling Sciences, and was used at 1:100. Secondary anti-rabbit::Alexa 568 was used at a concentration of 1:500

1. Patel, N.H. (1994). Imaging neuronal subsets and other cell types in whole mount *Drosophila* embryos and larvae using antibody probes. In *Methods in Cell Biology*, Volume 44, L.S.B. Goldstein and E. Fyrberg, eds. (New York: Academic Press).
2. Mazzone, E.O., Celik, A., Wernet, M.F., Vasiliauskas, D., Johnston, R.J., Cook, T.A., Pichaud, F., and Desplan, C. (2008). Iroquois complex genes induce co-expression of rhodopsins in *Drosophila*. *PLoS Biol.* 6, e97. 27.
3. Lynch, J.A., and Desplan, C. (2006). A method for parental RNA interference in the wasp *Nasonia vitripennis*. *Nat. Protoc.* 1, 486–494.
4. Buchta, T., Özüak, O., et al., Patterning the dorsal–ventral axis of the wasp *Nasonia vitripennis*. *Dev. Biol.* (2013), <http://dx.doi.org/10.1016/j.ydbio.2013.05.026>

## 2.3 Ancient and diverged TGF- $\beta$ signaling components in *Nasonia vitripennis*

Orhan Özüak\*, Thomas Buchta\*, Siegfried Roth, Jeremy A. Lynch

\*These authors contributed equally.

### **Abstract**

The TGF- $\beta$  signaling pathway and its modulators are involved in many aspects of cellular growth and differentiation in all metazoa. Although most of the core components of the pathway are highly conserved many lineage specific adaptations have been observed including changes regarding paralog number, presence and absence of modulators and functional relevance for particular processes. In the parasitic jewel wasp *Nasonia vitripennis* the Bone Morphogenetic Proteins (BMPs), one major subgroups the of the TGF- $\beta$  superfamily, play a more fundamental role in dorsoventral (DV) patterning than in all other insects studied so far. However, *Nasonia* lacks the BMP antagonist Short gastrulation/Chordin, which is essential for polarizing the BMP gradient along the DV axis in most bilaterian animals. Here, we present a broad survey of TGF- $\beta$  signaling in *Nasonia* with aim to detect other lineage specific peculiarities and to identify potential mechanisms, which explain how BMP-dependent DV patterning occurs in the early *Nasonia* embryo in the absence of Sog.

### **Introduction**

The TGF- $\beta$  signaling pathway controls various processes throughout development, which include dorsoventral axis specification, cell proliferation, appendage formation as well as central nervous system patterning (1, 2). It consists of the extracellular ligands and their modulators, which interact with each other to control ligand availability and distribution, of the receptors and of intracellular components, which assure signaling transduction and target gene expression (1, 3).



Most of the ligands belong to either the Bone Morphogenetic Protein (BMP) subfamily or the Activin/TGF- $\beta$  subfamily (4, 5). Around 30 TGF- $\beta$  ligands have been described in vertebrates and 7 for *Drosophila* and *Tribolium* (6, 7). Decapentaplegic (Dpp), Glass bottom boat (Gbb) and Screw (Scw) are the BMPs in *Drosophila* (8-10). Activin (Act), Activin-like protein 23b, which is also called Dawdle (Daw), and Myoglianin (Myo) belong to the Activin/TGF- $\beta$  subfamily (11-13). Maverick (Mav) is highly diverged, and is not easily placed into either of the ligand subfamilies (14).

All TGF- $\beta$  ligands form dimers and bind to a heteromeric receptor complex of two type I and two type II serine-threonine kinase receptors (3). In *Drosophila* the BMPs as well as the Activins use Punt as a common type II receptor, while specificity is generated by the type I receptors. BMP ligands bind the type I receptors Thickveins (Tkv) and Saxophone (Sax), whereas Activin/TGF- $\beta$  ligands signal through the type I receptor Baboon (Babo) (1).

Upon ligand binding, the type I receptors become phosphorylated, which in turn phosphorylate and thereby activate receptor-regulated SMADs (R-SMADs). Tkv and Sax activate Mothers against Dpp (Mad) and Babo activates Smad on X (Smox). Once phosphorylated, R-Smads bind to the Co-Smad Medea and form a complex that translocates into the nucleus where they regulate target gene expression (1).

Inhibitory SMADs such as Daughters against Dpp (Dad) in *Drosophila* can compete with Medea and bind to R-Smads, thereby inhibiting translocation and target gene regulation (1).

On the extracellular level, a large variety of modulators are involved in controlling ligand availability and distribution. A prominent group of modulators, which usually act as BMP antagonists are characterized by an array of conserved cysteine-rich domains that form cysteine knot structures (15). On the basis of spacing of the cysteine residues within the cysteine ring they have been grouped into several subgroups, e.g. the Noggin family, the Chordin family, the Twisted gastrulation-like proteins, the Crossveinless 2 and the Dan family (15). In *Drosophila*, the main BMP antagonist in dorsoventral patterning is the

Chordin homolog Short gastrulation (Sog), which interacts with Twisted gastrulation and is cleaved by the metalloprotease Tolloid (16).

Besides diffusible, secreted proteins several membrane-bound and extracellular matrix proteins have been shown to influence the efficiency of TGF- $\beta$  signaling (17). Thus, in the *Drosophila* wing two glypicans, the GPI anchored Heparan-Sulphate Proteoglycans Dally and Dally-like are required for efficient BMP signaling activity (18) while type IV collagens control the range of the BMP signaling gradient in the embryo (19).

In our previous work we showed that the parasitic jewel wasp *Nasonia vitripennis* uses the BMP pathway to pattern the DV axis despite the fact that no *sog* ortholog is present in *Nasonia* (Özüak et al, unpublished). The main goal of this work is to provide an overview of the TGF- $\beta$  pathway in *Nasonia* and to identify components, which might help to explain how the BMP signaling gradient is established during DV patterning in the wasp embryo.

Similar work was already done for the short germ beetle *Tribolium castaneum*, which revealed that the beetle retained a more ancestral composition of TGF- $\beta$  signaling components compared to *Drosophila* (7, 20, 21).

In this work we describe, members of all different signaling components for the wasp. Interestingly, we found a case of parallel evolution, involving the duplication and divergence of the BMP 5/6/7/8 ligands in *Nasonia* and *Drosophila*. In addition we identified the BMP ligand ADMP, which is not present in *Drosophila* and *Tribolium*, but plays an important role in vertebrates (22). As we were unable to find a *sog* homolog in *Nasonia* we were especially interested to identify alternative BMP antagonists, which might be expressed at the ventral side of the embryo. However, we failed to identify such inhibitors corroborating our functional studies which indicated that the DV BMP gradient of *Nasonia* is not shaped by an opposing inhibitory gradient, but rather by diffusion from a dorsal source region (Özüak et al. unpublished). Interestingly, the RNA of the type I receptor Tkv is localized to the dorsal midline of the developing *Nasonia* oocyte. In addition, one of the type II receptors is dorsally expressed in the early embryo. Based on these observations we discuss a

possible scenario of how the embryonic BMP gradient in *Nasonia* is established in the absence of a ventral inhibitor.

## Results/Discussion:

### Ligands

So far seven TGF- $\beta$  ligands are described in *Drosophila* and *Tribolium*. In the wasp *Nasonia* we found eight potential TGF- $\beta$  ligands in the genome. In our previous work we described the important role of *Nv-dpp* in patterning the dorsal-ventral axis of the wasp embryo (Özüak et al. unpublished). Knocking down *Nv-dpp* leads to the loss of dorsal fates and an almost complete ventralization of the embryo. In our phylogenetic analysis, *Nv-dpp* groups perfectly with other insect Dpp sequences as well as their vertebrate homologs Bmp2/4 (Fig. 1A). During oogenesis *Nv-dpp* is expressed in the nurse cells and localized at the posterior pole of the oocyte (Fig. 2A). In the early embryo, *Nv-dpp* is ubiquitously expressed and after gastrulation is completed, it is expressed in two stripes that flank the extraembryonic region on the dorsal side of the embryo (Fig. 1 B, C).

Another important ligand for embryonic DV patterning in *Drosophila* is Screw, which represents a diverged paralog of Gbb (8, 10). *Drosophila* Gbb plays no role in DV patterning, but is required in later developmental processes such as wing formation (16). We found two paralogs of Nv-Gbb, but unlike in *Tribolium*, where both Gbb paralogs are closer related to each other than to any other Gbb (7), the *Nasonia* Gbb paralogs are not closely related. Instead, Nv-Gbb1 groups together with other insect Gbbs and the vertebrate homologs Bmp 5/6/7/8, while Nv-Gbb2 shows signs of a very fast evolving gene such as *Drosophila screw*. Both genes are ubiquitously expressed during oogenesis as well as during early embryogenesis (Fig 1 D, F; Fig. 2 B, C). After gastrulation *Nv-gbb1* is expressed like *Nv-dpp* in two stripes at the dorsal side (Fig 1 E), while *Nv-gbb2* expression is gone. The knockdown of Nv-Gbb2 leads, like the

knockdown of Nv-Dpp to a ventralization of the embryo (Özüak et al. unpublished). Interestingly, the knockdown of Nv-Gbb1 has no embryonic phenotype, suggesting that it plays no role in early embryonic DV patterning. It might however play a role in later embryonic or in postembryonic stages, which we could not, targeted by parental RNAi. Thus, the situation might be similar to *Drosophila* where one Bmp 5/6/7/8 paralog (*screw*) was subject to fast evolutionary changes adapting to the special requirements of early embryonic DV patterning while the other one (*gbb*) retaining ancestral sequence features is required for later (more generic) developmental processes.

ADMP (anti-dorsalizing morphogenetic protein) has a BMP-like activity in *Xenopus* (22). Despite its important role in vertebrates during D-V patterning, ADMP is not present in *Drosophila* and *Tribolium*. However, it is present in the Honeybee and we found an ortholog of ADMP in the wasp (Fig 1 A). It will be interesting to further investigate ADMP function in *Nasonia* to see if it also plays a role in self-regulation during embryonic D-V patterning.

Orthologs of ligands belonging to the Activin subfamily such as *act*, *daw*, and *myo* are found in *Nasonia*. All three are ubiquitously expressed in the early embryo and later no expression is detectable (Fig 1G-I). The last of the eight detected ligands is Maverick, which is not clearly grouped into one of the two large subfamilies. In *Drosophila*, Mav is required for growth in the wing disc. A knockdown of Mav leads to wing size reduction with normal veins pattern (23). We investigated the expression pattern of *Nv-mav* and found out that there is no expression in the early embryo, but later after completion of gastrulation *Nv-mav* is expressed in two very narrow stripes flanking the extraembryonic region on the dorsal side (Fig 1 J, K).

## Receptors

The extracellular BMP signal is transmitted via tetrameric receptor complexes formed by type I and type II receptors. Altogether our analyses revealed six *Nasonia* orthologs of *Drosophila* Serine-Threonine kinase receptors: two BMP

type I receptors, *tkv* and *sax*, and the Activin receptor type I ortholog *babo* as well as type II receptors *wishful thinking* (*wit*) and two *punt* orthologs (Fig 3A). Aside from these receptors we also found BAMBI (not shown), which in vertebrates is known to be a pseudo receptor (24) and might play a role in inhibiting BMP signaling in *Nasonia* as well .

*Nv-sax* is ubiquitously expressed in the nurse cells and ubiquitously distributed in the oocyte (Fig 2D). *Nv-tkv* is also expressed in all nurse cells. However, in the oocyte, it shows a striking pattern of localization. Besides an anterior accumulation the RNA is found in a narrow stripe along the dorsal midline (Fig. 2G-I). The dorsal side can be identified via the position of the oocyte nucleus. (data not shown, (25)). Thus, *Nv-tkv* RNA localization during oogenesis closely resembles that of the *Nv-tgf- $\alpha$* , which is involved in establishing the DV axis in *Nasonia* (25). In early embryos *Nv-tkv* is no longer localized and shows like *Nv-sax* ubiquitous expression (Fig. 3B, C). Knock down of both receptors using pRNAi has been performed in previous studies and resulted in the case of *Nv-sax* as well as *Nv-tkv* in a strong ventralization of the embryo (Özüak et al unpublished).

Similar to the type I receptors, *Nv babo* shows a uniform expression pattern in early *Nasonia* embryos (Fig. 3D). The presence of a *babo* homolog in *Nasonia* is interesting since previous studies on *Apis mellifera* revealed a lack of this gene (7), indicating that the loss of Activin signaling via Baboon is not a general feature of the hymenoptera.

Furthermore, two homologous genes of the type II receptor Punt are present. *punt1* is not expressed during oogenesis (Fig 2E) However, it shows a distinct expression pattern along the dorsal midline in early blastoderm embryos (Fig. 3E), which strongly resembles the early expression patterns of previously described BMP signaling target genes in *Nasonia* (26).

In contrast to this, *punt2* is expressed during oogenesis and is localized at the posterior pole of the oocyte (Fig. 2F). This localization is not present in the embryo where *punt2* mRNA is distributed ubiquitously (Fig. 3F). Because of its maternal distribution, we knocked down *punt2*. Eclosed females that were

injected with *punt2* dsRNA during yellow pupae stage, laid no eggs and had degenerated ovaries (data not shown). This phenotype could be due to defects in Activin or BMP signaling as *punt2* might be essential for both pathways.

### Smads

SMADs are characterized by the presence of two Mad Homology (MH1 and MH2) domains. In addition, R-Smads have a C-terminal SXS motif. Upon ligand binding, the receptors pass on the signal by phosphorylating both serines in the SXS motif thereby activating the R-Smads (27). We identified four proteins with a MH1 and MH2 domain in the *Nasonia* genome, three of which contained a SXS motif (Fig. S1). Phylogenetic analysis revealed that two of the SXS motif containing proteins group together with *Drosophila* Mad and the third one with *Drosophila* Smox (Fig. 4A). It is worth mentioning that Nv-Mad2 is, similar to Nv-Gbb2 and Nv-Punt1, significantly more diverged in comparison to Nv-Mad1 and the other insect Mad orthologs. The fourth identified protein displayed clear homology to the Co-Smad Medea (Fig 4A). We could not identify any orthologs of known inhibitory Smads like Daughters against dpp (Dad).

During oogenesis *Nv-mad1* is ubiquitously expressed in the nurse cells and oocytes while *Nv-mad2* RNA accumulates at the posterior pole of the oocyte (Fig. 2J,K). *Nv-mad1* does not seem to have a conserved role in embryogenesis since it did not show any phenotype after pRNAi mediated knockdown. However, embryos of females injected with *Nv-mad2* dsRNA were severely ventralized as seen from the expansion of the ventral *twist* domain (Fig. 4C). This phenotype closely resembles the previously described knockdown phenotype of *Nv-dpp* and *Nv-gbb2* (Özüak et al unpublished).

*Nv-smox* is ubiquitously expressed during oogenesis (Fig. 2L) and pRNAi mediated knockdown resulted in sterile females (not shown) indicating an important role of Activin signaling during oogenesis. The *Nv-smox* phenotype

suggests that the sterility caused by *Nv-punt2* knockdown is due to interference with Activin, rather than BMP signaling.

### **TGF- $\beta$ modulators**

At the extracellular level, the TGF- $\beta$  pathway is influenced in many ways to fine tune ligand and receptor activity. While antagonists bind to ligands and inhibit them, cell surface proteins modulate the flux of the ligands (17). In our previous work we provided evidence that *Nasonia* is lacking *sog*, which is the main BMP antagonist in *Drosophila* and other insects. Sog belongs to the Chordin family, one of the subgroups of BMP antagonists. We searched for orthologs of other groups such as Noggin or members of the Dan family. While in *Tribolium* two members of the Dan family, Dan and Gremlin, are present, no orthologs of members of the Dan family nor Noggin are present in the *Nasonia* genome. However, like in *Drosophila* and *Tribolium* we found an ortholog of Follistatin, which preferentially antagonizes Activin rather than BMP (28). In *Nasonia*, *follistatin* is ubiquitously expressed during early embryogenesis and later after gastrulation in two narrow stripes that flank the extraembryonic region on the dorsal side of the embryo (Fig 5. A, E)

Despite the absence of *sog* three *Nasonia* orthologs of Twisted gastrulation/Crossveinless1 (*Nv-Cva-c*) were discovered in an earlier study (21). In *Drosophila* Tsg is thought to be a part of the Sog–Dpp complex. In this complex Tsg can have a pro- as well as an anti-BMP function. It was suggested that Tsg acts anti-BMP by enhancing the binding of Sog to Dpp and pro-BMP by enhancing the cleavage of Sog by the metalloprotease Tolloid (16). In our previous studies with *Nasonia* using *Nv-tsg1* pRNAi a pro BMP role for Tsg during embryogenesis was observed since embryos of injected females were severely ventralized (Özüak et al, unpublished). An exclusively pro BMP role for Tsg was also observed in *Tribolium castaneum* (21). Interestingly, this pro-BMP function of Tc-Tsg was described to be Sog independent. Since *Nasonia* apparently lacks Sog, the pro-BMP function of Tsg in *Nasonia* should also be Sog-independent.



Finally, we were able to identify four Crossveinless 2 like molecules (Cv2a- Cv2d) (Fig. 5Q). Cv2 proteins consist of similar domains as Sog/chordin proteins, but are thought to tightly interact with the type I receptors and /or membrane anchored proteoglycans and therefore lack diffusibility (29). *cv2c* and *cv2d* show a uniform expression in early *Nasonia* blastoderm embryos and weak uniform expression during later embryonic development (Fig.5 C,D,G,H). *cv2a* is first expressed in small patches on the dorsal side at cellularized blastoderm stage (Fig 5B). During development these patches widen towards the anterior and elongate towards posterior. At the onset of gastrulation *cv2A* is expressed in two narrow stripes flanking the presumptive serosa (Fig. 5F). We were not able to clone *cv2b* indicating that this gene might be a pseudogene, or is expressed only during postembryonic development.

Besides the antagonists we found several orthologs of cell surface proteins that are candidates for modulating the flux of BMP ligands and facilitating long range signaling activity. Among these are orthologs of Dally, Glypican4, CollagenIV and Pentagone (17, 30). In early blastoderm embryos all are ubiquitously expressed (Fig. 5I-L). Later, after gastrulation is completed, all of them show a distinct pattern. *Nv-dally* is expressed in a dotted pattern of two stripes flanking the ventral midline (Fig. 5M). *Nv-glypican4* is expressed in segmental stripes on the ventral half of the embryo (Fig. 5N). *Nv-collagenIV* is expressed in small patches at the anterior and posterior of the embryo (Fig. 5O). The expression pattern of *Nv-pentagone*, two ventral stripes, resembles strongly that of *Nv-ind*, a neuroectodermal marker, which we described in our previous work (Fig. 5P) (26).

Taken together this work indicates that *Nasonia* has retained some components of an ancestral TGF- $\beta$  signaling network, such as ADMP and Bambi that have been lost in other insect lineages (7). However, *Nasonia* also shows high degrees of divergence in some key signaling components with essential functions for embryonic DV patterning like Gbb2, Mad2 and Punt1. The most striking observation is that *Nasonia* has lost some families of BMP antagonists including Sog, which plays a crucial in DV patterning in most

bilaterian animals (31). Our earlier work indicates that *Nasonia* indeed radically deviates from the mode of DV patterning found in most other animals. Apparently, *Nasonia* establishes its DV axis in a bipolar fashion using independent signaling sources along the ventral and dorsal midline (Özüak et al., unpublished). These signaling sources are established during oogenesis. The oocytes of *Nasonia* like those of *Apis*, the other hymenopteran species studied so far, show an amazing ability to precisely localize mRNAs not only to the anterior and posterior poles (Fig. 2AG), but also along the dorsal midline (25, 32, 33). Thus, in *Nasonia* and *Apis* the RNA of TGF- $\alpha$  is localized in narrow dorsal stripe and the secreted TGF- $\alpha$  ligand initiates EGF signaling at the dorsal side of the follicular epithelium along the entire egg length (25, 34). In *Nasonia* functional studies show that EGF signaling negatively regulates the formation of eggshell cues required to localize a ventral source for embryonic DV patterning (25). However, both hymenopteran species are also able to localize the RNA for BMP signaling components along the dorsal midline of the oocyte. For *Apis* the RNA of the ligand Dpp is localized (34) while in *Nasonia* as shown in this study the RNA of the type I receptor Tkv is localized. If proteins produced by these localized RNAs are inserted into the membrane and remain there until egg deposition and early embryogenesis they might become sources for establishing signaling gradients in the embryo. In this context our finding is interesting that one of the type II receptors *punt1* is expressed along the dorsal midline in early embryos. This indicates that in *Nasonia* a positive feedback of BMP signaling is established along the dorsal midline at early stages of development. Further studies are required to investigate whether maternal receptor localization coupled to zygotic positive feedback are sufficient to account for the long range BMP gradient from which we have shown earlier that it is crucial for patterning the entire DV axis of the embryo (Özüak et al., unpublished).

References:

1. L. Parker, D. G. Stathakis, K. Arora, Regulation of BMP and activin signaling in *Drosophila*., *Prog. Mol. Subcell. Biol.* 34, 73–101 (2004).
2. H. Chang, C. W. Brown, M. M. Matzuk, Genetic analysis of the mammalian transforming growth factor-beta superfamily., *Endocr. Rev.* 23, 787–823 (2002).
3. C. Sieber, J. Kopf, C. Hiepen, P. Knaus, Recent advances in BMP receptor signaling., *Cytokine Growth Factor Rev.* 20, 343–55 (2009).
4. Y. Yamamoto, M. Oelgeschläger, Regulation of bone morphogenetic proteins in early embryonic development., *Naturwissenschaften* 91, 519–34 (2004).
5. A. P. Hinck, Structural studies of the TGF- $\beta$ s and their receptors - insights into evolution of the TGF- $\beta$  superfamily., *FEBS Lett.* 586, 1860–70 (2012).
6. B. Schmierer, C. S. Hill, TGFbeta-SMAD signal transduction: molecular specificity and functional flexibility., *Nat. Rev. Mol. Cell Biol.* 8, 970–82 (2007).
7. M. Van der Zee, R. N. da Fonseca, S. Roth, TGFbeta signaling in *Tribolium*: vertebrate-like components in a beetle., *Dev. Genes Evol.* 218, 203–13 (2008).
8. K. Arora, M. S. Levine, M. B. O'Connor, The screw gene encodes a ubiquitously expressed member of the TGF-beta family required for specification of dorsal cell fates in the *Drosophila* embryo., *Genes Dev.* 8, 2588–601 (1994).
9. R. W. Padgett, R. D. St Johnston, W. M. Gelbart, A transcript from a *Drosophila* pattern gene predicts a protein homologous to the transforming growth factor-beta family., *Nature* 325, 81–4 (1987).
10. K. A. Wharton, G. H. Thomsen, W. M. Gelbart, *Drosophila* 60A gene, another transforming growth factor beta family member, is closely related

- to human bone morphogenetic proteins., *Proc. Natl. Acad. Sci. U. S. A.* 88, 9214–8 (1991).
11. G. Kutty et al., Identification of a new member of transforming growth factor-beta superfamily in *Drosophila*: the first invertebrate activin gene., *Biochem. Biophys. Res. Commun.* 246, 644–9 (1998).
  12. L. Parker, J. E. Ellis, M. Q. Nguyen, K. Arora, The divergent TGF-beta ligand Dawdle utilizes an activin pathway to influence axon guidance in *Drosophila*., *Development* 133, 4981–91 (2006).
  13. P. C. Lo, M. Frasch, Sequence and expression of myoglianin, a novel *Drosophila* gene of the TGF-beta superfamily., *Mech. Dev.* 86, 171–5 (1999).
  14. M. Nguyen, L. Parker, K. Arora, Identification of maverick, a novel member of the TGF-beta superfamily in *Drosophila*., *Mech. Dev.* 95, 201–6 (2000).
  15. D. W. Walsh, C. Godson, D. P. Brazil, F. Martin, Extracellular BMP-antagonist regulation in development and disease: tied up in knots., *Trends Cell Biol.* 20, 244–56 (2010).
  16. M. B. O'Connor, D. Umulis, H. G. Othmer, S. S. Blair, Shaping BMP morphogen gradients in the *Drosophila* embryo and pupal wing., *Development* 133, 183–93 (2006).
  17. M.-C. Ramel, C. S. Hill, Spatial regulation of BMP activity., *FEBS Lett.* 586, 1929–41 (2012).
  18. J. L. Erickson, Formation and maintenance of morphogen gradients: an essential role for the endomembrane system in *Drosophila melanogaster* wing development., *Fly (Austin)*. 5, 266–71 (2011).
  19. H. L. Ashe, Type IV collagens and Dpp: positive and negative regulators of signaling., *Fly (Austin)*. 2, 313–5 (2008).
  20. M. van der Zee, O. Stockhammer, C. von Levetzow, R. Nunes da Fonseca, S. Roth, Sog/Chordin is required for ventral-to-dorsal Dpp/BMP

- transport and head formation in a short germ insect., *Proc. Natl. Acad. Sci. U. S. A.* 103, 16307–12 (2006).
21. R. Nunes da Fonseca, M. van der Zee, S. Roth, Evolution of extracellular Dpp modulators in insects: The roles of tolloid and twisted-gastrulation in dorsoventral patterning of the *Tribolium* embryo., *Dev. Biol.* 345, 80–93 (2010).
  22. B. Reversade, E. M. De Robertis, Regulation of ADMP and BMP2/4/7 at opposite embryonic poles generates a self-regulating morphogenetic field., *Cell* 123, 1147–60 (2005).
  23. C. F. Hevia, J. F. de Celis, Activation and function of TGF $\beta$  signalling during *Drosophila* wing development and its interactions with the BMP pathway., *Dev. Biol.* 377, 138–53 (2013).
  24. D. Onichtchouk et al., Silencing of TGF-beta signalling by the pseudoreceptor BAMBI., *Nature* 401, 480–5 (1999).
  25. J. A. Lynch, A. D. Peel, A. Drechsler, M. Averof, S. Roth, EGF signaling and the origin of axial polarity among the insects., *Curr. Biol.* 20, 1042–7 (2010).
  26. T. Buchta, O. Ozüak, D. Stappert, S. Roth, J. a Lynch, Patterning the dorsal-ventral axis of the wasp *Nasonia vitripennis*., *Dev. Biol.* , 1–14 (2013).
  27. X.-H. Feng, R. Derynck, Specificity and versatility in tgf-beta signaling through Smads., *Annu. Rev. Cell Dev. Biol.* 21, 659–93 (2005).
  28. J. Pentek, L. Parker, A. Wu, K. Arora, Follistatin preferentially antagonizes activin rather than BMP signaling in *Drosophila*., *Genesis* 47, 261–73 (2009).
  29. A. L. Ambrosio et al., Crossveinless-2 Is a BMP feedback inhibitor that binds Chordin/BMP to regulate *Xenopus* embryonic patterning., *Dev. Cell* 15, 248–60 (2008).
  30. R. Vuilleumier et al., Control of Dpp morphogen signalling by a secreted feedback regulator., *Nat. Cell Biol.* 12, 611–7 (2010).

31. C. M. Mizutani, E. Bier, *EvoD/Vo: the origins of BMP signalling in the neuroectoderm.*, *Nat. Rev. Genet.* 9, 663–77 (2008).
32. J. A. Lynch, A. E. Brent, D. S. Leaf, M. A. Pultz, C. Desplan, *Localized maternal orthodenticle patterns anterior and posterior in the long germ wasp Nasonia.*, *Nature* 439, 728–32 (2006).
33. M. J. Wilson, P. K. Dearden, *RNA localization in the honeybee (Apis mellifera) oocyte reveals insights about the evolution of RNA localization mechanisms.*, *Dev. Biol.* 375, 193–201 (2013).
34. M. J. Wilson, H. Abbott, P. K. Dearden, *The evolution of oocyte patterning in insects: multiple cell-signaling pathways are active during honeybee oogenesis and are likely to play a role in axis patterning.*, *Evol. Dev.* 13, 127–37 (2011).

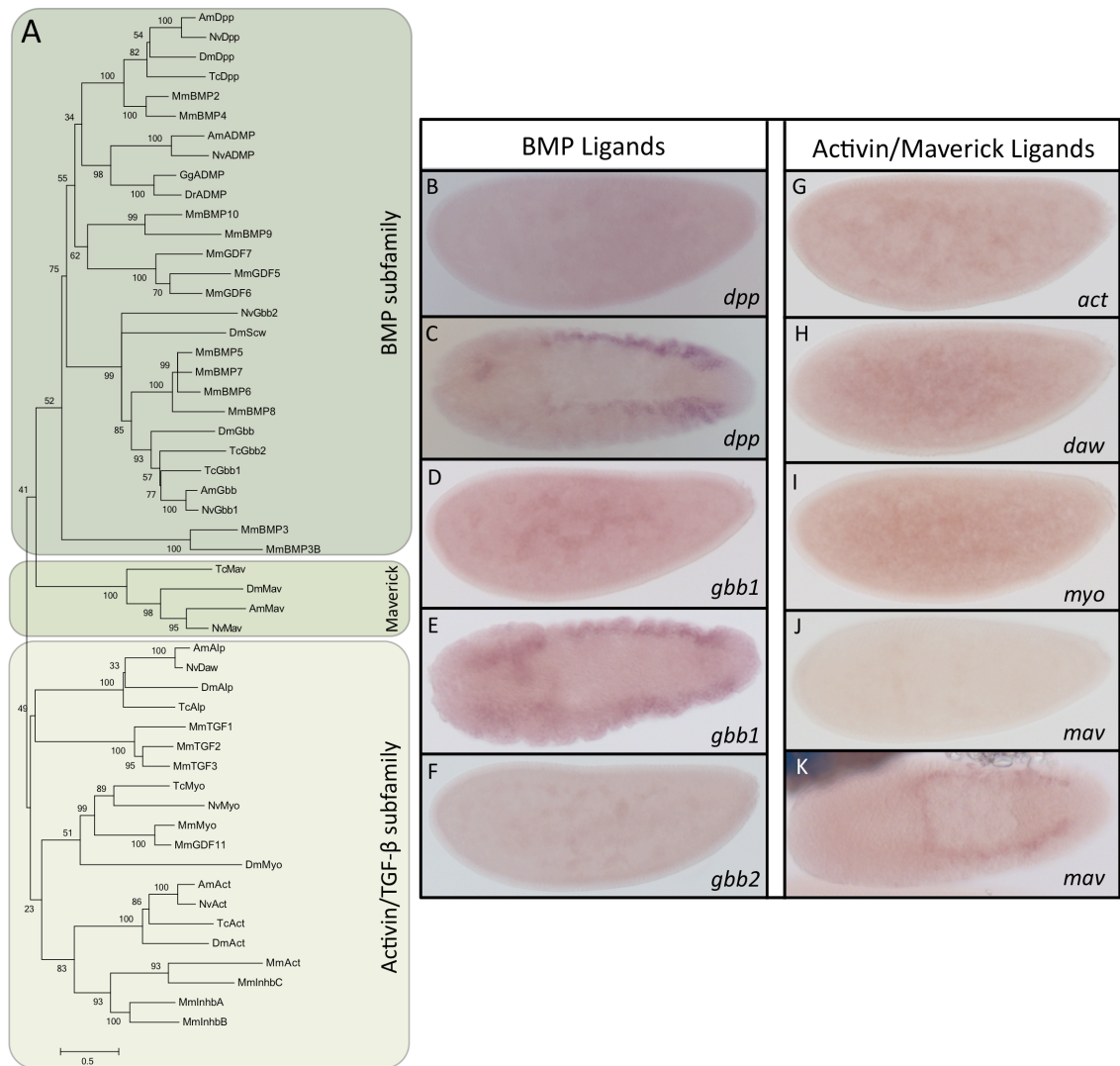


**Figure 1. Ligands**

**(A)** Maximum likelihood tree of TGF- $\beta$  ligands in different insect and vertebrate species. Bootstrap values (1,000 replicates) are indicated in percentages. Amino acid substitution model: WAG+*i*+*g*. Nv *Nasonia vitripennis*; Am *Apis mellifera*; Dm *Drosophila melanogaster*; Tc *Tribolium castaneum*; Mm *Mus musculus*; Gg *Gallus gallus*; Dr *Danio rerio*.

**(B, D, F, G, H, I, J)** Early and **(C, E, K)** late ISH of BMP Ligands **(B-F)** and Activin/Maverick ligands **(G-K)** for *dpp* **(B, C)**, *gbb1* **(D, E)**, *gbb2* **(F)**, *act* **(G)**, *daw* **(H)**, *myo* **(I)**, *mav* **(J, K)**. **B, D, F, G, H, I, J** lateral view. **C, E, K** dorsal view. Anterior is left.



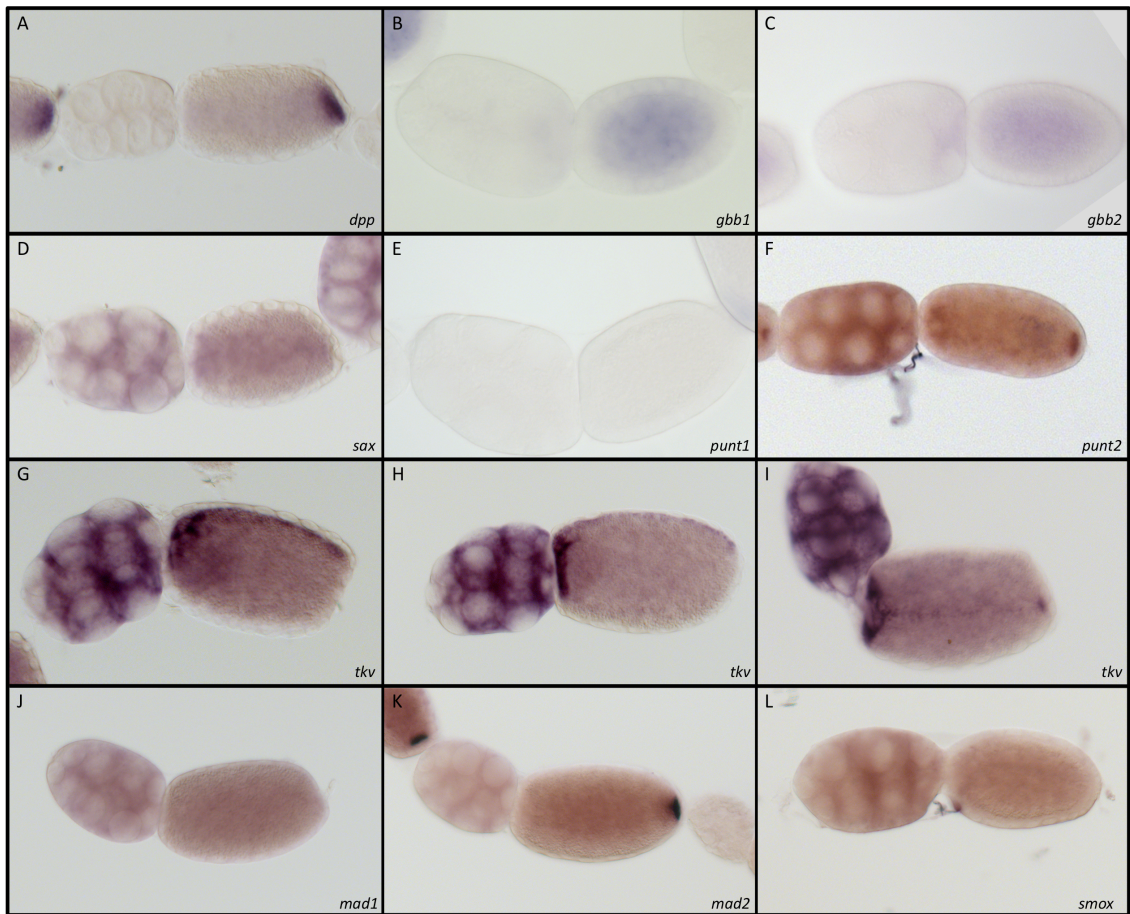


**Figure 2. BMP components in *Nasonia* ovaries**

Expression of (A) *dpp*, (B) *gbb1*, (C) *gbb2*, (D) *sax*, (E) *punt1*, (F) *punt2*, (G-I) *tkv* in lateral (G-H) and dorsal (I) view, *mad1* (J), *mad2* (K) and *smox* (L) in *Nasonia* ovaries.

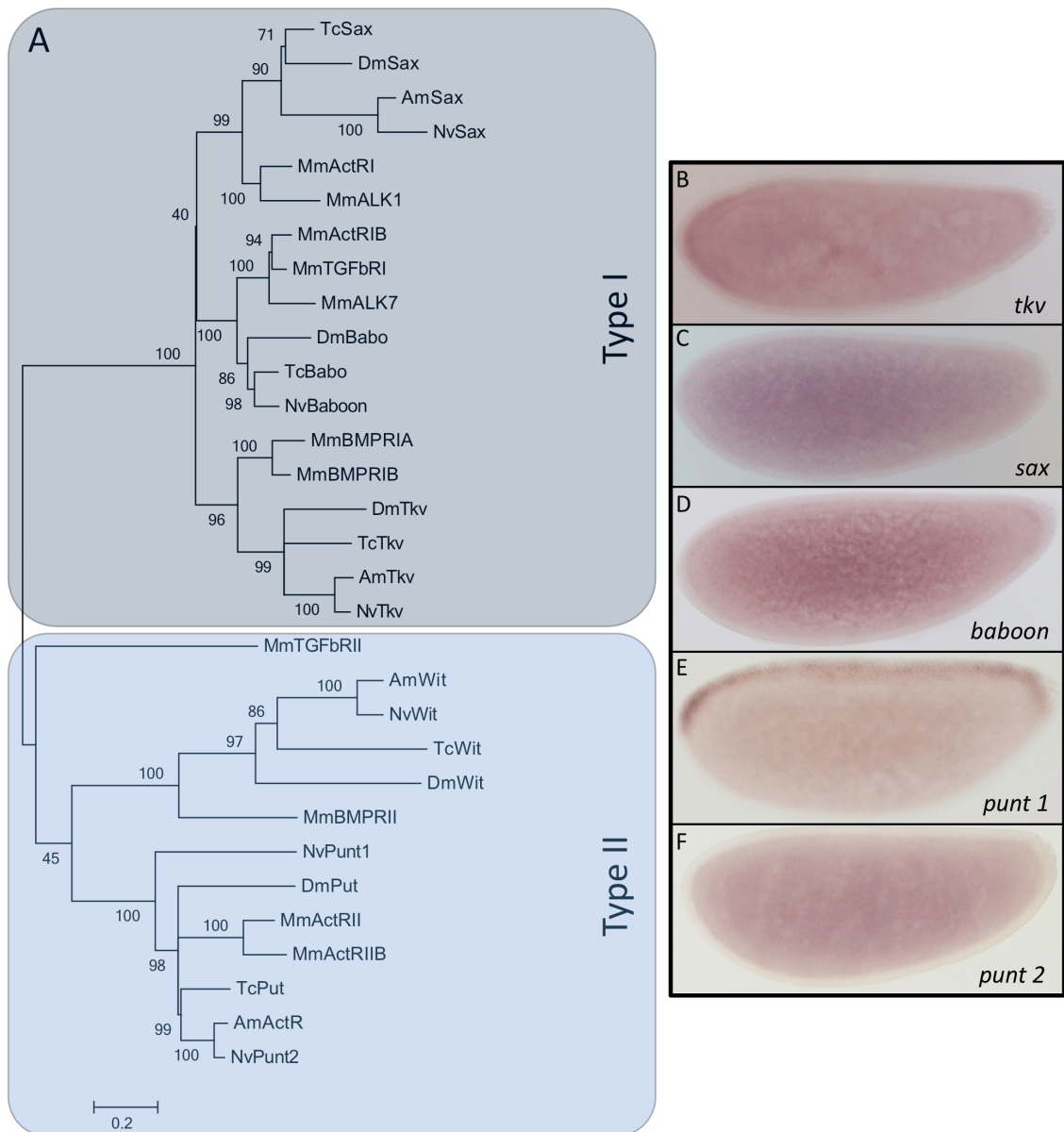


**Figure 3. Receptors**

(A) Maximum likelihood tree of type I and type II receptors in different insect and vertebrate species. Bootstrap values (1,000 replicates) in percentages. Amino acid substitution model: WAG+i+g. Nv *Nasonia vitripennis*; Am *Apis mellifera*; Dm *Drosophila melanogaster*; Tc *Tribolium castaneum*; Mm *Mus musculus*, see main text for protein abbreviations. (B-F) expression pattern of (B) *thickveins*, (C) *saxophone*, (D) *baboon*, (E) *punt1*, (F) *punt2* in *Nasonia* embryos. Anterior is left.

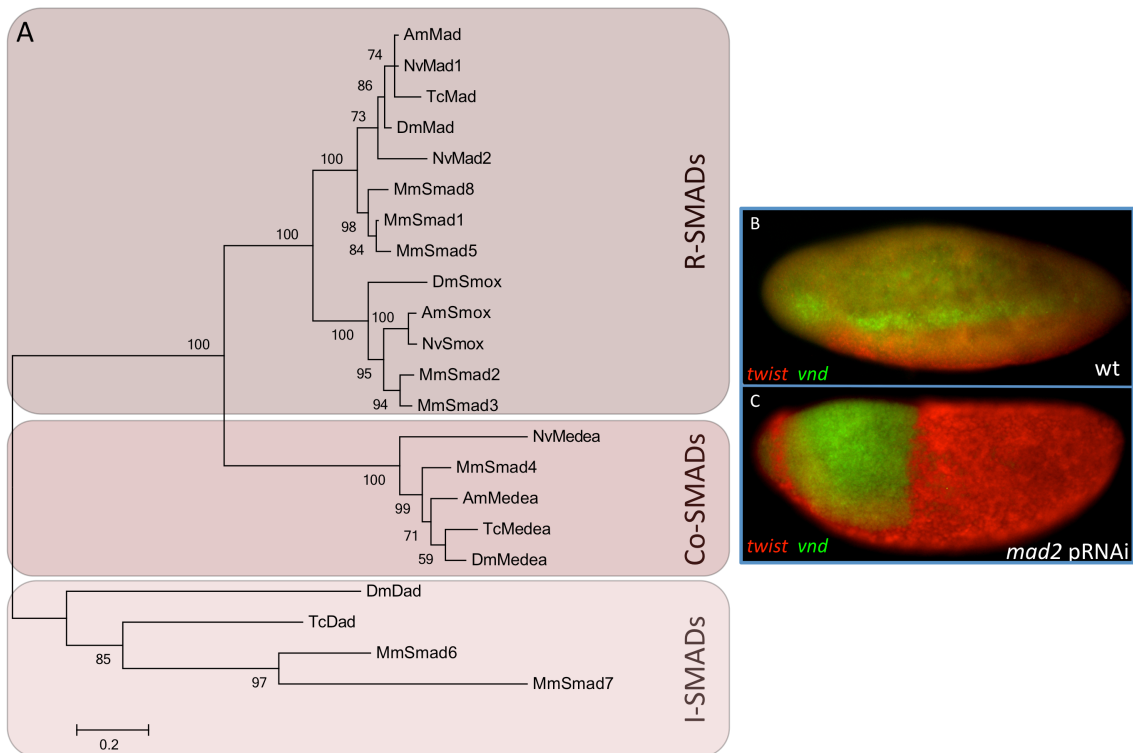


**Figure 4. SMADs**

(A) Maximum likelihood tree of SMADs in different insect and vertebrate species. Bootstrap values (1,000 replicates) in percentages. Amino acid substitution model: WAG+i+g. Nv *Nasonia vitripennis*; Am *Apis mellifera*; Dm *Drosophila melanogaster*; Tc *Tribolium castaneum*; Mm *Mus musculus*. (B-C) Lateral view of wildtype (B) and *mad2* knockdown (C) *Nasonia* embryos showing expression pattern of *twi* (red) and *vnd* (green). Anterior is left.

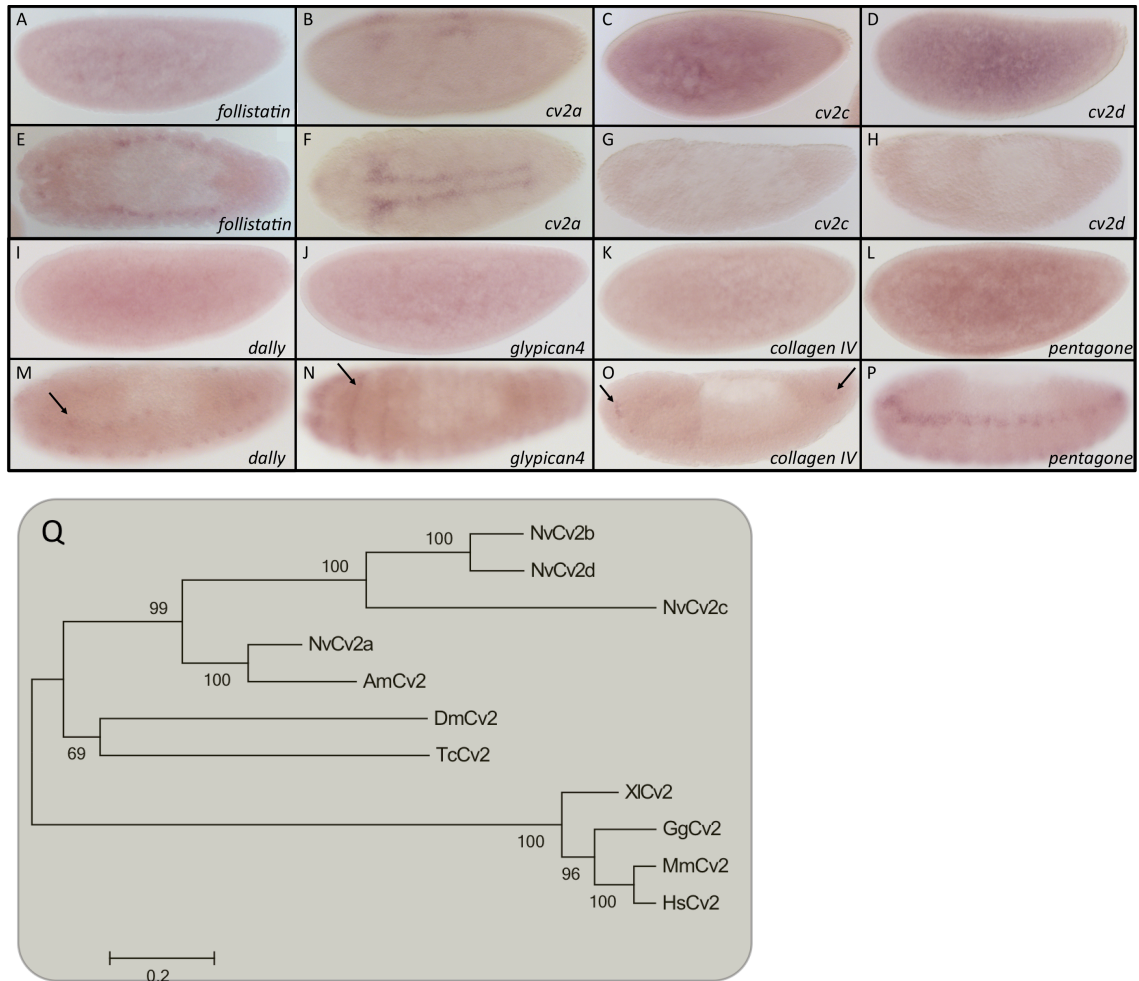


### Figure 5. Extracellular modulators

Early (A-D, I-L) and late (E-H, M-P) expression of *follistatin* (A, E), *cv2a* (B, F), *cv2c* (C, G), *cv2d* (D, H), *dally* (I, M), *glypican4* (J, N), *collagen IV* (K, O), *pentagone* (L, P) in *Nasonia* embryos. A-D, I-L, O, P lateral view. E, F dorsal view. G, H, O dorsolateral view. N ventral view. Anterior is the right. (Q) Maximum likelihood tree of *crossveinless2* in different insect and vertebrate species. Bootstrap values (1,000 replicates) in percentages. Amino acid substitution model: WAG+i+g. Nv *Nasonia vitripennis*; Am *Apis mellifera*; Dm *Drosophila melanogaster*; Tc *Tribolium castaneum*; Mm *Mus musculus*; Hs *Homo sapiens*; Gg *Gallus gallus*; Xl *Xenopus laevis*.

	MH2			SXS		
MmSmad8	WGAEYHRQDV	TSTPCWIEIH	LHGPLQWLDK	VLTMGSPHN	PISSVS	-----
MmSmad1	WGAEYHRQDV	TSTPCWIEIH	LHGPLQWLDK	VLTMGSPHN	PISSVS	-----
MmSmad5	WGAEYHRQDV	TSTPCWIEIH	LHGPLQWLDK	VLTMGSPHN	PISSVS	-----
NvMad2	WGAEYHRQDV	TSTPCWIEIH	LNGPLQWLDN	VLTRMGSPHN	AISSVS	-----
TcMad	WGAEYHRQDV	TSTPCWIEIH	LHGPLQWLDK	VLTMGSPHN	AISSVS	-----
DmMad	WGAEYHRQDV	TSTPCWIEIH	LHGPLQWLDK	VLTMGSPHN	AISSVS	-----
AmMad	WGAEYHRQDV	TSTPCWIEAH	LHGPLQWLDK	VLTMGSPHN	AISSVS	-----
NvMad1	WGAEYHRQDV	TSTPCWIEIH	LHGPLQWLDK	VLTMGTPHN	AISSVS	-----
DmSmox	WGAEYRRQTV	TSTPCWIELH	LNGPLQWLDR	VLTMGSPRL	PCSSMS	-----
AmSmox	WGAEYRRQTV	TSTPCWIELH	LNGPLQWLDR	VLTMGSPRL	PCSSMS	-----
NvMad3	WGAEYRRQTV	TSTPCWIELH	LNGPLQWLDR	VLTMGSPRL	PCSSMS	-----
MmSmad2	WGAEYRRQTV	TSTPCWIELH	LNGPLQWLDK	VLTMGSPSV	RCSSMS	-----
MmSmad3	WGAEYRRQTV	TSTPCWIELH	LNGPLQWLDK	VLTMGSPSI	RCSSVS	-----
NvMedea	FGSDYPRQSI	KETPCWIEIR	LHRPLQLLDD	ELLKMRSSGP	PT-----	-----
MmSmad4	WGPDYPRQSI	KETPCWIEIH	LHRALQLLDE	VLHTM--PIA	DPQLD-----	-----
DmMedea	WGPDYPRQSI	KETPCWIEIH	LHRALQLLDE	VLHAM--PID	GPRAAA-----	-----
AmMedea	WGPDYPRQSI	KETPCWIEIH	LHRALQLLDE	VLHTM--PID	GPRGIE-----	-----
TcMedea	WGPDYPRQSI	KETPCWVEIH	LHRALQLLDE	VLHTM--PID	GPRGIE-----	-----
DmDad	WGRDYKRQDI	MGPCWLEVI	F-----	-----	---SHLR-----	-----
TcDad	WGPLYKRQEI	TSCPCWLEIL	LAPCSDDDDH	KAEFFNLLKE	RCCAVALLPVSLRLMCLATG	-----
MmSmad6	WGPCYSRQFI	TSCPCWLEIL	LNNHR-----	-----	-----	-----
MmSmad7	WGQCYTRQFI	SSCPCWLEVI	FNSR-----	-----	-----	-----

### Supplementary Figure 1

Part of a Smad protein alignment showing the conserved MH2 and SXS domain.

## Material and methods

### Embryo and ovary collection

All *N. vitripennis* embryos were collected using the *Waspinator* and fixed as described in [1]. Nasonia ovaries were dissected and fixed as described in [2].

### ISH

Single in Situ hybridizations for *Nasonia* and *Drosophila* were performed as previously described [3]. Two-color ISH was performed as described in [4]

### RNAi

Young *N. vitripennis* pupae were injected as in [5].



1. Buchta, T., Özüak, O., et al., Patterning the dorsal–ventral axis of the wasp *Nasonia vitripennis*. *Dev. Biol.* (2013), <http://dx.doi.org/10.1016/j.ydbio.2013.05.026>
2. Lynch, J.A., Peel, A.D., Drechsler, A., Averof, M., Roth, S., 2010. EGF signaling and the origin of axial polarity among the insects. *Curr. Biol.: CB* 20, 1042–1047.
3. Brent, A.E., Schweitzer, R., Tabin, C.J., 2003. A somitic compartment of tendon progenitors. *Cell* 113, 235–248. *Bull*,
4. Mazzoni, E.O., Celik, A., Wernet, M.F., Vasiliauskas, D., Johnston, R.J., Cook, T.A., Pichaud, F., and Desplan, C. (2008). Iroquois complex genes induce co-expression of rhodopsins in *Drosophila*. *PLoS Biol.* 6, e97. 27.
5. Lynch, J.A., and Desplan, C. (2006). A method for parental RNA interference in the wasp *Nasonia vitripennis*. *Nat. Protoc.* 1, 486–494.

### Gene identification, phylogenetic analysis

Conserved domains of TGF $\beta$  signaling components were identified by TBLASTN (Altschul et al. 1997) on NCBI. The protein sequences were aligned with muscle 3.7 (<http://www.drive5.com/muscle/index.htm>). Alignment refinement was performed using GBLOCKS 0.91b (<http://molevol.cmima.csic.es/castresana/Gblocks.html>). Maximum likelihood Trees were edited in MEGA5.2.2 (Kumar et al. 2004)(<http://www.megasoftware.net/index.php>).

### NCBI accession numbers for ligands

Am Dpp XP\_001122815.2; Dm Dpp AAN10431.1; Tc Dpp EFA02913.1; Mm BMP2 NP\_031579.2; Mm BMP4 AAC37698.1; Mm BMP10 NP\_033886.2; Mm BMP9 AAD56961.1; Mm GDF5 NP\_032135.2; Mm GDF6 NP\_038554.1; Mm GDF7 NP\_038555.1; Dm Scw AAN11056.2; Dm Gbb AAF47075.1; Am Gbb XP\_394252.1; Tc Gbb1 EFA04645.1; Tc Gbb2 EFA04646.1; Mm BMP5

NP\_031581.2; Mm BMP8 NP\_001242948.1; Mm BMP6 NP\_031582.1; Mm BMP7 NP\_031583.2; Mm BMP3 NP\_775580.1; Mm BMP3B NP\_665684.2; Am ADMP XP\_003251013.1; Gg ADMP AAD52011.1; Dr ADMP NP\_571951.2; Tc Mav EFA11885.1; Dm Mav AAF59328.1; Am Mav XP\_001122118.2; Am Alp XP\_001122210.1; Dm Alp NP\_523461.1; Tc Alp EFA11884.1; Am Act XP\_001123044.2; Dm Act NP\_651942.2; Tc Act EFA05602.1; Mm Act NP\_032408.2; Mm InhbA NP\_032406.1; Mm InhbB NP\_032407.1; Mm InhbC NP\_034695.1; Dm Myo AAF59319.1; Tc Myo EFA05753.1; Mm Myo AAO46885.1; Mm GDF11 NP\_034402.1; Mm TGF1 NP\_035707.1; Mm TGF2 NP\_033393.2; Mm TGF3 NP\_033394.2; Nv Dpp XP\_001607677.1; Nv Gbb1 XP\_001603876.1; Nv Gbb2 XP\_001603269.2; Nv ADMP XP\_001604750.2; Nv Myo XP\_001602255.2; Nv Mav XP\_001606148.2; Nv Act XP\_001602284.1; Nv Alp XP\_003425497.1

#### **NCBI accession numbers for receptors**

Tc Tkv EFA09250.1; Dm Tkv AAN10533; Am Tkv XP\_391989; Mm BMPRIA P36895; Mm BMPRIB NP\_031586; Tc Sax EFA07576.1; Dm Sax AAF59189; Am Sax XP\_001121528; Mm ActRI NP\_031420; Mm ActRIB NP\_031421; Mm ALK1 Q61288; Tc Babo EFA01312.1; Dm Babo AAF59011; Mm TGFbrI XM\_006537756.1; Mm ALK7 NP\_620790; Tc Wit XP\_974821.1; Am Wit XP\_397334; Dm Wit AAF47832; Mm BMPRII NP\_031587; Tc Put EEZ97734.1; Am ActR XP\_395928; Dm Put AAF55079; Mm ActRII CAM14875; Mm ActRIIB NP\_031423; Nv Wit XP\_003428148.1; Nv Tkv XP\_001601240.2; Nv Sax XP\_003426889.1; Nv Babo XP\_003427942.1; Nv Put1 XP\_001606053.1; Nv Put2 XP\_001603863.1;

#### **NCBI accession numbers for SMADs**

Dm Mad AAF51142.1; Dm Smox NP\_511079.1; Am Mad XP\_392819.3; Am Smox XP\_396056.4; Mm Smad1 NP\_032565.2; Mm Smad5 NP\_032567.1; Mm Smad8 AAF77079.2; Mm Smad2 NP\_034884.2; Mm Smad3 NP\_058049.3; Dm Dad NP\_477260.1; Tc Dad EEZ99343.1; Mm Smad6 NP\_032568.3; Mm Smad7

NP\_001036125.1; Am Medea XP\_392838.4; Tc Medea EFA11586.1; Dm Medea NP\_524610.1; Mm Smad4 NP\_032566.2; Nv Mad1 XP\_001601460.2; Nv Mad2 XP\_001602991.1; Nv Mad3 XP\_001608214.2; Nv Medea XP\_003427724.1; Tc Mad EFA05663.1

### NCBI accession numbers for Crossveinless2

Nv Cv2a XP\_001601040.2; Nv Cv2b XP\_001599339.1; Nv Cv2c XP\_001603432.2; Nv Cv2d XP\_001599102.2; Dm Cv2 AAG01337.2; Tc Cv2 EFA10783.1; Am XM\_006570432.1; Gg NP\_001007081.1; Mm Cv2 AAN45857.1; Xl Cv2 AAX12852.1; Hs Cv2 AAP89012.1;

### ISH Primers

Gene	Primer	Sequence	Accession Nr.
<i>twist</i>	Forward	ggccgcggGCTTCTCGCCCAGTAACAAC	XM_001605767
	Reverse	cccggggcACGTTAGCCATGACCCTCTG	XM_001605767
<i>vnd</i>	Forward	ggccgcggGTCGGACTGCTCAACAACCTG	XM_001604500
	Reverse	cccggggcAGGTTCCAGGAGCTTCGACT	XM_001604500
<i>dpp</i>	Forward	ggccgcggGTGGTGGCGAGGCGGTAAA	XP_001607677.1
	Reverse	cccggggcCACGACCTTGTTCCTCCTCGT	XP_001607677.1
<i>gbb1</i>	Forward	ggccgcggCCAAGTTCCTCCTGGACATC	XP_001603876.1
	Reverse	cccggggcGATGATCCAGTCCTGCCACT	XP_001603876.1
<i>gbb2</i>	Forward	ggccgcggATCCTGCTGCAGTTCGACTT	XP_001603269.2
	Reverse	cccggggcCCCTGATGATCATGTTGTGG	XP_001603269.2
<i>activin</i>	Forward	ggccgcggGACGACTTCTACGCGAGGAC	XP_001602284.1
	Reverse	cccggggcCTCGATCACGTGCGTGTAGT	XP_001602284.1
<i>alp</i>	Forward	ggccgcggAGCTTCTACGGCAAGACCAA	XP_003425497.1
	Reverse	cccggggcGAGCAGCAGGGCACTATTTTC	XP_003425497.1
<i>myostatin</i>	Forward	ggccgcggCTCTCGCTTTGGATCTACGG	XP_001602255.2
	Reverse	cccggggcCGATCTGGTACTCGTTGTTCG	XP_001602255.2
<i>maverick</i>	Forward	ggccgcggGCCGAGTCAAAGAAGTGCTG	XP_001606148.2
	Reverse	cccggggcTCAGGAGCAAGCGCACTC	XP_001606148.2
<i>mad1</i>	Forward	ggccgcggGCCCCACAACGTCTCATACT	XP_001601460.2
	Reverse	cccggggcACATCCTGGCGATGGTACTC	XP_001601460.2
<i>mad2</i>	Forward	ggccgcggTGAATCAACCATGCCTCAA	XP_001602991.1



	Reverse	cccggggcGCATCTCGATCCAACAAGGT	XP_001602991.1
<i>mad3</i>	Forward	ggccgcggCAGAAGAGGGACGAGGTCTG	XP_001608214.2
	Reverse	cccggggcTGTCGTCTTGTTGCTCGAC	XP_001608214.2
<i>tkv</i>	Forward	ggccgcggTACCCACATCCAGGAGAAG	XP_001601240.2
	Reverse	cccggggcGAAGATCTCGGTGTGCAGGT	XP_001601240.2
<i>sax</i>	Forward	ggccgcggCTCTTACCCTCCAGACACG	XP_003426889.1
	Reverse	cccggggcTGCTTTTGTGTGCCAACATT	XP_003426889.1
<i>baboon</i>	Forward	ggccgcggTGCGAAACTGATGGCTACTG	XP_003427942.1
	Reverse	cccggggcTCCGACGATCTCCATGTGTA	XP_003427942.1
<i>puntI</i>	Forward	ggccgcggTCTCAAGCAGAGCAGGGAAT	XP_001606053.1
	Reverse	cccggggcGAAGCAAGTTCCAGAGCAC	XP_001606053.1
<i>puntII</i>	Forward	ggccgcggGCGCCTACCTAGCGATACTG	XP_001603863.1
	Reverse	cccggggcCTTCTCAACGCCGATAAAGC	XP_001603863.1
<i>follistatin</i>	Forward	ggccgcggAGCGAGGAGGACTACGACAA	XP_001607105.2
	Reverse	cccggggcCAGCTCGGATAGGTGACGTTG	XP_001607105.2
<i>cv2a</i>	Forward	ggccgcggGGCGTTATTACGGAATCGAA	XP_001601040.2
	Reverse	cccggggcTCGCCGAAGACAGTACACAC	XP_001601040.2
<i>cv2c</i>	Forward	ggccgcggGTTGTCTCATTGCGAAGGT	XP_001603432.2
	Reverse	cccggggcTCGGTATGGCAAATCAACAA	XP_001603432.2
<i>cv2d</i>	Forward	ggccgcggAGCGTCACTGCACAACCTGTC	XP_001599102.2
	Reverse	cccggggcCAAGTTGTCTGCTGCTCTCG	XP_001599102.2
<i>dally</i>	Forward	ggccgcggGCGACATTCCCAAACAGATT	XP_003425386.1
	Reverse	cccggggcGACAACCGTCTTGCGTATT	XP_003425386.1
<i>glypican4</i>	Forward	ggccgcggGCACACAAGGGCCACTAAAT	XP_001607767.2
	Reverse	cccggggcCGTCGTCGATCTCTTTGTGA	XP_001607767.2
<i>collagenIV</i>	Forward	ggccgcggCTTCGGAACGTGGAGAGAAG	XP_003427100.1
	Reverse	cccggggcGCCAACCAGAAGCTGAACTC	XP_003427100.1
<i>pentagone</i>	Forward	ggccgcggCCTAGACCGGGACGAGTACA	XP_001601094.2
	Reverse	cccggggcGTACCTCGGCAGTTTCTTGC	XP_001601094.2

### 3 Additional Material & Methods

In the following, all Materials and Methods used for the experiments described in chapter 4 are listed:

#### 3.1 *Nasonia vitripennis* Stock Keeping

Eclosed *Nasonia vitripennis* were honey fed for two days, using a honey-water soaked filter paper and plastic vial with foam cover. Afterwards, 20-30 females were transferred together with freshly pupated flesh fly larvae (e.g. *Calliphora* sp. pupae) that served as host for the next generation in a plastic vial with foam lid and kept there for 4-5 days at room temperature. Development is temperature sensitive. Un-parasitized hosts were kept at 4°C.

#### 3.2 Ovary preparation & Fixation

Ovaries were dissected from adult females in PBS with fine forceps. The ovaries were then fixed in 5% electron microscopy-grade formaldehyde in PBT (13 PBS, 0.1% Tween-20) for 30 min, and either used immediately or dehydrated in methanol, and stored at -20°C until needed.

#### 3.3 Embryo Collection & Fixation

The *Waspinator* (see chapter 2.1 supplementary data) was used for embryo collection. To fix the embryos, parasitized hosts are opened at the anterior. Immersing the anterior part of the host pupae causes the *Nasonia* embryos to detach from it into the fixing solution, where they assemble in the interphase. Embryos were fixed overnight. After fixation, formaldehyde/PBT (lower phase) was removed and replaced by the same amount of 100% methanol (stored at -20°C). Subsequent, vigorous shaking of the fixation vial for least a minute will causes embryos to lose their vitelline membrane and sink to the bottom where they can be collected and transferred to an Eppendorf vial with a

glass pipette. There, embryos were washed several times with methanol and either stored at -20°C or used for further experiments.

Fixation solution: 2.5ml 10% formaldehyde  
2.5ml PBS 1x  
5ml Heptane

### 3.4 *In Situ* Hybridization Probe & dsRNA Synthesis

(modified from Jeremy A. Lynch)

#### 3.4.1 Obtaining the Sequence

- Go to flybase.org
- Enter the name of the gene into the quick search box
- Click on the search result corresponding to your gene
- In the text box above the “Get FASTA”, chose “translations” to get the protein sequence of the gene
- Select the resulting protein sequence (highlight, then ctrl+C)
- Go back to flybase.org homepage, and click “blast” at the top of the page
  - For Database, choose GenBank protein
  - For Program, choose blastp
  - Past your sequence (ctrl+v) in the sequence box
  - Under the Species section, make sure only *Nasonia* box is checked
- Click on BLAST button, and wait for results
- Typically the *Nasonia* gene of interest will have the highest score (and lowest E-value) among multiple results. Click on the link (top-left) to the GenBank accession for the highest scoring *Nasonia* gene
- Scroll Down on this page, and click on the link for “CDS” (This will give you the DNA sequence coding for the protein that you have just found)
- On this page, change the Display box (lower right) to FASTA
- Select and copy the sequence (ctrl+c). You might want to also paste into a text document for later use.

### 3.4.2 Designing the primers

- We will be using the online version of the program Primer3. Go to <http://frodo.wi.mit.edu/>
- Paste your sequence from above into large box at top of page
- Parameters:
  - Product size range should be in the range of 700-850bp. PCR products of this size work well in both making dsRNA and single stranded probes
  - The maximum primer size should be set to 22, but 20 bp is ideal
  - Leave other settings as default
- Press “pick primers” button
- By default, you will be given up to 5 primer pairs. Usually the first pair has the best characteristics (in regard to self and between primer complementarities)
- Select and copy the forward and reverse primers, and paste them into a text document (make sure you label and keep track of which is forward and which is reverse!)
- We will be using special Universal primers to make templates for RNAi and in situ probes, for this we need linker sequences on the 5' end of each primer:
  - For the forward (sense) primer add the sequence ggccgcgg to the 5' end
  - For the reverse (antisense) add the sequence cccggggc to the 5' end

### 3.4.3 PCR

#### Primers

- Dissolve stock to 0.1 nanomole/microliter (100 microMolar) in distilled water
- Make working solution in eppi by diluting stock to 5 micromolar concentration (i.e. dilute primer stock 1:20)

#### First PCR:

- Do a 25 microliter reaction using the Red Taq mix from sigma
- The PCR mix is at 2x concentration
- The final concentration of each primer should be 0.2 micromolar
- Use 1 microliter of cDNA (made by the SMART RACE protocol)
- Use an annealing temperature of 57°C and do 35 cycles
- Check the reaction on a gel; you should have a single, bright band at the expected size. If this is so, purify PCR and sequence (if desired. If you will not sequence the product, you do not have to purify and can proceed directly to second PCR). If other bands are present, either try the PCR again at a higher annealing temperature, or gel purify the correct band.

#### Second PCR:

- To make template for a labelled antisense probe, use the gene specific forward primer with the 3' T7 universal primer (sequence: agggatcctaatacgaactcactatagggcccgggc)
- To make a control sense probe, use the gene specific reverse primer with the T7 5' universal (Sequence: gagaattctaatacgaactcactatagggcccggg)
- To make template for dsRNA, use both the T7 5' and 3' Universal primers.
- The concentrations of primers are the same as the first PCR
- Use 1 microliter of first PCR as template in each reaction
- Use same cycling parameters as first PCR

### 3.4.4 Making dig labelled probes

1. Make the T7 reaction master mix (Using Ambion T7 Maxiscript kit) in order below (volumes given for 1 reaction)

- 8 microliter RNase free water
- 2 microliter transcription buffer
- 2 microliter dig labelling mix
- 2 microliter T7 RNA polymerase

- Using **Roche T7 Polymerase + Roche RNase Inhibitor** (40U/microliter) (volumes given for 1 reaction)

- 7.5 microliter RNase free water
- 2 microliter transcription buffer
- 2 microliter dig labelling mix
- 2 microliter T7 RNA polymerase
- 0.5 microliter RNase inhibitor (20U/rxn)

2. Mix well, and quickly pipette into individual reaction tubes (14 microliter each)
3. Add 6 microliter PCR template to each reaction tube. Mix well.
4. Put reactions at 37 degree for 2-4 hours
5. Stop the reaction by adding 30 microliter water, and 50 microliter 2x stop solution (can remove 1-2 microliter to check on gel)
6. Add 5 microliter tRNA and 10 microliter Lithium Chloride
7. Add 300 microliter 100% ethanol, and precipitate for at least 30 minutes at -20°C
8. Centrifuge at 4 degrees 14000 rpm for 15 minutes
9. Decant supernatant
10. Add 300 microliter 70% ethanol, spin again for 5 minutes
11. Carefully remove all supernatant with pipette
12. Allow pellet to dry for about 5 minutes
13. resuspend pellet in 100 microliter resuspension solution
14. store at -20°C

resuspension solution:    50% formamide  
                                      5x SSC  
                                      in H<sub>2</sub>O

#### 3.4.5 Making dsRNA

1. Dilute the dsRNA template PCR reaction with an equal amount RNase free water
2. Prepare the 20 microliter master mix, using the Ambion T7 Megascript Kit:
  - a. 2 microliters each of the NTPs
  - b. 2 microliters T7 transcription buffer
  - c. 2 microliter of T7 polymerase mix
3. If making multiple dsRNAs, pipette 12 microliters each of master mix into individual reaction tubes
4. Add 8 microliter of dsRNA PCR template to master mix.
5. Mix well and place at 37°C for 4 hours- overnight
6. Stop reaction by adding 115 microliter RNase free water, and 15 microliter Ammonium acetate stop solution.
7. Purify by adding 150 microliter Phenol:Chloroform
  - a. Vortex or shake for about 1 minute
  - b. Centrifuge at 5000 rpm for 5 minutes
  - c. Take upper, aqueous layer, avoiding the interface
8. Precipitate by adding 150 microliters of isopropanol
  - a. Incubate at -20°C for 30minutes-1hour
9. Spin at full speed in refrigerated centrifuge (4°C) for 15 minutes
10. Decant supernatant, add 300 microliter 70% ethanol, mix gently
11. spin again at full speed for 5 minutes in refrigerated centrifuge
12. Carefully pipette away ethanol, and allow pellet to dry in open tube 5 minutes
13. Resuspend in 50 microliter RNase free water.

14. Check concentration on spectrophotometer
15. run 1 microliter of reaction on gel
16. if multiple bands, heat reaction to boiling, and allow to cool on bench at room temperature.

Concentration and purity of total RNA samples were determined via NanoDrop™

### **3.5 *In Situ* Hybridization (ISH)**

(Modified from Ava Brent & Jeremy A. Lynch)

The following protocol can be used for a single or double *In Situ* and will take 3 days.

1. Wash in PBT 3 x 5 min
2. Proteinase K digest 5 µg/mL (in PBT) for 5 minutes.
3. Rinse 2x in PBT
4. Fix in 5% formaldehyde/PBT 25 min
5. Wash in PBT 4x 5min
6. Wash in 50/50 PBT/Hyb 5 min
7. Prehyb 1 or more hour at 65°C
8. Remove prehyb, add diluted probe mix (1µl probe in 50µl hyb), and incubate overnight at 60°C.
9. Wash in hyb wash solution 3x 25 min each at 60°C
10. Wash in 50/50 MABT/hyb wash for 5 min at room temp
11. Wash 4x 10minutes in MABT
12. Block in 2%BBR MABT + 10% NGS 1 or more hours
13. incubate with appropriate anti-hapten antibodies (for double in situ use a combination of anti-dig::POD (Roche) at 1:100, anti-biotin or anti-dig::AP at 1:5000 or anti-fluorescein::AP at 1:2500 overnight at 4C in 2%BBR MABT/ 10% NGS serum (for antibody+ISH experiments, add primary antibody here)
14. Wash 4x 15 minutes in MABT
15. continue with normal HRP and/or AP detection methods (see below)



16. If you are doing antibody+ISH, block 1 or more hours , then add secondary antibody, overnight 4C
17. Wash 4x 10minutes, detect secondary antibody by preferred means

For AP NBT/BCIP detection:

1. Wash 2x 5 min each in AP buffer
2. For each mL of desired detection solution, add 20 uL of NBT/BCIP stock solution to AP buffer (Roche)
3. add about 500uL of detection solution to each sample
4. To stop reaction, wash several times in PBT

For the red fluorescent staining use the HNPP detection kit and Fast Red tablets from Roche:

1. Wash 2x 5 minute each in AP buffer
2. Dissolve 1 fast red tablet in 2mL of AP buffer
3. filter solution using a syringe driven filter unit, Nylon, 0.2 um
4. add 10uL HNPP solution to each mL of filtered fast red solution you want to use.
5. add 400uL of this to each sample, a visible red stain should appear, which will also be brightly fluorescent
6. Wash and mount, or go to green TSA staining steps

For Green tyramide (Using TSA detection kit with alex488 tyramide from Molecular Probes):

1. After last wash, rinse 2x in PBS, or PBT with only 0.05% tween
2. Dilute 30% H<sub>2</sub>O<sub>2</sub> 1:100 in amplification buffer
3. Add 1uL of above dilution to 100uL amplification buffer for a final dilution of 0.0015% H<sub>2</sub>O<sub>2</sub>
4. Add 1uL tyramide stock to above solution and immediately add to embryos

5. stain in the dark for 1 - 2 hour at room temperature (can go longer)
6. Wash and mount in vecta shield

**Solutions for ISH:****PBT**

1x PBS

0.1% Tween 20

**Hybridization solution**

50% formamide	25ml of 100% formamide
5x SSC	12,5ml of 20x SSC
2% SDS	10ml of 10% SDS
2% BBR	1g (Roche)
250 ug / mL tRNA	0.0125g
50 µg / mL heparin	100µl
H <sub>2</sub> O	fill up to 50ml

BBR (Boehringer Blocking reagent for nucleic acids, available from roche)

tRNA (can also substitute ssDNA, as in other standard hyb solutions)

Dissolve BBR at 55-65°C (can be stored at -20°C).

**Hyb wash solution**

50% formamide	25ml of 100% formamide
2x SSC	5ml of 20x SSC
1% SDS	5ml of 10% SDS
0.1% Tween	250µl of 20% Tween
H <sub>2</sub> O	fill up to 50ml

**MABT (maleic acid buffer containing Tween 20)**

1x MAB	10ml of 5x stock of MAB
--------	-------------------------

0.1% Tween 20	250µl of 20% Tween
H <sub>2</sub> O	fill up to 50ml

**Blocking Solution: MABT + 2% Börringer Blocking Reagent (BBR) + 10% NGS**

1x MAB	10ml of 5x stock of MAB
0.1% Tween 20	250µl of 20% Tween
10% NGS	2,5ml of 100% NGS
2% BBR	1g (Roche)
H <sub>2</sub> O	fill up to 50ml

**5x stock of MAB:**

58g Maleic Acid  
 approx 32g NaOH pellets  
 43.8g NaCl  
 pH to 7.5 with 10N NaOH  
 water to 1L

**AP Buffer:**

	<b>20 mL of AP buffer</b> (always fresh)
100 mM NaCl	400 uL 5M NaCl
100mM Tris pH 9.5	2mL 1M Tris pH 9.5
50mM MgCl (2)	1mL 1M MgCl
0.1% Tween 20	100 uL of 20% Tween
H <sub>2</sub> O	fill up to 20ml

Dissolve the MABT/2%BBR solution at 55-65°C. Once the BBR is dissolved, use it at room temperature.

### 3.6 Analysis of Toll pathway components

#### 3.6.1 NCBI Accession numbers

In the following, accession numbers of protein sequences used for the phylogenetic analysis of Toll pathway components in chapter 4 are listed:

##### Windbeutel

Nv_Wbl	XP_001604220.2
Am_Wbl	XP_001120162.1
Dm_Wbl	NP_725867.1
Tc_Wbl	XP_970926.1
Cq_Wbl	XP_001851101.1
Pc_Wbl	XP_002426577.1

##### Slalom / Medial glomeruli

Nv_Sll	XP_001599843.1
Dm_Sll	NP_524389.1
Cq_Sll	XP_001866162.1
Tc_Sll	EFA07569.1
Am_Sll	XP_395892.2
Pc_Sll	XP_002423693.1

Nv_Meigo	XP_001602973.2
Dm_Meigo	NP_650949.1
Cq_Meigo	XP_001847658.1
Tc_Meigo	XP_974276.1
Am_Meigo	NP_001229484.1
Pc_Meigo	XP_002423558.1

##### Pipe / $\alpha/\beta$ Hydrolase2

Nv_Pip	XP_003424424.1
Dm_Pip	AAD04925.1
Cq_Pip	XP_001841883.1
Tc_Pip	EFA12172.1
Am_Pip	XP_395133.3
Pc_Pip	XP_002429954.1

Nv_Hydr2	XP_001601996.2
Dm_Hydr2	NP_608751.2
Cq_Hydr2	XP_001850774.1
Tc_Hydr2	XP_966390.1
Am_Hydr2	XP_397036.3
Pc_Hydr2	XP_002429976.1

**Nudel / Corin / CG4386**

Nv_Nd	XP_003424379.1
Dm_Nd	NP_523947.2
Cq_Nd	XP_001843380.1
Tc_Nd	XP_974954.2
Am_Nd	XP_623911.3
Pc_Nd	XP_002426731.1

Nv_Corin	NP_001166078.1
Dm_Corin	NP_995773.1
Cq_Corin	XP_001865263.1
Tc_Corin	XP_001814556.1
Am_Corin	XP_001121114.2
Pc_Corin	XP_002429879.1

Nv_CG4386	NP_001166078.1
Dm_CG4386	NP_611611.1
Cq_CG4386	XP_001845720.1
Tc_CG4386	XP_974141.1
Am_CG4386	XP_394832.1
Pc_CG4386	XP_002430303.1

**Gastrulation defective / CG7432**

Nv_Gd	XP_003427708.1
Dm_Gd	NP_001259478.1
Cq_Gd	XP_001849079.1
Tc_Gd_1	XP_973195.2
Tc_Gd_2	EFA09210.1
Am_Gd	XP_001121433.2
Pc_Gd	XP_002433014.1

Nv_CG7432	XP_001606018.2
Dm_CG7432	NP_650825.2
Cq_CG7432	XP_001859951.1
Tc_CG7432_1	XP_970121.2
Tc_CG7432_2	EFA11600.1
Am_CG7432	XP_001121456.2
Pc_CG7432	XP_002423000.1

**Snake (Snk) / Notopleura (Np) / Spirit**

Nv_Snk	XP_003426550.1
Dm_Snk	NP_524338.2
Cq_Snk_1	XP_001851229.1
Cq_Snk_2	XP_001844337.1
Cq_Snk_4	XP_001845292.1

---

Cq_Snk_6	XP_001844334.1
Tc_Snk_1	XP_969745.2
Tc_Snk_5	EFA11659.1
Tc_Snk_6	XP_973839.1
Tc_Snk_10	EFA12222.1
Tc_Snk_7	XP_971578.1
Tc_Snk_4	EFA04603.1
Am_Snk	XP_001122420.2
Pc_Snk_2	XP_002429841.1
Nv_Np	NP_001166061.1
Dm_Np	NP_651662.1
Cq_Np	XP_001842493.1
Tc_Np	EFA12385.1
Am_Np_1	XP_001120043.2
Am_Np_2	XP_001119978.2
Dm_Spirit	CAL85477.1
Cq_Spirit	XP_001844336.1
Tc_Spirit	EEZ99345.1
Am_Spirit	XP_001121032.1
Pc_Spirit	XP_002422611.1
<b>Easter (Ea) / Melanization Protease1 (MP1)</b>	
Nv_Ea_1	NP_001155077.1
Nv_Ea_1	XP_001600074.1
Dm_Ea	NP_524362.2
Cq_Ea_1	XP_001850931.1
Cq_Ea_2	XP_001866674.1
Cq_Ea_3	XP_001866672.1
Cq_Ea_4	XP_001866675.1
Tc_Ea_1	XP_972628.1
Tc_Ea_3	EEZ99203.1
Tc_Ea_4	EFA07560.1
Tc_Ea_5	EFA07561.1
Tc_Ea_8	EFA07451.1
Tc_Ea_VA	EFA01246.1
Am_Ea	XP_001122011.2
Pc_Ea_1	XP_002430853.1
Pc_Ea_2	XP_002431768.1
Nv_MP1_1	NP_001155043.1
Nv_MP1_2	XP_003424740.1
Dm_MP1	NP_649450.3
Cq_MP1_1	XP_001866671.1
Cq_MP1_2	XP_001870698.1

---

Tc_MP1_1	EEZ99205.1
Tc_MP1_3	XP_972679.1
Tc_MP1_4	EFA07452.1
Am_MP1	XP_001122037.2

**Serpin27A (Spn27A) / Serpin42Da (Spn42Da)**

Nv_Spn27A	XP_001602351.1
Dm_Spn27A	NP_652024.1
Cq_Spn27A_1	XP_001866683.1
Cq_Spn27A_2	XP_001866679.1
Cq_Spn27A_3	XP_001866680.1
Cq_Spn27A_4	XP_001866682.1
Tc_Spn27A_1	XP_969874.1
Am_Spn27A	XP_001122067.2
Pc_Spn27A	XP_002427026.1

Nv_Spn42Da_1	XP_001606111.2
Nv_Spn42Da_2	XP_003425280.1
Dm_Spn42Da	NP_995755.1
Cq_Spn42Da_1	XP_001865070.1
Cq_Spn42Da_2	XP_001865071.1
Tc_Spn42Da_1	XP_973349.2
Tc_Spn42Da_3	XP_974388.1
Tc_Spn42Da_7	EFA09187.1
Tc_Spn42Da_4	EFA09186.1
Tc_Spn42Da_9	XP_974209.1
Tc_Spn42Da_6	XP_974182.1
Am_Spn42Da_1	XP_003251813.1
Am_Spn42Da_2	XP_395991.3

**Spätzle (Spz) / Neurotrophin (NT1)**

Nv_Spz_1	XP_001606369.2
Nv_Spz_2	XP_003426647.1
Nv_Spz_3	XP_003424967.1
Nv_Spz_4	XP_003424972.1
Dm_Spz	NP_524526.1
Cq_Slpz_1	XP_001848412.1
Cq_Slpz_2	XP_001864596.1
Tc_Spz_1	XP_975083.1
Tc_Spz_2	EEZ99268.1
Pc_Spz_1	XP_002432638.1

Nv_NT1	XP_001607462.2
Dm_NT1	NP_001163348.1

---

Cq_NT1_1	XP_001841845.1
Cq_NT1_2	XP_001841846.1
Pc_NT1	XP_002423418.1

**Toll**

NvToll_2	XP_001604577.1
NvToll_3	XP_001604871.2
NvToll_4	XP_003425965.1
NvToll8	XP_001603014.1
NvToll6_1	XP_001601629.2
NvToll6_2	XP_003424932.1
NvToll7	XP_003425317.1

DmToll_C	NP_001262995.1
DmToll_B	NP_524518.1
DmToll_D	NP_733166.1
DmToll2/18w	NP_476814.1
DmToll3	AAF86229.1
DmToll4	AAF52747.3
DmToll5	AAF86227.1
DmToll6	AAF86226.1
DmToll7	NP_523797.1
DmToll8/Tollo	NP_524757.1
DmToll9	NP_001246845.1

TcToll1	XP_967154.1
TcToll2	XP_973926.2
TcToll3	XP_967796.1
TcToll4	XP_967716.2
TcToll6	XP_971999.1
TcToll10	XP_393717.2
TcToll7	XP_972409.1
TcToll8	XP_972104.2
TcToll13	XP_973341.2

AmToll	XP_396158.1
AmToll6	XP_393712.2
AmToll10	XP_393717.2
AmToll8	XP_393713.2
AmToll18w	NP_001013379.1

**Pelle / Tube**

Nv Pelle	XP_001599847.1
Nv Pelle-like	XP_001601124.2
Dm Pelle	NP_476971.1



---

Tc Pelle	XP_966383.1
Am Pelle	XP_624002.3
Mm IRAK1	EDL29849.1
Mm IRAK4	AAH51676.1
Nv Tube	XP_001606360.1
Dm Tube	AAA28994.1
Tc TC011895	EFA09756.1
Am Tube	XP_001121229.2

**Myeloid differentiation primary response gene 88 (Myd88) / CG42795**

Nv_Myd88	XP_001602490.1
Dm_Myd88	NP_610479.1
Cq_Myd88_1	XP_001868621.1
Cq_Myd88_2	XP_001850286.1
Tc_Myd88_1	EFA01304.1
Tc_Myd88_2	XP_973419.2
Am_Myd88_1	AGM19319.1
Am_Myd88_2	AGM19359.1
Am_Myd88_3	AGM19327.1
Pc_Myd88	XP_002431564.1

Nv_CG42795	XP_003426839.1
Dm_CG42795	NP_649988.2
Cq_CG42795	XP_001845012.1
Tc_CG42795	EFA12119.1
Am_CG42795	XP_393843.3
Pc_CG42795	XP_002423273.1

**Cactus (Cact)**

Nv_Cact_1	XP_001603027.1
Nv_Cact_2	XP_001603057.1
Nv_Cact_3	XP_001603141.1
Dm_Cact	AAA85908.1
Cq_Cact	XP_001846384.1
Tc_Cact_1	NP_001157182.1
Am_Cact_1	ACT66872.1
Am_Cact_3	XP_394485.2
Am_Cact_4	XP_001121575.2
Pc_Cact	XP_002427786.1

**Dorsal (DI) / Relish (Rel) / Dorsal immune response factor (Dif)**

Nv-DI_1	XP_001602675.2
Nv-DI_2	XP_001603465.2
Nv-DI_3	XP_001602435.2
Nv-DI_4	XP_003427515.1
Dm-DI	NP_724054.1
Cq-DI_1	XP_001844078.1
Cq-DI_2	XP_001866031.1
Cq-DI_4	XP_001844076.1
Cq-DI_5	XP_001861958.1
Cq-DI_6	XP_001843106.1
Tc-DI_1	EFA02850.1
Tc-DI_3	XP_974806.2
Am-DI_1	NP_001164477.1
Am-DI_3	XP_395180.4
Pc-DI	XP_002431518.1
Am-Rel	XP_624626.3
Nv-Rel_1	XP_001602212.2
Dm-Rel	NP_996187.1
Cq-Rel	XP_001862276.1
Tc-Rel	XP_970894.1
Pc-Rel	XP_002429240.1
Dm-Dif	NP_001162998.1

### 3.6.2 Phylogenetic analysis

The Phylogenetic trees in chapter 4 were generated using the tools available at:

<http://www.phylogeny.fr/> (Dereeper et al., 2008)

The maximum likelihood phylogeny in Fig. 4.17 was generated with PhyML (Guindon and Gascuel 2003). Tree was edited in MEGA5.2.2.

(<http://www.megasoftware.net/index.php>)

### 3.6.3 ISH Primers of Toll Pathway genes

<i>dorsal 1</i>	Fw	AAACATGACCGTTTCCTTCG
	Rev	TGAGGCATTTGTTTCAGCAG
<i>dorsal 2</i>	Fw	CAACAGTTGCTGGTGGATTG
	Rev	TGTCGGTTGGATTGAAACA
<i>dorsal 3</i>	Fw	GGAAAGCTCGCTAGAGGTGA
	Rev	GTGCTGTCATTTGCTCGAAA
<i>dorsal 4</i>	Fw	TTCTTGCGTCACAAAAGACG
	Rev	AACATTTTGCTCGGGTATGC
<i>cact 1</i>	Fw	ACTTGGATATGGGCAAGTCG
	Rev	CTACTGTCGCTGCTGCTGTC
<i>cact 2</i>	FW	CCTGAACCTGCTAAGGCTTG
	Rev	ATGAGCTCCTTGGCTAGTCG
<i>cact 3</i>	FW	CCTACAGCTCCGAATTGTCTTC
	Rev	ACTCCTGGATCAGACAGAGGAA
<i>easter1</i>	FW	TCCGCCTTTGATTGCTATTC
	Rev	AGGCCTGCTTGTCTACCAGA
<i>easter 2</i>	Fw	ATATTCATTTTGCCGCTTGC
	Rev	CTGGCCTTCTTCTCGATTTG
<i>snake</i>	Fw	CGTCCAAACGAATCTGGTCT
	Rev	TCTCGATCCAGTCGACGTAA
<i>gastrulation defective</i>	Fw	AAAATACGTTGGGCGCATAG
	Rev	CTGGTTTTCCCATCCAAAGA

---

<i>nudel</i>	Fw	ACAGATAGGCACGGACAACC
	Rev	CAGTGCAAGCCTCTTTAGCC
<i>pipe</i>	Fw	AAACCGTTGCCGTCTCTCTA
	Rev	TGAGCAACGAGAATTCGTGTC
<i>slalom</i>	Fw	TGCTTTGTGGGTACCAGTGA
	Rev	TACAACCTGACCCGTGGTTGA
<i>windbeutel</i>	Fw	ACATAGGTGGGAGTCGATGC
	Rev	GTGCGTGAAAGACTGCAAAA
<i>serpin27A</i>	Fw	CACAGCATCTCGTCCTTCAA
	Rev	ATCAGCGGAATCACCGATAC
<i>TollB</i>	Fw	CGACAAATCCAATGTCATGC
	Rev	TTGTTGCGAAGCGTTAGTTG
<i>Toll2</i>	Fw	TGCGCTTCAACAACATATCC
	Rev	TTGCTCGAGTTGGAGAGCTT
<i>Toll 3</i>	Fw	GAACTCGCCAAACTGGTCTC
	Rev	AACGGATTGTTTCGTCAGCTC
<i>Toll4</i>	Fw	ATTGTCCGGTCAAAACGAAC
	Rev	GCTTCGAGTACAGCCAAACC
<i>spz2</i>	Fw	CACAGTGGCCAACCTAACCT
	Rev	ACTCTTCTTCCGCGTCATGT
<i>spz1</i>	Fw	AGCTGATCATAACCCGTCCAA
	Rev	GCCACCAACTGCCTGTAGAT
<i>myd88</i>	Fw	TCGTGCAGACCAAATCTCAG
	Rev	TTGGGCTCTTGAAGTGGAGT
<i>pelle</i>	Fw	GCTGCAACTGACAACTGGAA
	Rev	CGGTTGACATTTGTGGTCTG
<i>tube</i>	Fw	AATTCATCGCCTGACAATC
	Rev	TCAGTCTGTTTCGCCCTTCT

Fw = forward primer  
Rev = reverse primer

### 3.7 Transcriptome

#### 3.7.1 RNA isolation

1. Homogenize *Nasonia vitripennis* embryos in 50µl TRIZOL Reagent (Invitrogen) with a pistill in a 1.5 ml Eppendorf tube.
2. Incubate homogenized tissue in TRIZOL Reagent for 5 minutes at room temperature.
4. Bring volume up to 1ml TRIZOL.
5. Add 200 µl of Chloroform.
6. Shake tube vigorously by hand for 15 seconds.
7. Incubate 2 to 3 minutes at room temperature.
8. Centrifuge at 11,600 rcf for 15 minutes at 4°C
9. Transfer upper aqueous phase to a new Rnase-free 1.5 ml tube
10. Add 500µl Isopropyl alcohol.
11. Incubate overnight at -20°C
12. Centrifuge at 11,600 rcf for 15 minutes at 4°C
13. Remove supernatant thoroughly
14. Add 1ml 70% ethanol.
15. Wash pellet 20-30 min on a shaker
16. Centrifuge at 9,700 rcf for 15 minutes at 4°C
17. Remove supernatant thoroughly
18. Dry RNA pellet for 5 minutes at room temperature
19. Resuspend pellet in 10-20µl RNase-free water.

Concentration and purity of samples were determined via NanoDrop™

#### 3.7.2 cDNA generation

cDNA was generated with the SuperScript® VILO cDNA Synthesis Kit and Master Mix using 2,5 µg/µl RNA.

### 3.7.3 Quantitative polymerase chain reaction (qPCR)

qPCR was used to quantify and compare the relative amount of *twist* mRNA in wild type, BMP- knockdown and Toll- knockdown embryos. For each knockdown condition (BMP<sup>-</sup>/Toll<sup>-</sup>) four independent biological replicates, using 4 different dsRNA probes were generated (*dpp*, *gbb*, *Toll3*, *Toll3\**). *Toll3* dsRNA and *Toll3\** dsRNA target the same mRNA (*Toll3* mRNA). However, *Toll3* is approx 700bp whereas *Toll3\** is approx 250bp long. Each of the two dsRNA probes targets a different region of the *Toll3* mRNA. Four qPCR experiments were performed. In parallel to each experiment, a dilution series of known template concentrations was used to establish a standard curve for assessing the reaction efficiency (Fig. 3.1). Each experiment was performed on a 96-well plate, using one biological replicate of each knockdown condition together with a wild type control (see table 3.1 & Fig. 3.2). To control for the validity of the method, three technical replicates (triplicates) of each primer sample were used in each experiment.

All knockdown WT samples were generated by pRNAi injection, RNA isolation and cDNA synthesis as described above.

For normalization of the qPCR data, *polyubiquitin* (XM\_001599384.1) and *actin 5c* (XM\_001601007.1) were used as reference genes.

**Table 3.1 pRNAi knockdown samples used for qPCR**

Each triplet corresponds to a single experiment.

Concentration and purity of total RNA samples were determined via NanoDrop™

Sample Name	Conc. ( $\mu\text{g}/\mu\text{l}$ )
WT 20.10.	1,8
<i>Toll3</i> <sup>-</sup> 20.10.	1,6
<i>dpp</i> <sup>-</sup> 20.10.	0,9
<u>2<sup>nd</sup> experiment</u>	
WT 26.10.	0,18
<i>Toll3</i> <sup>-</sup> 26.10.	0,6
<i>dpp</i> <sup>-</sup> 26.10.	0,6
<u>3<sup>rd</sup> experiment</u>	
WT 02.11.	0,4
<i>Toll3</i> <sup>-*</sup> 02.11.	0,9
<i>gbb1</i> <sup>-</sup> 02.11.	0,8
<u>4<sup>th</sup> experiment</u>	
WT 16.11.	0,7
<i>Toll3</i> <sup>-*</sup> 16.11.	3,9
<i>gbb1</i> <sup>-</sup> 16.11.	2,3

**qPCR mix**

12,5 $\mu\text{l}$	SYBR Green®
1 $\mu\text{l}$	Forward Primer
1 $\mu\text{l}$	Reverse Primer
8,5 $\mu\text{l}$	Water
2 $\mu\text{l}$	DNA
-----	
25 $\mu\text{l}$	1 Reaction

	1	2	3	4	5	6	7	8	9	10
A	twi1FW/twi1REV	twi1FW/twi1REV	twi1FW/twi1REV	twi1FW/twi1REV	twi1FW/twi1REV	twi1FW/twi1REV	twi1FW/twi1REV	twi1FW/twi1REV	twi1FW/twi1REV	twi1FW/twi1REV
	NTC	1:10000	1:10000	1:1000	1:1000	1:100	1:100	1:100	1:10	1:10
B	twi2FW/twi2REV	twi2FW/twi2REV	twi2FW/twi2REV	twi2FW/twi2REV	twi2FW/twi2REV	twi2FW/twi2REV	twi2FW/twi2REV	twi2FW/twi2REV	twi2FW/twi2REV	twi2FW/twi2REV
	NTC	1:10000	1:10000	1:1000	1:1000	1:100	1:100	1:100	1:10	1:10
C	twi3FW/twi3REV	twi3FW/twi3REV	twi3FW/twi3REV	twi3FW/twi3REV	twi3FW/twi3REV	twi3FW/twi3REV	twi3FW/twi3REV	twi3FW/twi3REV	twi3FW/twi3REV	twi3FW/twi3REV
	NTC	1:10000	1:10000	1:1000	1:1000	1:100	1:100	1:100	1:10	1:10
D	Pol1FW/Pol1REV	Pol1FW/Pol1REV	Pol1FW/Pol1REV	Pol1FW/Pol1REV	Pol1FW/Pol1REV	Pol1FW/Pol1REV	Pol1FW/Pol1REV	Pol1FW/Pol1REV	Pol1FW/Pol1REV	Pol1FW/Pol1REV
	NTC	1:10000	1:10000	1:1000	1:1000	1:100	1:100	1:100	1:10	1:10
E	Pol2FW/Pol2REV	Pol2FW/Pol2REV	Pol2FW/Pol2REV	Pol2FW/Pol2REV	Pol2FW/Pol2REV	Pol2FW/Pol2REV	Pol2FW/Pol2REV	Pol2FW/Pol2REV	Pol2FW/Pol2REV	Pol2FW/Pol2REV
	NTC	1:10000	1:10000	1:1000	1:1000	1:100	1:100	1:100	1:10	1:10
F	Act1FW/Act1REV	Act1FW/Act1REV	Act1FW/Act1REV	Act1FW/Act1REV	Act1FW/Act1REV	Act1FW/Act1REV	Act1FW/Act1REV	Act1FW/Act1REV	Act1FW/Act1REV	Act1FW/Act1REV
	NTC	1:10000	1:10000	1:1000	1:1000	1:100	1:100	1:100	1:10	1:10
G	Act2FW/Act2REV	Act2FW/Act2REV	Act2FW/Act2REV	Act2FW/Act2REV	Act2FW/Act2REV	Act2FW/Act2REV	Act2FW/Act2REV	Act2FW/Act2REV	Act2FW/Act2REV	Act2FW/Act2REV
	NTC	1:10000	1:10000	1:1000	1:1000	1:100	1:100	1:100	1:10	1:10

**Figure 3.1 Pipetting scheme for standard curve dilution**

The scheme reflects the arrangement of wells on a standard 96 well plate. Top panel in each line refers to the used primer combination. Bottom panel refers to the dilution of DNA (1 = 2,5µg/µl). NTC = none template control; twi = *twist*; Pol = *polyubiquitin*; Act = *actin 5c*; FW = forward primer; REV = reverse primer.

	1	2	3	4	5	6	7	8	9
A	twi1FW/twi1REV	twi1FW/twi1REV	twi1FW/twi1REV	twi1FW/twi1REV	twi1FW/twi1REV	twi1FW/twi1REV	twi1FW/twi1REV	twi1FW/twi1REV	twi1FW/twi1REV
	wt cDNA	wt cDNA	wt cDNA	Toll-cDNA	Toll-cDNA	Toll-cDNA	Toll-cDNA	dpp-cDNA	dpp-cDNA
B	twi2FW/twi2REV	twi2FW/twi2REV	twi2FW/twi2REV	twi2FW/twi2REV	twi2FW/twi2REV	twi2FW/twi2REV	twi2FW/twi2REV	twi2FW/twi2REV	twi2FW/twi2REV
	wt cDNA	wt cDNA	wt cDNA	Toll-cDNA	Toll-cDNA	Toll-cDNA	Toll-cDNA	dpp-cDNA	dpp-cDNA
C	twi3FW/twi3REV	twi3FW/twi3REV	twi3FW/twi3REV	twi3FW/twi3REV	twi3FW/twi3REV	twi3FW/twi3REV	twi3FW/twi3REV	twi3FW/twi3REV	twi3FW/twi3REV
	wt cDNA	wt cDNA	wt cDNA	Toll-cDNA	Toll-cDNA	Toll-cDNA	Toll-cDNA	dpp-cDNA	dpp-cDNA
D	Pol1FW/Pol1REV	Pol1FW/Pol1REV	Pol1FW/Pol1REV	Pol1FW/Pol1REV	Pol1FW/Pol1REV	Pol1FW/Pol1REV	Pol1FW/Pol1REV	Pol1FW/Pol1REV	Pol1FW/Pol1REV
	wt cDNA	wt cDNA	wt cDNA	Toll-cDNA	Toll-cDNA	Toll-cDNA	Toll-cDNA	dpp-cDNA	dpp-cDNA
E	Pol2FW/Pol2REV	Pol2FW/Pol2REV	Pol2FW/Pol2REV	Pol2FW/Pol2REV	Pol2FW/Pol2REV	Pol2FW/Pol2REV	Pol2FW/Pol2REV	Pol2FW/Pol2REV	Pol2FW/Pol2REV
	wt cDNA	wt cDNA	wt cDNA	Toll-cDNA	Toll-cDNA	Toll-cDNA	Toll-cDNA	dpp-cDNA	dpp-cDNA
F	Act1FW/Act1REV	Act1FW/Act1REV	Act1FW/Act1REV	Act1FW/Act1REV	Act1FW/Act1REV	Act1FW/Act1REV	Act1FW/Act1REV	Act1FW/Act1REV	Act1FW/Act1REV
	wt cDNA	wt cDNA	wt cDNA	Toll-cDNA	Toll-cDNA	Toll-cDNA	Toll-cDNA	dpp-cDNA	dpp-cDNA
G	Act2FW/Act2REV	Act2FW/Act2REV	Act2FW/Act2REV	Act2FW/Act2REV	Act2FW/Act2REV	Act2FW/Act2REV	Act2FW/Act2REV	Act2FW/Act2REV	Act2FW/Act2REV
	wt cDNA	wt cDNA	wt cDNA	Toll-cDNA	Toll-cDNA	Toll-cDNA	Toll-cDNA	dpp-cDNA	dpp-cDNA

**Figure 3.2 Pipetting scheme for qPCR experiment**

The scheme reflects the arrangement of wells on a standard 96 well plate. Top panel in each line refers to the used primer combination. Bottom panel refers to the used cDNA. twi = *twist*; Pol = *polyubiquitin*; Act = *actin 5c*; FW = forward primer; REV = reverse primer; wt = wild type; Toll  $\hat{=}$  *Toll3* or *Toll3*\*knockdown cDNA; dpp  $\hat{=}$  *dpp* or *gbb* knockdown cDNA

**Primers used for qPCR:**

For each experiment three different sets of twist primers, and two different sets of polyubiquitin/actin primers were used:

<i>twist 1</i>	Fw	AGCTCGCCACCAAGTACATC
	Rev	CTCTCACTGCGTTTTGTGGA
<i>twist 2</i>	Fw	CGAGGTGCAAGAAGAGGAAG
	Rev	ACGTTAGCCATGACCCTCTG
<i>twist 3</i>	Fw	TCCAGCAGCATCAGCTCTAC
	Rev	GGGAAGGTCTTGCTCTCGT
<i>actin 1</i>	Fw	TGTCATGGTTCGGTATGGAGA
	Rev	AGCCTCGGTCAGGAGGAC



---

<i>actin 2</i>	Fw	GTCCATCGTCCACAGGAAGT
	Rev	CTTCTCTCGTCTCGCGTGT
<i>polyubiquitin 1</i>	Fw	CTCGAAGATGGACGCACA
	Rev	CCCGTGAGTGTCTTAACGAA
<i>polyubiquitin 2</i>	Fw	AATCCAGGACAAAGAGGGAAT
	Rev	TTCCACCCCTAAGACGTAAGA

Fw = forward primer  
Rev = reverse primer

#### Primers used for RNAi probe synthesis

<i>Toll</i>	Fw	GAACTCGCCAAACTGGTCTC
	Rev	AACGGATTGTTCGTCAGCTC
<i>Toll*</i>	Fw	GAACTCGCCAAACTGGTCTC
	Rev	AACGGATTGTTCGTCAGCTC
<i>decapentaplegic (dpp)</i>	Fw	GTGGTGGGCGAGGCGGTAAA
	Rev	CACGACCTTGTTCTCCTCGT
<i>glass bottom boat 1 (gbb1)</i>	Fw	ATCCTGCTGCAGTTCGACTT
	Rev	CCCTGATGATCATGTTGTGG

Fw = forward primer  
Rev = reverse primer

qPCR was performed using **Applied Biosystems 7500 Fast Real-Time PCR System**

### 3.7.4 Transcriptome data generation and evaluation

The transcriptome was sequenced at the **Cologne Center for Genomics (CCG)** using an Illumina GAIIX genome analyzer (<http://portal.ccg.uni-koeln.de/ccg/ngs/>). Samples in Table 3.2 were used for sequencing. All samples were generated by pRNAi injection, RNA isolation and cDNA synthesis as described above.

**Table 3.2 pRNAi knockdown samples used for RNA seq.**

Concentration and purity of total RNA samples were determined via NanoDrop™

Name	Conc. ( $\mu\text{g}/\mu\text{l}$ )	Vol ( $\mu\text{l}$ )
WT 17.04	1,1	3
<i>TollA</i> <sup>-</sup> 26.10.	0,6	3
<i>dpp</i> <sup>-</sup> 26.10.	0,6	3
WT 08.05.	2,2	2
<i>TollA</i> <sup>*</sup> 16.11.	3,9	2
<i>gbb1</i> <sup>-</sup> 16.11.	2,3	2

**Further evaluation of the raw transcriptome data was processed and performed by Dr. Jeremy A. Lynch using the following programs and protocols:**

- Bowtie software (<http://bowtie-bio.sourceforge.net/index.shtm/>)
- SAM tools (<http://samtools.sourceforge.net/>)
- TopHat software (<http://tophat.cbcb.umd.edu/>)
- Cufflinks software (<http://cufflinks.cbcb.umd.edu/>)
- Differential gene and transcript expression analysis of RNA-seq experiments with TopHat and Cufflinks. (Trapnell et al., 2012)

### 3.7.5 High through-put ISH Primers

Primers of genes that displayed a distinct expression pattern:  
(The whole transcriptome data set and a list of all differentially expressed genes is available in the Roth group)

2EG025794/ <i>epithelial membrane protein (emp)</i>	Fw	CCTGAAGATCAAGCCTTTCG
	Rev	TTGATCTGGATCCTGGCTCT
2EG013778	Fw	GCGTCGAAGTTGAACCATCT
	Rev	CTGCAGATCTCCGACAATGA
2EG000923	Fw	TACCAGGGATTCCTTTGCTG
	Rev	GTACAGACACCCGGCCTAGA
2EG007407/ <i>homeobrain (hbn)</i>	Fw	AGATCGAAGGGACACATTGC
	Rev	CCTGAACTCTGGCTTCAGAAA
2EG009116/ <i>longitudinals lacking (lola)</i>	Fw	GGTTTGTACCCGATCGAAGA
	Rev	TTACCGAGAGCCTGGTTGTT
2EG023469/ <i>rotund (rn)</i>	Fw	GCAAGAGCTACACCCAGGAG
Rev		CGGATCTGGTGGAGACTGAT
2EG017550/ <i>fk506-binding protein2 (fk506-bp2)</i>	Fw	CGCATCAGCACGTCTCTCTA
	Rev	CTTCTTCACCTCGTCGCTCT
2EG001522/ <i>ankyrin (ank)</i>	Fw	TATCCTCTGCACATCGCTTG
	Rev	TCACGCTTCCTCGATCTTCT
2EG006076/ <i>general transcription factor IIF subunit1 (gtf2f1)</i>	Fw	AGCGACGAGAAGGAAAACAA
	Rev	TTCTGAAGAAGCTCCGTCGT
2EG011947/ <i>calsyntenin (cals)</i>	Fw	TACACCGTTCCGAGTCAGAG
	Rev	CTCAGACAGGTCAGCACGTC
2EG006715/ <i>ankyrin-2 (ank2)</i>	Fw	AAAGGTTCACTGCTCCGAGA
	Rev	AGTAGCAGCTCCGTCAGCT
2EG014953/ <i>pathetic (pth)</i>	Fw	ATATTGCTGCTTCCGCTGAT
	Rev	TCCAAATCCAATGTCCCAGT

2EG008134/ <i>kin of IRRE (kirre)</i>	Fw	GCCAGGACTCGACGAATTTA
	Rev	GCCGTAAAGGGGACTAGAGG
2EG013616/ <i>semaphorin-5c (sema-5c)</i>	Fw	TCAGACGAAGGAGGAGGAGA
	Rev	TAGATGCACATGACGGTGGT
2EG009552/ <i>optomotor blind (omb)</i>	Fw	ATCAGCACCCTACCGGAAC
	Rev	CGGAACTCGCAACAACATAA
2EG004843/ <i>drumstick (drm)</i>	Fw	TCCTGGCAACAACAACAAAA
	Rev	GCTCGGCTGTATCGAGTTTC

Fw = forward primer

Rev = reverse primer

### 3.7.6 High through-put in ISH

High through ISH is an adapted *Drosophila* protocol described in (Berns et al., 2012). Solutions and order of single steps is identical to the one color ISH using NBT/BCIP detection method described in chapter 3.4 except for the following solutions/steps:

#### Hybridization solution

50% formamide	25ml of 100% formamide
5x SSC	12,5ml of 20x SSC
2% SDS	10ml of 10% SDS
1% <b>BBR</b>	<b>0.5g (Roche)</b>
250 ug/mL tRNA	0.0125g
50 µg/mL heparin	100µl
H <sub>2</sub> O	fill up to 50ml

Additionally, following items are required:

Vacuum pump

96-well filter plates (0.45-µm pore size)

Multi-channel pipette

## 4 Additional Results

### 4.1 The Toll signaling cascade in *Nasonia vitripennis*

Up to now, most analyzed *Nasonia* Toll pathway related genes in this thesis were mainly orthologs of zygotically expressed *Drosophila melanogaster* (*Dm*) Dorsal target genes. However, as described earlier Dorsal's nuclear activity in *Dm* is the result of a hierarchical signaling cascade that originates in the follicular epithelium of the egg chamber during oogenesis (see chapter 1.4.1 - 1.4.4).

To investigate whether the upstream and downstream components of the Toll receptor are conserved between *Drosophila melanogaster* (Diptera) and *Nasonia vitripennis* (Hymenoptera), an analysis of the respective genes was performed using the sequenced genome of *Nasonia* (Werren et al., 2010) on NCBI. The NCBI Basic Local Alignment Search Tool (BLAST) revealed *Drosophila*-related sequences of all investigated Toll pathway components in the *Nasonia* genome. For additional phylogenetic analysis, the related sequences of *Culex quinquefasciatus* (Diptera), *Tribolium castaneum* (Coleoptera), *Apis mellifera* (Hymenoptera) and *Pediculus humanus corporis* (Phthiraptera) (Fig. 4.1) were also identified by protein BLAST in the corresponding genomes on NCBI. The protein sequences of those genes were further investigated by a phylogenetic analysis using “*Phylogeny.fr Robust Phylogenetic Analysis For The Non-Specialist*” (Dereeper et al., 2008). To confirm that the putative *Nasonia* orthologs are indeed closest related to the *Dm*-query-sequence each phylogenetic tree was outgroup-rooted by using the second best hit of the BLAST search as outgroup. In this context, the second best hit of a *Nasonia* BLAST search is defined as the first *Nasonia* sequence in the list of BLAST hits, which does not lead back to the original *Dm*-query sequence when BLASTed back against the *Dm* database. The resulting *Dm*-sequence served as outgroup sequence and was also BLASTed in the genomes of the other five species. The outgroup sequences are supposed to group together and branch off ancestrally to all other presumed

operational taxonomic units (OTUs = sequence or organism used as the terminal nodes of a phylogenetic tree) in the phylogeny. The indicated names of the sequences in the phylogenetic trees are derived from the order of appearance in the BLAST search results and thus preceded the generation of the phylogenetic trees. For further information please look up the corresponding NCBI accession numbers in chapter 3.6.1 Material & Methods.

The BLASTs and phylogenetic trees were performed using full protein sequences of all six species except for the tree combining Tube and Pelle orthologous sequences which is based on previous research on sequence homology between *Dm*-Tube and *Mus musculus* (*Mm*) IRAK 4 (Towb et al., 2009). The phylogenetic tree is based on a Death Domain alignment of Tube and Pelle orthologs from *Dm*, *Tc*, *Am*, *Nv*, and *Mm* (Fig. 4.17).

Additionally, the Windbeutel tree (Fig. 4.2) is not outgroup-rooted since the corresponding outgroup-sequences (Sallimus) are too diverged to be aligned with the Windbeutel sequences.

Furthermore, the Toll phylogenetic analysis (Fig. 4.14) is based on all Toll and Toll like receptors (TLRs) identified in *Apis*, *Tribolium*, *Nasonia* and *Drosophila*.

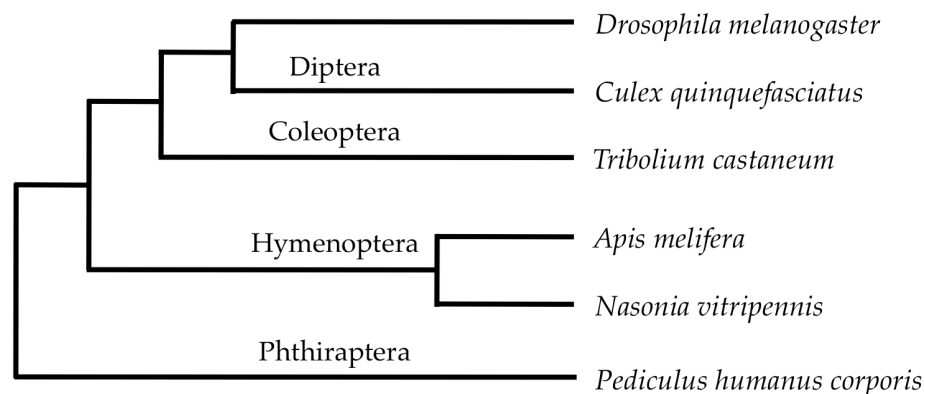


**Figure 4.1 Phylogenetic tree**

The tree shows the relation between the species used for the phylogenetic comparison of Toll pathway components.

The phylogenetically analyzed *Nasonia* genes of the Toll pathway were further analyzed by *In situ* hybridization (ISH) with the exception of *Nv-pelle-like*, *Nv\_spz\_1* and *Nv\_spz\_2*, *Nv\_Toll8* (since these genes were recently identified). ISH was performed in ovarioles and embryos of *Nasonia* (3–6h after egg lay).

### The *Nasonia* Ovariole

Similar to *Drosophila*, the *Nasonia* ovariole represents the polytrophic meroistic type of oogenesis (see Chapter 1.2). However, unlike the *Drosophila* egg chamber, where nurse cells and oocyte are combined in one compartment, the *Nasonia* nurse cells form a separate compartment. Figure 4.2 shows a scheme of a honeybee (*Apis mellifera*) ovariole (Dearden, 2006), which is quite similar to the *Nasonia* ovariole. The figure should facilitate the reader the interpretation of the following *Nasonia* ovariole stainings.

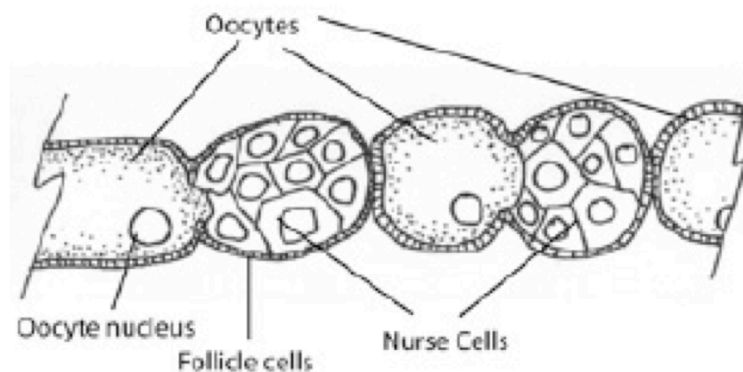


**Figure 4.2 Structure of the Honeybee ovary**

Morphology of a polytrophic meroistic ovariole. (Dearden, 2006)

## 4.2 Analyses of Toll pathway components

The described components are subdivided into chapters corresponding to the compartment in which they are expressed/ active in *Drosophila*:

- Components of the follicular epithelium
- Components of the perivitelline fluid
- Components of the oocyte membrane (*Toll receptors*)
- Intracellular oocyte components

#### 4.2.1 Analysis of components of the follicular epithelium

The Toll pathway components expressed in the follicle cells of the *Drosophila* egg chamber are *windbeutel*, *slalom*, *pipe* and *nudel*. Related sequences of all four genes were identified in the genomes of all six species.

##### Windbeutel

In a comparison between Windbeutel (Wbl) related protein sequences of all six species, *Nv*-Wbl is closest related to the other hymenopteran sequence of *Apis mellifera* (Fig. 4.3). ISH did not show an expression pattern in ovarioles or embryos.

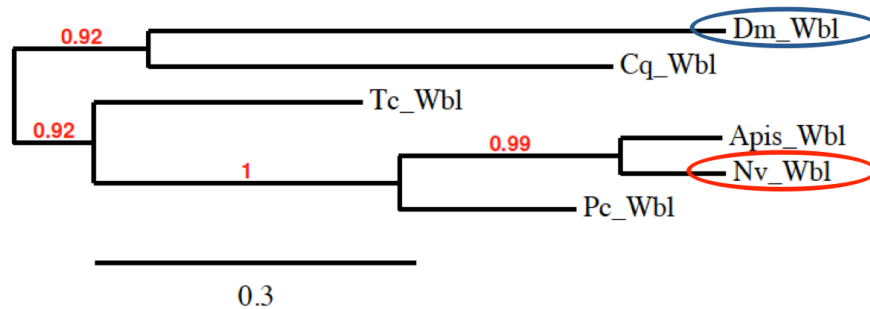


**Figure 4.3 Phylogenetic analysis of Windbeutel**

SH-aLRT tree based on muscle alignment of Windbeutel protein sequences. The tree describes the relationship between Windbeutel proteins in different insect species. Red values indicate branch support (SH-aLRT) in percentages (x 100). Red ellipses highlight *Nasonia* sequences and blue ellipses highlight *Drosophila* sequences. Wbl = Windbeutel; Am = *Apis mellifera*, Dm = *Drosophila melanogaster*; Tc = *Tribolium castaneum*; Cq = *Culex quinquefasciatus*; Nv = *Nasonia vitripennis*; Pc = *Pediculus corporis*.

##### Slalom

In a phylogenetic analysis comparing Slalom protein sequences with the closely related Medial glomeruli (Meigo) protein sequence of all species, the Slalom sequences branch separately. Within the Slalom branch, the Dipteran sequences of *Dm*-Slalom and *Cq*-Slalom seem closer related to each other whereas *Nv*-Slalom clusters with the other sequences. Within this cluster, the



*Nasonia* sequence is most similar to *Am*-Slalom (Fig. 4.4). ISH did not show an expression pattern in ovarioles or embryos.

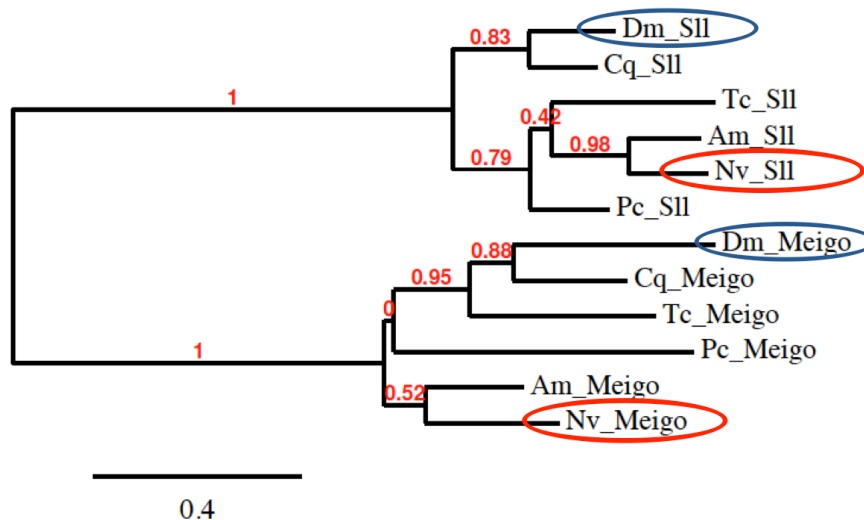


**Figure 4.4 Phylogenetic analysis of Slalom**

The tree describes the relationship between Slalom homologs and the closely related protein Medial glomeruli in different insect species. Red values indicate branch support (SH-aLRT) in percentages (x 100). Red ellipses highlight *Nasonia* sequences and blue ellipses highlight *Drosophila* sequences. Sll = Slalom; Meigo = Medial glomeruli; Am = *Apis mellifera*; Dm = *Drosophila melanogaster*; Tc = *Tribolium castaneum*; Cq = *Culex quinquefasciatus*; Nv = *Nasonia vitripennis*; Pc = *Pediculus corporis*.

### Pipe

For the phylogenetic analysis of Pipe, the *Drosophila* isoform ST2, which was shown to be essential for DV patterning (Zhang et al., 2009b) was used as query sequence. The phylogenetic analysis of Pipe and the outgroup sequence of  $\alpha/\beta$  Hydrolase2 (Hydr2) revealed that *Nv*-Pipe groups with the other Pipe homologs but forms a sister branch to the remaining Pipe sequences (Fig. 4.5). ISH did not show an expression pattern in ovarioles or embryos.

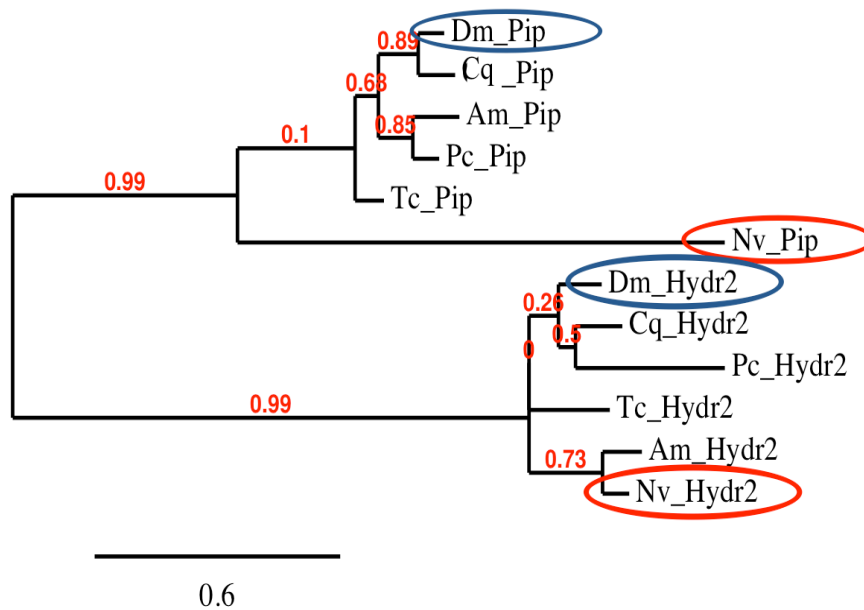


**Figure 4.5 Phylogenetic analysis of Pipe**

The tree describes the relationship between Pipe homologs and the closely related protein  $\alpha/\beta$  hydrolase2 in different insect species. Red values indicate branch support (SH-aLRT) in percentages (x 100). Red ellipses highlight *Nasonia* sequences and blue ellipses highlight *Drosophila* sequences. Pip = Pipe; Hydr2 =  $\alpha/\beta$  Hydrolase2; Am = *Apis mellifera*; Dm = *Drosophila melanogaster*; Tc = *Tribolium castaneum*; Cq = *Culex quinquefasciatus*; Nv = *Nasonia vitripennis*; Pc = *Pediculus corporis*.

### Nudel

In a phylogenetic comparison of Nudel (Ndl) related sequences with the closely related outgroup sequences Corin and CG4386, *Nv*-Nudel forms a sister branch to the Dipteran sequences of *Drosophila* and *Culex*, whereas the other hymenopteran sequence *Am*-Nudel branches more basally (Fig. 4.6).

*Nv-ndl* mRNA expression is detected in the oocyte and the follicle cells surrounding the oocyte (Fig. 4.12a). *Nv-ndl* expression is not detected in the embryo.

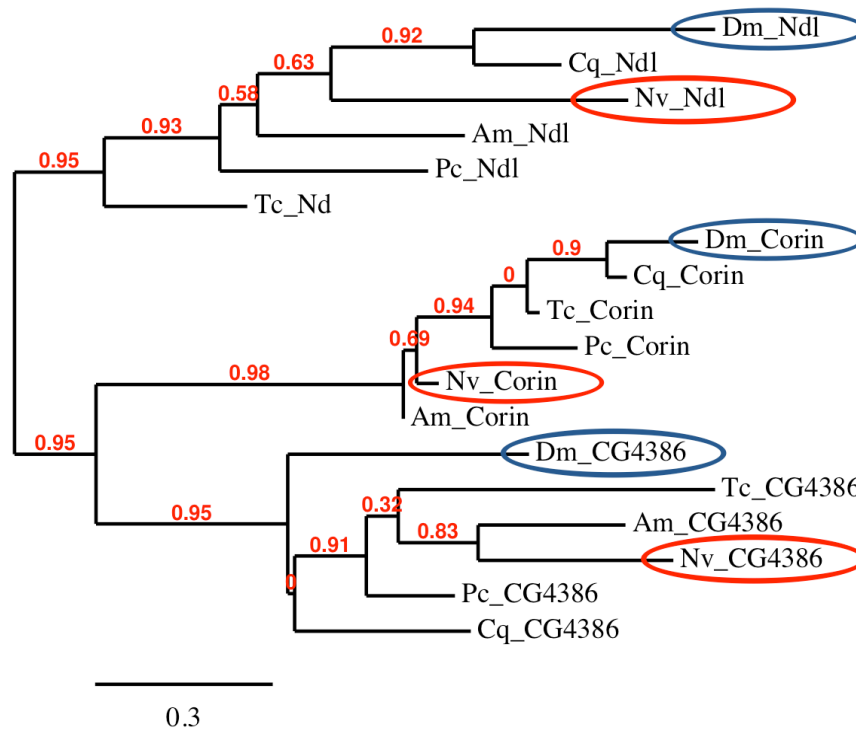


**Figure 4.6 Phylogenetic analysis of Nudel**

The tree describes the relationship between Nudel homologs and the closely related proteins CG4386 and Corin in different insect species. Red values indicate branch support (SH-aLRT) in percentages ( $\times 100$ ). Red ellipses highlight *Nasonia* sequences and blue ellipses highlight *Drosophila* sequences. Ndl = Nudel; Am = *Apis mellifera*; Dm = *Drosophila melanogaster*; Tc = *Tribolium castaneum*; Cq = *Culex quinquefasciatus*; Nv = *Nasonia vitripennis*; Pc = *Pediculus corporis*.

#### 4.2.2 Analysis of perivitelline fluid components

Together with Nudel protein, three sequentially acting proteases are active in the perivitelline fluid (Gastrulation defective, Snake and Easter). Their activity culminates in the generation of the active form of Spätzle, which is the ligand of the oocyte-transmembrane receptor Toll. Related sequences to all components were identified in the *Nasonia* genome database on NCBI.

### Gastrulation defective

Protein BLAST for Gastrulation defective (Gd) related sequences revealed two homologous *Tribolium* sequences, Tc\_Gd\_1 and Tc\_Gd\_2. Phylogenetic analysis including the sequences of the closely related protein sequence of CG7432 shows that Tc\_Gd\_1 clusters together with the query sequences of *Drosophila* and the related sequences of *Apis* and *Nasonia*. Within this cluster, the *Nasonia* homologous sequence of Gd is most similar to *Apis* (Fig. 4.7). Tc\_Gd\_2 is more similar to Cq\_Gd and Pc\_Gd. The Gd related sequences Dm\_Gd, Tc\_Gd\_1, Am\_Gd and Nv\_Gd are closer related to the outgroup CG7432 than to the Gd related sequences Cq-Gd, Tc-Gd and Pc-Gd (Fig. 4.7)

The *Nasonia gastrulation defective* homolog (*Nv-gd*) is expressed in the oocyte and the surrounding follicle cells. In later stages, expression is restricted to one side of the follicle epithelium (Fig. 4.12b). It is not expressed during embryogenesis.

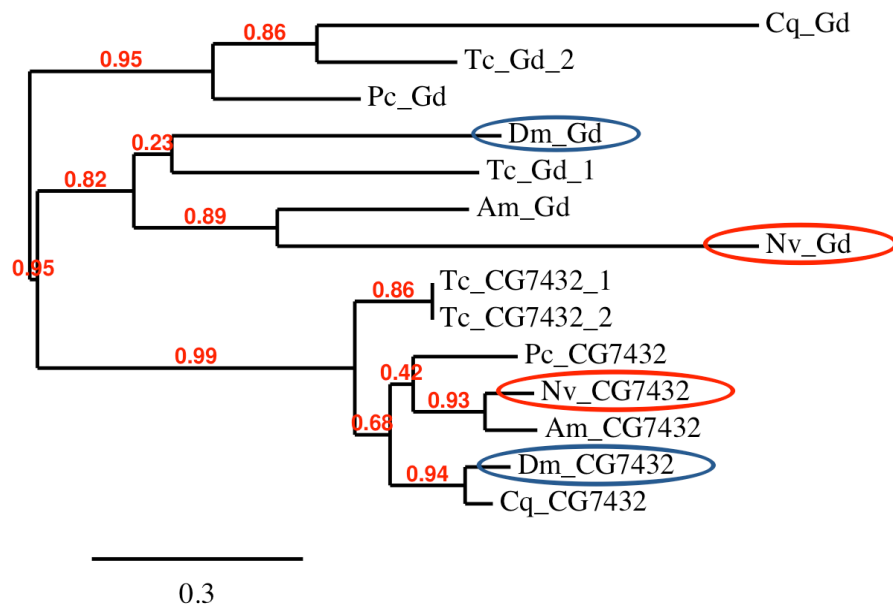


**Figure 4.7 Phylogenetic analysis of Gastrulation defective**

The tree describes the relationship between Gastrulation defective homologs and the closely related protein CG7432 in different insect species. Red values indicate branch support (SH-aLRT) in percentages (x 100). Red ellipses highlight *Nasonia* sequences and blue ellipses highlight *Drosophila* sequences. Gd = Gastrulation defective; Am = *Apis mellifera*; Dm = *Drosophila melanogaster*; Tc = *Tribolium castaneum*; Cq = *Culex quinquefasciatus*; Nv = *Nasonia vitripennis*; Pc = *Pediculus corporis*.

### Snake

BLAST analysis of Snake (Snk) related sequences revealed four different homologous sequences in *Culex* and six in the *Tribolium* genome whereas for each of the other species one homologous sequence was identified.

BLAST analysis of the outgroup sequence, Notopleura (*Dm-NP*), revealed that there is no related sequence to this protein present in the genome of *Pediculus*. To add an appropriate outgroup for *Pediculus*, the second best hit of the *Tribolium* BLAST search, Spirit, was included into the phylogenetic analysis. However, there was no homologous Spirit sequence detected in the genome of *Nasonia*. In a phylogenetic analysis comparing the Snake related sequences to the closely related sequences of NP and Spirit, *Nv-Snake* as well as *Nv-Notopleura*, are both leaves within a branch that has a hypothetical ancestor (the node of the branch) with the sister branch containing the closely related *Dm-Snake* and *Cq-Snake* (Fig. 4.8). In general, the selected outgroup sequences NP and Spirit don't branch separately and thus are impractical to outgroup-root the tree.

Although *Nv-snk* was detected in the *Nasonia* genome, ISH did not show an expression pattern in ovarioles. However, *Nv-snk* is faintly and ubiquitously expressed in embryos (Fig. 4.13i).

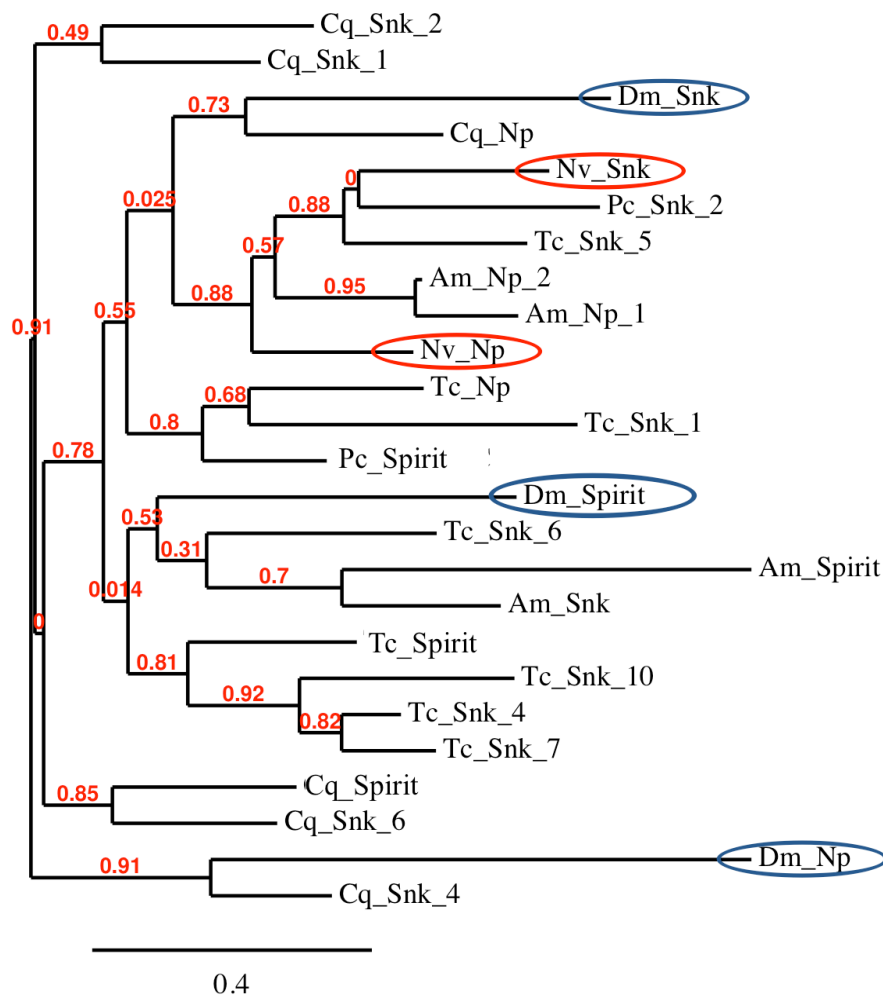


**Figure 4.8 Phylogenetic analysis of Snake**

The tree describes the relationship between Snake homologs and the closely related proteins Notopleura and Spirit in different insect species. Red values indicate branch support (SH-aLRT) in percentages (x 100). Red ellipses highlight *Nasonia* sequences and blue ellipses highlight *Drosophila* sequences. Snk = Snake; Np = Notopleura; Am = *Apis mellifera*; Dm = *Drosophila melanogaster*; Tc = *Tribolium castaneum*; Cq = *Culex quinquefasciatus*; Nv = *Nasonia vitripennis*; Pc = *Pediculus corporis*.

### Easter

BLAST analysis of Easter (Ea) revealed two different homologous sequences in *Nasonia* (*Nv\_Ea\_1* and *Nv\_Ea\_2*), four different Easter like molecules in *Culex* (*Cq\_Ea\_1, 2, 3* and *4*) and two in *Pediculus* (*Pc\_Ea\_1* and *2*). Furthermore, the BLAST analysis revealed five different Easter like molecules in *Tribolium* (*Tc\_Ea\_1, 3, 4, 5* and *8*). Additionally, a functional *Tribolium* ortholog of Easter

(Tc\_Ea\_VA), which was discovered by Van Anh Dao, was added to the phylogeny (V.A. Dao and S. Roth unpublished results). Interestingly, Tc\_Ea\_VA was not identified via the protein BLAST search as described above, since it did not have sufficient sequence homology to the query sequence *Dm\_Ea*.

In a phylogenetic analysis of Easter homologs and the closely related sequence of Melanization Protease 1 (MP1), *Nv\_Ea\_1* is closest related to *Am\_Ea*. Both are leaves on a sister branch to *Nv\_Ea\_2* (Fig. 4.9). The clade containing both branches is a sister clade to the one containing both present MP1 homologs (*Nv\_MP1\_1* and 2). *Dm\_Ea* is leaf on a basal branch and closest related to the assumed outgroup *Dm\_MP1*. Therefore, the selected outgroup sequence MP doesn't branch separately and thus is impractical to outgroup-root the tree.

Of the two identified *easter* homologs (*Nv-ea1* and *Nv-ea2*) only *Nv-ea1* showed an expression pattern in the oocyte and the posterior part of the nurse cell compartment (Fig. 4.12c). Expression of both *Nasonia easter* homologs is not detected during embryogenesis.

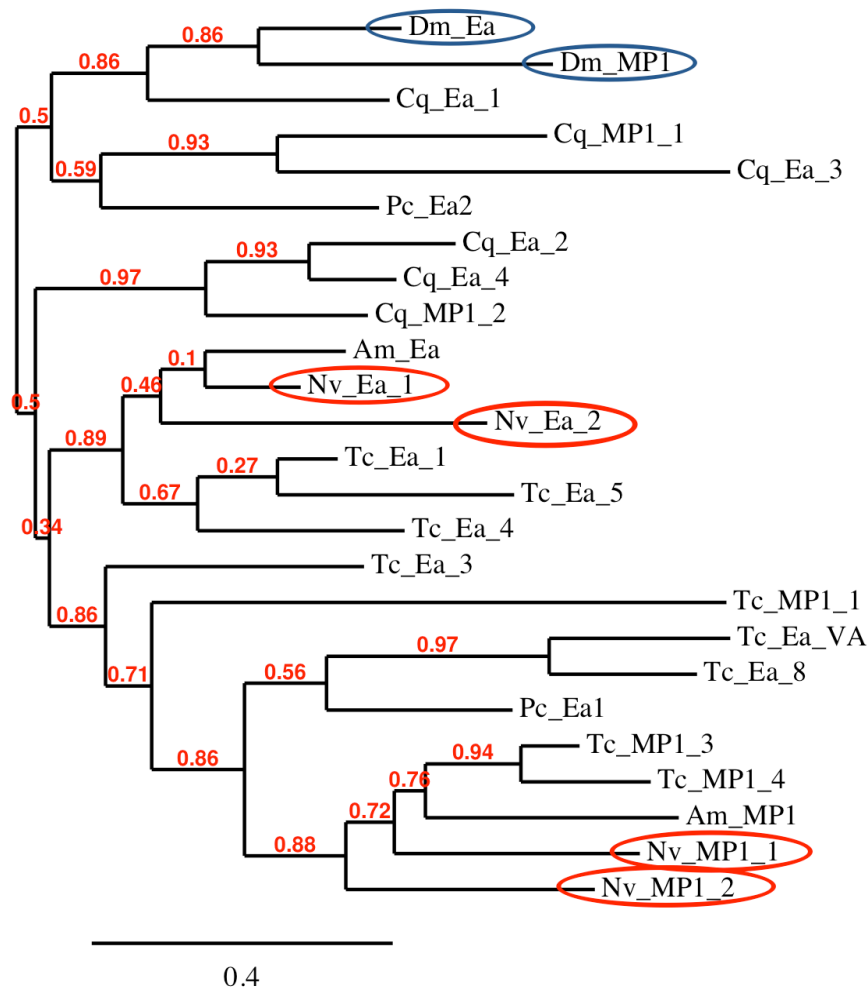


**Figure 4.9 Phylogenetic analysis of Easter**

The tree describes the relationship between Easter homologs and the closely related protein Melanization protease 1 in different insect species. Red values indicate branch support (SH-aLRT) in percentages ( $\times 100$ ). Red ellipses highlight *Nasonia* sequences and blue ellipses highlight *Drosophila* sequences. Ea = Easter; MP1 = Melanization protease 1; Am = *Apis mellifera*; Dm = *Drosophila melanogaster*; Tc = *Tribolium castaneum*; Cq = *Culex quinquefasciatus*; Nv = *Nasonia vitripennis*; Pc = *Pediculus corporis*.

### Serpin 27A

Three different Serpin 27A (Spn27A) related sequences were identified in the *Culex* genome (*Cq\_Spn27A\_1*, 2, 3 and 4) and one homologous sequence in each other species. In a phylogenetic tree including the closely related Serpin 42Da (Spn42Da) as outgroup, *Nv\_Spn27A* groups together with *Dm\_Spn27A*, *Cq\_Spn27A\_2* and *Am\_Spn27A* in a sister branch to *Tc\_Spn27A* (Fig. 4.10).



*Cq\_Spn27A\_1* branches more basally. Additionally, *Cq\_Spn27A\_3* and 4 are part of the outgroup branch of *Spn42Da* homologs.

*Nv-spn27A* was detected in the *Nasonia* genome but ISH did not show expression in ovarioles. In embryos *Nv-spn27A* is initially expressed in a narrow stripe at the anterior dorsal midline (Fig. 4.13a). The stripes elongates towards the posterior pole (Fig. 4.13b). During gastrulation the stripe retracts from the posterior pole and expands laterally (Fig. 21c-d). After gastrulation *Nv-spn27A* is expressed in the anterior part of the presumptive serosa (Fig. 4.13e).

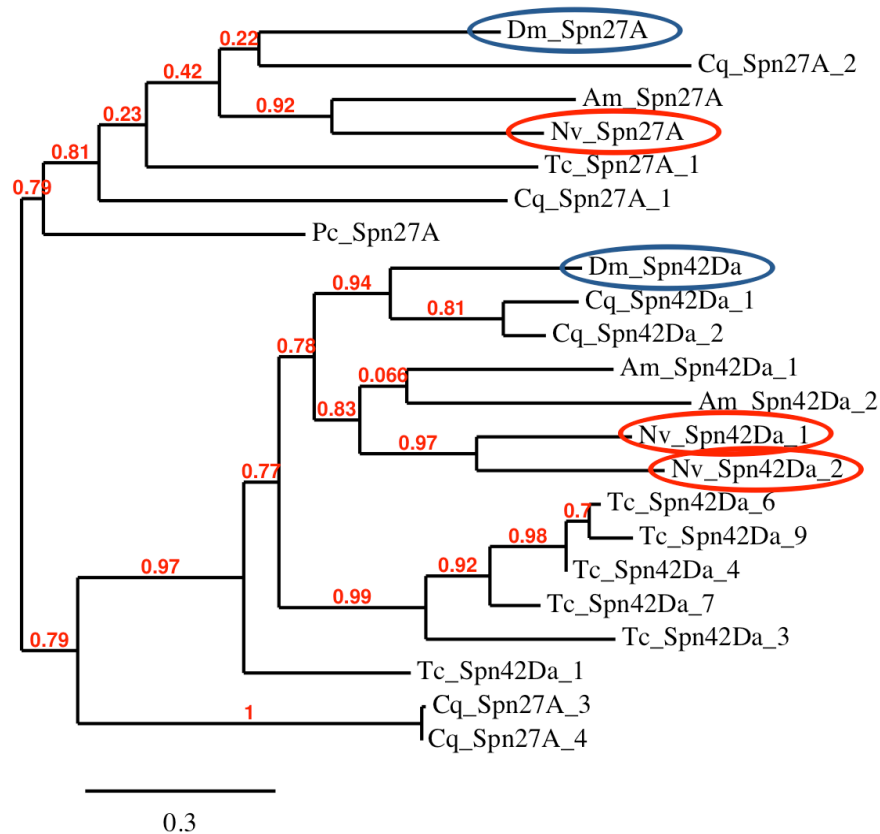


**Figure 4.10 Phylogenetic analysis of Serpin27A**

The tree describes the relationship between Serpin27A homologs and the closely related Serpin24Da protein in different insect species. Red values indicate branch support (SH-aLRT) in percentages (x 100). Red ellipses highlight *Nasonia* sequences and blue ellipses highlight *Drosophila* sequences. Spn27A = Serpin27A; Spn24Da = Serpin24Da; Am = *Apis mellifera*; Dm = *Drosophila melanogaster*; Tc = *Tribolium castaneum*; Cq = *Culex quinquefasciatus*; Nv = *Nasonia vitripennis*; Pc = *Pediculus corporis*.

### Spätzle

NCBI protein BLAST revealed four different Spätzle (Spz) related proteins in *Nasonia* (*Nv\_Spz\_1*, 2, 3, and 4) and two in *Culex* (*Cq\_Spz\_1* and 2). No related sequence was found in *Apis*. In a phylogenetic tree including the closely related Neurotrophin 1 (NT1) sequence (which was not detected in *Apis* and *Tribolium*) *Nv\_Spz\_3* and 4 branch in a clade with *Cq\_Spz\_1* and 2 and the query sequence *Dm\_Spz*. This clade is a sister branch to *Tc\_Spz\_1* and to a clade containing, *Pc\_Spz\_1*, *Tc\_Spz\_2*, *Nv\_Spz\_1* and 2. All present NT1 sequences branch in a separate clade (Fig. 4.11). However, some branches have very low branch support.

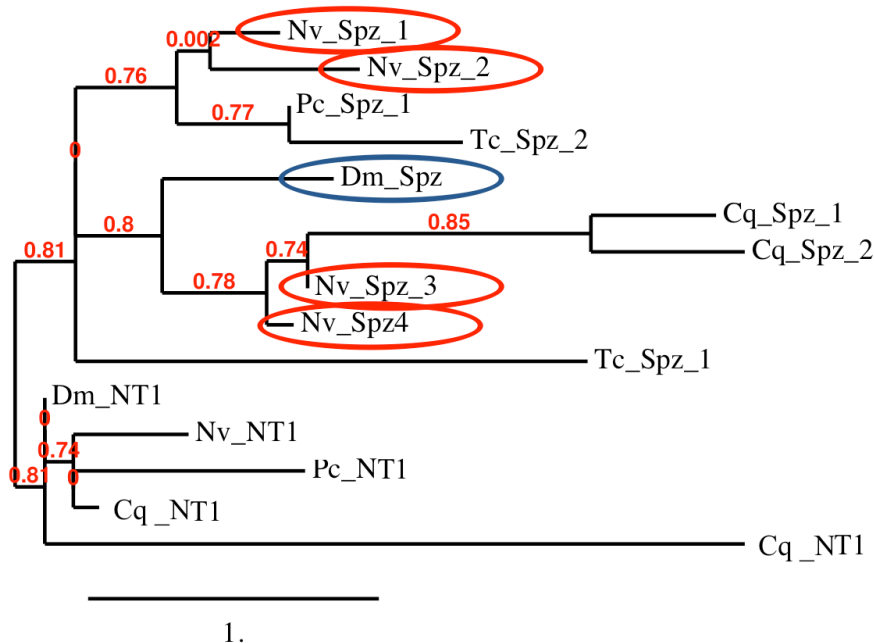


**Figure 4.11 Phylogenetic analysis of Spätzle**

The tree describes the relationship between Spätzle homologs and the closely related protein Neurotrophin in different insect species. Red values indicate branch support (SH-aLRT) in percentages (x 100). Red ellipses highlight *Nasonia* sequences and blue ellipses highlight *Drosophila* sequences. Spz = Spätzle; NT1 = Neurotrophin 1; Am = *Apis mellifera*; Dm = *Drosophila melanogaster*; Tc = *Tribolium castaneum*; Cq = *Culex quinquefasciatus*; Nv = *Nasonia vitripennis*; Pc = *Pediculus corporis*.

Of the two investigated *spätzle* homologs (*Nv-spz1* and *Nv-spz2*) only *Nv-spz1* showed an expression pattern in the oocyte and the posterior part of the nurse

cell compartment (Fig. 12d). In the early embryo, *Nv-spz2* is ubiquitously expressed with increased expression levels along the dorsal midline (Fig. 4.13g). In later stages expression levels are additionally enhanced in a broad central domain around the entire embryonic circumference (Fig. 13h). The other identified *spz* related gene, *Nv-spz1*, did not show expression during embryogenesis. *Nv-spz3* and *Nv-spz4* have not been investigated, yet.

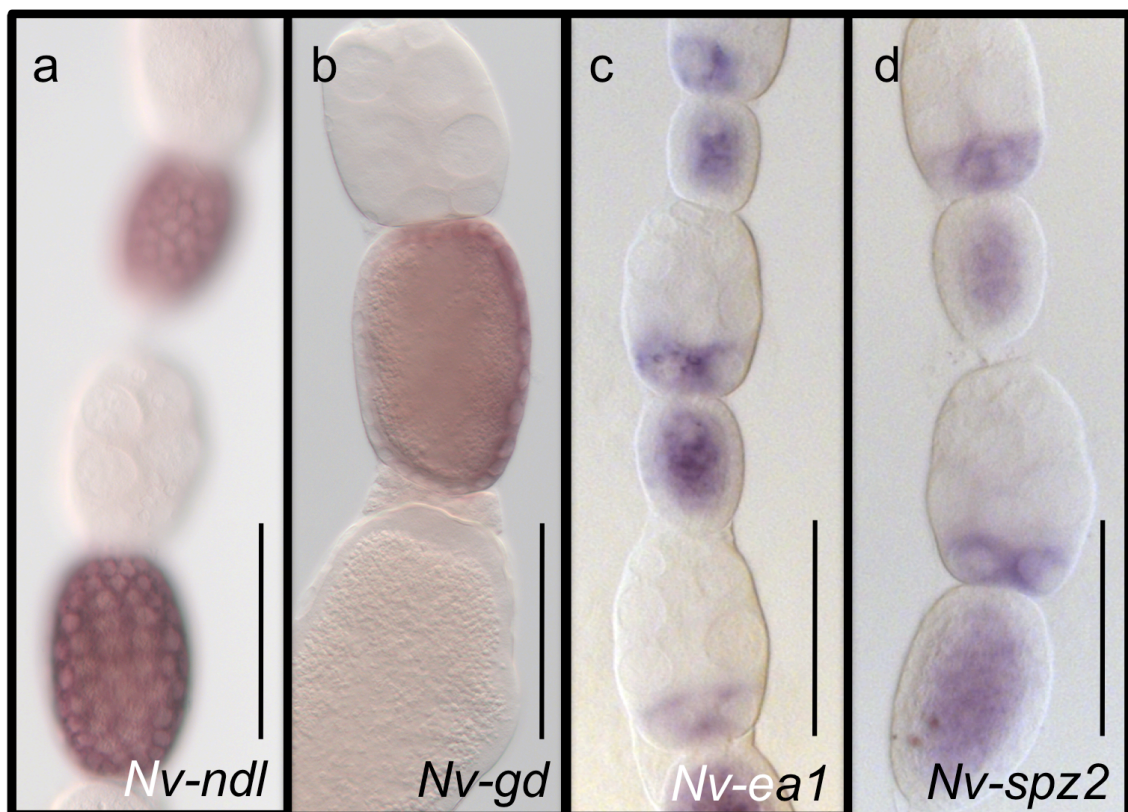


**Figure 4.12 Expression of Toll pathway protease cascade components in *Nasonia vitripennis* ovaries**

(a-d) Expression of *nudel* (a), *gastrulation defective* (b), *easter* (c) and *spätzle* (d) mRNA in the ovariole of *Nasonia vitripennis*. (a) *Nv-ndl* mRNA is ubiquitously expressed in the developing oocyte and the follicular epithelium. (b) *Nv-gd* mRNA is ubiquitously expressed in the oocyte. Expression in the follicle cells and perivitelline fluid is restricted to one hemisphere of the oocyte. (c) *Nv-ea1* mRNA expression is equally distributed in the oocyte and locally expressed in the posterior nurse cells. (d) *Nv-spz2* mRNA expression is equally distributed in the oocyte and locally expressed in the posterior nurse cells. *Nv* = *Nasonia vitripennis*; *ndl* = *nudel*; *gd* = *gastrulation defective*; *ea* = *easter*; *spz* = *spätzle*. Anterior is on top. Scale bars represent 100  $\mu\text{m}$ .

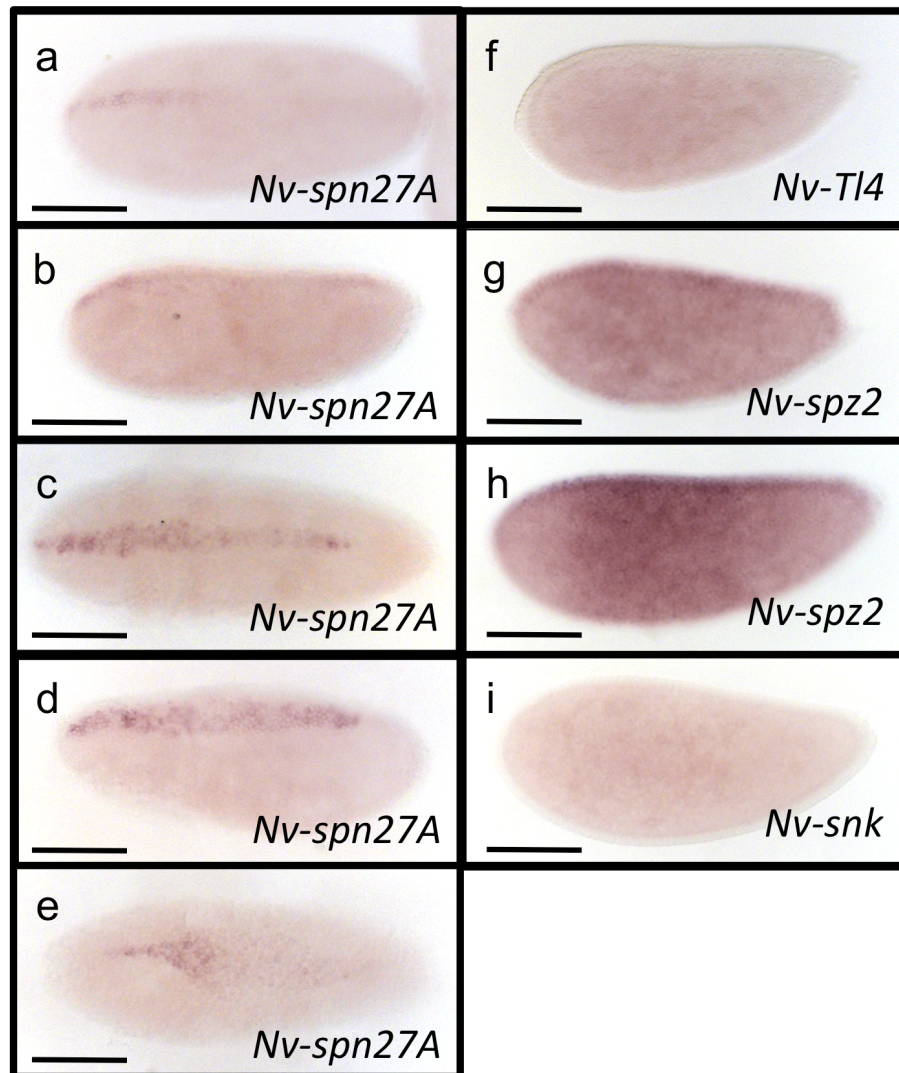


**Figure 4.13 Dynamics of *Nv-serpin27A* expression during embryogenesis and *Nv-Toll*, *Nv-spätzle* and *Nv-snake* mRNA expression in *Nasonia* embryos**

(a,c,e) Dorsal (b) lateral and (d) dorso-lateral views of *Nasonia* embryos in (a) cycle 10, (b) cycle 11-12, (c) initiation of gastrulation, (d) ongoing gastrulation and (e) post gastrulation showing *Nv-serpin27A* mRNA expression. *Nv-serpin27A* is initially expressed as a narrow stripe along the anterior part of the dorsal midline (a). The stripe elongates towards the posterior pole (b). During gastrulation the stripe retracts from the posterior pole (c), expands laterally (d) and is later expressed in the presumptive extraembryonic tissue (e). (a-i) Lateral views of *Nasonia* embryos in (g,i) cycle 10, (f) cycle 10-11 and (h) cycle 11 showing (f) *Nv-Toll4*, (g-h) *Nv-spätzle2* and *Nv-snake* mRNA expression. *Nv-Toll4* is ubiquitously expressed in the embryo (f). *Nv-spätzle* is ubiquitously expressed with a localized stripe of mRNA expression along the dorsal midline (g). During embryogenesis *Nv-spätzle* expression becomes stronger in a broad ring covering thoracic and anterior-abdominal segments along the whole dorso-ventral embryo circumference. Scale bar represents 100  $\mu\text{m}$ . Anterior is left.

### 4.2.3 Analysis of Toll

#### Toll and Toll like receptors (TLRs)

For the phylogenetic analysis of Toll and TLRs only *Nasonia*, *Tribolium*, *Apis* and *Drosophila* were considered. NCBI BLAST identified four *DmToll* related sequences in *Nasonia* (*NvTollB*, *NvToll\_2*, *NvToll\_3* and *NvToll\_4*). In a phylogenetic tree, they branch in a clade with *AmToll*, which is a sister clade to the one containing *DmToll* (Fig. 4.14). One *DmToll8/Tollo* homologous sequence (*NvToll8*) was identified in *Nasonia*. It branches in a clade with *DmToll8/Tollo* and is closest related to *AmToll8*. Two *DmToll6* related sequences were identified in *Nasonia* (*NvToll6\_1* and *NvToll6\_2*) whereas in the tree only one of them (*NvToll6\_2*) groups with *DmToll6*. The other one (*NvToll6\_1*) branches with *Toll10* of *Apis* and *Tribolium*. One *Toll7* homolog was identified (*NvToll7*).

*NvToll2* (*Nv-Tl2*) is expressed in the posterior part of the nurse cell compartment and in the oocyte with tight mRNA localization at both the anterior and posterior pole (Fig. 4.15a). *NvToll3* (*Nv-Tl3*) is expressed in the posterior part of the nurse cell compartment and throughout the oocyte with tight mRNA localization at posterior pole (Fig. 4.15b). *NvToll4* (*Nv-Tl4*) is expressed throughout the oocyte and the nurse cell compartment. Dense particles containing *Nv-Toll4* mRNA are observed within the nurse cells and oocyte (Fig. 4.15c). *NvTollB* was identified as a *Dm-Toll* related gene however ISH did not show expression in ovarioles. In embryos, only *Nv-Tl2*, *Nv-Tl3* and *Nv-Tl4* are expressed. *Nv-Tl4* has a faint ubiquitous expression pattern (Fig. 4.13f). *Nv-Tl2* is initially expressed in a spot like pattern at both the anterior and posterior pole (Fig. 4.16a). The expression pattern at both poles elongate to stripes along the ventral midline (Fig 4.16b), and later fuse to a pattern that outlines the mesoderm while the spot like expression pattern on both poles is still present on the ventral side (Fig 4.16c-e). In later stages, expression retracts from the anterior pole and becomes activated throughout the whole mesoderm (Fig. 4.16f). At the onset of gastrulation, *Nv-Tl2* is strongly expressed in the mesoderm (Fig. 4.16g). *Nv-Tl3* is ubiquitously expressed in the early embryo



with increased expression levels on both poles along the AP axis (Fig. 4.16h). During development expression becomes tightly localized at the poles and disappears from the rest of the embryo. From both poles tendencies of a stripe along the ventral midline are initiated (Fig. 4.16i-j). The expression of *NvToll7*, *NvToll8*, *NvToll6\_1* and *NvToll6\_2* has not been analyzed, yet.

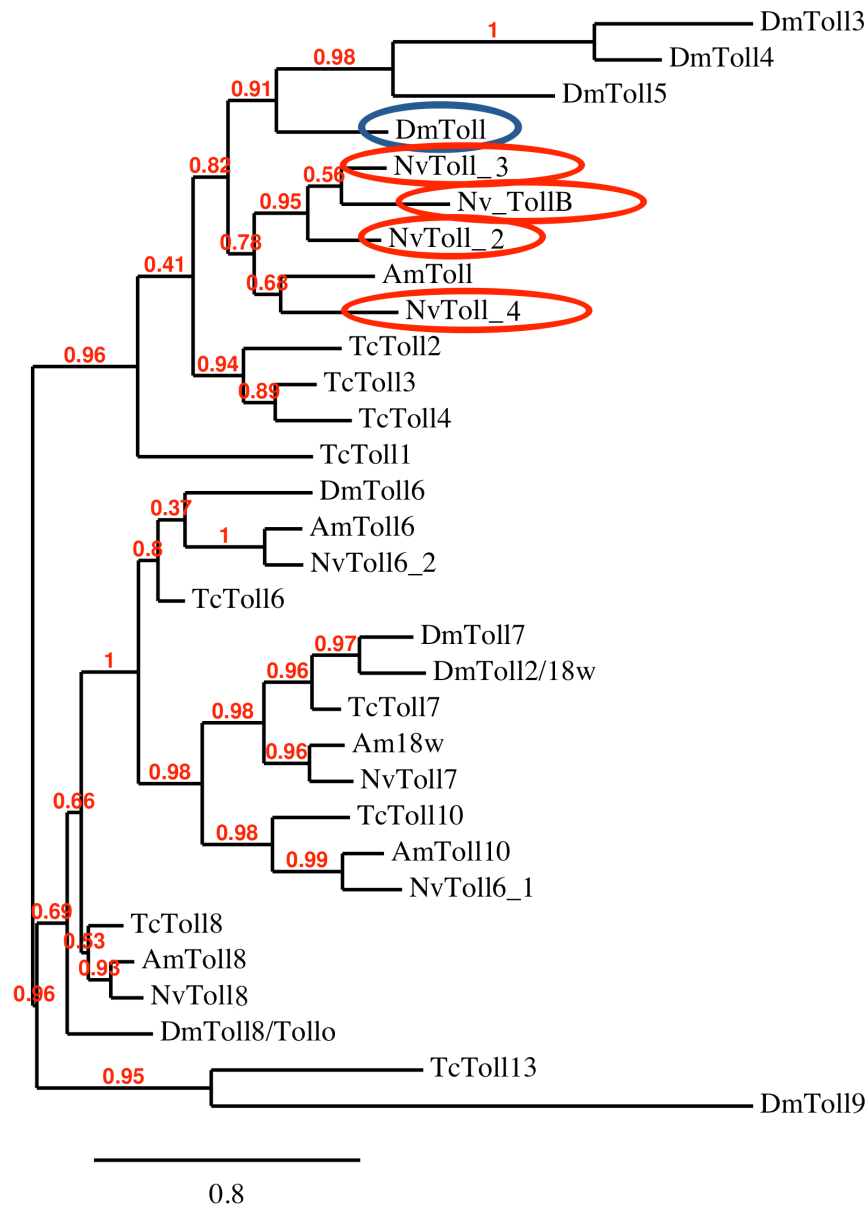


**Figure 4.14 Phylogenetic analysis of Toll**

SH-aLRT tree of Toll and Toll related proteins in different insect species. Red values indicate branch support (SH-aLRT) in percentages (x 100). Red ellipses highlight *Nasonia* sequences and blue ellipses highlight *Drosophila* sequences. Am = *Apis mellifera*, Dm = *Drosophila melanogaster*, Tc = *Tribolium castaneum*; Nv = *Nasonia vitripennis*.

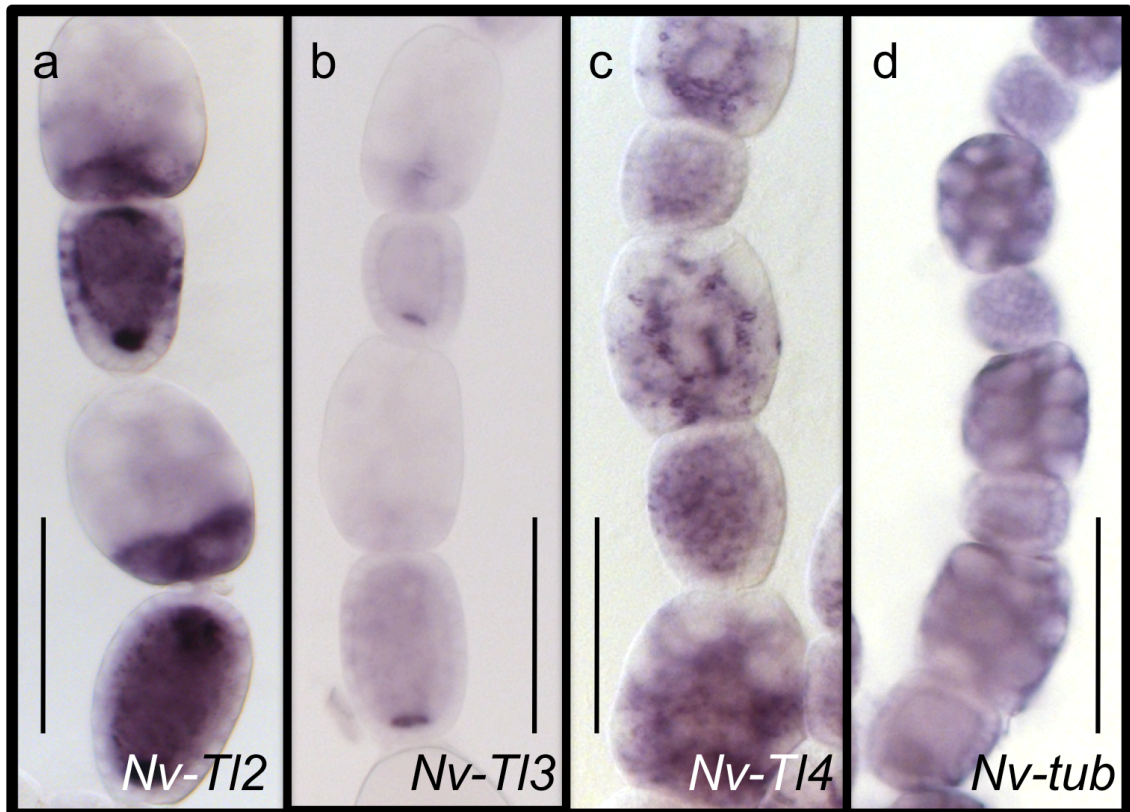


**Figure 4.15 Expression of Toll and Tube in *Nasonia vitripennis* ovarioles**

(a-d) Expression of *Toll2* (a), *Toll3* (b), *Toll4* (c) and *tube* (d) mRNA in the ovariole of *Nasonia vitripennis*. (a) *Nv-Toll2* mRNA is ubiquitously expressed in the oocyte and nurse cells with tight localization of *Nv-Toll2* mRNA at both the anterior and posterior poles of the oocyte and in the posterior part of the nurse cell compartment. (b) *Nv-Toll3* mRNA is ubiquitously expressed in the oocyte with tight localization of *Nv-Toll3* mRNA at the posterior pole in the oocyte. *Nv-Toll3* expression is restricted to the posterior part of the nurse cell compartment. (c) *Nv-Toll4* mRNA is ubiquitously expressed in the oocyte and the nurse cell compartment. Dense particles containing *Nv-Toll4* mRNA are observed within the nurse cells and oocyte. (d) *Nv-tube* mRNA is ubiquitously expressed in the ovariole. *Nv* = *Nasonia vitripennis*; *TI2* = *Toll2*; *TI3* = *Toll3*; *TI4* = *Toll4*; *tub* = *tube*. Anterior is on top. Scale bars represent 100  $\mu\text{m}$ .

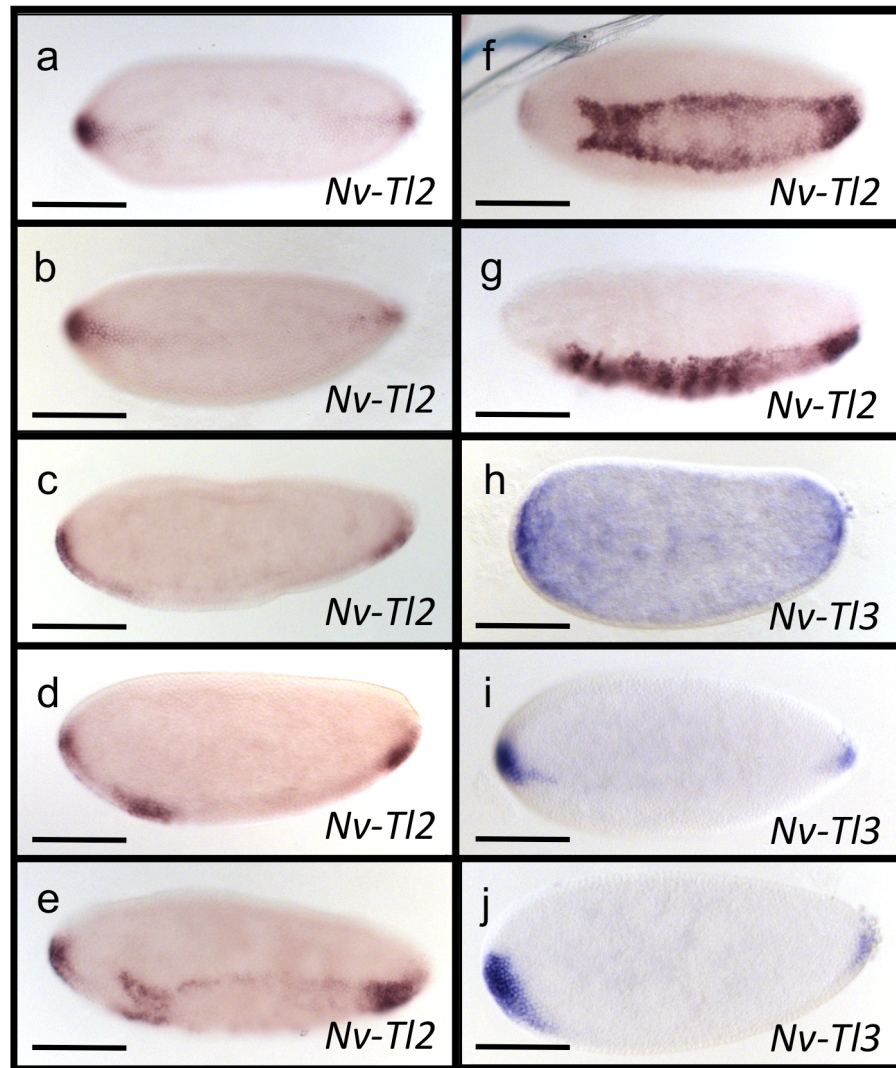


**Figure 4.16 Dynamics of *Nv-Toll2* and *Nv-Toll3* expression during embryogenesis** (a,b,f) Ventral (c,d,h) lateral and (e,i) ventro-lateral views of *Nasonia* embryos in (a,b) cycle 10-11, (c) cycle 11, (d,e,i,j), cycle 12 and (g) initiation of gastrulation showing *Nv-Toll2* (a-g) and *Nv-Toll3* (h-j) mRNA expression. *Nv-Toll2* is initially expressed in two terminal spots on both the anterior and posterior pole of the embryo (a). The expression pattern at both poles elongates to stripes along the ventral midline (b-d) and later form a 2-4 nuclei wide row of mRNA expression that outlines the mesoderm-ectoderm border (e). These narrow stripes expand ventrally (f) until by the initiation of gastrulation *Nv-Toll2* is expressed in the whole mesoderm (g). In parallel gene expression clears at the anterior pole (e-g). Initial *Nv-Toll3* expression is found throughout the embryo with tight localization of *Nv-Toll3* mRNA on both the anterior and posterior pole (h). In later stages *Nv-Toll3* mRNA expression is tightly localized at the poles and disappears from the rest of the embryo. From both poles tendencies of a stripe along the ventral midline are initiated (i,j). Scale bar 100  $\mu$ m. Anterior is left.



#### 4.2.4 Analysis intracellular Components

Inside the oocyte, the extracellular signal is transmitted via Myd88, Tube and Pelle to the Cactus/Dorsal complex. As a result Cactus is degraded and Dorsal translocates into the nucleus where it activates target gene expression. Related sequences to all components were identified in the *Nasonia* genome Database on NCBI.

##### Tube and Tube-like kinases (TTLKs) and Pelle

NCBI protein BLAST revealed one Tube related (*Nv* Tube) and two different Pelle related (*Nv* Pelle and *Nv* Pelle like) sequences. The phylogenetic tree with sequences of *Nv*, *Am*, *Tc* and *Mm* generates two major branches. One branch contains all Tube related sequences together with *Mm* IRAK4 and *Mm* IRAK1. The other branch contains all Pelle related sequences (Fig. 4.17a). Within the Tube branch, *Nv* Tube is closest related to *Am* Tube. Both cluster with *Dm* Tube and the *Tribolium* homolog (*Tc* TC011895) in a sister branch to *Mm* IRAK4. Within the Pelle branch, *Nv* Pelle and *Nv* Pelle like are both leaves on a sister branch to *Am* Pelle. The Phylogenetic tree is based on a death domain sequences alignment (Fig. 4.17b) since previous studies revealed that the kinase domain of Tube and TLKs is not conserved in *Drosophila*, *Nasonia* and *Apis* (see also Towb et al., 2009). A phylogenetic analysis with full protein sequences causes artificial aggregation of those three sequences.

*Nv-tube* (*Nv-tub*) mRNA is ubiquitously expressed in the *Nasonia* ovariole (Fig. 4.15d) and in embryos (Fig. 4.23k). *Nv-pll* was detected in the *Nasonia* genome however ISH did not show expression in ovarioles. Nevertheless, *Nv-pll* is faintly and ubiquitously expressed in embryos (Fig. 4.23h). *Nv-pelle like* has not been investigated, yet.

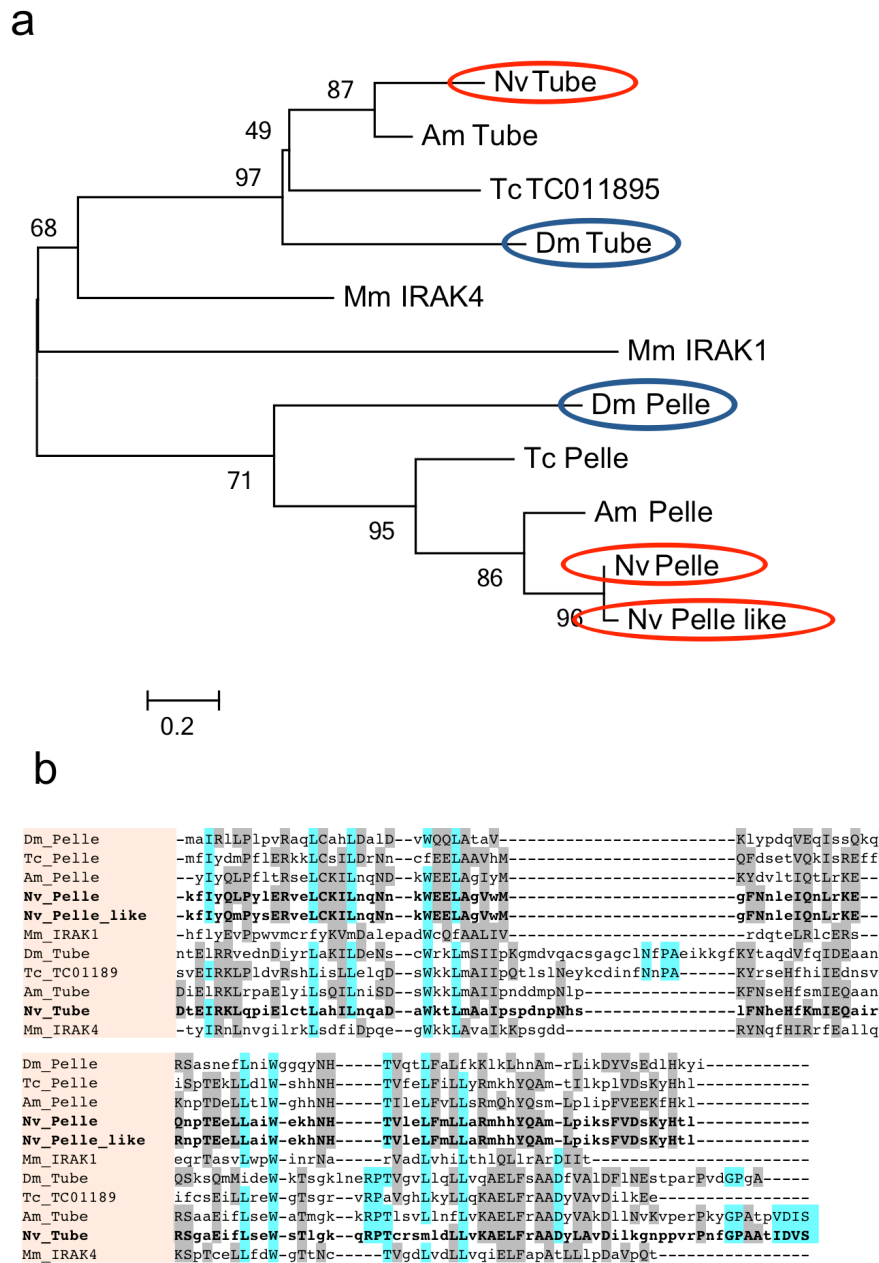


**Figure 4.17 Maximum likelihood tree based on death domain sequence of TTLK and Pelle proteins**

(a) The tree shows the relationship of TTLK and Pelle proteins in different insect species based on the death domain sequence. Bootstrap values (1,000 replicates) are indicated in percentages. Red ellipses highlight *Nasonia* homologs and blue ellipses highlight *Drosophila* homologs. (b) Muscle alignment of the death domains of TTLK and Pelle proteins. Similar residues are colored as the most conserved one (according to BLOSUM62). Average BLOSUM62 score: Max: 3.0 (blue), Low: 0.5 (grey). Am = *Apis mellifera*; Dm = *Drosophila melanogaster*; Tc = *Tribolium castaneum*; Nv = *Nasonia vitripennis*; Mm = *Mus musculus*.

### Myd88

One Myd88 related sequence was identified in *Nasonia* as well as in each of the other analyzed species. In a phylogenetic tree including the closely related sequence of CG42795 as outgroup all Myd88 related sequences branch separately whereas *Nv*\_Myd88 is a sister branch to all other Myd88 homologs (Fig. 4.18). However, some branches have very low branch support.

Although *Nv-myd88* was detected in the *Nasonia* genome, ISH did not show expression in ovarioles. It is faintly and ubiquitously expressed in embryos (Fig. 4.23h).

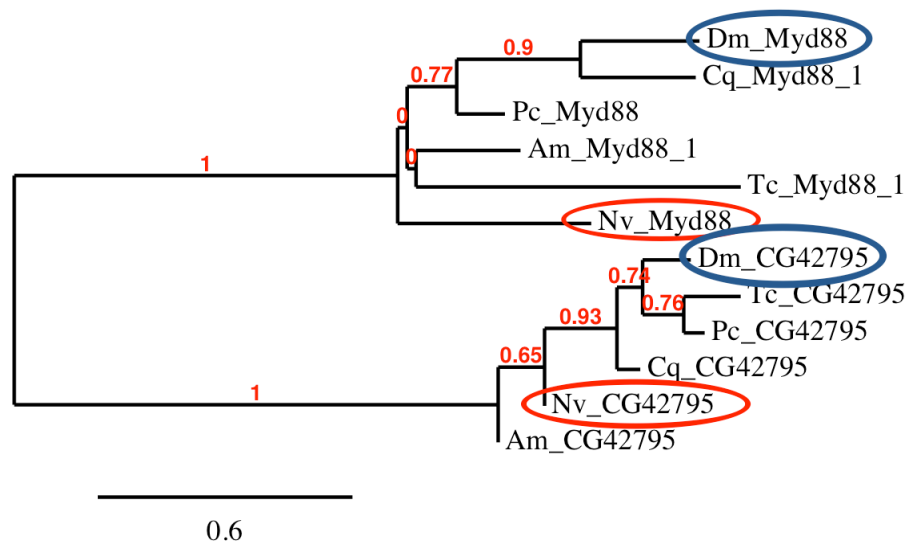


**Figure 4.18 Phylogenetic analysis of Myeloid differentiation primary response gene 88 (Myd88)**

The tree describes the relationship between Myd88 homologs and the closely related protein CG42795 in different insect species. Red values indicate branch support (SH-aLRT) in percentages (x 100). Red ellipses highlight *Nasonia* sequences and blue ellipses highlight *Drosophila* sequences. Myd88 = Myeloid differentiation primary response gene 88; Am = *Apis mellifera*; Dm = *Drosophila melanogaster*; Tc = *Tribolium castaneum*; Cq = *Culex quinquefasciatus*; Nv = *Nasonia vitripennis*; Pc = *Pediculus corporis*.

### Cactus

In the *Nasonia* genome, three Cactus (Cact) related proteins were identified (*Nv\_Cact\_1*, 2 and 3). In a tree with the closely related Relish (Rel) sequence as outgroup, all hymenopteran sequences (*Nv*-Cact and *Am*-Cact) cluster in a branch. Together they form a sister branch to one containing the query sequence *Dm\_Cact* (Fig. 4.19). The *Nasonia* and *Apis* homologs of Rel are closer related to Cactus than the other Rel related sequences.

*Nasonia cactus1* (*Nv-cact1*) is expressed throughout the whole ovariole with reduced expression levels at the anterior part of the nurse cell compartment (Fig. 4.20a). *Nasonia cactus2* (*Nv-cact2*) is ubiquitously expressed throughout the whole ovariole and dense particles containing *Nv-cact2* mRNA are observed in the anterior compartments (Fig. 4.20b). *Nasonia cactus3* (*Nv-cact3*) is ubiquitously expressed with higher expression levels in the oocyte and the posterior part of the nurse cell compartment (Fig. 4.20c).

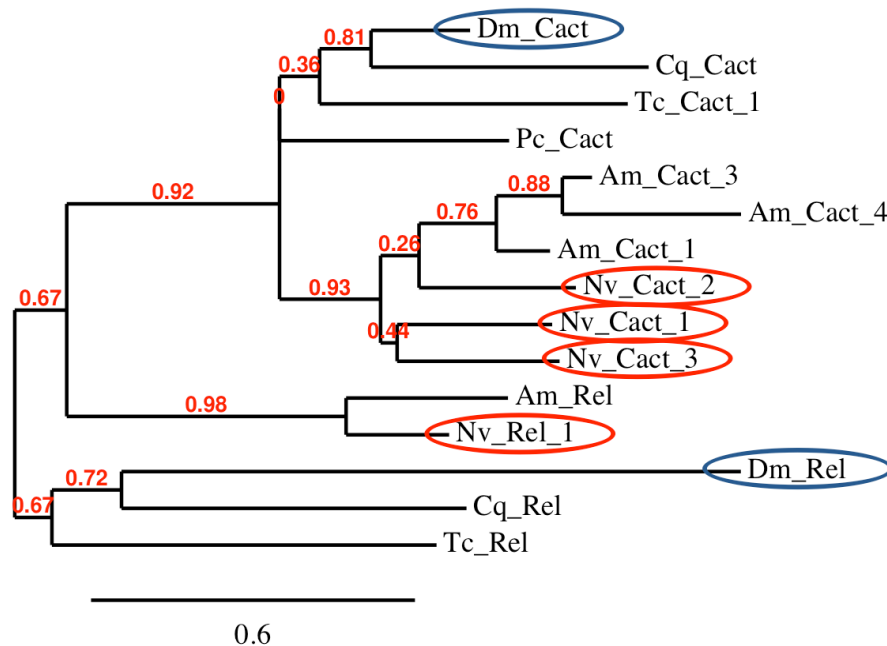


**Figure 4.19 Phylogenetic analysis of Cactus**

The tree describes the relationship between Cactus homologs and the closely related protein Relish in different insect species. Red values indicate branch support (SH-aLRT) in percentages (x 100). Red ellipses highlight *Nasonia* sequences and blue ellipses highlight *Drosophila* sequences. Cact = Cactus; Rel = Relish; Am = *Apis mellifera*; Dm = *Drosophila melanogaster*; Tc = *Tribolium castaneum*; Cq = *Culex quinquefasciatus*; Nv = *Nasonia vitripennis*; Pc = *Pediculus corporis*.

In embryos, *Nv-cact1* is expressed as a narrow stripe along ventral midline (Fig. 4.23e-g) prior to gastrulation, whereas *Nv-cact2* is ubiquitously expressed during early embryogenesis (Fig. 4.23i). During later stages expression levels of *Nv-cact2* are increased along the ventral midline (Fig. 4.23j). A stripe, similar but weaker to the one observed in *Nv-cact1* ISH stainings, appears to form. *Nv-cact3* is not expressed in embryos.

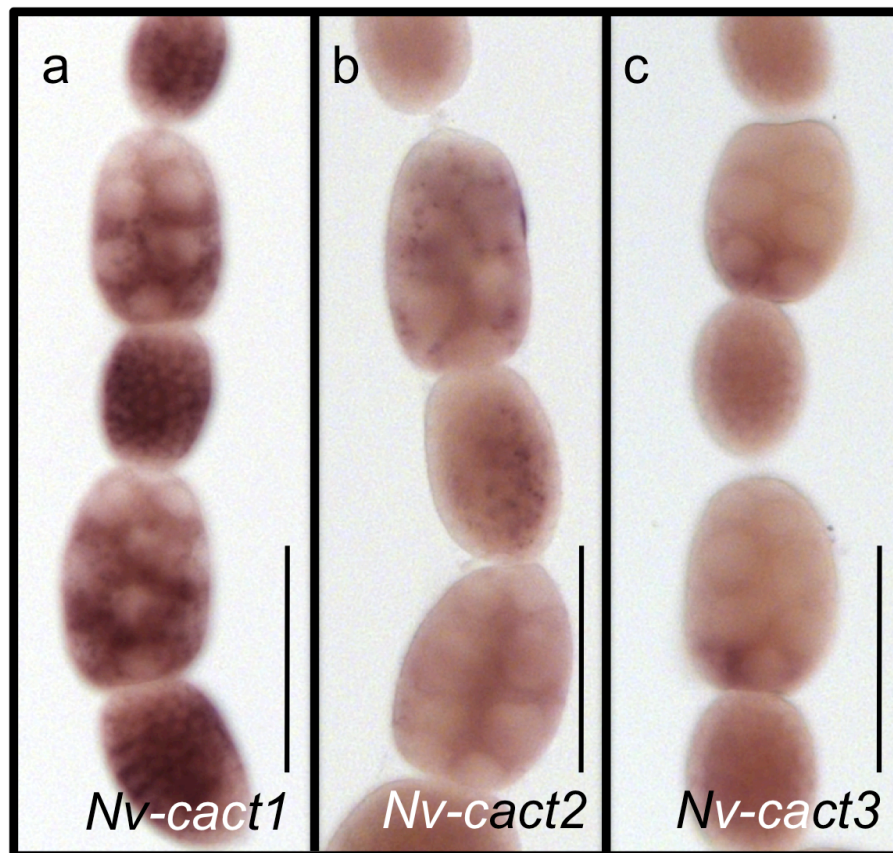


**Figure 4.20 Expression of *cactus* in *Nasonia vitripennis* ovarioles**

(a-c) Expression of *cact1* (a), *cact2* (b) and *cact3* (c) mRNA in the ovariole of *Nasonia vitripennis*. (a) *Nv-cact1* mRNA is ubiquitously expressed in the developing oocyte and the follicular epithelium. In the nurse cell compartment expression levels are reduced towards the anterior pole. (b) *Nv-cact2* mRNA is ubiquitously expressed in the oocyte, follicle cells and nurse cell compartment. (c) *Nv-cact3* mRNA is ubiquitously expressed with higher expression levels in the oocyte and the posterior part of the nurse cell compartment. *Nv* = *Nasonia vitripennis*; *cact1* = *cactus1*; *cact2* = *cactus2*; *cact3* = *cactus3*. Anterior is on top. Scale bars represent 100  $\mu$ m.

## Dorsal

The protein BLAST for Dorsal (DI) related sequences identified four putative Dorsal homologs in *Nasonia* (*Nv\_DI\_1*, 2, 3 and 4). In a phylogenetic analysis including the sequences of the closely related Rel/Dif protein as outgroup, all Rel related sequences branch off separately. *Nv\_DI1* branches with the other Dorsal homologs whereas the three remaining Dorsal related sequences of *Nasonia* (*Nv\_DI\_2*, 3 and 4) branch off more basally. *Dm\_Dif* branches together with *Dm\_DI* (Fig. 4.21).

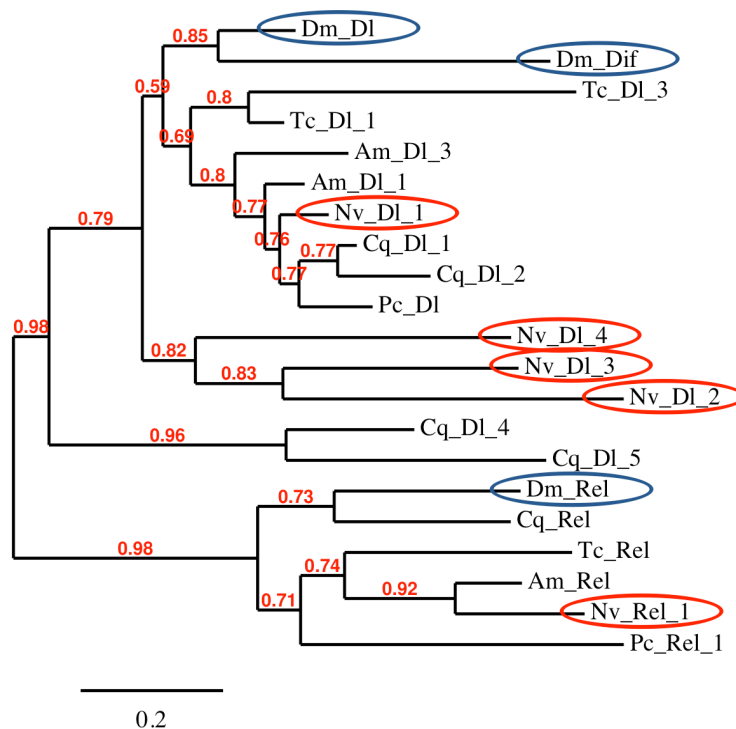


**Figure 4.21 Phylogenetic analysis of Dorsal**

The tree describes the relationship between Dorsal homologs and the closely related proteins Relish and Dorsal-related immunity factor in different insect species. Red values indicate branch support (SH-aLRT) in percentages (x 100). Red ellipses highlight *Nasonia* sequences and blue ellipses highlight *Drosophila* sequences. DI = Dorsal; Rel = Relish; Dif = Dorsal-related immunity factor; Am = *Apis mellifera*; Dm = *Drosophila melanogaster*; Tc = *Tribolium castaneum*; Cq = *Culex quinquefasciatus*; Nv = *Nasonia vitripennis*; Pc = *Pediculus corporis*.



Of the four *dorsal* related genes identified in the *Nasonia* genome (*Nv-dl1-4*), *Nv-dl1* is ubiquitously expressed in the ovariole (Fig. 4.22a). *Nv-dl2* is expressed in the posterior part of the nurse cell compartment and ubiquitously in the oocyte (Fig. 4.22b). *Nv-dl3* mRNA is expressed in the oocyte and nurse cells with reduced expression levels at the anterior part of the nurse cell compartment (Fig. 4.22c). *Nv-dl4* is expressed in the posterior part of the nurse cell compartment and ubiquitously in the oocyte (Fig. 4.22d). All four *Nasonia dorsal* homologs are ubiquitously expressed during embryogenesis (Fig. 4.23a-d).

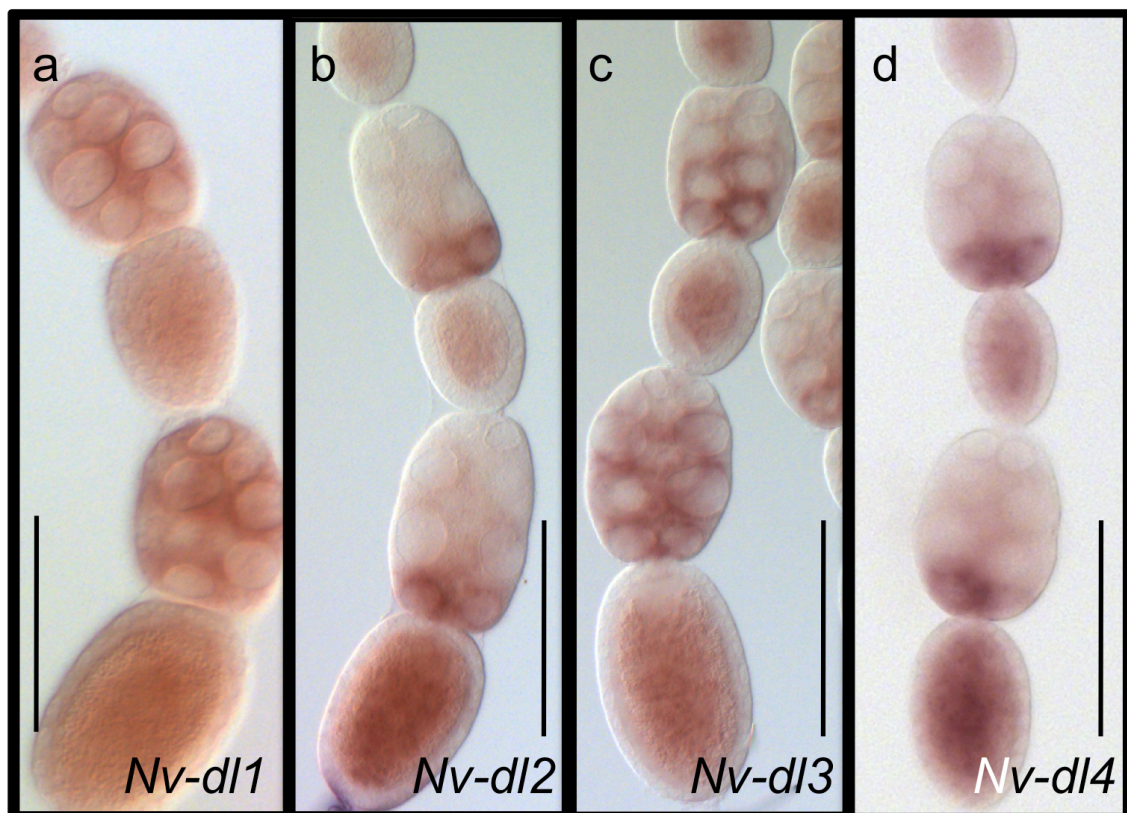


**Figure 4.22 Expression of *dorsal* in *Nasonia vitripennis* ovarioles**

(a-d) Expression of *dorsal1* (a), *dorsal2* (b), *dorsal3* (c) and *dorsal4* (d) mRNA in the ovariole of *Nasonia vitripennis*. (a) *Nv-dorsal1* mRNA is ubiquitously expressed throughout the ovariole. (b) *Nv-dorsal2* mRNA is ubiquitously expressed in the oocyte and locally expressed in the posterior nurse cells. Expression levels are increased in older compartments. (c) *Nv-dorsal3* mRNA is ubiquitously expressed in the oocyte. In the nurse cell compartment expression levels are reduced towards the anterior pole. (d) *Nv-dorsal4* mRNA expression is equally distributed in the oocyte. In the nurse cell compartment expression levels are increased towards the anterior pole. *Nv* = *Nasonia vitripennis*; *dl1* = *dorsal1*; *dl2* = *dorsal2*; *dl3* = *dorsal3*; *dl4* = *dorsal4*. Anterior is on top. Scale bars represent 100  $\mu\text{m}$

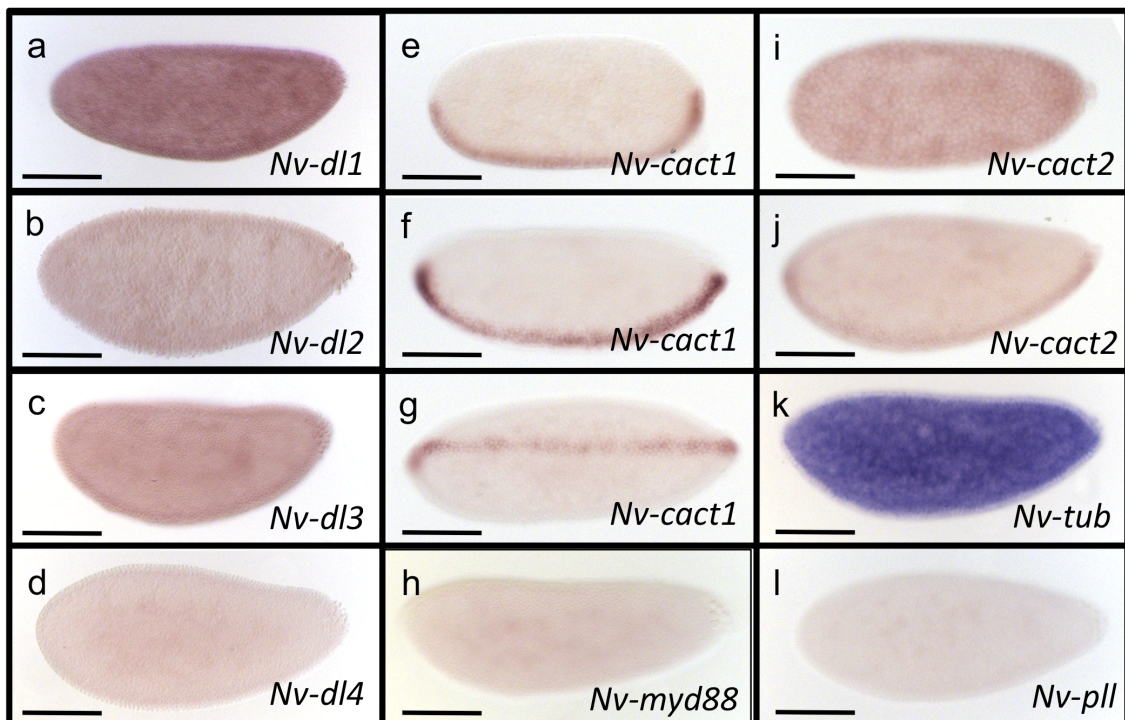


**Figure 4.23 Dynamics of *Nv-cact* expression during embryogenesis and mRNA expression of *Nv-dorsal*, *Nv-tube* and *Nv-pelle* in *Nasonia* embryos**

(a-f, h-l) lateral and (g) ventral views of *Nasonia* embryos in (e,i) cycle 9, (b) cycle 10-11 (c,d,f,g,j,k,l) cycle 11, (a,h) cycle 12 showing (a-d) *Nv-dorsal1-4*, (e-g) *Nv-cact1*, (h) *Nv-myd88*, (i,j) *Nv-cact2*, (k) *Nv-tube* and (l) *Nv-pelle* mRNA expression. *Nv-dorsal1*, *Nv-dorsal2*, *Nv-dorsal3*, *Nv-dorsal4*, *Nv-myd88*, *Nv-tube* and *Nv-pelle* mRNA expression is detected ubiquitously in *Nasonia* embryos (a-d, h, k, l). *Nv-cactus1* mRNA is expressed as a narrow stripe along the ventral midline (e-g). *Nv-cactus2* is ubiquitously expressed in early embryos (i) and in later stages expression is increased along the ventral midline (j). *Nv* = *Nasonia vitripennis*; *dl1* = *dorsal1*; *dl2* = *dorsal2*; *dl3* = *dorsal3*; *dl4* = *dorsal4*; *cact1* = *cactus1*; *cact2* = *cactus2*; *myd88* = myeloid differentiation primary response gene 88; *tub* = *tube*; *pll* = *pelle*. Scale bar 100  $\mu$ m. Anterior is left.

### 4.3 Transcriptome

So far, all *Nasonia* homologs identified are the result of a candidate gene approach. The choice for the genes picked was based on their influence on *Drosophila* DV axis formation. Additionally, a rather unbiased next generation sequencing method, using RNA sequencing (Whole Transcriptome Shotgun Sequencing (WTSS)), was performed. RNA isolation and cDNA synthesis was



performed on embryos of *Nasonia* females injected with dsRNA of *BMP* (BMP<sup>-</sup>), *Toll* (Toll<sup>-</sup>) as well as embryos of H<sub>2</sub>O treated control females (WT).

#### 4.3.1 Quantitative polymerase chain reaction (qPCR)

Prior to the RNA-seq analysis, the isolated RNA / cDNA samples were tested for relative amounts of *twist* mRNA by qPCR (Fig. 4.24). Data was normalized to the WT samples. In average, BMP RNAi treated embryos show a 2.34 fold increased value of *twist* mRNA whereas in Toll RNAi treated embryos a 13.34 fold decreased value of *twist* mRNA is observed.

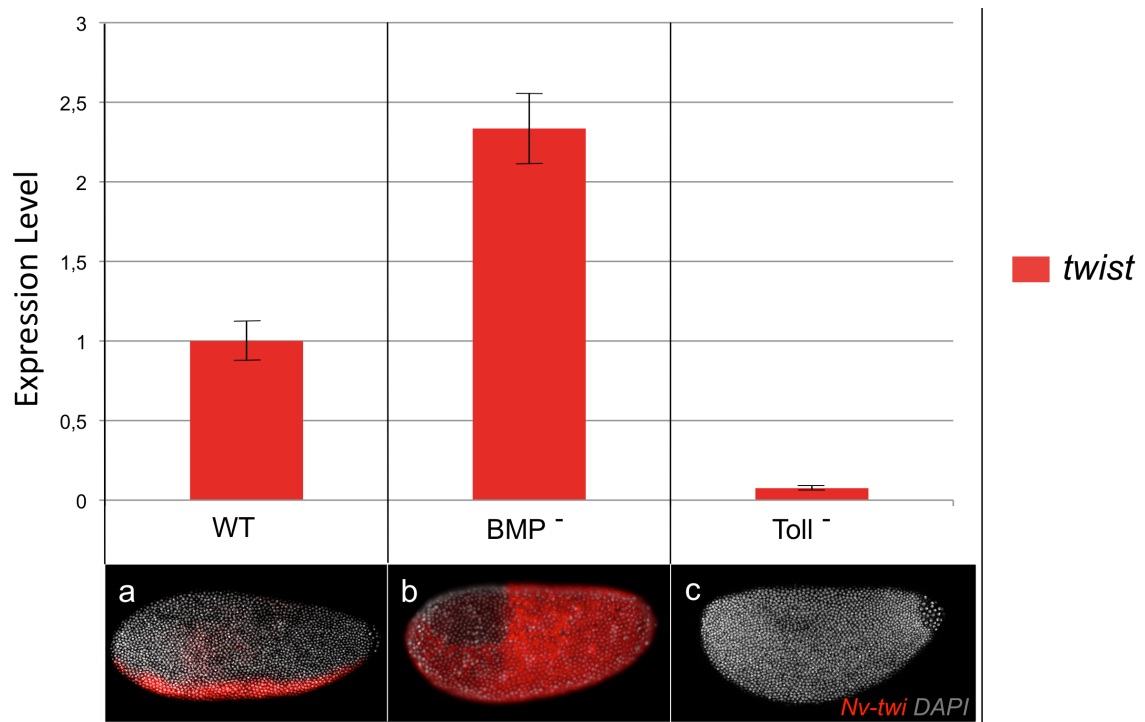


**Figure 4.24 qPCR validation of *twi* mRNA expression levels**

qPCR data showing relative amounts of *Nv-twist* mRNA in wildtype, BMP<sup>-</sup> and Toll<sup>-</sup> embryos as quantified by SYBR Green®. Data are normalized to the wildtype samples. (a-c) lateral views of *Nasonia* embryos in cycle 11-12 showing *Nv-twist* mRNA expression in wild-type (a), BMP knockdown (b) and Toll knockdown (c). Anterior is left. *Nv* = *Nasonia vitripennis*; qPCR = quantitative polymerase chain reaction; WT = wildtype; BMP = *bone morphogenetic protein*; *twi* = *twist*.

### 4.3.2 High throughput ISH

Comparison of the analyzed transcriptome data of *BMP* RNAi treated (*BMP*<sup>-</sup>) and *Toll* RNAi treated (*Toll*<sup>-</sup>) embryos identified ~290 genes that show significantly divergent expression levels when compared to the wildtype (WT) transcriptome data set. The wildtype expression of those genes was analyzed in a high throughput ISH screen. The high throughput ISH is performed in a 96 well plate, in which each well represents a separate reaction tube. This way, up to 96 genes can be stained and screened in parallel.

In the first round of high throughput ISH 48 genes were analyzed. The genes analyzed were the 48 genes with the most diverged expression levels of both the *BMP*<sup>-</sup> and the *Toll*<sup>-</sup> transcriptome. Analysis of these genes by high throughput ISH was part of two Bachelor theses and performed by the Bachelor students Jessica Pietsch and Selma Wolff. Orhan Özüak and Thomas Buchta supervised both students. The results of this analysis have been documented in the Bachelor theses “Neue Zielgene des BMP-Signalwegs bei der dorsoventralen Musterbildung in *Nasonia vitripennis*” by Jessica Pietsch and “Neue Zielgene des Toll-Signalwegs bei der dorsoventralen Musterbildung in *Nasonia vitripennis*” by Selma Wolff, respectively.

In a second high throughput screen, 96 genes of the remaining genes with significantly diverged expression levels were analyzed. In the following, expression of genes with a distinct expression pattern are described in Fig. 4.25-26, whereas the genes are subdivided into genes with DV pattern (Fig. 4.25) and AP pattern (Fig. 4.26), corresponding to the spatial distribution of their expression. All other genes did not show any expression or only a ubiquitous, equally distributed expression (not shown). Although the genes *Nv-Toll2* and *Nv-punt2* were identified as differentially expressed and *Nv-Toll2* additionally exhibit a DV expression pattern, they are not described in this section, since they were already known and previously described in chapter 2.3 (*Nv-punt2*) and chapter 4.4.3 (*Nv-Toll2*).

#### 4.3.2.1 Gens with a DV axis expression pattern

Evaluation of the transcriptome data revealed that the gene *Nv-2EG01377* is expressed significantly lower in BMP<sup>-</sup> embryos than WT embryos. Tblastx search against the NCBI *Drosophila melanogaster* database revealed no sequence homology to any *Drosophila* protein. Tblastx search against the whole NCBI insect database revealed closest homology to the sequence defined as “hypothetical protein EAI\_13565” (NCBI Accession Nr.: EFN84382) of *Harpegnathos saltator*, a hymenopteran species of ant. The gene is initially expressed in a narrow stripe along the dorsal midline with stronger signal at the posterior 50 % (Fig. 4.25a-b). During development, the expression levels are increased and prior to gastrulation, *Nv-2EG01377* is expressed in a narrow dorsal stripe along the whole AP axis (Fig. 4.25c-d).

The *Nasonia* homolog of *pathetic* (*Nv-ptb*) is significantly down regulated in BMP<sup>-</sup> embryos. Close to gastrulation, it is faintly, ubiquitously expressed and has increased expression in a narrow stripe like domain along the dorsal midline (Fig. 4.25e).

The *Nasonia* homolog of *semaphorin-5c* (*Nv-sema-5c*) is significantly down regulated in BMP<sup>-</sup> embryos. Close to gastrulation, it is faintly, ubiquitously expressed and has increased expression in a narrow stripe domain along the dorsal midline (Fig. 4.25f).

The *Nasonia* homolog of *epithelial membrane protein* (*Nv-emp*) is significantly down regulated in Toll<sup>-</sup> embryos. It is expressed as a narrow stripe in the anterior part of the ventral midline (Fig. 4.25g). In later stages it is expressed in a faint, narrow stripe along the ventral midline (Fig. 4.25h).

The *Nasonia* homolog of *optomotor blind* (*Nv-omb*) is significantly down regulated in BMP<sup>-</sup> embryos. It is expressed as a broad stripe covering the ventral midline excluding both the anterior and posterior pole (Fig. 4.25i). In later stages, the expression domain clears along the dorsal midline leaving two 4-8 nuclei wide stripes of expression on either side of the dorsal midline (Fig. 4.25j). In the gastrulating embryo both stripes are narrowed and more prominent in the anterior part (Fig. 4.25k).

The *Nasonia* homolog of *ankyrin* (*Nv-ank*) is significantly down regulated in BMP<sup>-</sup> embryos. It is ubiquitously expressed with weakly enhanced expression along the dorsal midline in embryos close to gastrulation (Fig. 4.25l).

The *Nasonia* homolog of *kin of irre* (*Nv-kirre*) is significantly down regulated in BMP<sup>-</sup> embryos. It is expressed in a narrow stripe along the dorsal midline (Fig. 4.25m-n).

The gene *Nv-EG000923* is significantly lower expressed in BMP<sup>-</sup> than WT embryos. Tblastx search against the NCBI *Drosophila melanogaster* database revealed no sequence homology to any *Drosophila* molecule. Tblastx search against the whole NCBI insect database revealed closest homology to a gene defined as “PREDICTED: LOW QUALITY PROTEIN: myosin-XV-like” (NCBI Accession Nr.: XP\_003491207) of *Bombus impatiens*, a hymenopteran species of bumble bees. The gene is expressed in a stripe along the dorsal midline excluding both the anterior and posterior pole (Fig. 4.25o). In gastrulating embryos it is expressed in the presumptive serosa (Fig. 4.25p).

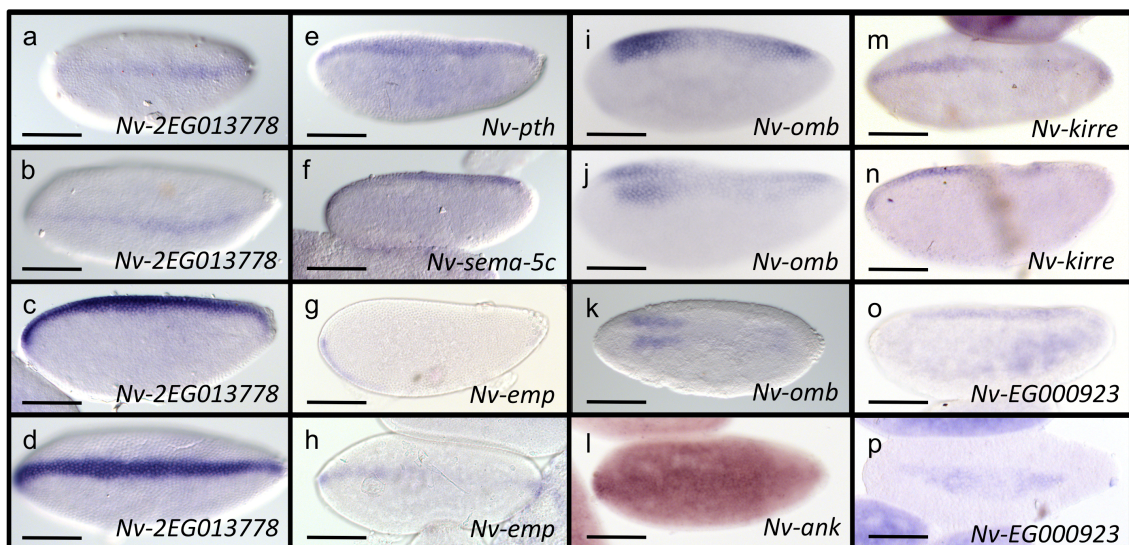


**Figure 4.25 High through put ISH genes with DV expression pattern**

(a,b,d,k,l,m,p) Dorsal (c,f,g,l,n,o) lateral, (e,j) dorso-lateral and (h) ventral views of *Nasonia* showing (a-d) *Nv-2EG01377*, (e) *Nv-ptb*, (f) *Nv-sema-5c*, (g,h) *Nv-emp*, (i-k) *Nv-omb*, (l) *Nv-ank*, (m,n) *Nv-kirre*, (o,p) *Nv-EG000923* mRNA expression. *Nv* = *Nasonia vitripennis*; *ptb* = *pathetic*; *sema-5c* = *semaphorin-5c*; *emp* = *epithelial membrane protein member 1*; *omb* = *optomotor blind*; *ank* = *ankyrin*; *kirre* = *kin of irre*. Scale bar 100  $\mu$ m. Anterior is left.

#### 4.3.2.2 Gens with an AP axis expression pattern

The *Nasonia* homolog of *longitudinals lacking* (*Nv-lola*) is significantly down regulated in BMP<sup>-</sup> embryos. The gene is expressed in two posterior patches on both lateral sides (Fig. 4.26a-b). In gastrulating embryos it is expressed at the posterior pole and in an additional domain as faint narrow stripe along the dorsal midline (Fig. 4.26c). After gastrulation it is ubiquitously expressed with faintly enhanced stripe like signals along the AP axis, similar to a segmental pattern (Fig. 4.26d).

The *Nasonia* homolog of *homeobrain* (*Nv-hbn*) is significantly down regulated in BMP<sup>-</sup> embryos. It is ubiquitously expressed during embryogenesis with a strong spot like signal on both the anterior and posterior pole (Fig. 4.26e).

The *Nasonia* homolog of *FK506-binding protein 2* (*Nv- fk506-bp2*) is significantly down regulated in BMP<sup>-</sup> embryos. In blastoderm embryos it is faintly, ubiquitously expressed with a cap like expression domain at the anterior pole of the embryo (Fig. 4.26f-h).

The *Nasonia* homolog of *general transcription factor IIF subunit 1* (*Nv-gtf2f1*) is significantly down regulated in BMP<sup>-</sup> embryos. The gene is ubiquitously expressed with enhanced expression of a dorsa-ventral ring domain at the anterior of the embryo (Fig. 4.26i). In later stages (close to gastrulation), the ring is reduced to patches on both lateral sides and additional dorsal stripe along the anterior appears (Fig. 4.26j).

The *Nasonia* homolog of *ankyrin 2* (*Nv- ank2*) is significantly down regulated in BMP<sup>-</sup> embryos. The gene is ubiquitously expressed with exception of both the anterior and posterior most region. Additionally, is shows enhanced expression of a dorsa-ventral ring domain at the anterior of the embryo (Fig. 4.26k-l).

The *Nasonia* homolog of *calsyntenin* (*Nv- cals*) is significantly down regulated in BMP<sup>-</sup> embryos. After gastrulation, *Nv-cals* is expressed in ubiquitously in the head region and in a stripe along the DV axis of each

following segment with enhanced signal on the ventral side and head region (Fig. 4.26m).

The *Nasonia* homolog of *drumstick* (*Nv-drm*) is significantly down regulated in BMP<sup>+</sup> embryos. Its expression is only detected after gastrulation. Similar to *Nv-cals*, *Nv-drm* exhibits a segmental stripe pattern with more complex patterning in the head region (Fig. 4.26n).

The *Nasonia* homolog of *rotund* (*Nv-rn*) is significantly down regulated in BMP<sup>+</sup> embryos. It is expressed in a broad domain on both lateral sides at the posterior part of the embryo (Fig. 4.26o). Its expression pattern is cleared along the dorsal midline (Fig. 4.26p).

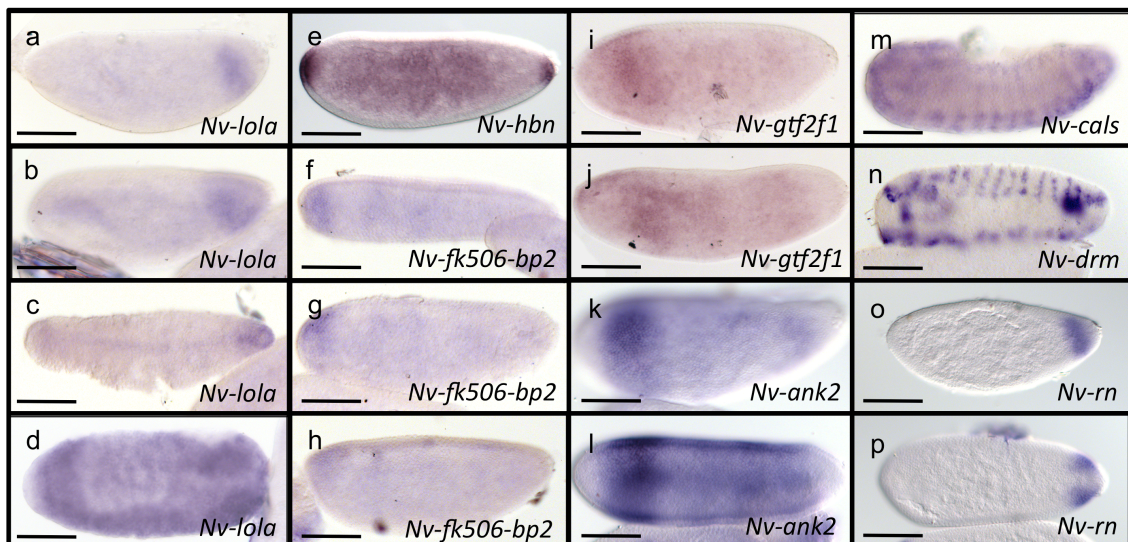


**Figure 4.26 High through put ISH genes with AP expression pattern**

(c,d,n,p) Dorsal and (a,b,e,f,g,h,i,j,k,l,m,o) lateral views of *Nasonia* showing (a-d) *Nv-lola*, (e) *Nv-hbn*, (f,g,h) *Nv-fk506-bp2*, (i,j) *Nv-gtf2f1*, (k,l) *Nv-ank2*, (m) *Nv-cals*, (n) *Nv-drm*, (o,p) *Nv-rn* mRNA expression. *Nv* = *Nasonia vitripennis*; *lola* = *longitudinals lacking*; *fk506-bp2* = *FK506-binding protein 2*; *gtf2f1* = *general transcription factor IIF subunit 1*; *ank2* = *ankyrin2*; *cals* = *calsyntenin*; *drm* = *drumstick*; *rn* = *rotund*. Scale bar 100  $\mu$ m. Anterior is left.



## 5 Discussion and outlook

### 5.1 The fate mapping analysis

Analysis of *Nasonia* embryogenesis showed, that prior to gastrulation most of the investigated DV marker genes are expressed in similar domains with similar expression patterns when compared to their corresponding orthologs in *Drosophila*. Nevertheless, detailed analysis of the dynamics in WT embryos indicates clear differences between *Nasonia* and *Drosophila*.

#### 5.1.1 Dynamic gene expression on the ventral side

Interestingly, all marker genes of the prospective mesoderm are initiated as a narrow stripe along the ventral midline in *Nasonia*. This indicates a significant divergence to *Drosophila* where the type-I target genes *twi* and *sna* are already initiated in relatively broad domains that undergo only minor expansion before they achieve their final shape.

Additionally, the I- $\kappa$ B homolog *cact*, which is hypothesized to be a read out for Toll/NF $\kappa$ B signaling, is initially expressed in a narrow stripe in *Nasonia*. The narrowness of the *cact* domain raises the question whether the area of Cactus protein activity and its function as repressor is congruent with its mRNA expression domain. In this case it would be imaginable that the zygotic *cactus* expression reflects the Dorsal activity. With regard to the tightness of gene regulation observed in zygotic genes in *Nasonia*, it is conceivable that Toll signaling activates Dorsal in a very confined narrow stripe instead of a broad gradient. The subsequently occurring expansion of mesodermal marker genes could be a result of zygotic gene regulation. A confined regulation of *cact* expression is also observed in the self-regulatory system of *Tribolium*. However, unlike in *Nasonia*, it is initially expressed in a broad domain that progressively shrinks to a narrow stripe on the ventral side thereby following the dynamic progression of nuclear Tc-Dorsal (Nunes da Fonseca et al., 2008).

Another significant divergence to *Drosophila* is observed in the expression of *Nv-sim*. In *Drosophila*, *Dm-sim* expression is initially detected in a

posterior domain followed by a narrow stripe on both sides of the mesoderm. Moreover, *Dm-sim* is known to be absent from the ventral side because it is repressed by *Dm-sna* (Kasai et al., 1992; Nambu et al., 1990; Park and Hong, 2012). *Nv-sim*, similar to the other type-I genes, starts as a narrow stripe and expands laterally during embryogenesis. Besides, the *Nv-sim* expression domain is always 1-2 nuclei broader than *Nv-twi* and *Nv-sna* domain. Furthermore, *Nv-sim* progressively clears on the ventral side where its expression overlaps with the domains of *Nv-twi* and *Nv-sna* leaving it expressed in two narrow stripes that cover a single row of nuclei on both sides of the mesoderm. Despite the differences in dynamics observed between *Drosophila* and *Nasonia*, at the onset of gastrulation, *Nv-sim* and *Dm-sim* display a strikingly similar expression pattern in both organisms.

In *Tribolium* *sim* is initiated in a ventral domain. *Tc-sim* expression progressively clears in later stages after *Tc-sna* is activated indicating a correlation between *sna* expression and *sim* inhibition. The described mesoderm dependent inhibition of *sim* expression in *Drosophila* and *Tribolium* is also observed in *Nasonia*. However, in contrast to *Dm-sim*, the repression does not seem to be primary since *Nv-sim*, *Nv-sna* and also *Nv-twi* are initially co-expressed on the ventral side (see chapter 2.1).

The general observation that all described mesodermal marker genes are initially co-expressed in overlapping domains that broaden to their final shape, in combination with the progressive repression of *sim*, already indicates that the ventral patterning GRN has strong dynamics and probably self-regulatory properties that are in stark contrast to what is known from *Drosophila*.

To investigate the relation of *sim*, *twi* and *sna* in *Nasonia*, and in particular how initial activation and later inhibition of the genes is regulated in more detail, it would be interesting to perform knockdown experiments. Detailed analysis of the enhancer and promoter region by Chromatin Immunoprecipitation (ChIP) sequencing would give further insights into the regulation of those genes.



### 5.1.2 Lateral gene expression

*Nv-brk* is the only ectodermal marker expressed in the early blastoderm embryo. Its expression appears at the same time *Nv-twi*, *Nv-sna* and *Nv-sim* expression is detected and covers the whole neurogenic ectoderm.

In later cycles, the laterally expressed columnar genes are activated. First *Nv-vnd* expression is detected. It is the most ventral of the lateral genes and it is initially expressed in the anterior, prospectively thoracic regions of the blastoderm. In following cycles this expression domain extends towards the posterior end.

While *vnd* expression expands, *Nv-msh* expression is activated, followed by *Nv-ind* expression. Like *vnd*, *msh* and *ind* are initially expressed in an anterior region and expand during development towards the posterior. This anterior to posterior expansion indicates that besides the dorsal ventral pattern information another source of information with an AP orientation is present and gives positional information to regulate gene expression along the DV axis.

Interestingly, this anterior to posterior dynamic of ectodermal marker genes is also reflected in the gastrulation movement and represents another divergence between *Nasonia* and *Drosophila*. In *Drosophila*, the process of gastrulation constitutes the internalization of mesoderm and is initiated by the invagination of cells within the mesoderm (Sweeton et al., 1991). Unlike *Drosophila*, gastrulation in *Nasonia* starts at the anterior. Here neuroectodermal cells abutting the mesoderm start to migrate ventrally across mesoderm until they fuse on ventral midline. This process continues to the posterior in until the complete mesoderm is internalized. During gastrulation, the two ventro-lateral *Nv-sim* stripes constitute the leading edge of the migrating ectoderm.

The fact that *Nv-brk* expression initially covers the whole neurogenic ectoderm plus the observation that *Nv-brk* expression is detected earlier than other lateral genes, which are involved in the partitioning of the neurogenic ectoderm (e.g. *Nv-vnd*, *Nv-ind* and *Nv-msh1*), could be an indication that *Nv-brk* has a role in the refinement of positional information in the *Nasonia* embryo, at least in lateral domains.

### 5.1.3 Gene expression on the dorsal side

Target genes on the dorsal side display features of tight regulation already in the early blastoderm stages assuming that already during early embryogenesis, a refined informational input is provided on the dorsal side, most probably by BMP signaling. Several dorsal marker genes are already initiated as narrow stripes along the dorsal midline (chapter 2.1). Genes that initially display a broad expression domain like *Nv-zen* or *Nv-hnt*, quickly refine to narrow stripes.

The pMAD staining demonstrates, that the phosphorylated MAD protein, which served as read out for BMP signaling, is similar to *Nv-zen* expression initially observed in a relatively broad dorsal domain. In following cycles this domain is refined to a thin stripe along the dorsal midline, too.

Interestingly, the two BMP pathway receptors genes *tkv* and *put* are also expressed in a stripe like dorsal domain. However, they are not co-expressed. Their localized expression is temporally separated since *Nv-tkv*'s dorsal domain is only observed during oogenesis and *Nv-put* only during embryogenesis. That this early localization of pathway components could indicate a mechanism for the establishment of a BMP gradient in *Nasonia* will be discussed in more detail in chapter 5.5.2.

Later embryonic stages indicate further divergence from the *Drosophila* model concerning the establishment of the extraembryonic tissue. In most insect embryos, the extraembryonic tissue consists of two separate membranes, the amnion and the serosa. The dorsal most fate of the *Drosophila* blastoderm embryo develops into a single extraembryonic epithelium, the amnioserosa, which covers the embryo only at the dorsal side. Cell movements on the dorsal domain of the post-gastrulating *Nasonia* embryo indicate that the two membranes are separated in *Nasonia* (see chapter 2.1). Unlike in *Drosophila*, in *Nasonia* the corresponding cells expand and migrate ventrally, which presumably results in the complete encompassing of the embryo by those cells. This covering effect is typical for serosal cells and similarly observed in other

insects like the honeybee *Apis mellifera* (Fleig and Sander, 1988) but also the scuttlefly *Megaselia* (Rafiqi et al., 2008). Genes like *ara* and *pnr* are reliable marker for amniotic tissue in *Tribolium* (Nunes da Fonseca et al., 2008; van der Zee et al., 2006). Both are also expressed on the dorsal side in the *Nasonia* embryo, where they flank the expression of serosal markers like *Nv-zen* and are both also considerably amniotic markers in *Nasonia*. To further clarify the separation and role of amnion and serosa in *Nasonia* one would have to trace the movement of cells expressing these marker genes in more detail and perform functional experiments by generating knockdown embryos.

## 5.2 Functional analysis

To further investigate the function of the BMP and Toll pathway in DV axis formation of *Nasonia*, knockdown embryos for either or both of the pathways were generated by pRNAi. These embryos were further analyzed by two-color and three-color ISH.

### 5.2.1 Toll knockdown embryos are still polarized

*Drosophila* embryos lacking Toll signaling display a complete loss of polarity along the dorsal-ventral axis and fail to establish different embryonic fates. Instead they show a consistent tissue where dorsal marker genes and those of the dorsal ectoderm are ubiquitously expressed (Stathopoulos et al., 2002). This phenotype results due to the lack of Toll dependent repression of Dpp.

*Nasonia* embryos negative for Toll signaling show a loss of mesoderm, which is indicated by the absence of *twi* expression on the ventral side. The absence of mesoderm upon lack of Toll signaling indicates a conserved role of Toll in mesoderm formation between *Drosophila* and *Nasonia*. Nevertheless, unlike in *Drosophila*, *Nasonia* embryos negative for Toll signaling are still highly polarized. Gene expression of dorsal marker genes is not affected upon loss of mesoderm when compared to WT indicating a BMP gradient with peak levels along the dorsal midline. Additionally, both the dorsal ectoderm and the

dorsal-ventral ectoderm border stay stable. Since Toll signaling is strongly reduced it seems natural, that the informational input specifying these borders is a result of BMP signaling. Although unlikely, it cannot be ruled out, that minor traces of Toll signaling are sufficient to polarize the ventral domain of embryo. This cannot be excluded since RNAi causes only a strong reduction in gene expression instead of a complete knockout of the gene.

The described loss of mesoderm in Toll negative embryos is accompanied by an expansion of ectoderm towards the ventral side indicated by the expansion of *Nv-brk* expression towards the ventral side. Thus, the activation of *Nv-brk* mRNA expression appears to be independent of Toll signaling and mesoderm formation since it is still expressed in Toll negative embryos lacking mesoderm. However, the *Nv-brk* expression domain is expanded ventrally covering the whole ventral side. This is in contrast to *Drosophila* where no early *brinker* expression is detected in the absence of Toll signaling (Jaźwińska et al., 1999).

In a more detailed analysis of Toll negative embryos we observed a series of phenotypes reaching from a moderate to strong reduction of mesoderm up to a complete loss of mesoderm, which is indicated by reduction or loss of *twi* expression, respectively. In minor to moderate phenotypes *Nv-twi* expression is narrowed with respect to its lateral expansion when compared to WT, whereas in moderate to strong phenotypes reduction of *Nv-twi* expression along the DV-axis is accompanied by its reduction along the AP-axis. However, in most cases no *Nv-twi* expression is detected at all.

Reduction of *Nv-twi* expression is accompanied by a shift of *Nv-vnd* expression. In WT embryos *Nv-vnd* expression marks the ventral neuroectoderm. In contrast to *Nv-brk*, *Nv-vnd* expression does not expand towards the ventral midline upon reduction of *Nv-twi* expression in Toll negative embryos. Instead, the width of *Nv-vnd* expression remains wildtype in regard to its DV expansion. However, the whole domain shifts towards the ventral side. This shift is in correlation to the narrowing *twi* expression domain. In rare cases *vnd* expression is detected on the most ventral side of embryos

completely lacking mesoderm/*twi* expression. This phenotype shows that the remnants of Toll signaling in those knockdown embryos are sufficient to induce ectoderm but not mesoderm formation. Furthermore it shows that ectoderm can be induced without the formation of mesoderm.

The I- $\kappa$ B homolog Cact is one of the first targets of Toll signaling in *Drosophila*. Its mRNA expression pattern in *Nasonia* matches the early narrow stripe like expression of mesodermal markers that only respond to high levels of nuclear Dorsal and was used as proxy to indicate Toll/NF- $\kappa$ B signaling. In Toll negative embryos neither *twi* nor *cact* expression is detected, further affirming that *Nv-cact* indeed is a direct downstream target of Toll signaling.

### 5.2.2 Toll signaling in the absence of BMP

Upon loss of BMP signaling in *Nasonia* we observed a dramatic expansion of mesoderm indicated by expanded *Nv-twi* expression. In these embryos mesoderm covers the complete embryo circumference leaving only a small anterior-dorsal domain with *brk/vnd* expression. Interestingly, this is not true for the *Nv-cact* expression domain. In BMP minus embryos the *Nv-cact* expression is unaffected and does not follow the expansion of the *twi* domain.

The fact that in BMP minus embryos *Nv-cact* expression is not affected by mesoderm expansion can be seen as further evidence that Toll/NF- $\kappa$ B signaling does not act as a global morphogen but rather as an inductive signal along the ventral midline that triggers mesoderm formation in *Nasonia* rather than forming a gradient with several thresholds that provides positional information for pattern formation as observed in *Drosophila*. In *Nasonia*, final borders and shape of gene expression of mesodermal and ectodermal markers are determined by BMP, implying that BMP signaling apparently functions as morphogen along the whole DV axis. This assumption is further reinforced by the observation that in early BMP minus embryos, like in WT, *Nv-twi* is expressed in a narrow stripe. In this case Toll signaling could establish a steep gradient of nuclear dorsal with peak levels along the ventral midline. Along this stripe target genes like *twi*, *sna* and *sim* are activated and presumably

feedback on each other and putative downstream target genes. Activation of these feedback loops expands the domains. However, the final borders of these domains are not actively defined by the Toll signal but by BMP dependent inhibition as in BMP negative embryos refinement of the mesoderm border is impaired and results in massive expansion of mesoderm.

Additionally, a knockdown of both pathways was performed by simultaneous injection of the respective dsRNAs in female *Nasonia* pupa. Embryos of those females expressed the ectodermal marker *Nv-brk* only when stained for *twi*, *brk* and *zen*. This indicates that the expansion of mesoderm in the BMP knock-down embryos at least requires the induction of Toll signaling, which further emphasizes Toll's conserved role in mesoderm induction (see also chapter 2.2).

### 5.2.3 Future functional analyses

To further analyze the mechanism of the GRN one would have to knockdown potentially important zygotic marker genes along the DV axis like *twi*, *brk* or *zen*. Knock down of those genes was performed by pRNAi. However, embryonic pattern formation and development was unaffected. It seems that a parental knockdown in the ovaries is not affecting zygotically expressed genes. The problem could be evaded by injecting dsRNA into freshly laid *Nasonia* eggs. The establishment of egg/embryonic injections would additionally provide the option to generate constant knockout lines by stably introducing an appropriate DNA construct into the germline. A first attempt to perform embryonic injections was already made which requires further improvement since the survival rates of injected *Nasonia* embryos are not stable, yet.

### 5.3 Analysis of Toll pathway components

All analyzed genes of the *Drosophila* Toll signaling cascade are conserved in the *Nasonia* genome. The *Nasonia* homologs of *Nv-Sll* and *Nv-Wbl* are closest related to the other Hymenoptera species *Apis mellifera*, whereas the other follicle cell component, *Nv-Pipe*, seems to be distantly related to the others, since it branches more basally. Furthermore, neither *Nv-pipe* nor one of the other two follicle cell components is expressed during *Nasonia* oogenesis. In *Drosophila*, *pipe* expression specifies the domain for the formation of the morphogen gradient on the ventral side. The absence of *Nv-pipe*, *Nv-wbl* and *Nv-sll* could indicate that despite the conserved role of *Nv-Toll*, no gradient (as observed in *Drosophila*) is established in *Nasonia*. On the other hand it could also mean, that a gradient is formed but simply does not depend on the expression of those genes in the follicular epithelium.

Nevertheless, the components of the protease cascade, involved in the formation of the Spätzle morphogen gradient in *Drosophila*, are conserved in *Nasonia*. *Nv-ndl*, and *Nv-gd* are both expressed in *Nasonia* ovarioles (Fig. 4.12a-b) and in the corresponding phylogenetic trees both genes group together with *Drosophila* in a branch or in a sister branch (Fig 4.6 and Fig. 4.7). Interestingly, *Nv-snk* is detected in the genome but not expressed. The phylogenetic analysis of *Nv-Snk* allows no conclusion since both outgroup sequences do not root the tree (Fig. 4.8). A more distantly related molecule would be required to root the tree properly. The same is true for the phylogenetic analysis of *Nv-Ea* (Fig. 4.8). Nevertheless, mRNA expression of one of the two *Nv-ea* genes (*Nv-ea1*) is detected during *Nasonia* oogenesis (Fig. 4.12c).

The substrate of Easter, *Spz*, is conserved in *Nasonia*. All four *Nasonia* Spätzle sequences are closely related to the *Drosophila* homolog. Of the two analyzed *Nasonia* sequences (*Nv-spz1* and *Nv-spz2*), only *Nv-spz1* is expressed in ovarioles (Fig. 4.12d). Furthermore, *Nv-spz1* seems to be a ligand for the Toll receptor and has an important function in DV patterning since the pRNAi knockdown phenotype (not shown) is identical to the *Nv-Toll3* knockdown (see chapter 2.2). In addition to that it has an interesting embryonic expression

pattern with a localized domain on the dorsal side of the embryo that later expands towards the ventral midline (Fig. 4.13 g-h) which could indicate an involvement in the establishment of dorsal fates during embryogenesis. The two remaining homologs *Nv-spz3* and *Nv-spz4* are not yet analyzed by ISH or pRNAi but look very interesting, since both are closely related to *Dm-spz*, too, according to the phylogenetic analysis (Fig. 4.11).

The inhibitory substrate, *Nv-spn27A*, is not expressed during oogenesis. Interestingly, it is expressed in a dorsal domain during embryogenesis and in later stages it is expressed in the anterior part of the presumptive serosa (Fig. 4.13), an expression pattern quite identical to *Nv-zen*. *zen* orthologs are markers for serosa and other extraembryonic tissues in other insects (van der Zee et al., 2005).

Four of the five Toll and TLR homologs in *Nasonia* group in a sister branch to *DmToll* (Fig. 4.14). *Nv-Toll3* seems crucial for DV axis formation since it leads to dorsalized embryos when knocked down by pRNAi (see chapter 2.2). *Nv-TollB* is not expressed, neither during oogenesis nor embryogenesis. Interestingly, *Nv-Toll2* expression resembles the expression pattern of *Nv-Toll3* during oogenesis (compare Fig. 4.15a and b) and early embryogenesis (compare Fig. 4.16a-c and Fig. 4.16i-j) whereas prior to gastrulation it strongly resembles the expression pattern of *Nv-twi* (compare Fig 4.16 f-g and chapter 2.1 or 2.2). Anyhow, pRNAi against *Nv-TollB* and *Nv-Toll2* did not show any phenotype. *Nv-Toll4*, which is ubiquitously expressed during oogenesis and embryogenesis, seems to play an important role in the immune system of *Nasonia* since dsRNA treated females had severely reduced live span after eclosion. Additionally, those females displayed reduced motility (not shown). Moreover, these females did not lay eggs, which could be a side effect of the restricted immune response. On the other hand it could also indicate an additional role for *Nv-Toll4* in DV axis formation. Knockdown ovarioles of *Nv-Toll4* injected females were morphologically indistinguishable from WT ovarioles. However, they have not been further analyzed by ISH, which might



provide deeper insight into putative degenerations of the ovariole that would explain the disability to lay eggs.

The same is true for the intracellular components, *mydd 88*, *pelle* and *tube*. Like the knockdown of *Nv-Toll4*, dsRNA treatment of any of the three components leads to severely reduced live span, motility and loss of egg production. Since only one copy of each is present in the *Nasonia* genome (Fig. 4.12 - 4.13), it is likely, that all three function as signal mediator for both immune response signaling as well as DV specific Toll signaling. It seems reasonable that reduced expression of any of the three components, negatively affects the immune response of *Nasonia* to such a degree, that stock keeping conditions quickly cause an infection, responsible for the symptoms described above.

Only *Nv-tube* is expressed and shows a ubiquitous distribution during oogenesis and embryogenesis (Fig. 4.15d and Fig. 4.23k), whereas *Nv-mydd88* and *Nv-pelle* are not expressed in oogenesis. During embryogenesis all three components display a ubiquitous expression (Fig. 4.23h, k, l). However, the other *pelle* homolog (*Nv-pelle like*) needs to be investigated by ISH and pRNAi, too.

Four NF- $\kappa$ B related and three I- $\kappa$ B related genes are present in the *Nasonia* genome (Fig. 4.19 - 4.20). All are expressed during oogenesis (Fig. 4.20 and 4.22) whereas all except *Nv-cact3* are expressed during embryogenesis. In previous studies, it was already assumed, that *Nv-cact1* could be a functional component in DV axis formation because of its ventrally restricted expression domain resembles the initial expression domain of the first detected zygotically expressed genes on the ventral side (chapter 2.1 and 2.2). Interestingly, *Nv-cact2* shows a narrow ventral stripe (Fig. 4.23j) that is quite similar to the previously described stripe detected in *Nv-cact1* stainings (chapter 2.1 and 2.2 and Fig. 4.23e-g). To find out, which *dorsal* and *cact* genes contribute to DV axis formation, functional analyzes using pRNAi was performed. Unfortunately, knockdown by pRNAi of all seven genes alone and in combination did not alter

embryogenesis in terms of morphology or gene expression (see also chapter 5.2.4).

In summary, it can be concluded, that there is conservation between *Nasonia* and *Drosophila* within the general architecture of the Toll signaling cascade and in terms of the components that it comprises. However, gene expression and functional analysis indicates, that the cascade does not culminate in the generation of a morphogen gradient as observed in *Drosophila*. It rather seems that Toll signaling defines a very narrow field along the ventral midline, which is reflected by the narrow expression of *Nv-cact1/2* and the narrow domains of the zygotically expressed genes *Nv-twi*, *Nv-sna* and *Nv-sim* (see also chapter 2.1). It is conceivable, that within these narrow stripes of expression zygotic genes trigger self-regulatory loops that cause the dynamic expansion of the mesoderm.

Another interesting aspect is the previously mentioned absence of follicle cell components that are substantial for the determination of the field of the *Dm*-Dorsal gradient in the embryo of *Drosophila*. The fact that all three components of the follicle epithelium are not expressed during *Nasonia* oogenesis plus the observation that *Nv-pipe* is the most diverged of all six *pipe* homologs (Fig. 4.5) could be another indication that they are not involved in DV axis formation in *Nasonia*.

Nevertheless, as previously discussed, *Nv-Spz* and *Nv-Toll* are both crucial for DV axis formation in *Nasonia*. In addition, the upstream protease cascade is mostly conserved, which makes it likely that Spätzle is also processed by those proteases in *Nasonia*. However, this does not necessarily mean, that a Spätzle gradient is formed. It is imaginable, that the Toll receptor is equally distributed throughout the oocyte membrane and that it is only activated in a narrow domain, which later in the embryo is reflected by the expression pattern of *Nv-cact*.

One observation that could support this hypothesis is the unilateral restricted expression of *Nv-gd* mRNA during late oogenesis. In *Drosophila* *gd* mRNA is uniformly expressed. However, Gd protein is ventrally localized and

this localization presumably depends on Pipe-sulfated proteins (Cho et al., 2012). The ventrally located Gd protein is assumed to form a complex with Snake and Easter. Within this complex Gd facilitates the activation of Easter and thus the activation of Spätzle. If one assumes that in *Nasonia* the protein distribution of all proteases is reflected by their mRNA distribution, *Nv*-Easter and *Nv*-Spätzle would be uniformly distributed throughout the perivitelline fluid whereas *Nv*-Gd would be restricted to one side along the DV axis. In this case, the *Nv-gd* expression domain would determine the area of Spätzle/Toll activation and thus constitute a way to circumvent the lack of *Nv-pipe* in *Nasonia*. To test whether the side of *Nv-gd* mRNA expression reflects the ventral side could be investigated by visualization of the oocyte nucleus. Since in *Nasonia*, like in *Drosophila*, asymmetric positioning followed by EGF signaling defines the dorsal side of the embryo (Lynch et al., 2010), *Nv-gd* expression should oppose the oocyte nucleus location. However, common nuclear staining using 4',6-diamidino-2-phenylindole (DAPI) does not apply since during the desired stages the oocyte nucleus is haploid and dim, and very close to the polyploid and bright follicle cells. Nevertheless, one can passively visualize the oocyte nucleus by using marker genes that are localized within the oocyte near the asymmetrically positioned oocyte nucleus, like *Nv-tgf* (Lynch et al., 2010) or *Nv-tkv* (chapter 2.3). In both cases, a double ISH staining would be required to visualize the expression of both *Nv-gd* and the oocyte nucleus marker gene.

Another interesting observation is the absence of *Nv-serpin27A* expression during oogenesis. In *Drosophila*, Serpin27A's function as protease inhibitor is assumed to provide an important control element in the proteolytic cascade that leads to the formation of the Dorsal gradient. The concept of a narrow activation domain instead of a broad gradient could be connected to the expendability of Spn27A during oogenesis. However, a narrower domain could also mean a steeper gradient, which one could argue, needs even more regulation.

To be sure, whether the system is set up by a gradient, similar to *Drosophila* or by a narrow induction along the ventral midline as reflected by

the domains of *cact* (or *twi*, *sna* and *sim*), an analysis of the distribution of nuclear Dorsal along the DV axis is necessary. Additionally, an analysis of the Toll receptor distribution could also give further insights about the mechanism, since it cannot be ruled out that evenly distributed Spätzle activates an ventrally localized Toll receptor in the oocyte membrane.

## 5.4 DV axis formation without *short gastrulation* (*sog*)

### 5.4.1 Sog is not conserved in the *Nasonia vitripennis* genome

In *Drosophila*, one lateral marker gene with high affinity dorsal binding site is *short gastrulation* (*sog*). In *Drosophila*, Sog plays a major role in the establishment of a sharp gradient of BMP signal the dorsal side. *Dm-sog* is expressed in a broad domain on both lateral sides in the neurogenic ectoderm. In the syncytial blastoderm embryo Sog protein diffuses dorsally and concurrently binds Dpp protein. The Sog/Dpp complex diffuses dorsally where Sog becomes cleaved by the metalloprotease Tolloid. After being cleaved by Tolloid, Sog releases Dpp, which in turn leads to the accumulation of Dpp on the dorsal side. The process results in a steep gradient with peak levels of Dpp along the dorsal midline.

To this date no *sog* ortholog was detected in any published *Nasonia* genome. Additionally, in our independent transcriptome analysis of blastoderm stage embryos we did not detect *Nv-sog* expression indicating a loss of this BMP inhibitor in *Nasonia*. Furthermore, the *Nasonia* ortholog of *tolloid* is expressed in blastoderm embryo stages but only in a small domain of the head region on the dorsal side (Chapter 2.2). Knockdown of *tolloid* by pRNAi did not lead to an alteration of embryogenesis suggesting that *Nv-tolloid* has no function in early DV axis formation. This would be reasonable since the proteolytic role of Tolloid as inhibitor of Sog would be expendable during embryogenesis in the absence of Sog.

The fact that *sog* is missing raises the question whether there is another gene substituting for *sog*'s anti BMP function in the syncytial blastoderm

embryo of *Nasonia* and if not, how peak levels of BMP signaling are established and stabilized. The formation of dorsal fates without the inhibitory function of Sog was previously observed in another hymenopteran species, the honeybee *Apis mellifera* (*Am*). In contrast to *Nasonia*, the *Apis* genome holds a *sog* ortholog. However, *Am-sog* it is not expressed during embryogenesis (Wilson and Dearden, 2011) and thus not part of DV axis determination. Additionally, in *Apis* the RNA of the ligand Dpp is localized (Wilson et al., 2011). One possible hypothesis would be that a Sog independent system represents an ancestral mode, which would also be in accordance with the fact that both *Nasonia* and *Apis* are basal members of the holometabola. However, it is more likely that the loss or the loss of functionality of *sog* as inhibitor in axis formation is a hymenoptera specific phenomenon, since recent studies revealed a role of *sog* during embryogenesis of the hemimetabolous milkweed bug *Oncopeltus fasciatus* (*Of*) (Lena Sachs, Yen-Ta Chen and S. Roth unpublished data).

#### 5.4.2 A BMP gradient without Sog

ISH analyses of BMP components may provide indication that the positional cues for the BMP gradient of the *Nasonia* embryo already arise during oogenesis. The mRNA of the gene *Nv-tkv*, which encodes an ortholog of the type-I receptor protein Thickvein, is expressed in a dorsal stripe already in the oocyte. *Nv-tkv* is the only BMP pathway component analyzed to far, that has a localized DV expression domain during oogenesis. The other type-I receptor ortholog, *Nv-sax* shows a ubiquitous expression pattern in the oocyte. After egg lay, both *Nv-tkv* and *Nv-sax* are ubiquitously expressed in the embryo.

The gene *punt* encodes the type-II receptor Punt in *Drosophila*. Interestingly, one of the *Nasonia* orthologs of *punt* (*Nv-put1*) shows a localized expression domain in the embryo that constitutes also a narrow stripe along the dorsal midline (see chapter 2.3). Moreover, its expression is not detected during oogenesis.

Combining these observations, it is conceivable that DV specific BMP signaling is determined by a complex consisting of a BMP ligand (Dpp/Gbb)

and the type-I and type-II receptor combination *Nv-Tkv* and *Nv-Put* in *Nasonia*. Channeling of the signal could be accomplished by the restricted localization of one of the receptor heteromer components while the other components are equally distributed. In particular, the dorsal localization of *Nv-Tkv* during oogenesis and *Nv-Put* during embryogenesis could be part of a system, which defines the peak level of the BMP gradient along the dorsal midline.

However, it remains to be answered, what causes the tight mRNA localization of these components during oogenesis and whether the localized mRNA expression of those genes indeed also reflects the actual position of the receptor in the plasmamembrane. Theoretically a localized mRNA could also serve as a source for a subsequent protein gradient. However, this is not necessarily in contrast to the aforementioned ideas.

## 5.5 Transcriptome

The differences observed between *Nasonia* and *Drosophila* is reflected in differences in gene expression along the DV axis. To detect important DV patterning genes by an unbiased approach a transcriptome analysis was performed. Since the knockdown of key components of the Toll and BMP pathway leads to drastic changes in the fate map of the embryo it is obvious to assume, that these changes in tissue size are also reflected in altered gene expression levels. In other words, the severe reduction or expansion of different cell fates along the DV axis should lead to an increase or decrease in transcription levels of marker genes of the respective tissue. Previous quantitative analysis of *Nv-twi* mRNA expression in both knockdown conditions confirmed this assumption since the measured expression levels reflected the observed expansion and reduction of mesoderm, respectively (Fig. 24). It is likely to assume that other target genes of both the Toll and BMP pathway display a similar alteration in expression levels.

The analysis of the three transcriptome data sets lead to the detection of common as well as unknown genes that are potentially important for the establishment of the *Nasonia* dorsal-ventral GRN. Interestingly, most of the

detected genes with a DV localized expression domain are observed to be expressed on the dorsal side. The only gene of the second round of high throughput ISH displaying an expression pattern on the ventral side is the ortholog of *epithelial membrane protein (emp)* (Fig. 4.25g-h) a member of the Scavenger Receptors Class B Type I (SR-BI). Interestingly, its expression pattern resembles the initial expression of the other early ventral marker genes of *Nasonia*. So far, no statement can be made about its dynamic since detailed analyses in temporal staged embryos has not been performed. In *Drosophila* *emp* is described to be expressed during embryogenesis in various epithelial cell types derived from the ectoderm (Hart and Wilcox, 1993). Together with other SR-BI's *emp* is described to play a role in endocytosis (Uvila et al., 2006), absorption of carotenoid or pheromone recognition and immunity (Herboso et al., 2011). The most obvious connection can be made to the Toll receptor, which is also known to play a role in immunity as well as in DV patterning. However, *emp*'s concrete role in immunity is not validated and to find out which or whether it has a function at all in *Nasonia* DV pattern formation further analysis and functional studies would be required.

Genes on the dorsal side, like *Nv-2EG013778* and *Nv-EG000923* (Fig 4.25a-d and 4.25o-p) show high similarity to important dorsal marker genes like *Nv-zen* concerning their temporal and spatial distribution and additionally seem to be hymenoptera specific. Other genes are promising candidates, since their known function makes them putative components of the dorsal-ventral GRN in *Nasonia*. For example *omb* (Fig. 4.25 i-k) is known to act downstream of Dpp signaling during *Drosophila* wing formation. Together with genes like *brk* it is important for gene regulation and domain organization during wing vein development (Cook et al., 2004; Jaźwińska et al., 1999; Sivasankaran et al., 2000; Zhang et al., 2013). It is imaginable, that *Nv-omb* has a similar role in gene regulation and expression pattern refinement during *Nasonia* embryogenesis and thus, theoretically, represents one of the missing links in understanding how tight gene regulation on the dorsal side of the early blastoderm embryo is

achieved in a *sog* independent manner. The same is true for any other dorsally as well as ventrally expressed gene.

In addition to the genes with DV specific expression pattern, genes with AP specific expression were detected (Fig. 26). There is good reason that gene expression along the AP axis is also affected, considering the extreme fate shifts and tissue size alterations in both knockdown conditions. Those genes also represent potentially important components of the dorsal-ventral GRN since it is not clear, to what extent both the AP and DV system are connected in *Nasonia*. Anyhow, the observed dynamism of ectodermal marker genes along the AP axis, together with the anterior to posterior progression of the gastrulation movement indicates that there is a connection between both axes, which could also be reflected in the transcriptome data set.

In summary, to use the whole potential of the transcriptome, further screening of the data set and investigation of all genes with diverged expression levels is required. Additionally, all identified genes have to be investigated more thoroughly by detailed temporal and spatial expression analysis as well as by functional studies. Especially those candidates that show no homology to previously described genes have to be analyzed on a sequence level to determine potentially conserved protein domains that could further elucidate the function of the respective gene in DV axis formation or any other biological process.



## 6 References

- Akiyama-Oda, Y., Oda, H., 2006. Axis specification in the spider embryo: *dpp* is required for radial-to-axial symmetry transformation and *sog* for ventral patterning. *Development* 133, 2347–57.
- Anderson, K. V, Bokla, L., Nüsslein-Volhard, C., 1985a. Establishment of dorsal-ventral polarity in the *Drosophila* embryo: the induction of polarity by the Toll gene product. *Cell* 42, 791–8.
- Anderson, K. V, Jürgens, G., Nüsslein-Volhard, C., 1985b. Establishment of dorsal-ventral polarity in the *Drosophila* embryo: genetic studies on the role of the Toll gene product. *Cell* 42, 779–89.
- Andreu, M.J., González-Pérez, E., Ajuria, L., Samper, N., González-Crespo, S., Campuzano, S., Jiménez, G., 2012. Mirror represses pipe expression in follicle cells to initiate dorsoventral axis formation in *Drosophila*. *Development* 139, 1110–4.
- Ashe, H.L., Levine, M., 1999. Local inhibition and long-range enhancement of Dpp signal transduction by Sog. *Nature* 398, 427–31.
- Ashe, H.L., Mannervik, M., Levine, M., 2000. Dpp signaling thresholds in the dorsal ectoderm of the *Drosophila* embryo. *Development* 127, 3305–12.
- Attisano, L., Wrana, J.L., 1998. Mads and Smads in TGF beta signalling. *Curr. Opin. Cell Biol.* 10, 188–94.
- Bastock, R., St Johnston, D., 2008. *Drosophila* oogenesis. *Curr. Biol.* 18, R1082–7.
- Bergmann, A., Stein, D., Geisler, R., Hagenmaier, S., Schmid, B., Fernandez, N., Schnell, B., Nüsslein-Volhard, C., 1996. A gradient of cytoplasmic Cactus degradation establishes the nuclear localization gradient of the dorsal morphogen in *Drosophila*. *Mech. Dev.* 60, 109–23.
- Berns, N., Woichansky, I., Kraft, N., Hüsken, U., Carl, M., Riechmann, V., 2012. “Vacuum-assisted staining”: a simple and efficient method for screening in *Drosophila*. *Dev. Genes Evol.* 222, 113–8.
- Biehs, B., François, V., Bier, E., 1996. The *Drosophila* short gastrulation gene prevents Dpp from autoactivating and suppressing neurogenesis in the neuroectoderm. *Genes Dev.* 10, 2922–34.
- Cha, B.J., Koppetsch, B.S., Theurkauf, W.E., 2001. In vivo analysis of *Drosophila* bicoid mRNA localization reveals a novel microtubule-dependent axis specification pathway. *Cell* 106, 35–46.
- Chasan, R., Anderson, K. V, 1989. The role of easter, an apparent serine protease, in organizing the dorsal-ventral pattern of the *Drosophila* embryo. *Cell* 56, 391–400.
- Chasan, R., Jin, Y., Anderson, K. V, 1992. Activation of the easter zymogen is regulated by five other genes to define dorsal-ventral polarity in the *Drosophila* embryo. *Development* 115, 607–16.
- Chen, G., Handel, K., Roth, S., 2000. The maternal NF-kappaB/ dorsal gradient of *Tribolium castaneum*: dynamics of early dorsoventral patterning in a short-germ beetle. *Development* 127, 5145–56.

- Cho, Y.S., Stevens, L.M., Sieverman, K.J., Nguyen, J., Stein, D., 2012. A ventrally localized protease in the *Drosophila* egg controls embryo dorsoventral polarity. *Curr. Biol.* 22, 1013–8.
- Cook, O., Biehs, B., Bier, E., 2004. *brinker* and *optomotor-blind* act coordinately to initiate development of the L5 wing vein primordium in *Drosophila*. *Development* 131, 2113–24.
- Das, P., Maduzia, L.L., Wang, H., Finelli, A.L., Cho, S.H., Smith, M.M., Padgett, R.W., 1998. The *Drosophila* gene *Medea* demonstrates the requirement for different classes of Smads in *dpp* signaling. *Development* 125, 1519–28.
- Davis, G.K., Patel, N.H., 2002. Short, long, and beyond: molecular and embryological approaches to insect segmentation. *Annu. Rev. Entomol.* 47, 669–99.
- Dearden, P.K., 2006. Germ cell development in the Honeybee (*Apis mellifera*); *vasa* and *nanos* expression. *BMC Dev. Biol.* 6, 6.
- DeLotto, R., Spierer, P., 1986. A gene required for the specification of dorsal-ventral pattern in *Drosophila* appears to encode a serine protease. *Nature* 323, 688–92.
- Dennler, S., Itoh, S., Vivien, D., ten Dijke, P., Huet, S., Gauthier, J.M., 1998. Direct binding of Smad3 and Smad4 to critical TGF beta-inducible elements in the promoter of human plasminogen activator inhibitor-type 1 gene. *EMBO J.* 17, 3091–100.
- Dereeper, a, Guignon, V., Blanc, G., Audic, S., Buffet, S., Chevenet, F., Dufayard, J.-F., Guindon, S., Lefort, V., Lescot, M., Claverie, J.-M., Gascuel, O., 2008. Phylogeny.fr: robust phylogenetic analysis for the non-specialist. *Nucleic Acids Res.* 36, W465–9.
- Derynck, R., Feng, X.H., 1997. TGF-beta receptor signaling. *Biochim. Biophys. Acta* 1333, F105–50.
- Drier, E.A., Govind, S., Steward, R., 2000. Cactus-independent regulation of Dorsal nuclear import by the ventral signal. *Curr. Biol.* 10, 23–6.
- Drier, E.A., Huang, L.H., Steward, R., 1999. Nuclear import of the *Drosophila* Rel protein Dorsal is regulated by phosphorylation. *Genes Dev.* 13, 556–68.
- Edwards, D.N., Towb, P., Wasserman, S.A., 1997. An activity-dependent network of interactions links the Rel protein Dorsal with its cytoplasmic regulators. *Development* 124, 3855–64.
- Ferguson, E.L., Anderson, K. V, 1992a. Localized enhancement and repression of the activity of the TGF-beta family member, *decapentaplegic*, is necessary for dorsal-ventral pattern formation in the *Drosophila* embryo. *Development* 114, 583–97.
- Ferguson, E.L., Anderson, K. V, 1992b. *Decapentaplegic* acts as a morphogen to organize dorsal-ventral pattern in the *Drosophila* embryo. *Cell* 71, 451–61.
- Fernandez, N.Q., Grosshans, J., Goltz, J.S., Stein, D., 2001. Separable and redundant regulatory determinants in *Cactus* mediate its dorsal group dependent degradation. *Development* 128, 2963–74.
- Fleig, R., Sander, K., 1988. Honeybee morphogenesis: embryonic cell movements that shape the larval body 534, 525–534.

- François, V., Bier, E., 1995. *Xenopus* chordin and *Drosophila* short gastrulation genes encode homologous proteins functioning in dorsal-ventral axis formation. *Cell* 80, 19–20.
- Fuller, M.T., Spradling, A.C., 2007. Male and female *Drosophila* germline stem cells: two versions of immortality. *Science* 316, 402–4.
- González-Reyes, A., Elliott, H., St Johnston, D., 1995. Polarization of both major body axes in *Drosophila* by gurken-torpedo signalling. *Nature* 375, 654–8.
- Grosshans, J., Bergmann, A., Haffter, P., Nüsslein-Volhard, C., 1994. Activation of the kinase Pelle by Tube in the dorsoventral signal transduction pathway of *Drosophila* embryo. *Nature* 372, 563–6.
- Häcker, U., Nybakken, K., Perrimon, N., 2005. Heparan sulphate proteoglycans: the sweet side of development. *Nat. Rev. Mol. Cell Biol.* 6, 530–41.
- Han, J.H., Lee, S.H., Tan, Y.Q., LeMosy, E.K., Hashimoto, C., 2000. Gastrulation defective is a serine protease involved in activating the receptor toll to polarize the *Drosophila* embryo. *Proc. Natl. Acad. Sci. U. S. A.* 97, 9093–7.
- Hart, K., Wilcox, M., 1993. A *Drosophila* gene encoding an epithelial membrane protein with homology to CD36/LIMP II. *J. Mol. Biol.* 234, 249–53.
- Hashimoto, C., Hudson, K.L., Anderson, K. V., 1988. The Toll gene of *Drosophila*, required for dorsal-ventral embryonic polarity, appears to encode a transmembrane protein. *Cell* 52, 269–79.
- Hashimoto, C., Kim, D.R., Weiss, L. a, Miller, J.W., Morisato, D., 2003. Spatial regulation of developmental signaling by a serpin. *Dev. Cell* 5, 945–50.
- Hayashi, H., Abdollah, S., Qiu, Y., Cai, J., Xu, Y.Y., Grinnell, B.W., Richardson, M.A., Topper, J.N., Gimbrone, M.A., Wrana, J.L., Falb, D., 1997. The MAD-related protein Smad7 associates with the TGFbeta receptor and functions as an antagonist of TGFbeta signaling. *Cell* 89, 1165–73.
- Herboso, L., Talamillo, A., Pérez, C., Barrio, R., 2011. Expression of the Scavenger Receptor Class B type I (SR-BI) family in *Drosophila melanogaster*. *Int. J. Dev. Biol.* 55, 603–11.
- Hogan, B.L., 1996. Bone morphogenetic proteins: multifunctional regulators of vertebrate development. *Genes Dev.* 10, 1580–94.
- Hong, C.C., Hashimoto, C., 1995. An unusual mosaic protein with a protease domain, encoded by the nudel gene, is involved in defining embryonic dorsoventral polarity in *Drosophila*. *Cell* 82, 785–94.
- Hong, J.-W., Hendrix, D. a, Papatsenko, D., Levine, M.S., 2008. How the Dorsal gradient works: insights from postgenome technologies. *Proc. Natl. Acad. Sci. U. S. A.* 105, 20072–6.
- Hu, X., Yagi, Y., Tanji, T., Zhou, S., Ip, Y.T., 2004. Multimerization and interaction of Toll and Spätzle in *Drosophila*. *Proc. Natl. Acad. Sci. U. S. A.* 101, 9369–74.
- Hudson, J.B., Podos, S.D., Keith, K., Simpson, S.L., Ferguson, E.L., 1998. The *Drosophila* Medea gene is required downstream of dpp and encodes a functional homolog of human Smad4. *Development* 125, 1407–20.
- Huguet, C., Crepieux, P., Laudet, V., 1997. Rel/NF-kappa B transcription factors and I kappa B inhibitors: evolution from a unique common ancestor. *Oncogene* 15, 2965–74.

- Imamura, T., Takase, M., Nishihara, A., Oeda, E., Hanai, J., Kawabata, M., Miyazono, K., 1997. Smad6 inhibits signalling by the TGF-beta superfamily. *Nature* 389, 622–6.
- Isoda, K., Nüsslein-Volhard, C., 1994. Disulfide cross-linking in crude embryonic lysates reveals three complexes of the *Drosophila* morphogen dorsal and its inhibitor cactus. *Proc. Natl. Acad. Sci. U. S. A.* 91, 5350–4.
- Januschke, J., Gervais, L., Gillet, L., Keryer, G., Bornens, M., Guichet, A., 2006. The centrosome-nucleus complex and microtubule organization in the *Drosophila* oocyte. *Development* 133, 129–39.
- Jaźwińska, a, Rushlow, C., Roth, S., 1999. The role of brinker in mediating the graded response to Dpp in early *Drosophila* embryos. *Development* 126, 3323–34.
- Jonk, L.J., Itoh, S., Heldin, C.H., ten Dijke, P., Kruijer, W., 1998. Identification and functional characterization of a Smad binding element (SBE) in the JunB promoter that acts as a transforming growth factor-beta, activin, and bone morphogenetic protein-inducible enhancer. *J. Biol. Chem.* 273, 21145–52.
- Kamiyama, S., Suda, T., Ueda, R., Suzuki, M., Okubo, R., Kikuchi, N., Chiba, Y., Goto, S., Toyoda, H., Saigo, K., Watanabe, M., Narimatsu, H., Jigami, Y., Nishihara, S., 2003. Molecular cloning and identification of 3'-phosphoadenosine 5'-phosphosulfate transporter. *J. Biol. Chem.* 278, 25958–63.
- Kanodia, J.S., Rikhy, R., Kim, Y., Lund, V.K., DeLotto, R., Lippincott-Schwartz, J., Shvartsman, S.Y., 2009. Dynamics of the Dorsal morphogen gradient. *Proc. Natl. Acad. Sci. U. S. A.* 106, 21707–12.
- Kasai, Y., Nambu, J.R., Lieberman, P.M., Crews, S.T., 1992. Dorsal-ventral patterning in *Drosophila*: DNA binding of snail protein to the single-minded gene. *Proc. Natl. Acad. Sci. U. S. A.* 89, 3414–8.
- Kingsley, D.M., 1994. The TGF-beta superfamily: new members, new receptors, and new genetic tests of function in different organisms. *Genes Dev.* 8, 133–46.
- Konrad, K.D., Goralski, T.J., Mahowald, A.P., Marsh, J.L., 1998. The gastrulation defective gene of *Drosophila melanogaster* is a member of the serine protease superfamily. *Proc. Natl. Acad. Sci. U. S. A.* 95, 6819–24.
- Konsolaki, M., Schüpbach, T., 1998. windbeutel, a gene required for dorsoventral patterning in *Drosophila*, encodes a protein that has homologies to vertebrate proteins of the endoplasmic reticulum. *Genes Dev.* 12, 120–31.
- Kretzschmar, M., Massagué, J., 1998. SMADs: mediators and regulators of TGF-beta signaling. *Curr. Opin. Genet. Dev.* 8, 103–11.
- Kugler, J.-M., Lasko, P., n.d. Localization, anchoring and translational control of oskar, gurken, bicoid and nanos mRNA during *Drosophila* oogenesis. *Fly (Austin)*. 3, 15–28.
- Lagna, G., Hata, A., Hemmati-Brivanlou, A., Massagué, J., 1996. Partnership between DPC4 and SMAD proteins in TGF-beta signalling pathways. *Nature* 383, 832–6.

- Lemaitre, B., Nicolas, E., Michaut, L., Reichhart, J.M., Hoffmann, J.A., 1996. The dorsoventral regulatory gene cassette *spätzle/Toll/cactus* controls the potent antifungal response in *Drosophila* adults. *Cell* 86, 973–83.
- LeMosy, E.K., Hashimoto, C., 2000. The nudel protease of *Drosophila* is required for eggshell biogenesis in addition to embryonic patterning. *Dev. Biol.* 217, 352–61.
- Liberman, L.M., Reeves, G.T., Stathopoulos, A., 2009. Quantitative imaging of the Dorsal nuclear gradient reveals limitations to threshold-dependent patterning in *Drosophila*. *Proc. Natl. Acad. Sci. U. S. A.* 106, 22317–22.
- Ligoxygakis, P., Roth, S., Reichhart, J.-M., 2003. A Serpin Regulates Dorsal-Ventral Axis Formation in the *Drosophila* Embryo. *Curr. Biol.* 13, 2097–2102.
- Lin, H., Spradling, A.C., 1993. Germline stem cell division and egg chamber development in transplanted *Drosophila* germaria. *Dev. Biol.* 159, 140–52.
- Lüders, F., Segawa, H., Stein, D., Selva, E.M., Perrimon, N., Turco, S.J., Häcker, U., 2003. Slalom encodes an adenosine 3'-phosphate 5'-phosphosulfate transporter essential for development in *Drosophila*. *EMBO J.* 22, 3635–44.
- Lynch, J. a, Peel, A.D., Drechsler, A., Averof, M., Roth, S., 2010. EGF signaling and the origin of axial polarity among the insects. *Curr. Biol.* 20, 1042–7.
- Lynch, J. a, Roth, S., 2011. The evolution of dorsal-ventral patterning mechanisms in insects. *Genes Dev.* 25, 107–18.
- Lynch, J. a., El-Sherif, E., Brown, S.J., 2012. Comparisons of the embryonic development of *Drosophila*, *Nasonia*, and *Tribolium*. *Wiley Interdiscip. Rev. Dev. Biol.* 1, 16–39.
- Lynch, J.A., Desplan, C., 2006. A method for parental RNA interference in the wasp *Nasonia vitripennis*. *Nat. Protoc.* 1, 486–94.
- Ma, Q., Guo, C., Barnewitz, K., Sheldrick, G.M., Soling, H.-D., Uson, I., Ferrari, D.M., 2003. Crystal structure and functional analysis of *Drosophila* Wind, a protein-disulfide isomerase-related protein. *J. Biol. Chem.* 278, 44600–7.
- Margolis, J., Spradling, A., 1995. Identification and behavior of epithelial stem cells in the *Drosophila* ovary. *Development* 121, 3797–807.
- Marqués, G., Musacchio, M., Shimell, M.J., Wünnenberg-Stapleton, K., Cho, K.W., O'Connor, M.B., 1997. Production of a DPP activity gradient in the early *Drosophila* embryo through the opposing actions of the SOG and TLD proteins. *Cell* 91, 417–26.
- Massagué, J., 1998. TGF-beta signal transduction. *Annu. Rev. Biochem.* 67, 753–91.
- Massagué, J., Seoane, J., Wotton, D., 2005. Smad transcription factors. *Genes Dev.* 19, 2783–810.
- Medzhitov, R., Preston-Hurlburt, P., Kopp, E., Stadlen, A., Chen, C., Ghosh, S., Janeway, C.A., 1998. MyD88 is an adaptor protein in the hToll/IL-1 receptor family signaling pathways. *Mol. Cell* 2, 253–8.
- Minakhina, S., Yang, J., Steward, R., 2003. Tamo selectively modulates nuclear import in *Drosophila*. *Genes Cells* 8, 299–310.
- Misra, S., Hecht, P., Maeda, R., Anderson, K. V, 1998. Positive and negative regulation of Easter, a member of the serine protease family that controls

- dorsal-ventral patterning in the *Drosophila* embryo. *Development* 125, 1261–7.
- Mizutani, C.M., Bier, E., 2008. EvoD/Vo: the origins of BMP signalling in the neuroectoderm. *Nat. Rev. Genet.* 9, 663–77.
- Moussian, B., Roth, S., 2005. Dorsoventral axis formation in the *Drosophila* embryo—shaping and transducing a morphogen gradient. *Curr. Biol.* 15, R887–99.
- Nakao, A., Afrakhte, M., Morén, A., Nakayama, T., Christian, J.L., Heuchel, R., Itoh, S., Kawabata, M., Heldin, N.E., Heldin, C.H., ten Dijke, P., 1997. Identification of Smad7, a TGFbeta-inducible antagonist of TGF-beta signalling. *Nature* 389, 631–5.
- Nakayama, T., Cui, Y., Christian, J.L., 2000. Regulation of BMP/Dpp signaling during embryonic development. *Cell. Mol. Life Sci.* 57, 943–56.
- Nambu, J.R., Franks, R.G., Hu, S., Crews, S.T., 1990. The single-minded gene of *Drosophila* is required for the expression of genes important for the development of CNS midline cells. *Cell* 63, 63–75.
- Neuman-Silberberg, F.S., Schüpbach, T., 1993. The *Drosophila* dorsoventral patterning gene *gurken* produces a dorsally localized RNA and encodes a TGF alpha-like protein. *Cell* 75, 165–74.
- Nunes da Fonseca, R., von Levetzow, C., Kalscheuer, P., Basal, A., van der Zee, M., Roth, S., 2008. Self-regulatory circuits in dorsoventral axis formation of the short-germ beetle *Tribolium castaneum*. *Dev. Cell* 14, 605–15.
- O'Connor, M.B., Umulis, D., Othmer, H.G., Blair, S.S., 2006. Shaping BMP morphogen gradients in the *Drosophila* embryo and pupal wing. *Development* 133, 183–93.
- Park, K.W., Hong, J.-W., 2012. Mesodermal repression of single-minded in *Drosophila* embryo is mediated by a cluster of Snail-binding sites proximal to the early promoter. *BMB Rep.* 45, 577–82.
- Pascucci, T., Perrino, J., Mahowald, A.P., Waring, G.L., 1996. Eggshell assembly in *Drosophila*: processing and localization of vitelline membrane and chorion proteins. *Dev. Biol.* 177, 590–8.
- Rafiqi, A.M., Lemke, S., Ferguson, S., Stauber, M., Schmidt-Ott, U., 2008. Evolutionary origin of the amnioserosa in cyclorrhaphan flies correlates with spatial and temporal expression changes of *zen*. *Proc. Natl. Acad. Sci. U. S. A.* 105, 234–9.
- Ray, R.P., Arora, K., Nüsslein-Volhard, C., Gelbart, W.M., 1991. The control of cell fate along the dorsal-ventral axis of the *Drosophila* embryo. *Development* 113, 35–54.
- Reach, M., Galindo, R.L., Towb, P., Allen, J.L., Karin, M., Wasserman, S.A., 1996. A gradient of cactus protein degradation establishes dorsoventral polarity in the *Drosophila* embryo. *Dev. Biol.* 180, 353–64.
- Reeves, G.T., Trisnadi, N., Truong, T. V, Nahmad, M., Katz, S., Stathopoulos, A., 2012. Dorsal-ventral gene expression in the *Drosophila* embryo reflects the dynamics and precision of the dorsal nuclear gradient. *Dev. Cell* 22, 544–57.

- Robertis, E.M. De, 2008. Evo-devo: variations on ancestral themes. *Cell* 132, 185–195.
- Robinson, D.N., Cooley, L., 1996. Stable intercellular bridges in development: the cytoskeleton lining the tunnel. *Trends Cell Biol.* 6, 474–9.
- Rose, T., LeMosy, E.K., Cantwell, A.M., Banerjee-Roy, D., Skeath, J.B., Di Cera, E., 2003. Three-dimensional models of proteases involved in patterning of the *Drosophila* Embryo. Crucial role of predicted cation binding sites. *J. Biol. Chem.* 278, 11320–30.
- Roth, S., 2003. The origin of dorsoventral polarity in *Drosophila*. *Philos. Trans. R. Soc. Lond. B. Biol. Sci.* 358, 1317–29; discussion 1329.
- Roth, S., Lynch, J. a, 2009. Symmetry breaking during *Drosophila* oogenesis. *Cold Spring Harb. Perspect. Biol.* 1, a001891.
- Roth, S., Schüpbach, T., 1994. The relationship between ovarian and embryonic dorsoventral patterning in *Drosophila*. *Development* 120, 2245–57.
- Roth, S., Stein, D., Nüsslein-Volhard, C., 1989. A gradient of nuclear localization of the dorsal protein determines dorsoventral pattern in the *Drosophila* embryo. *Cell* 59, 1189–202.
- Rushlow, C.A., Han, K., Manley, J.L., Levine, M., 1989. The graded distribution of the dorsal morphogen is initiated by selective nuclear transport in *Drosophila*. *Cell* 59, 1165–77.
- Savard, J., Tautz, D., Richards, S., Weinstock, G.M., Gibbs, R. a, Werren, J.H., Tettelin, H., Lercher, M.J., 2006. Phylogenomic analysis reveals bees and wasps (Hymenoptera) at the base of the radiation of Holometabolous insects. *Genome Res.* 16, 1334–8.
- Schmierer, B., Hill, C.S., 2007. TGFbeta-SMAD signal transduction: molecular specificity and functional flexibility. *Nat. Rev. Mol. Cell Biol.* 8, 970–82.
- Schüpbach, T., Wieschaus, E., 1989. Female sterile mutations on the second chromosome of *Drosophila melanogaster*. I. Maternal effect mutations. *Genetics* 121, 101–17.
- Sen, J., Goltz, J.S., Konsolaki, M., Schüpbach, T., Stein, D., 2000. Windbeutel is required for function and correct subcellular localization of the *Drosophila* patterning protein Pipe. *Development* 127, 5541–50.
- Sen, J., Goltz, J.S., Stevens, L., Stein, D., 1998. Spatially restricted expression of pipe in the *Drosophila* egg chamber defines embryonic dorsal-ventral polarity. *Cell* 95, 471–81.
- Shimell, M.J., Ferguson, E.L., Childs, S.R., O'Connor, M.B., 1991. The *Drosophila* dorsal-ventral patterning gene *tolloid* is related to human bone morphogenetic protein 1. *Cell* 67, 469–81.
- Sivasankaran, R., Vigano, M.A., Müller, B., Affolter, M., Basler, K., 2000. Direct transcriptional control of the Dpp target omb by the DNA binding protein Brinker. *EMBO J.* 19, 6162–72.
- Srinivasan, S., Rashka, K.E., Bier, E., 2002. Creation of a Sog morphogen gradient in the *Drosophila* embryo. *Dev. Cell* 2, 91–101.
- St Johnston, D., Nüsslein-Volhard, C., 1992. The origin of pattern and polarity in the *Drosophila* embryo. *Cell* 68, 201–19.

- Stathopoulos, A., Levine, M., 2004. Whole-genome analysis of *Drosophila* gastrulation. *Curr. Opin. Genet. Dev.* 14, 477–84.
- Stathopoulos, A., Van Drenth, M., Erives, A., Markstein, M., Levine, M., 2002. Whole-genome analysis of dorsal-ventral patterning in the *Drosophila* embryo. *Cell* 111, 687–701.
- Steward, R., 1987. Dorsal, an embryonic polarity gene in *Drosophila*, is homologous to the vertebrate proto-oncogene, *c-rel*. *Science* 238, 692–4.
- Steward, R., 1989. Relocalization of the dorsal protein from the cytoplasm to the nucleus correlates with its function. *Cell* 59, 1179–88.
- Sweeton, D., Parks, S., Costa, M., Wieschaus, E., 1991. Gastrulation in *Drosophila*: the formation of the ventral furrow and posterior midgut invaginations. *Development* 112, 775–89.
- Towb, P., Bergmann, A., Wasserman, S.A., 2001. The protein kinase Pelle mediates feedback regulation in the *Drosophila* Toll signaling pathway. *Development* 128, 4729–36.
- Towb, P., Galindo, R.L., Wasserman, S.A., 1998. Recruitment of Tube and Pelle to signaling sites at the surface of the *Drosophila* embryo. *Development* 125, 2443–50.
- Towb, P., Sun, H., Wasserman, S. a, 2009. Tube Is an IRAK-4 homolog in a Toll pathway adapted for development and immunity. *J. Innate Immun.* 1, 309–21.
- Trapnell, C., Roberts, A., Goff, L., Pertea, G., Kim, D., Kelley, D.R., Pimentel, H., Salzberg, S.L., Rinn, J.L., Pachter, L., 2012. Differential gene and transcript expression analysis of RNA-seq experiments with TopHat and Cufflinks. *Nat. Protoc.* 7, 562–78.
- Tsuneizumi, K., Nakayama, T., Kamoshida, Y., Kornberg, T.B., Christian, J.L., Tabata, T., 1997. Daughters against dpp modulates dpp organizing activity in *Drosophila* wing development. *Nature* 389, 627–31.
- Ulvila, J., Parikka, M., Kleino, A., Sormunen, R., Ezekowitz, R.A., Kocks, C., Rämetsä, M., 2006. Double-stranded RNA is internalized by scavenger receptor-mediated endocytosis in *Drosophila* S2 cells. *J. Biol. Chem.* 281, 14370–5.
- Uv, A.E., Roth, P., Xylourgidis, N., Wickberg, A., Cantera, R., Samakovlis, C., 2000. *members only* encodes a *Drosophila* nucleoporin required for rel protein import and immune response activation. *Genes Dev.* 14, 1945–57.
- Van der Zee, M., Berns, N., Roth, S., 2005. Distinct functions of the *Tribolium* *zerknüllt* genes in serosa specification and dorsal closure. *Curr. Biol.* 15, 624–36.
- Van der Zee, M., Stockhammer, O., von Levetzow, C., Nunes da Fonseca, R., Roth, S., 2006. *Sog/Chordin* is required for ventral-to-dorsal Dpp/BMP transport and head formation in a short germ insect. *Proc. Natl. Acad. Sci. U. S. A.* 103, 16307–12.
- Werren, J.H., Richards, S., Desjardins, C.A., Niehuis, O., Gadau, J., et al., 2010. Functional and evolutionary insights from the genomes of three parasitoid *Nasonia* species. *Science* 327, 343–8.



- Wharton, K.A., Ray, R.P., Gelbart, W.M., 1993. An activity gradient of decapentaplegic is necessary for the specification of dorsal pattern elements in the *Drosophila* embryo. *Development* 117, 807–22.
- Whitman, M., 1998. Smads and early developmental signaling by the TGF $\beta$  superfamily. *Genes Dev.* 12, 2445–62.
- Wilson, M.J., Dearden, P.K., 2011. Diversity in insect axis formation: two orthodenticle genes and hunchback act in anterior patterning and influence dorsoventral organization in the honeybee (*Apis mellifera*). *Development* 138, 3497–507.
- Wisotzkey, R.G., Mehra, A., Sutherland, D.J., Dobens, L.L., Liu, X., Dohrmann, C., Attisano, L., Raftery, L.A., 1998. Medea is a *Drosophila* Smad4 homolog that is differentially required to potentiate DPP responses. *Development* 125, 1433–45.
- Wolper, L., Jessel, T., Lawrence, P., Mayerowitz, E., Robertson, E., Smith, J., 2007. *Principles of Development*, Third Edit. ed. Oxford University Press.
- Yamashita, H., Ten Dijke, P., Heldin, C.H., Miyazono, K., 1996. Bone morphogenetic protein receptors. *Bone* 19, 569–74.
- Zhang, X., Luo, D., Pflugfelder, G.O., Shen, J., 2013. Dpp signaling inhibits proliferation in the *Drosophila* wing by Omb-dependent regional control of bantam. *Development* 140, 2917–22.
- Zhang, Y., Musci, T., Derynck, R., 1997. The tumor suppressor Smad4/DPC 4 as a central mediator of Smad function. *Curr. Biol.* 7, 270–6.
- Zhang, Z., Stevens, L.M., Stein, D., 2009a. Sulfation of eggshell components by Pipe defines dorsal-ventral polarity in the *Drosophila* embryo. *Curr. Biol.* 19, 1200–5.
- Zhang, Z., Zhu, X., Stevens, L.M., Stein, D., 2009b. Distinct functional specificities are associated with protein isoforms encoded by the *Drosophila* dorsal-ventral patterning gene pipe. *Development* 136, 2779–89.
- Zhao, T., Graham, O.S., Raposo, A., St Johnston, D., 2012. Growing microtubules push the oocyte nucleus to polarize the *Drosophila* dorsal-ventral axis. *Science* 336, 999–1003.

## 7 Summary

Analysis of the DV axis of *Nasonia* revealed that all investigated Toll pathway components and most zygotically expressed DV patterning genes known from *Drosophila* are also present in the *Nasonia* genome. Prior to gastrulation, gene expression is quite similar when compared to *Drosophila*. However, regulation of gene expression is more dynamic.

The functional analysis revealed a conserved role for Toll signaling in embryonic DV axis polarization. However, in contrast to *Drosophila*, Toll's function in providing pattern information is reduced to the formation of ventral fates in *Nasonia*. Additionally, it seems that Toll signaling does not result in a broad stable gradient of nuclear Dorsal. It induces a narrow domain of zygotic gene expression that dynamically expands independent of Toll signaling. Furthermore, the *Drosophila* Toll signaling target gene *sog*, which is essential for the formation of the dorsal BMP gradient is absent in *Nasonia*. Nevertheless, peak levels of BMP signaling along the dorsal midline are established and even obtained in the absence of Toll signaling in *Nasonia*. This suggests, that the *Nasonia* DV axis is established by bipolar signal induction from both the ventral and the dorsal side, which is in contrast to the unipolar Toll dependent axis determination observed in *Drosophila*. Moreover, the functional analysis of the GRN provides strong evidence for the assumption that BMP signaling plays the dominant role in providing DV polarity in the early embryo of *Nasonia*.

To investigate the influence of the BMP and Toll pathway on early embryogenesis in an unbiased way, a transcriptome analysis was performed. The generated transcriptome data set provides an optimal tool to investigate genes that are putative downstream targets of Toll and BMP signaling. A preliminary screen based on a high throughput variant of ISH already discovered previously described *Drosophila* orthologs as well as unknown hymenoptera specific genes that hold a potentially important role in the DV GRN of *Nasonia*.

## 8 Zusammenfassung

Die Analyse des dorsal-ventralen (DV) genregulatorischen Netzwerkes (GRN) von *Nasonia vitripennis* ergab, dass alle untersuchten Toll-Signalweg-Komponenten und die meisten zygotisch exprimierten DV-Mustergene von *Drosophila* auch im Genom von *Nasonia* vorhanden sind. Zu Beginn der Gastrulation ist die Expression ähnlich wie in *Drosophila*, allerdings ist diese dynamischer reguliert.

Die funktionelle Analyse mittels parentaler RNA-Interferenz (pRNAi) ergab, dass die Funktion des Toll Signalwegs in der embryonalen DV-Achsenpolarisation konserviert ist. Jedoch ist im Vergleich zu *Drosophila* die Funktion von Toll, in Bezug auf die von ihm bereitgestellte Musterinformation, auf die Ausbildung der ventralen Gewebe des Embryos beschränkt. Zusätzlich kann angenommen werden, dass der Toll Signalweg nicht in der Bildung eines breiten, stabilen Gradienten nukleären Dorsals resultiert, sondern eher einen schmalen Bereich der zygotische Genexpression induziert, die sich anschließend, unabhängig vom Toll-Signalweg, dynamisch erweitert. Des Weiteren ist *short gastrulation (sog)*, ein Zielgen des Toll-Signalwegs, welches für die Formation des dorsalen BMP Gradienten in *Drosophila* essenziell ist, nicht vorhanden in *Nasonia*. Dennoch wird in *Nasonia* der Höchstwert des BMP-Signals entlang der dorsalen Mittellinie gebildet und sogar in Abwesenheit von Toll aufrechterhalten. Daher ist naheliegend, dass in *Nasonia* die Festlegung der DV-Achse durch beidseitige Induktion, sowohl von ventraler als auch von dorsaler Seite, bestimmt wird; anders als die einseitige Toll-abhängigen Achsenfestlegung, in *Drosophila*. Zudem liefert die funktionelle Analyse überzeugende Beweise für die Vermutung, dass der BMP-Signalweg die Hauptrolle in der Bereitstellung der DV Polarität im frühen Embryo von *Nasonia vitripennis* spielt.

Um den Einfluss des BMP- und Toll-Signalwegs auf die frühe Embryogenese unvoreingenommen zu untersuchen, wurde eine Transkriptomanalyse mit wildtypischen und RNAi behandelten Embryos

durchgeführt. Der erzeugte Transkriptomdatensatz eignet sich optimal zur Untersuchung mutmaßlicher, dem Toll bzw. BMP-Signalweg nachgeschalteter Gene. Erste, auf einer Hochdurchsatzvariante der *In-situ* Hybridisierung beruhende Untersuchungen, zeigen, dass sowohl *Drosophila*-orthologe, als auch bislang unbekannte, Hymenoptera-spezifische Gene eine wichtige Rolle im dorsal-ventralen GRN von *Nasonia vitripennis* spielen könnten.

## 9 Anhang über die Eigenbeteiligung an den aufgeführten Veröffentlichungen

### 9.1 Patterning the dorsal–ventral axis of the wasp *Nasonia vitripennis*

Thomas Buchta a,1, Orhan Özüak a,1, Dominik Stappert a, Siegfried Roth a,n, Jeremy A. Lynch a,b,nn a Institute for Developmental Biology, University of Cologne, Zùlpichstrasse 47b, 50674 Cologne, Germany b Department of Biological Sciences, University of Illinois at Chicago, 900 S Ashland Ave., Chicago, IL 60607, USA

#### 9.1.1 Gene identification

Conserved domains of the following genes have been identified using TBLASTN

([http://blast.ncbi.nlm.nih.gov/Blast.cgi?PROGRAM=tblastn&BLAST\\_PROGRAMS=tblastn&PAGE\\_TYPE=BlastSearch&SHOW\\_DEFAULTS=on&LINK\\_LOC=blasthome](http://blast.ncbi.nlm.nih.gov/Blast.cgi?PROGRAM=tblastn&BLAST_PROGRAMS=tblastn&PAGE_TYPE=BlastSearch&SHOW_DEFAULTS=on&LINK_LOC=blasthome)) in the *Nasonia vitripennis* genome:

<i>twist</i>	( <i>Nv-twi</i> )
<i>snail</i>	( <i>Nv-sna</i> )
<i>single-minded</i>	( <i>Nv-sim</i> )
<i>cactus1</i>	( <i>Nv-cact1</i> )
<i>brinker</i>	( <i>Nv-brk</i> )
<i>ventral nervous system defective</i>	( <i>Nv-vnd</i> )
<i>intermediate neuroblasts defective</i>	( <i>Nv-ind</i> )

Conserved domains of the following genes have been identified using TBLASTN in the *Drosophila melanogaster* genome:

<i>twist</i>	( <i>Dm-twi</i> )
<i>snail</i>	( <i>Dm-sna</i> )
<i>single-minded</i>	( <i>Dm-sim</i> )
<i>brinker</i>	( <i>Dm-brk</i> )
<i>ventral nervous system defective</i>	( <i>Dm-vnd</i> )
<i>intermediate neuroblasts defective</i>	( <i>Dm-ind</i> )

### 9.1.2 Primer design

For all in 8.1.1 identified genes specific primers were designed using Primer3 (<http://bioinfo.ut.ee/primer3-0.4.0/>).

### 9.1.3 cDNA generation

cDNA used for specific gene amplification was created using *Superscript 3* (Invitrogen).

### 9.1.4 *In situ* hybridization (ISH) probe synthesis

Amplicons created using gene specific primers described in 8.1.2 were used for ISH probe synthesis.

### 9.1.5 Single/two color fluorescent ISH with DAPI

ISH with DAPI was performed for the following genes:

<i>Dm-twi</i> / <i>Dm-sna</i>	(Figure 1 A-C)
<i>Nv-twi</i> / <i>Nv-sna</i>	(Figure 1 D-F)
<i>Dm-twi</i> / <i>Dm-sim</i>	(Figure 2 A-C)
<i>Nv-twi</i> / <i>Nv-sim</i>	(Figure 2 D-F)
<i>Nv-twi</i> / <i>Nv-Cact</i>	(Figure 3)
<i>Dm-brk</i> / <i>Dm-twi</i>	(Figure 4 A-C)
<i>Nv-brk</i> / <i>Nv-twi</i>	(Figure 4 D-F)
<i>Dm-vnd</i> / <i>Dm-ind</i>	(Figure 5 A-C)
<i>Nv-vnd</i> / <i>Nv-ind</i>	(Figure 5 D-F)
<i>Dm-sna</i> / <i>Dm-sim</i>	(Supplementary Figure 2 A-D)
<i>Nv-sna</i> / <i>Nv-sim</i>	(Supplementary Figure 2 E-H)
<i>Nv-sim</i> / <i>Nv-twi</i>	(Supplementary Figure 3 A/B)
<i>Nv-vnd</i> / <i>Nv-twi</i>	(Supplementary Figure 2 C-E)

### 9.1.6 DAPI staining

Characterization of syncytial divisions in the early embryo of *Nasonia* at all stages stained with DAPI (Supplementary Figure 1) was performed.

### 9.1.7 Microscopy, picture processing and figure design

Pictures for the following figures were taken, processed and assembled \*:

Figure 1. Simultaneous detection of *twist* and *snail* in *Nasonia*, *Drosophila* and *Tribolium* embryos.

Figure 2. Simultaneous detection of *twist* and *single-minded* in *Nasonia*, *Drosophila* and *Tribolium* embryos.

Figure 3. Characterization of the expression and dynamics of *cact* in *Nasonia*.

Figure 4. Comparison of *brinker* expression dynamics in *Drosophila* and *Nasonia*.

Figure 5. Comparison of columnar gene dynamics in *Drosophila* and *Nasonia*. (A-F)

Supplementary Figure 1. Characterization of syncytial divisions in the early embryo of *Nasonia* Embryos at all stages stained with DAPI to demonstrate the arrangement of the nuclei.

Supplementary Figure 2. Double fluorescent ISH of *snail* and *sim* in *Nasonia*, *Drosophila* and *Tribolium* embryos

Supplementary Figure 3. Postgastrular dynamics of *Nv-vnd* and *Nv-sim*  
(\**Tribolium* pictures taken by D. Stappert)

### 9.1.8 Embryo collection and fixation

Embryos used in 8.1.3 and 8.1.5 were collected by using the Waspinator and fixed as described in the paper

### 9.1.9 Waspinator

Idea and design for the *Waspinator* by T. Buchta & O. Özüak.

### 9.1.10 Text

Orhan Özüak wrote the Manuscript of “Patterning the dorsal–ventral axis of the wasp *Nasonia vitripennis*”.

The Manuscript of “Patterning the dorsal–ventral axis of the wasp *Nasonia vitripennis*” was proofread and finalized in co-operation with Thomas Buchta.

## 9.2 Novel deployment of Toll and BMP signaling pathways leads to a convergent patterning output in a wasp

Orhan Özüak\*, Thomas Buchta\*, Siegfried Roth, Jeremy A. Lynch

### 9.2.1 Gene identification

Conserved domains of the following genes have been identified using TBLASTN

([http://blast.ncbi.nlm.nih.gov/Blast.cgi?PROGRAM=tblastn&BLAST\\_PROGRAMS=tblastn&PAGE\\_TYPE=BlastSearch&SHOW\\_DEFAULTS=on&LINK\\_LOC=blasthome](http://blast.ncbi.nlm.nih.gov/Blast.cgi?PROGRAM=tblastn&BLAST_PROGRAMS=tblastn&PAGE_TYPE=BlastSearch&SHOW_DEFAULTS=on&LINK_LOC=blasthome)) in the *Nasonia vitripennis* genome:

<i>twist</i>	( <i>Nv-twi</i> )
<i>cactus1</i>	( <i>Nv-cact1</i> )
<i>brinker</i>	( <i>Nv-brk</i> )
<i>ventral nervous system defective</i>	( <i>Nv-vnd</i> )
<i>Toll</i>	( <i>Nv-Toll</i> )
<i>decapentaplegic</i>	( <i>Nv-dpp</i> )

### 9.2.2 Primer design

For all in 8.2.1 identified genes specific primers were designed using Primer3 (<http://bioinfo.ut.ee/primer3-0.4.0/>).



### 9.2.3 cDNA generation

cDNA used for specific gene amplification was created.

### 9.2.4 *In situ* hybridization (ISH) probe synthesis

Amplicons created using gene specific primers for

<i>twist</i>	( <i>Nv-twi</i> )
<i>cactus1</i>	( <i>Nv-cact1</i> )
<i>brinker</i>	( <i>Nv-brk</i> )
<i>ventral nervous system defective</i>	( <i>Nv-vnd</i> )

were used for ISH probe synthesis.

### 9.2.5 Two-color and three-color fluorescent ISH with DAPI

ISH with DAPI for the following genes:

<i>Nv-zen</i> / <i>Nv-brk</i> / <i>Nv-twi</i>	(Figure 1. A,B,D)
<i>Nv-zen</i> / <i>Nv-ara</i> / <i>Nv-brk</i>	(Figure 2. L,M,M')
<i>Nv-twi</i> / <i>Nv-vnd</i>	(Figure 2. A,B,C,D)
<i>Nv-twi</i> / <i>Nv-cact</i>	(Figure 2. I,J,K)
<i>Nv-doc</i> / <i>Nv-twi</i>	(Supplementary Figure 1. A,B)

### 9.2.6 Double stranded RNA synthesis

Amplicons created using gene specific primers for

<i>Toll</i>	( <i>Nv-Toll</i> )
decapentaplegic	( <i>Nv dpp</i> )

were used for dsRNA synthesis.

### 9.2.7 dsRNA single and double injections

Following dsRNA were injected:

Nv-Toll
Nv-dpp / Nv-Toll (double injection)

### 9.2.8 Microscopy, picture processing and figure design

Pictures for the following figures were taken, process and assembled\*:

- Figure 1. Effects of *Toll*, *dpp*, and *Toll/dpp* double pRNAi.
- Figure 2. Detailed effects of *Nv-dpp* and *Nv-Toll* pRNAi.
- Figure 4. Relative roles of BMP and Toll signalling in *Drosophila* and *Nasonia*.
- Supplementary Figure 1. *Nasonia dorsocross* (*Nv-doc*) as a marker in *Nv-dpp* RNAi.

\*except Figure1C/E/F, Figure2E-H, Suppl.Fig.1c-f  
by O. Özüak

### 9.2.9 Embryo collection and fixation

Embryos used in 8.2.3 and 8.2.5 were collected by using the Waspinator and fixed as described in the paper

### 9.2.10 Text

Thomas Buchta wrote the Manuscript of “Novel deployment of Toll and BMP signaling pathways leads to a convergent patterning output in a wasp”.

The Manuscript of “Patterning the dorsal–ventral axis of the wasp *Nasonia vitripennis*” was proofread and finalized in co-operation with Orhan Özüak.

### 9.3 Ancient and diverged TGF- $\beta$ signaling components in *Nasonia vitripennis*

Orhan Özüak\*, Thomas Buchta\*, Siegfried Roth, Jeremy A. Lynch

#### 9.3.1 Gene identification

Conserved domains of the following genes have been identified using TBLASTN

([http://blast.ncbi.nlm.nih.gov/Blast.cgi?PROGRAM=tblastn&BLAST\\_PROGRAMS=tblastn&PAGE\\_TYPE=BlastSearch&SHOW\\_DEFAULTS=on&LINK\\_LOC=blasthome](http://blast.ncbi.nlm.nih.gov/Blast.cgi?PROGRAM=tblastn&BLAST_PROGRAMS=tblastn&PAGE_TYPE=BlastSearch&SHOW_DEFAULTS=on&LINK_LOC=blasthome)) in the *Nasonia vitripennis* genome:

<i>mother against dpp 1</i>	( <i>Nv-mad1</i> )
<i>mother against dpp 2</i>	( <i>Nv-mad2</i> )
<i>mother against dpp 3</i>	( <i>Nv-mad3</i> )
<i>medea</i>	( <i>Nv-med</i> )
<i>dally</i>	( <i>Nv-dally</i> )
<i>glypican4/dally-like</i>	( <i>Nv-dly</i> )
<i>collagen type IV</i>	( <i>Nv-dcg1</i> )
<i>pentagone</i>	( <i>Nv-pent</i> )
<i>follistatin</i>	( <i>Nv-flt</i> )
<i>crossveinless 2A</i>	( <i>Nv-cv2A</i> )
<i>crossveinless 2B</i>	( <i>Nv-cv2B</i> )
<i>crossveinless 2C</i>	( <i>Nv-cv2C</i> )
<i>crossveinless 2D</i>	( <i>Nv-cv2D</i> )

The putative *Nasonia* protein sequences were aligned with muscle 3.7

(<http://www.drive5.com/muscle/index.htm>)

Alignment refinement was performed using GBLOCKS 0.91b

(<http://molevol.cmima.csic.es/castresana/Gblocks.html>)

Maximum likelihood phylogenies were generated with PhyML 3.0

(<http://atgc.lirmm.fr/phyml/binaries.html>)

Trees were edited in MEGA5.2.2

(<http://www.megasoftware.net/index.php>)

### 9.3.2 Primer design

For all in 8.3.1 identified genes specific primers were designed using Primer3. (<http://bioinfo.ut.ee/primer3-0.4.0/>)

### 9.3.3 cDNA generation

cDNA used for specific gene amplification was created using *Superscript 3* (Invitrogen)

### 9.3.4 *In situ* hybridization (ISH) probe synthesis

Amplicons created using gene specific primers described in 8.3.2 were used for ISH probe synthesis.

### 9.3.5 Single/ two color fluorescent ISH with DAPI

ISH with DAPI was performed for the following genes:

<i>Nv-vnd / Nv-twi</i>	(Figure 3 B)
<i>dally</i>	(Figure 4 A/E)
<i>glypican 4</i>	(Figure 4 B/F)
<i>collagen IV</i>	(Figure 4 C/G)
<i>pentagone</i>	(Figure 4 D/H)
<i>follistatin</i>	(Figure 4 I/M)
<i>crossveinless 2A</i>	(Figure 4 J/N)
<i>crossveinless 2C</i>	(Figure 4 K/O)
<i>crossveinless 2D</i>	(Figure 4 L/P)

### 9.3.6 Double stranded RNA synthesis

Amplicons created using gene specific primers described in 8.3.2 were used for dsRNA synthesis.

### 9.3.7 dsRNA injection

Following dsRNA were injected:

<i>mother against dpp 1</i>	( <i>Nv-mad1</i> )
<i>mother against dpp 2</i>	( <i>Nv-mad2</i> )
<i>mother against dpp 3</i>	( <i>Nv-mad3</i> )
<i>medea</i>	( <i>Nv-med</i> )
<i>crossveinless 2A</i>	( <i>Nv-cv2A</i> )
<i>crossveinless 2C</i>	( <i>Nv-cv2C</i> )
<i>crossveinless 2D</i>	( <i>Nv-cv2D</i> )

### 9.3.8 Microscopy, picture processing, tree generation and figure design

Figure 3. Intracellular mediators.

Figure 4. Extracellular modulators.

### 9.3.9 Embryo collection and fixation

Embryos used in 8.3.3 and 8.3.5 were collected by using the *Waspinator* and fixed as described in the paper

### 9.3.10 Text

Thomas Buchta wrote the manuscript of „Ancient and diverged TGF- $\beta$  signaling components in *Nasonia vitripennis*“.

The Manuscript of “Ancient and diverged TGF- $\beta$  signaling components in *Nasonia vitripennis*“ will be proofread and finalized in co-operation with Orhan Özüak.

## **Danksagung**

Ich danke Prof. Dr. Siegfried Roth, für die Möglichkeit, in seinem Arbeitskreis meine Promotionsarbeit and diesem interessanten Thema anfertigen zu dürfen. Darüber hinaus bedanke ich mich für die hilfreiche Unterstützung und viele anregende Diskussionen.

Ich danke Prof. Dr. Günter Plickert für das Erstellen des Zweitgutachtens.

Im Besonderen danke ich Jeremy A. Lynch für kompetente Betreuung und fachkundige Beratung während dieser Arbeit.

Ein ganz besonderer Dank geht an Orhan Özüak für die gute Zusammenarbeit und Freundschaft.

Ich danke allen Mitarbeitern der AG Roth, die mir stets Ansprechpartner waren und mein Forschungsprojekt durch ihre Ideen, Anregungen und konstruktive Kritik bereicherten.

Und nicht zuletzt danke ich meiner Familie, die in jeglicher Hinsicht die Grundsteine für meinen Weg gelegt haben.

Bei der DFG bedanke ich mich für die finanzielle Unterstützung dieser Arbeit durch den SFB 680 "Molecular basis of evolutionary innovations".

## Erklärung

Ich versichere, dass ich die von mir vorgelegte Dissertation selbständig angefertigt, die benutzten Quellen und Hilfsmittel vollständig angegeben und die Stellen der Arbeit – einschließlich Tabellen, Karten und Abbildungen –, die anderen Werken im Wortlaut oder dem Sinn nach entnommen sind, in jedem Einzelfall als Entlehnung kenntlich gemacht habe; dass diese Dissertation noch keiner anderen Fakultät oder Universität zur Prüfung vorgelegen hat; dass sie – abgesehen von unten angegebenen Teilpublikationen – noch nicht veröffentlicht worden ist sowie, dass ich eine solche Veröffentlichung vor Abschluss des Promotionsverfahrens nicht vornehmen werde. Die Bestimmungen der Promotionsordnung sind mir bekannt. Die von mir vorgelegte Dissertation ist von Prof. Dr. Siegfried Roth betreut worden.

Teilpublikationen:

**Buchta T, Özüak O, Stappert D, Roth S, Lynch JA.** (2013) Patterning the dorsal-ventral axis of the wasp *Nasonia vitripennis*. *Dev Biol.* 2013 Sep 1;381(1):189-202. doi: 10.1016/j.ydbio.2013.05.026. Epub 2013 Jun 2.

In review:

**Orhan Özüak\*, Thomas Buchta\*, Siegfried Roth, Jeremy A. Lynch**

“Novel deployment of Toll and BMP signaling pathways leads to a convergent patterning output in a wasp”

**Orhan Özüak\*, Thomas Buchta\*, Siegfried Roth, Jeremy A. Lynch**

“Ancient and diverged TGF- $\beta$  signaling components in *Nasonia vitripennis*”

Ich versichere, dass ich alle Angaben wahrheitsgemäß nach bestem Wissen und Gewissen gemacht habe und verpflichte mich, jedmöglich, die obigen Angaben betreffenden Veränderungen, dem Dekanat unverzüglich mitzuteilen.

.....

Datum

.....

Unterschrift

## Lebenslauf

### Persönliche Daten

Name Thomas Martin Buchta  
Anschrift Thieboldsgasse 142  
50676 Köln  
Geburtsdatum/ -ort 09.11.81 Bretten

---

### Schulische Ausbildung

1988 – 1992 Grundschule Büchig  
1992 – 1993 Schiller-Schule Bretten  
1993 – 1999 Max-Planck-Realschule Bretten  
1999 – 2002 Handelslehranstalt Bruchsal

---

### Wehr-/Zivildienst

2002 – 2003 Kindertagesstätte Rath-Heumar

---

### Studium

2003 – 2004 Heinrich Heine Universität Düsseldorf  
2004 – 2009 Universität zu Köln  
Diplom-Prüfungsfächer: Genetik, Entwicklungsbiologie,  
Biochemie  
Diplomarbeit bei Prof. Dr. Carien Niessen  
am Zentrum für Molekulare Medizin Köln (ZMMK)  
Titel: „Role of classical cadherins in desmosome  
formation“  
seit 2010 Doktorarbeit bei Prof Dr. Siegfried Roth  
am Institut für Entwicklungsbiologie der Universität zu  
Köln  
Titel: „Analysis of the dorsal-ventral gene regulatory  
network of *Nasonia vitripennis*“



Publikationen:

**Michels C, Buchta T, Bloch W, Krieg T, Niessen CM.** (2009) Classical cadherins regulate desmosome formation. *J Invest Dermatol.* 2009 Aug;129(8):2072-5. doi: 10.1038/jid.2009.17. Epub 2009 Mar 5.

**Buchta T, Ozüak O, Stappert D, Roth S, Lynch JA.** (2013) Patterning the dorsal-ventral axis of the wasp *Nasonia vitripennis*. *Dev Biol.* 2013 Sep 1;381(1):189-202. doi: 10.1016/j.ydbio.2013.05.026. Epub 2013 Jun 2.

In review:

**Orhan Özüak\*, Thomas Buchta\*, Siegfried Roth, Jeremy A. Lynch**  
“Novel deployment of Toll and BMP signaling pathways leads to a convergent patterning output in a wasp”

**Orhan Özüak\*, Thomas Buchta\*, Siegfried Roth, Jeremy A. Lynch**  
“Ancient and diverged TGF- $\beta$  signaling components in *Nasonia vitripennis*”